STIMULATION OF CARBONATE RESERVOIRS USING A NEW EMULSIFIED ACID SYSTEM

A Dissertation

by

MOHAMMED ALI IBRAHIM SAYED

Submitted to the Office of Graduate Studies of
Texas A&M University
in partial fulfillment of the requirements for the degree of

DOCTOR OF PHILOSOPHY

Chair of Committee,	Hisham A. Nasr-El-Din
Committee Members,	Steven A. Holditch
	Alfred D. Hill
	Mahmoud El-Halwagi
Head of Department,	Alfred D. Hill

August 2013

Major Subject: Petroleum Engineering

ABSTRACT

The scope of work can be divided into; the measurement of the rheological properties of a new emulsified acid system that can be suitable for high temperature applications, a study of the performance of the new emulsified acid in stimulating both calcite and dolomite formations, measuring the reaction rate and diffusion coefficient when the new emulsified acid systems react with both calcite and dolomite, and testing the new emulsified acid using core samples obtained from carbonate reservoirs.

The droplet size has a practical impact on the performance of emulsified acid. A good understanding and characterization of the emulsified acid by its size distribution will lead to better understanding of its stability, rheology and how it reacts with carbonate rocks. The influence of the concentration of the new emulsifier on the droplet size, droplet size distribution and upon the rheology of emulsified acids is studied in detail.

The emulsified acid reaction kinetics with calcite rocks was studied before in few studies, and very little work was done with dolomite. One of the main objectives of the present work is to study in detail the reaction of the emulsified acid with both calcite and dolomite rocks using the rotating disk apparatus.

Most of the previous studies on the emulsified acid were done using core samples that were saturated with brine or deionized water. One of the main objectives of the present work is to study in detail the effect of the presence of crude oil in the reservoir rock on the performance of emulsified acids.

Lastly, an innovative technique of emulsifying the chelating agents is evaluated for high temperature applications. The rheology of the emulsified chelating agent is measured using an HPHT rheometer. Also, the reaction of the new emulsified chelating agent with calcite is studied using the rotating disk apparatus, and coreflood experiments were performed using chelating agents and calcite core samples.

DEDICATION

TO MY PARENTS, MY WIFE AND MY KIDS

ACKNOWLEDGEMENTS

I would like to express my sincere thanks to my supervising professor Dr. Hisham A. Nasr-El-Din I am grateful to his assistance and guidance throughout my study and research. I would like to thank him for his help and support without which this study could not have been accomplished.

My appreciation also goes to Dr. Steven A. Holditch, Dr. Mahmoud El-Halwagi, and Dr. Alfred D. Hill for devoting their invaluable time to review my research work and evaluate its results. Their comments during the course of my study are highly appreciated.

Thanks also go to my friends and colleagues and the department faculty and staff for making my time at Texas A&M University a great experience.

My deep appreciation to Ms. Kate Brady for proofreading my dissertation.

Finally, thanks to my mother, father and mother-in-law for their encouragement, and to my wife and my kids for their patience, love and making my life simply better.

NOMENCLATURE

A_c = cross-sectional area of the disk, cm^2

A_0 = initial surface area of the disk, cm^2

C_b = reactant concentration in the bulk solution, $gmole/cm^3$

C_s = concentration of H+ on the surface ($gmole/cm^3$)

D = diffusion coefficient, cm^2/s

D_B = Brownian diffusion coefficient, m^2/s

E_a = activation energy, kcal/gmole

J_{mt} = the mass transfer rate of HCl from the bulk to the disk ($gmole/cm^2.s$)

K = power-law consistency factor, $g/cm.s^{(n-2)}$

k = reaction rate constant ($gmole/cm^2.s$) $(gmole/cm^3)^{-m}$

k_o = pre-exponential factor (frequency factor, $gmole^{(1-m)}$ $cm^{(3m-2)}s^{-1}$

k_{mt} = the mass transfer coefficient (cm/s)

n = power-law index

N = K/ρ, $cm^2/s^{(n+2)}$

N_A = Avogadro's number, $6.022X10^{23}$ mol^{-1}

m = reaction rate order, dimensionless

r = radius of the disk, cm

R_{H+} = rate of reaction ($gmole/cm^2.s$)

r_D = radius of the dispersed phase droplets, m

R_{Dh+} = initial dissolution rate, $gmole/s.cm^2$

Re = modified Reynolds number

R_g = universal gas constant, 8.31 J/(mole.°K)

S_c = modified Schmidt number = ν/D

S_h = Sherwood number

TAN = the total acid number

TBN = the total base number

$\dot{\gamma}$ = shear rate, s^{-1}

β = coefficient to be determined in the Einstein equation for the effective viscosity of a dilute suspension of spheres

μ_a = apparent fluid viscosity, cp

μ" = the effective viscosity (μ") of a dilute suspension of spheres

ν = kinematic viscosity, cm^2/s

η = viscosity of the continuous phase, Pa-s

ρ = fluid density, g/cm^3

φ = core porosity, volume fraction

ϕ = acid volume fraction

$\varepsilon(n)$ = function that depends on the power-law index, n, and the wall radial velocity gradient

ω = disk rotational speed, rad/s

TABLE OF CONTENTS

Page

LIST OF FIGURES

Page

LIST OF TABLES

1. INTRODUCTION AND LITERATURE REVIEW

1.1 Introduction

Acid treatments have been applied to wells in oil and gas bearing rock formations for many years. Acidizing is probably the most widely used workover and stimulation practice in the oil industry (Fredd and Fogler 1997). By dissolving acid soluble components within underground rock formations, or removing material at the wellbore face, the rate of flow of oil or gas out of production wells or the rate of flow of oil-displacing fluids into injection wells may be increased. Acids are widely used to stimulate oil and gas wells to improve the rate of hydrocarbon production (Al-Anazi et al. 1998; Kasza et al. 2006), and to stimulate disposal wells and water injection wells, in order to increase the formation uptake of the injected fluids (Mohammed et al. 1999; Nasr-El-Din et al. 2000).

A number of different acids are used in conventional acidizing treatments, the most common are; hydrochloric (HCl), hydrofluoric (HF), acetic acid (CH_3COOH), formic acid (HCOOH), sulfamic [(NH_2) HSO_3] and chloroacetic ($ClCH_2COOH$). Fredd and Fogler (1996 and 1997) introduced ethylene di-amine tetra acetic acid (EDTA) to be used as an alternative fluid to acidize carbonate formations. These acids differ in their characteristics. Choosing the acid and any additives for a given situation depends on the underground reservoir characteristics and the specific intention of the treatment, for example, near-wellbore damage removal, dissolution of scale in fractures, etc.

In most carbonate-stimulation treatments, HCl is pumped as the main stimulation fluid. HCl is cheap, it has high rock-dissolving power, it generates soluble reaction

products, and it reacts very quickly with carbonates. The reaction between HCl and carbonates is very fast, and this rate becomes higher at higher downhole temperatures, which results in rapid HCl spending and failure of the treatment (Allen and Roberts 1989; Nasr-El-Din et al. 2003a). Other disadvantages of HCl are excessive tubing corrosion and associated high cost of inhibition, and a tendency to form acid/oil sludge in asphaltene-rich crudes.

The majority of acidizing treatments carried out utilize hydrochloric acid (HCl). However, the very fast reaction rate of hydrochloric acid, and other acids listed above, can limit their effectiveness in a number of applications. The problem of acid penetration and optimum wormhole growth is directly coupled to the acid placement problem. The low permeability or high skin sections in a heterogeneous formation accept very little acid. As a result, the velocity of the injected acid in these sections may actually be too low for wormholes to form and all of the acid will spend on the wellbore wall with little or no live acid penetrating deeper into the formation. This ‘‘compact dissolution’’ does not result in significant skin reduction and must be avoided if possible. In this situation, a retarded acid system such as viscosified acid or emulsified acid will improve the wormholing efficiency because it will provide deeper acid penetration (Buijse 2000)

The low viscosity of plain HCl acid (about equal to water) often results in poor wellbore coverage unless highly effective diversion methods are used to ensure treatment of the entire pay zone. Furthermore, the high reaction rate of HCl may prevent the formation of deeply penetrating wormholes and lead to compact dissolution, especially in zones in which the injection rate is low. The higher viscosity improves

wellbore coverage (Jones et al. 1995, Jones and Davies 1998) and at the same time it retards the acid spending rate (Buijse 2000)

Acid spending rate can be reduced by increasing viscosity. The fluid's access to the rock face will be reduced through decreasing the rate of acid leak off and acid mobility (Peters and Saxon 1989). There are several options to lower the acid spending rate, such as the use of organic acids (weak acids), gelled acids (Pabley et al. 1982; Deysarkar et al. 1984; Crowe et al. 1989), in-situ gelled acids (Johnson et al. 1988; Yeager and Shuchart 1997; Saxon et al. 2000), VES acids (Lynn and Nasr-El-Din 2001; Al-Muhareb et al. 2003; Nasr-El-Din et al. 2003b; 2006b;), and emulsified acids (Dill 1961; Knox et al. 1964; Crenshaw and Flippen 1968; Nasr-El-Din et al. 2001).

De Groote (1933) used acid-oil emulsions to remove damage from carbonate rocks, and at the same time, protect the metallic parts of the well from corrosion that may be caused by acid. After that, emulsified acid systems were used for different purposes. Harris (1961) reported the use of emulsified acetic acid in well completion and stimulation applications. Davis et al. (1965) used emulsified acid to test the effectiveness of their spearhead film technique. For emulsified acid, HCl acid is commonly used in these systems as the internal phase of an oil external emulsion. Emulsified acid combines a relatively high rock-dissolving power with a low acid/rock reaction rate.

The most common hydrocarbon that is used as an external phase is diesel, and its main function is to act as a diffusion barrier between acid and rock (Crowe and Miller 1974; Bergstrom and Miller 1975; Hoefner and Fogler 1985; Daccord et al. 1989; Peters and Saxon 1989). This diffusion barrier will result in a reduction in acid-rock reaction

rate, which will help in the creation of deep wormholes (Williams and Nierode 1972; Guidry et al. 1989; Navarrete et al. 1998a and b), and the creation of etched fractured surfaces which enhance well performance (Navarrete et al. 1998a and b; Nasr-El-Din et al. 2006a; 2008a). An acid-diesel emulsion has several advantages (Nasr-El-Din et al. 2000). Besides its slow reaction rate with carbonate rocks, it has a relatively high viscosity. As a result, it has a better sweep efficiency that will improve acid distribution in heterogeneous reservoirs (Buijse and van Domelen 2000). Also, the live acid does not come in contact with well tubulars; therefore, the corrosion level is very low.

1.2 Emulsified Acid

Emulsions are mixtures of two immiscible liquids with a non-vanishing interfacial tension at their interface (Bibette and Leal-Calderon 1996). An emulsion may be defined as a thermo-dynamically unstable heterogeneous system formed by at least two liquids that are at best only slightly soluble. The internal phase is dispersed in the other in the form of small droplets, with diameters higher than 0.1 μm (Clayton 1923, Sherman 1968, and Becher 1985). In general, the emulsion consists of droplets of fluid "A" dispersed in fluid "B"; these are simple A-in-B emulsions, but more complex systems can be prepared such as multiple emulsions where droplets of "A" are included inside droplets of "B" dispersed in "A" and so forth (Pal 1996). As there is interfacial tension, these systems are never at thermo-dynamical equilibrium; the total surface of the interface tends to decrease by various means. The interface decreases both by ripening (migration of phase A via B from the small droplets to the large ones) and by

coalescence. Use of surfactants can slow down both processes (Bibette and Leal-Calderon 1996).

The emulsified acid system consists of acid in diesel oil emulsion. The acid solution consists of hydrochloric acid and acid additives (such as corrosion inhibitor), while the oil phase consists of diesel oil (in most cases) and emulsifier (surfactant). The emulsifier is a surfactant which is used to reduce the interfacial tension between the diesel and acid solution, as both of them are not soluble in each other. Once the emulsified acid is formed, it should remain stable for a certain time, which allows it to be pumped to the formation.

1.3 Previous Work

According to Crowe (1971) the rate at which the acid reacts with the formation is a function of various factors including; the acid concentration, temperature, acid injection rate, type of rock and the surface area to acid volume ratio. To more efficiently treat the formation it is desirable to increase the reaction time of the acid. One method employed in the art of extending the reaction time is to employ acid-in-oil emulsions systems introduced by De Groote (1933). De Groote used this acid system (acid-in-oil emulsion) to remove the damage from carbonate rocks and at the same time, to protect the metallic parts of the well from corrosion that may be caused by acid while the solution is being introduced into the well. From this point of view, the emulsified acid was invented to be a corrosion inhibitor much more than being an improved stimulation fluid. De Groote (1933) used hydrochloric acid, nitric acid and a mixture of the two acids to prepare this acid system. He also used crude oil, coal tar distillates, and kerosene as dispersing

external phases. The emulsifier used to prepare these emulsions was sulfonic acid. The volume fractions of the mixture prepared were 33.3% for acid and 66.7% for crude oil.

Harris (1961) reported the use of emulsified acetic acid in well completion and stimulation applications. Davis et al. (1965) used emulsified acid to test the effectiveness of their spearhead film technique. The emulsified acid was composed of 90 percent by volume of 15 wt% HCl and 10 vol% kerosene.

Emulsified acid can be used in either acid fracturing or matrix acidizing. Matrix treatments (Hendrickson et al. 1965; Schechter and Gidley 1969) are performed at pressures below that required to produce hydraulic fracturing and have as their main purpose the removal of formation damage in the area immediately around the wellbore. Acid fracturing treatments are performed at pressures above fracturing pressures, usually at greatly increased injection rates. These treatments are designed primarily to improve the natural flow characteristics of the well by the creation of artificial flow channels deep into the formation. In contrast to ordinary hydraulic fracturing where fracture conductivity is produced by the placement of sand or other propping agent, acid fracturing achieves conductivity by the non-uniform etching of the fracture faces.

The need to retard acid reaction rate and thus increase fracture penetration has long been recognized (Knox et al. 1964; Smith et al. 1970). One of the earliest means of acid retardation was through the addition of gelling agents to the acid. Increasing the viscosity of the acid decreases the rate of mass transfer at the fracture face. This decreases reaction rate and increases the distance which the acid can penetrate before spending. Another effective means of thickening acids is through the use of acid-oil

emulsions. Emulsified acids have the advantage of good temperature stability and the viscosity can be controlled by varying the ratio of oil to acid. In order to achieve a high degree of retardation, it is usually necessary to employ highly viscous emulsions. This leads to high friction pressures encountered during pumping. These high friction pressures reduce the pump rate and thus nullify part of the advantage of the retarded acid.

Dill (1961) indicated that both formic and acetic acids have also been employed as retarded acids in well treating. These organic acids are used either alone or in combination with hydrochloric acid. The organic acids do have one very important advantage over hydrochloric acid; they are environmentally friendly, so they can be used in treatment of water wells. They can be inhibited in the presence of chrome plating and at much higher temperatures. Good corrosion inhibition is possible with the organic acids at temperatures up to at least 400°F.

Knox et al. (1964) indicated that surfactant type retarders have also been developed to slow the reaction rate of hydrochloric acid. These retarders function on limestone in much the same way that corrosion inhibitors protect metal against acid attack.

Broaddus et al. (1968) showed that different acids, including emulsified acid, cause different etching for the fracture surface and cause different flow capacities. They showed that emulsified acids provided excellent etching and better fracture flow capacity than regular hydrochloric acid. They advised to combine acid solutions having different

degrees of retardation to get the desired fracture conductivity. The most retarded acid will be pumped first and the least retarded acid will be pumped last.

Crenshaw and Flippen (1968) discussed why the emulsified acid was needed for stimulating the Ellenburger deep, hot gas wells in the Delaware Basin. In their opinion, the acid needed to be emulsified because there was no corrosion inhibitor that could stand the high concentration HCl at high temperature during the treatment time. The main problem was the high friction, especially in the case of the high injection rates. This problem can be solved by using friction reducers. Crenshaw and Flippen (1968) mentioned another problem with using the emulsified acid is the undesirable injection of a liquid hydrocarbon to a gas reservoir (in this special case).

Nierode and Williams (1971) determined a kinetic model for the reaction of hydrochloric acid with limestone. The reaction order and rate constant for this model were calculated from experiments where acid reacted with a single calcium carbonate plate. Experiments were performed so that acid flow past the plate and mass transfer rate to the rock surface could be calculated theoretically. Nierode and Williams (1971) showed that the combination of this model with existing theory allowed prediction of acid reaction during acid fracturing operations. Also, Nierode and Williams (1971) presented a model for acid reaction in wormholes created during matrix acidization treatments.

Nierode and Williams (1971) and Lund et al. (1975) found that the reaction rate of HCI acid with calcite is very fast. In conventional stimulation when 15 wt% HCI is used at low flow rates, the acid reacts with carbonate rocks and causes a face dissolution

or surface wash-out (Hoefner et al. 1987). Crowe and Miller (1974) and Bergstrom and Miller (1975) recommended using acid-in diesel emulsions as a way to overcome this problem.

Crowe and Miller (1974) introduced a highly retarded acid emulsion that has proven extremely effective in the stimulation of hot limestone and dolomite formations. They showed that the level of reaction rate retardation achieved with this acid is much greater than previously possible and is obtained through use of a unique surfactant system which both emulsifies the acid and forms a chemical barrier on the surface of the rock. Acid reaction rate studies performed in the laboratory under both static and flowing conditions demonstrated its high level of retardation. Crowe and Miller (1974) concluded that this emulsion has a viscosity of only 30 cp., thus greatly reducing pumping pressure and allowing increased injection rate. These results indicated improvements in acid pumpability and acid penetration.

Hoefner et al. (1987) developed a new type of retarded acid-in-oil micro-emulsion system to increase the efficiency of matrix treatments in carbonates. The microemulsion is of low viscosity but can exhibit acid diffusion rates two orders of magnitude lower than aqueous HC1. Decreased acid diffusion delays spending and allows live acid to penetrate the rock matrix more uniformly and to greater distances. Hoefner et al. (1987) performed some corefloods, where the results showed that the microemulsion can stimulate cores in fewer PV's and under conditions of low injection rates where aqueous HCl fails completely. The microemulsion could also conceivably

increase acid penetration along any natural fractures and fissures that may be present, thus increasing acidizing efficiency in this type of treatment.

Hoefner and Fogler (1985), Daccord et al. (1987), and Peters and Saxon (1989) stated that the role of diesel is to act as a diffusion barrier between the acid and the rock. Thus, the reaction rate of the acid with carbonate rocks becomes slower. According to this result, Williams and Nierode (1972), Hoefner et al. (1987), Guidry et al. (1989) and Buijse (2000) concluded that the reduction of the reaction rate of the acid with the rock gives the acid the ability to penetrate deeper into the formation by creating wormholes (i.e. channels with high permeability) and enhances well productivity.

Peters and Saxon (1989) introduced a second internal phase (nitrogen) that results in a further delay in the acid's ability to contact the formation. Their preliminary laboratory investigation indicated the technical and practical feasibilities of this tri-phase system. Peters and Saxon (1989) indicated some advantages of this tri-phase system over the conventional emulsified acids. First, the total volume of the system is increased (by approximately 30% in the system used to date), so the dissolving power of the acid is expanded into a greater volume. Second, the gaseous portion of the emulsion's inner phase, occupying approximately 32% of that phase, competes with the acid portion for release from the interfacial tension network that maintains stability in the system. Third, the compressibility of the gaseous phase gives it a clear advantage in the competition (with the acid droplets) for escape from the emulsion.

The permeability of the near-wellbore area containing the wormholes is usually several orders of magnitude larger than the original permeability of the rock and skin

values of -2 to -4 after an acid treatment are possible (Snow and Brownlee 1989, Sollman et al. 1990, Cannan et al. 1992 and Gilchrist and Lietard 1994)

Proper acid placement and fluid diversion is becoming increasingly important especially in heterogeneous formations in which the permeability contrast is large, injected fluids have the tendency to enter the sections that have the highest permeability and/or lowest skin. One method to improve zonal coverage is to use fluid systems with a viscosity significantly higher than the viscosity of the reservoir fluid (Lietard et al. 1997; Tambini et al. 1992). Acid-in-oil emulsions can have viscosities in the wellbore of 50 cp. or more and they improve zonal coverage considerably, compared to plain acid.

de Rozieres et al. (1994) measured diffusion coefficients for straight emulsified and gelled acids using both a diaphragm diffusion cell and a rotating disk apparatus. For emulsified acid, de Rozieres et al. (1994) found that the major observation is that values for the effective diffusion coefficient are 10 to 100 times smaller than for a gelled acid under the same conditions of temperature and acid concentration. It is known that emulsified acids retard the acid reaction. They demonstrated that the retardation is due to the reduction of the transfer of the acid to the surface. Also, when gels or emulsions are to be used, it is believed that values obtained with the rotating disk are more appropriate for use in acid fracturing models than those obtained in a diffusion cell.

Al-Anazi et al. (1998) evaluated the acid-in-diesel emulsion for field application. Experimental tests included rheology, thermal stability, compatibility, reactivity with reservoir rocks, and coreflood experiments. The experimental results indicated that the acid-in-diesel emulsion was a viscous and non-Newtonian fluid. The thermal stability of

the acid decreased as temperature was increased. The stability of emulsified acid also decreased in the presence of reservoir rock. The emulsified acid was found to be compatible with native crude oil and acid additives, except mutual solvents and demulsifiers. The reactivity of the emulsified acid with reservoir rock was slower than that of the 15 wt% HCl by a factor of 45 at 24°C. The reaction rate of the emulsified acid increased as temperature was increased. Al-Anazi et al. (1998) concluded that coreflood results showed that the emulsified acid formed deep wormholes in tight carbonate cores (< 50 md). At the same acid volume and flow rate, the emulsified acid penetrated deeper into the core compared to the regular acid which caused face dissolution. Permeability ratio (final/initial) of reservoir cores exponentially increased with the acid injection rate. The size and number of the wormholes depended on the acid injection rate.

Buijse and van Domelen (2000) discussed the use of emulsified acid as a stimulation fluid for matrix treatment in heterogeneous carbonate formations. Emulsified acid is especially effective when the injection rate is low, such as in low permeability formations or damaged formations. In these cases, plain HCI acid will spend on the formation face and will not create wormholes that penetrate deep into the formation. At comparable injection rates, emulsified acid is capable of forming deeply penetrating wormholes and efficiently stimulates the formation. The effects of the injection rate, viscosity and acid/oil volume ratio were analyzed on core samples. Rheological properties and temperature stability (up to 250°F) of the emulsion systems were analyzed. Buijse and van Domelen (2000) concluded the viscosity of the system will improve wellbore coverage and will divert fluid to the low permeability and/or damaged

sections of the well. The low diffusivity of emulsified acid provides for efficient wormholing at low injection rates. The wormholes are narrow but penetrate deep into the formation. Emulsified acid systems can be formulated in such a way that the emulsion breaks when the acid spends. In this way, excessively high treating pressures, caused by flow of high viscosity emulsions in the formation, can be avoided.

Navarrete et al. (1998a) evaluated two acid systems using laboratory fracture conductivity experiments and acid fracture simulations, the acid systems included neat 28 wt% HCl and an oil external emulsion that consisted of 30% by volume of diesel and 70% by volume of 28 wt% HCl. They found that emulsified 28 wt% HC1 is 8.5 times more retarded than the equivalent straight acid at 130°F. Emulsified acid provides a more efficient use of the acid capacity, allowing for longer fracture length without sacrificing fracture conductivity. Emulsified acids are a good way to maximize an etched half-length when treatments are pumped down large tubulars.

Navarrete et al. (1998b) presented a new emulsified acid system that is stable up to 350°F, highly retarded and significantly more viscous than straight acid. They presented laboratory data comparing emulsified acid with straight acid at temperatures ranging up to 350°F, including rheology and acid conductivity. They concluded that the new high-temperature emulsified acid system provides adequate stability in the temperature range of 250 to 350°F. Emulsified acid produces higher conductivities than straight acid at high closure stresses, in spite of larger etched widths, providing a more efficient use of the acid. The new high-temperature emulsified acid system is 14 to 19 times more retarded than straight acid at temperatures between 250 and 350°F in

fracturing applications and 6.6 times in matrix applications. Field case histories showed that emulsified acid improved production two to four times in the Smackover dolomite formation.

Nasr-El-Din et al. (2000) mentioned that acid-in-diesel emulsion has several advantages. Besides its slow reaction rate with the rock, it has a relatively high viscosity. As a result, it has better sweep efficiency that will improve acid distribution in heterogeneous reservoirs (Buijse and van Domelen 2000). Also, the live acid does not come in contact with the well tubulars; therefore, there is minimum corrosion to well casing and tubing. In addition, the concentration of iron in the live acid reaching the formation will be low (Al-Anazi et al. 1998). One of the main concerns is the presence of iron in the acid which may cause iron precipitation once the acid is spent (Taylor et al. 1999; Taylor and Nasr-El-Din 1999; Nasr-El-Din et al. 2000)

Nasr-El-Din et al. (2000) indicated that two wastewater disposal wells in a carbonate field in Saudi Arabia suffered loss of injectivity due to severe formation damage. Laboratory tests conducted on reservoir cores indicated that regular 15 wt% HCl did not form deep wormholes and caused surface wash-out only. They conducted a thorough experimental study to evaluate using acid-in-diesel emulsions to stimulate these wells which had several tight zones. The emulsified acid consisted of 70 vol% of 15 wt% HCl, 30 vol% diesel and an emulsifier (a cationic surfactant). Experimental results indicated that the acid-in-diesel emulsion behaved as a shear-thinning fluid. The stability of the acid was found to be a function of emulsifier concentration. The reaction rate of the emulsified acid with reservoir rocks depended also on emulsifier

concentration at the reservoir temperature (55°C). Very low reaction rates were obtained at emulsifier concentrations greater than 20 gals/1000 gals of acid. These results indicated that longer soaking times would be needed to stimulate disposal wells to ensure complete acid spending. Nasr-El-Din et al. (2000) indicated that the emulsified acid formed deep wormholes in tight carbonate cores (< 100 md), where the core permeability increased after the treatment. Permeability ratio (final/initial) of reservoir cores exponentially increased with the acid injection rate. The size and number of the wormholes depended on the acid volume, injection rate and initial core permeability. Field application of emulsified acid indicated that both wells responded favorably to the treatment. The injectivity of both wells has significantly increased after the treatment. Also, emulsified acid reduced corrosion of well tubing and casing compared to that of a regular acid.

Bazin and Abdulahad (1999) experimentally investigated some of the properties of emulsified acid systems. The systems used in their study were mixtures of acid, diesel oil, surfactant and a co-surfactant. Model systems made of anionic and nonionic surfactants were compared to the properties of a commercial emulsified acid. Experimental results were focused on the effect of the acid to oil volume ratio, the acid concentration and the surfactant nature. They analyzed rheological properties and temperature stability of the emulsion systems. Results of coreflood tests in limestone samples are presented which compare the behavior of emulsified acids to the behavior of plain HCl acid. Bazin and Abdulahad (1999) concluded that increasing the diesel volume increases emulsion stability but also viscosity. They indicated that systems with 50/50

diesel/acid ratio have acceptable properties. Also, increasing the acid concentration provides higher propagation rates and increasing the acid volume into the emulsion formulation does not decrease the acid breakthrough time significantly. At low flow rate, acid-in-diesel emulsions provide deeper wormhole penetration with lower injected volumes compared to plain acid.

Quantifying diffusivity is a key step for a successful acid fracturing design. Conway et al. (1999) measured the diffusion coefficients of straight acids, gelled acids, and emulsified hydrochloric acids using both the diaphragm cell and the rotating disk device. The results from the two methods show good agreement when comparing the acid diffusion coefficient from diaphragm cell experiments where acid is diffused against spent acid to that obtained from the rotating disk. Rotating disk data can be used to normalize the predicted diffusion coefficients to a specific reservoir. A correlation was developed to calculate diffusivity of HCl as a function of temperature, acid strength, and rock type.

Mohamed et al. (1999) studied acid stimulation of power water injectors and saltwater disposal wells. Three single systems were examined by conducting coreflood experiments using reservoir cores. The temperature was 140-150°F and the overburden pressure was 2000 psi. The results indicated that regular 15 wt% HCl caused surface washout and no deep wormholes were formed when this acid was injected into the cores at low flow rates. Emulsified acid, on the other hand, created deep wormholes that extended to the whole length of core plugs (2 inches). The size and number of wormholes were found to depend on the injection flow. Permeability enhancement due

to acid injection (1 pore volume) increased with injection flow rate. They recommended injecting this acid at the highest possible injection rate such that the injection pressure is below the fracture pressure of the formation.

There are a number of acid formulations that will generate deeply penetrating wormholes in carbonate formations. Two of the most widely used are diesel emulsified acid (DEA) and self-diverting polymer/HCl (in-situ gelled acid, or GA) (Lynn and Nasr-El-Din 2001). The acid volumes required for propagation of the wormholes, as well as the characteristics of the wormholes are significantly different in each of these formulations. Lynn and Nasr-El-Din (2001) evaluated two different service company implementations of GA, and one in-house developed DEA formulation for stimulation of a high temperature (250°F/121°C), low permeability Saudi Arabian gas and gas condensate producing carbonate. They compared the reaction characteristics of DEA to GA formulations using reservoir condition corefloods. The characteristics of the acids that were compared included wormhole propagation rates, volumes of carbonate consumed by the acids, wormhole geometric characteristics, and pressure response during injection. Since the acid formulations called for 28 percent HCl acid concentrations, high temperature stability and corrosion control chemicals of the packages were evaluated. From the coreflood study, they found that the GA formulations enhanced the permeability of core samples significantly more than the emulsified acid. The DEA was the more stable of the acid formulations at 250°F. Both of the GA formulations showed some degree of separation of the corrosion control components at reservoir temperature. Also, The GA was found to require larger volumes of acid to

achieve an equivalent penetration distance versus the DEA, and logically, the GA dissolved a larger volume of rock per volume of acid injected. The DEA has a higher rate of wormhole propagation and the DEA leaves no residual material in the generated wormholes. The GA left a residuum of polymeric material in the wormholes even after high rate injection condensate. The DEA was injected into tight cores without encountering any problems. The acid propagated through the core plug samples in almost straight lines. The acid propagation rate in the core plugs was very fast. The acid enhanced core permeability by a factor that depended on acid injection rate. The acid created clean wormhole without any residuals. However, residual diesel was noted in some areas of the cores.

Nasr-El-Din et al. (2001) described the optimization of an emulsified acid system to stimulate deep, sour gas reservoirs. The high temperatures encountered in deep wells have a tendency to destabilize emulsified acid and, as a result, this acid may lose its retardation effect. Extensive experimental studies were performed to evaluate the influence of temperature on emulsion stability and retardation effect. In addition, the effects of various acid additives on emulsion stability were examined in detail. The acid (28 wt% HCl) to diesel volume ratio was 70 to 30. Experimental results indicated that the emulsified acid is stable for more than two days at ambient conditions and more than four hours at 250°F. The retardation factor of the emulsified acid was found to be greater than ten times that of the conventional acid systems. Coreflood tests using tight carbonate plugs (dolomite cores) indicated that the emulsified acid could be injected into tight cores (permeability less than 10 md) without encountering any injectivity problems.

The acid created deep wormholes, which significantly increased the permeability of the treated cores. Nasr-El-Din et al. (2001) concluded that emulsified acid can be effectively used to stimulate deep sour, gas wells. Besides that, emulsified acids require minimum amounts of additives, protect well tubulars (even special types), and are a cost effective option to stimulate deep wells.

Bartko et al. (2003) studied the use of 28 wt% regular HCl, emulsified acid, and in-situ gelled acid in fracturing the Khuff formation which is heterogeneous in nature. Based on production results and the large database of acid fracture treatments (more than 70 wells); Bartko et al. (2003) concluded that there is a correlation between the acid type used and the lithology of the formation.

Typically, changing the acid volumes, placement techniques, or pumping rates, has optimized acid fracture treatments by creating longer and wider fractures. With this large database of acid fracture treatments, acid rock interactions were investigated to determine the relationship between lithology and acid type. Bartko et al. (2003) indicated that emulsified acid has become the preferred fluid of choice for the Khuff stimulation program, especially in low permeability intervals that are calcite dominated. When investigating the optimum volume of emulsified acid; the optimum volume for emulsified acid is less than that of the in-situ gelled acid. They found that the optimum volume is between 650 to 1,000 gal/ft. of perforation. The performance of the emulsified acid is better than the in-situ gelled acid.

Taylor et al. (2006) measured acid reaction rates in carbonate reservoir rocks. It was generally assumed that limestone reservoir rocks will react much more rapidly with

acid than dolomite reservoir rocks. Their work was the first to show that this assumption may be false in some cases, and this refers to the mineral impurities commonly found in these rocks. Trace amounts of clay impurities in limestone were found to reduce the acid dissolution rate by nearly an order of magnitude, to make the acid reactivity of these rocks similar to dolomite rocks. A rotating disk instrument was used to measure dissolution rates of reservoir rock from a deep, dolomitic gas reservoir in Saudi Arabia (275°F, and 7,500 psi). More than 60 experiments were made at temperatures of 23 and 85°C and HCl concentrations of 1.0 M (3.6 wt%). Eight distinctly different rock types that varied in composition from 0 to 100% dolomite were used. The mineralogy of each rock disk was examined before and after each rotating disk experiment with an Environmental Scanning Electron Microscope (ESEM) using secondary and backscattered electron imaging and energy dispersive X-ray (EDS) spectroscopy. Acid reactivity was correlated with the detailed mineralogy of the reservoir rock. It was also shown that bulk anhydrite in the rock samples was converted to anhydrite fines by the acid which is a potential source of formation damage.

Laws et al. (2005) tried to develop a strategy to optimize acid stimulation of the Harweel Cluster wells. Initial treatments involved bull heading 15 wt% gelled HCl. The latter treatments involved spotting 15 wt% HCl and emulsified acid with coiled tubing using a Dynamic Diversion Technique. In addition, they found that the emulsified acid system has shown superior diversion characteristics compared to gelled 15 wt% HCl. The emulsified acid results in a higher negative skin and better inflow distribution compared to the gelled acid. In over-pressured wells that are suitable for matrix

stimulation, they recommended using a combination of 15 wt% HCl and emulsified acid in sequential stages.

Kasza et al. (2006) indicated that a positive results of emulsified acidizing fluid were achieved during core flow tests. Six acidizing treatments have been performed using emulsified acid (Kasza et al. 2006). Kasza et al. observed an increase in oil and gas production and a decrease in pressure drop around the wellbore after these treatments. Based on these results, the treatment of other wells by emulsified acid was applied in other oil fields located in the same carbonate formation.

Nasr-El-Din et al. (2006a) studied the role the formation softening plays in production response. Fracture acidizing of carbonates has yielded increases in production in many areas of the world, but depending upon rock strength and reservoir closure pressure, this response may be lower than expected. Also, as a result of rock strength and closure pressure, production may decline at a higher rate than after a proppant fracture treatment. Nasr-El-Din et al. (2006a) presented laboratory results that describe the effect on strength reduction of limestone and dolomite formation samples after exposure to various acid systems. Formation samples were dry, saturated with potassium chloride water or saturated with synthetic oil prior to testing. Samples were exposed to neat, emulsified, gelled and crosslinked 15 wt% hydrochloric acids and each exhibited a distinct effect on rock strength reduction. Nasr-El-Din et al. (2006a) concluded that acid system choice makes a difference in the degree of rock softening of carbonates. Also, softening effects are greater on limestone than on dolomite and production responses from emulsified acid treatments are the best.

Al-Harbi et al. (2006) evaluated the acid treatment results for water injection wells in Saudi Arabia. Increasing the volume of emulsified acid in acid treatment stages will lead to improve wells injectivity. Therefore, there is a strong relationship between the emulsified acid volumes with the injectivity index for the selected wells.

Kalfayan (2007) indicated that emulsified acid systems offer perhaps the greatest chemical retardation. Their disadvantage has always been high friction pressure generation during injection; thus a well depth limitation. Improvements have been made in this regard in recent years, expanding the potential of this generally effective acid system to deeper completions.

For stimulation purposes, the most important properties of emulsified acid are reactivity, stability, and viscosity (Al-Mutairi et al. 2008a). The size distribution of the droplets of the emulsion affects these properties. Al-Mutairi et al (2008a) correlated the droplet size of the dispersed phase (acid) to the viscosity and stability of emulsified acids. Measurements of the droplet size were acquired with laser-diffraction techniques and analyzed by use of an advanced image-processing system. The apparent viscosity was measured with a Brookfield PVS rheometer at various temperatures. The stability of the emulsified acid was monitored by use of an HTHP see-through cell. Steady shear viscosity was measured for emulsions with droplet sizes ranging in diameter from 1 to 20 μm. The viscosity covered a shear rate range from 10 to 750 s^{-1} and a temperature ranging from 25 to 80°C. All measurements were regenerated for emulsifier concentrations of 1, 5, and 10 gpt. It was noted that finer emulsions had higher

viscosities. Likewise, similar measurements were performed with varying acid volume fractions.

Al-Mutairi et al. (2008a) noted that the most stable emulsion was at an acid volume fraction of nearly 0.7. Other volume fractions were stable for a few hours before diesel was expelled as a separate layer above the emulsion. Eventually, the remaining emulsion stabilized at an acid volume fraction of 0.7. Al-Mutairi et al. (2008a) concluded that fine emulsions were more stable than coarse ones. Other volume fractions discharged more diesel as the acid volume fraction was decreased. The viscosity of emulsified acid decreased with the increase in droplet size of the dispersed phase means that fine emulsions had higher viscosity than coarse ones. Also, the viscosity of emulsified acids was found to increase with the acid volume fraction at high emulsifier concentrations (10 gpt). However, at low concentrations (1 gpt), it increased as the acid volume fraction was increased from 0.4 to 0.6.

Al- Mutairi et al. (2008b) studied the fracture conductivity after acidizing it with the emulsified acids. The objective of this work was to study the effect of droplet size, acid volume fraction and emulsifier concentration on the fracture conductivity. They used Indiana limestone rocks acidized with different formulations of emulsified acid. A 15 wt% HC1 in diesel emulsion with 0.5, 0.6 and 0.7 acid volume fractions and with emulsifier concentrations of 1, 5 and 10 gpt were used in the tests. The tests were run at 200°F and 1,000 psi. The standard fracture conductivity measurements were done after each experiment and the etched fracture surfaces were characterized using a laser profilometer. Al-Mutairi et al. (2008b) showed that channeling and large-scale features

on the etched surfaces were the dominant factors for fracture conductivity for the course emulsions. Higher acid volume fractions weakened the rock and caused the fracture to loss its conductivity faster at high closure pressures. When emulsions with smaller droplet sizes were used (high emulsifier concentration), the acid penetrated deeper inside the rock and caused small-scale features on the surface rather than channeling. This feature formed a mesh-like surface that was conductive even at high closure pressures.

The emulsified acid should be stable at ambient conditions for a long period of time and should be stable also at downhole conditions for a period of time long enough to pump the acid without encountering operational problems (Nasr-El-Din et al. 2008a). Application of emulsified acid at higher temperatures requires 20 to 30 gpt of a cationic emulsifier. Nasr-El-Din et al. (2008a) conducted a thorough laboratory study to select an emulsifier that can be used at lower loadings, and meet the stability criteria that are needed to stimulate oil and gas wells. Laboratory work included measuring stability, apparent viscosity, and droplet size distribution as a function of emulsifier type and concentration, temperature, and additive type and concentration. A new emulsified acid was developed and used to acid fracture over ten wells in a deep gas reservoir in Saudi Arabia. The new emulsified acid used a significantly lower amount (4 to 6 gpt) of the emulsifier, and it produced a stable emulsion over a wide range of temperatures (from 75 to 275°F). The droplet size of this emulsified acid was much smaller and the apparent viscosity of the acid-in-diesel emulsion was higher. Field data showed greater reduction in the time needed to prepare the new emulsion in the field. The performance of wells

stimulated with the new emulsifier was significantly better than those stimulated with the old emulsifier.

Unlike other acid systems, such as gelled and viscoelastic surfactant-based (VES) acids, where the mobility of hydrogen ion controls the overall rate of the reaction, emulsified acid/calcite reaction involves the transport of acid droplets in the diesel phase to the rock surface, breaking of acid droplets, and then the actual reaction on the surface (Al-Mutairi et al. (2009a). Al-Mutairi et al (2009a) examined the effect of the acid droplet size on the reaction rate of emulsified acid with calcite. The acid was 15 wt% HCl emulsified in diesel with 70:30 acid/diesel volume ratio. The emulsifier concentration varied from 1 to 10 gpt. All emulsions were characterized by measuring the droplet size distribution, viscosity, and thermal stability. Diffusivities were measured using the rotating disk device. The experiments were carried out at 25, 50, and 85°C, under 1,000 psi pressure, and disk rotational speeds from 100 to 1,000 rev/min. They collected samples of the reacting acid and these samples were analyzed to measure calcium concentration in the reactor. The effect of the acid droplet size on the overall reaction rate was significant. Al-Mutairi et al. (2009a) concluded that the diffusion rate of acid droplets to the surface of the disk decreased with increasing emulsifier concentration because of the emulsion's high viscosity and the smaller droplet size. The effective diffusion coefficient of emulsified acid was found to increase linearly with the average droplet size of emulsified acid. The effect of temperature on the diffusion coefficient did not follow the Arrhenius law. It is suggested that the droplet size of emulsified acids can be adjusted to produce the desired diffusion rate coefficients for

acid fracturing treatments. They suggested that droplet size can be adjusted to produce the desired diffusion coefficients for acid fracturing treatments.

Al-Mutairi et al. (2009b) provided a detailed description of the droplet size distribution of emulsified acids. The core of their study was to introduce methods to measure and represent these data. They showed that coarse and fine emulsions can be produced by selecting the mode of mixing and speed of shearing; simple mixing and low shearing produce coarse emulsions while atomizing and high shearing produce fine emulsions. It is also demonstrated that the droplet size and specific surface area are affected by emulsifier concentration and acid volume fraction; the average droplet size decreases with increasing emulsifier concentration. Also the acid volume fraction has an effect; as the volume fraction increases, the diameter of the acid droplet also increases. The specific surface area of the droplets increases with increasing emulsifier concentration and decreases with increasing acid volume fraction. The change of droplet size has a practical impact on the stability, rheology and reactivity of emulsified acid.

Using emulsified acid to treat wells with asphaltene deposition will require removing asphaltene first using a suitable aromatic-based solvent, and then using a matrix acid treatment (Abdel Fatah and Nasr-El-Din 2010). Abdel Fatah and Nasr-El-Din (2010) used emulsified acid in xylene. Xylene was the external phase, and was used to dissolve asphaltenes. Then the acid, present as the dispersed phase dissolved the carbonate rock, thus enhancing well productivity. Extensive lab work was performed to ensure the stability of acid-in-xylene emulsion and measure its apparent viscosity. Acid concentration was 15 wt% HC1, the acid volume fraction was 0.7 and the balance was

xylene. All tests were conducted at room temperature and 160°F. The stability and apparent viscosity of emulsified acids were found to be a function of the type of hydrocarbon phase used to prepare emulsified acid. Emulsified acids prepared with xylene had a lower apparent viscosity and were stable for relatively shorter periods of time. This acid was used to treat four wells and there were no operational problems and the four wells responded to the new treatment without increasing water-cut except in one well.

While experimental studies have shown acid type significantly influences resulting fracture conductivity, there has been limited work on how fluid properties relate to etched fracture faces and hence the resulting conductivity. Pournik et al. (2010) studied the influence of acid-fracture fluid properties on fracture conductivity. A series of acid fracture conductivity tests were conducted using four commonly used acid fracturing fluids; gelled, in-situ gelled, emulsified, and surfactant-based acid. Detailed rheological properties were measured in order to explain trends noted with conductivity data. Acid system influences the degree of etching and the etching pattern due to differences in chemical and physical properties of acid systems. Pournik et al. (2010) concluded that viscoelastic acid generated the greatest degree of etching, the best etching pattern and the highest conductivity at low closure stress, while emulsified acid resulted in the largest retained conductivity at higher loads.

Xiong et al. (2010) used a selective emulsified acid system to stimulate heterogeneous reservoirs. In conventional acid treatment, acid fluid always flows into the pore path with high water saturation first, and broadens the pore path filled with

water. However, it can't stimulate the pore path filled with oil as well as that filled with water. This selective emulsified acid system viscosity will increase when it meets water and decrease when it meets oil in the formation. They used fluoroboric acid beside the hydrochloric acid as the acid internal phase. Fluoroboric acid offers some advantages such as no damaging products, the reaction products will stabilize particles and clays, and it also can slow down the reaction rate between acid and rock. Xiong et al. (2010) concluded that the average permeability increment of cores saturated by oil reaches to 96.1% after being treated by this acid system, while the average increment of cores saturated by water is only 10.1%. The novel selective emulsified acid system achieved good retardation and showed protective capability to the formation.

Appicciutoli et al. (2010) developed and evaluated new solvent blends to be used with emulsified acid and injected in carbonate reservoirs which suffer an asphaltene deposition problem. The results showed improved efficiency to dissolve asphaltenes in a major oil- producing field in Western Europe, easing operations and reducing health, safety, and environmental risks to zero without compromising product efficiency. Laboratory testing proved the newly developed solvent blends were also suitable for creating acid in oil emulsions. Laboratory testing allowed the determination of the most suitable solvent emulsifier for improved emulsion stability at BHT conditions. The emulsifying agent chosen provides static emulsion stability at 70°C for more than 120 min.

The increased viscosity of the emulsion and therefore increased injection pressure during the stimulation process is viewed as beneficial to the treatment because

it assists with diversion of the fluid. This benefit in easier diversion was not sacrificed because the wells were able to return the viscous fluid from the formation when the well was placed on production.

Maier et al. (2011) studied the stimulation treatment of an oil producing field in an environmentally sensitive area in Europe. The reservoir was located in a carbonate formation so it was treated using fluids based on HCl acid. Their research focused on the use of viscosified acid systems. From the different types of viscosified acids; emulsified acid was selected to treat that reservoir. The reservoir suffered an asphaltene deposition problem, and the need to add an environmentally safe solvent to remove this asphaltene was very important. After testing a new solvent, which was a blend of different commercial solvents, it was used as the continuous phase for emulsifying the HCl. The new solvent blend was used to create good and stable emulsions. So the new acid system can be used to create deep wormholes and to remove the asphaltene deposition.

Solares et al. (2011) discussed a case study for a gas well in a carbonate reservoir in Saudi Arabia. An effective diversion technique with polymer and new optimized acid formulations was successfully performed. The treatment included a delayed borate crosslinked fluid used as a pad to create and extend the hydraulic fracture, and two 26 wt% HCl acid blends of emulsified and gelled acids were used to penetrate and efficiently etch the rock surface. The implementation of this acid fracturing treatment resulted in a net rate gain of 1,450 % over its pre-stimulation rate.

Madyanova et al. (2012) described the application of a high temperature, highly retarded emulsified acid system that slows the reaction times by a factor of 5 to 15

compared to conventional HCl systems. The emulsified acid system combined with a self-diverting viscoelastic surfactant-based acid was able to achieve complete stimulation of a 197 ft. long perforated interval without the need of coiled tubing. The post-stimulation skin value was estimated to be -3.3.

Sabhapondit et al. (2012) studied the effect of the corrosion inhibitor on the efficiency of the acid treatment. They showed the common misconception that a stable emulsified acid can ensure a successful acid job without (or with a very little amount of) corrosion inhibitor. They concluded that using a suitable corrosion inhibitor in an appropriate concentration is as equally important as emulsion stability for successful completion of an emulsified acid job without encountering severe corrosion problems.

Al-Mutairi et al. (2012) discussed the effect of acid and its wormholing characteristic on tar and on carbonate rock that was saturated with crudes that have varying °API gravities. Experiments included acid flooding of core plugs that were saturated with different °API gravities. The extreme case included flooding the acid through tar saturated plugs. The tests involved regular hydrochloric acid and emulsified acids. Al-Mutairi et al. (2012) showed that regular and emulsified acids produced comparable wormhole penetration in tar. Tar formations were difficult to exhibit face dissolution even at extremely low injection rates. The benefit from emulsified acid was reduced when higher °API oil saturated the rock.

Dnistryansky et al. (2012) suggested some technologies to account for all challenges in stimulation of the Orenburg Oil, Gas and Condensate field (OOGCF).

They mentioned that highly retarded emulsified acid helped to create wormholes while treating long intervals with low pumping rate through coiled tubing (CT).

1.4 Objective

Emulsified acids have been extensively used in the oil industry for a long time. Most of the available research and publications discussed mainly its application in the field and a number of studies discussed the rheology of emulsified acid, especially viscosity, and relate the rheological behavior to the droplet size distribution of the dispersed phase. Some of the researchers studied the reactivity of emulsified acid with carbonate rocks. Some of these studies discussed the emulsified acid with sufficient details of its preparation, but others did not. Besides its chemical composition, and method of preparation of emulsified acid, there are other factors that will affect the rheology of the emulsified acid.

A new emulsifier was developed and used to prepare emulsified acids that can be used in stimulating deep wells drilled in carbonate reservoirs. In the present paper, the rheology of the new acid is compared to the rheology of another system formulated by a commercial emulsifier that has been used extensively in the field. All emulsified acid systems were formulated at 0.7 acid volume fraction, and the final acid concentration varied from 5 to 28 wt% HCl. The rheology measurements were conducted at temperatures up to 300°F for emulsifier concentration ranges from 0.5 to 2.0 vol% (5 to 20 gpt). The reaction between emulsified acid and both calcite and dolomite rocks was studied using a rotating disk apparatus at 230°F and rotation speeds up to 1,500 rpm. A coreflood study was conducted in order to study the efficiency of the new emulsified

acid to create wormholes and increase the efficiency of the treatment. The coreflood study was performed at 300°F and at different injection rates using both outcrop rocks (dolomite and limestone) and reservoir core samples. The effect of the presence of crude oil in the reservoir on the performance of emulsified acids was also studied.

1.5 Plan for the Work

The experimental work is conducted in the following sequence. First, a thorough understanding of the rheological behavior, especially the change of the emulsified acid viscosity with temperature, shear rate, and emulsifier concentration. The effect of changing the type and the concentration of the emulsifier, the acid volume fraction, the temperature and the type of dispersing phase on the viscosity and elasticity of the emulsified acid was studied first. Measurements of the droplet size distribution was performed in order to better characterize the emulsified acid and to better explain its rheological behavior.

After measuring the electrical conductivity of the acid and checking its quality, the apparent viscosity of the emulsified acid was measured using an HPHT Grace M5600 rheometer. Then, these measurements were correlated to emulsifier concentration and droplet size of the acid.

The next step in the study plan was to measure the diffusion and reaction rates of emulsified acid systems using the rotating disk apparatus. Both calcite and dolomite core samples were utilized in this part. The next step was to test the effect of different emulsified acid systems and different injection conditions on the behavior of emulsified acid with real rock through the use of a coreflood system, and using both outcrop and

reservoir carbonate cores (limestone and dolomite). The final step was the evaluation of a new technique for emulsifying chelating agents and testing these emulsions for high temperature stimulation treatments at a temperature above 350°F.

Every stage is discussed in a separate section. Each section is designed to stand for itself. Therefore, each section starts with an introduction giving background about the subject and reviewing the previous work done on the subject. Then, the experimental part describes the method of preparing the emulsion and the equipment and procedures for conducting the experiments. The results are then presented and discussed. Finally, the main conclusions are outlined.

2. VISCOSITY OF THE NEW EMULSIFIED ACID SYSTEMS

2.1 Introduction

Emulsions are mixtures of two immiscible liquids with a non-vanishing interfacial tension at their interface (Bibette and Leal-Calderon 1996). The internal phase is dispersed in the other in the form of small droplets, with diameters greater than 0.1 μm (Clayton 1923; Sherman 1968; Becher 1985). By contrast to micro-emulsion phases, emulsions are not thermodynamic states. Instead, emulsions are metastable dispersions; external shear energy is used to rupture large droplets into smaller ones during emulsification (Mason 1999). The interface decreases both by ripening and by coalescence. The use of surfactants can slow down both processes (Bibette and Leal-Calderon 1996).

Emulsions exhibit a highly varied rheological behavior that is useful and fascinating (Tadros 1994; Barnes 1994; Mason et al. 1996a; Lequeux 1998). The relationship between stress and strain depends on the emulsion composition (volume fraction of dispersed phase), microscopic droplet structure, and interfacial interactions. For years, measurements of emulsion rheology were not quantitatively understood because the droplet size distributions had not been controlled (Princen 1985; Princen 1986a; Princen 1986b; Princen and Kiss 1987; Princen 1989). Some measurements performed (Mason et al. 1995; Mason et al. 1996a; Mason et al. 1996b; Mason et al. 1997a) indicated that polydispersity is important in emulsion rheology, while (Borwankar 1997) showed another opinion. Rheology of dilute emulsions (Beenakker 1984; Ladd 1990; Lowenberg and Hinch 1996; Mason et al. 1996b) and compressed

emulsions (Weitz and Pine 1992; Mason and Weitz 1995; Mason et al. 1997b) has been studied before.

Based on the droplet size of the acid, emulsified acid systems can be classified as micro (Hoefner and Fogler 1985) or macro-emulsion (Al-Anazi et al. 1998). Macro emulsions have larger droplet sizes, use smaller amounts of emulsifier, and are the most widely used type in the field (Al-Anazi et al. 1998; Mohamed et al. 1999; Nasr-El-Din et al. 2000; Kasza et al. 2006).

The rheology of emulsified acid is a key parameter in evaluating the performance during well stimulation treatments. Emulsified acid systems may have a high viscosity, and the emulsion may be separated and lose its advantages (Bazin and Abdulahad 1999). Therefore, it is important to check the viscosity and the stability of the emulsified acids, prior to their injection into the porous medium. Nasr-El-Din et al. (2000) measured the viscosity of emulsified acid, and they found that the apparent viscosity decreased as the shear rate was increased, which indicated that the acid-in-diesel emulsion is a non-Newtonian shear-thinning fluid. Lynn and Nasr-El-Din (2001) performed rheology and coreflood studies to compare between gelled acid and emulsified acid. They concluded that the viscosity of emulsified acid decreased with shear rate, but at temperature 250°F, emulsified acid was more stable than gelled acid. Nasr-El-Din et al. (2008a) developed an emulsified acid that used a significantly lower amount of the emulsifier (4 to 6 gpt). The emulsion was stable over a temperature range of 75 to 275°F. The droplet size of emulsions produced from this emulsifier was much smaller, resulting in a higher apparent viscosity.

Acid stability, apparent viscosity, and droplet size distribution as a function of emulsifier type and concentration, temperature, and type and concentration of additive, was measured by Al-Mutairi et al. (2008a). Al-Mutairi et al. (2008a) noted that the emulsion was stable at an acid volume fraction of 0.7, and at other volume fractions the emulsion was stable for only few hours. Stability and viscosity were higher for fine emulsions (Al-Mutairi et al. 2008a). At high emulsifier concentrations (10 gpt), the viscosity of emulsified acids was found to increase with acid volume fraction, while at low concentrations (1 gpt) it increased as the acid volume fraction was increased from 0.4 to 0.6.

Al- Mutairi et al. (2008b) studied the effects of droplet size, acid volume fraction and emulsifier concentration of emulsified acid on fracture conductivity, and it was found that emulsions with a smaller droplet size, and hence higher viscosity, penetrated deeper inside the rock and caused small-scale features on the surface rather than channeling.

A new emulsifier was used to prepare emulsified acids that can be used in stimulating deep wells drilled in carbonate reservoirs. In the present chapter, the droplet size distribution of the new emulsified acid systems will be shown. The rheology of the new emulsified acid is compared to the rheology of another system formulated by a commercial emulsifier that has been used extensively in the field. All emulsified acid systems were formulated at 0.7 acid volume fraction, and the final acid concentration was 15 wt% HCl. The effect of the HCl concentration on the viscosity of emulsified acid was studied by changing the HCl acid concentration from 5 to 28 wt%. The rheology

measurements were conducted at temperatures up to 300°F for emulsifier concentration ranges from 0.5 to 2.0 vol% (5 to 20 gpt).

2.2 Experimental Studies

2.2.1 Materials

The emulsions were prepared using diesel and an acid solution (HCl and water). The water used throughout the experiments was de-ionized water, obtained from a water purification system that has a resistivity of 18.2 MΩ.cm at room temperature. Hydrochloric acid was titrated using 0.1 N sodium hydroxide solution, and the acid concentration was found to be 36.8 wt%. Additives, such as corrosion inhibitor and emulsifier, were added to the acid solution and the diesel, respectively. Two types of emulsifier from two different companies were used to prepare the emulsified acid systems. These two emulsifiers will be denoted as A (the commercial emulsifier) and B (the new developed emulsifier). Both emulsifiers are cationic, and the new emulsifier is a blend of cationic surfactant, isopropanol, and petroleum distillate.

2.2.2 Procedures

The acid solution was prepared by mixing corrosion inhibitor, de-ionized water and HCl acid. The diesel solution was prepared by adding emulsifier to diesel oil, and mixing at a high speed (1200 rpm). Then, the acid solution was added slowly to the diesel solution and mixed at high speed (1200 rpm) for 30 min. After that, the electric conductivity of the final mixture was measured in a conductivity cell to check the quality of the final emulsion. If the electric conductivity is nearly equal to 0, then we have a good emulsified acid. In the case that there is some conductivity, extend mixing to 1 hour at

maximum possible speed, and measure conductivity again, to be sure of the quality of the prepared emulsified acid.

2.2.3 Equipment

An HPHT rheometer was used to measure the viscosity of live emulsified acids under different conditions. The wetted material is Hastelloy C-276, an acid-resistant alloy. The rheometer can perform measurements at various temperatures up to 500°F over shear rates of 0.00004 to 1,870 s^{-1}. A B5 bob was used in this work, which required a sample volume of 52 cm^3. The test was applied by varying the shear rate from 0.1 to 1000 s^{-1}.

The droplet size distribution was measured using a Zeiss Axiophot microscope. Images were analyzed using Image-J software (Abramoff et al. 2004). This microscope can measure particles as small in size as 0.03 μm. A fluorescence microscope uses the phenomena of fluorescence and phosphorescence, instead of or in addition to, reflection and absorption. A sample is illuminated with a light of a wavelength, which causes fluorescence in the sample. The light emitted by fluorescence, which is at a different, longer, wavelength than the illumination, is then detected through a microscope objective.

2.3 Results and Discussion

2.3.1 Droplet Size Distribution of Emulsified Acids

The average droplet size of the emulsified acid system was measured before (Guidry et al. 1989; Al-Anazi et al. 1998; and Al-Mutairi et al. 2009a). **Table 2-1** lists the measured average droplet size of the emulsified acid systems used in these studies.

The acid volume fraction was 0.7 and the emulsifier concentration was varied from 0.5 to 2.0 vol% (5 to 20 gpt). A small sample of each emulsified acid system was examined using the Zeiss Axiophot microscope in order to measure the droplet size distribution of acid droplets. The photomicrographs of the emulsified acids prepared using emulsifier concentrations of 0.5, 1.0, and 2.0 vol% are shown in **Figs. 2-1a to 2-1c**, respectively. As the emulsifier concentration was increased from 0.5 to 2.0 vol%, the droplet size of the emulsified acid decreased. The photomicrographs were analyzed using Image-J software, and the droplet size of emulsified acid was measured. The droplet size distributions of the three emulsified acid systems are shown in **Figs. 2-2a through 2-2c.** The droplet size distribution of emulsified acid systems formulated at 2.0 vol% emulsifier shows the classical "bell curve" shape of a normal distribution. For emulsified acids prepared using 0.5 and 1.0 vol% emulsifier, the droplet size distribution of emulsified acid is not symmetric, and the distribution is negatively skewed. The average, median, standard deviation and errors with 95% confidence limits of these distributions are presented in **Table 2-2.** The photomicrographs and droplet size measurements showed that as the emulsifier concentration increased from 0.5 vol% to 2.0 vol%, the average droplet size decreased from 8.1 to 2.8 μm, which indicates that emulsifier concentration has a great effect on the average droplet size and droplet size distribution of the produced emulsions. These results are in agreement with what was noted by Al-Mutairi et al. (2009a).

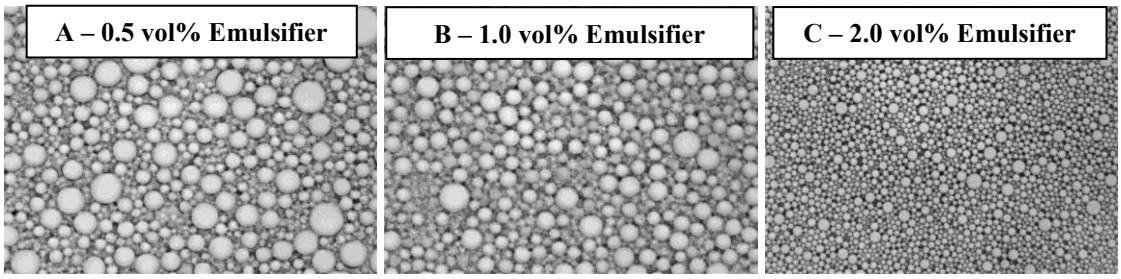

Fig. 2-1: Droplet size distributions of emulsified acid systems (40x objective: 0.0960 micrometers per pixel).

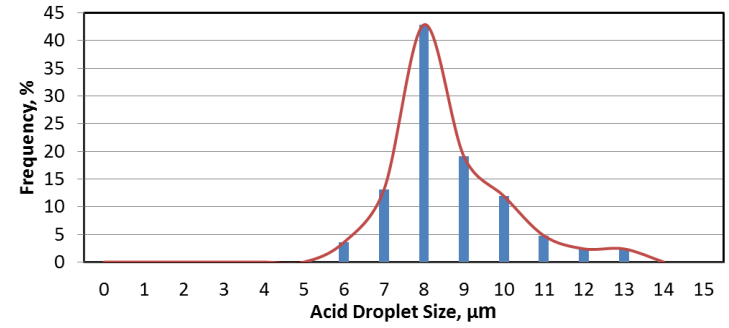

A – 0.5 vol% emulsifier concentration

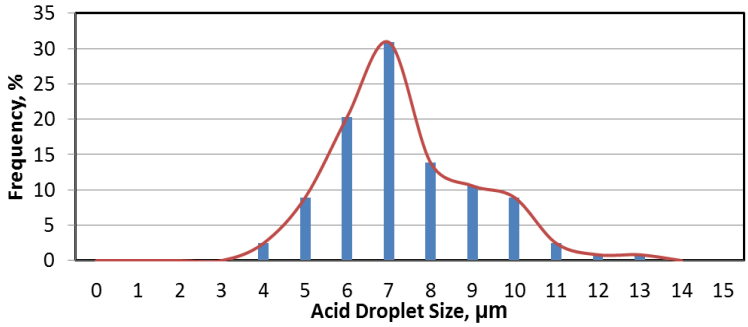

B – 1.0 vol% emulsifier concentration

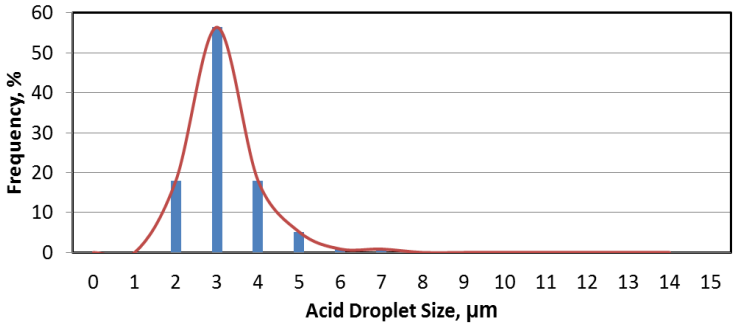

C – 2.0 vol% emulsifier concentration

Fig. 2-2: Droplet size distributions of emulsified acids

Table 2-1: Average droplet size for emulsified acid systems published by other authors.

Authors	Average Droplet Size
Guidry et al. (1989)	0.2 mm
Al-Anazi et al. (1998)	77 μm
Al-Mutairi et al. (2009a)	6 to 12.4 μm

Table 2-2: Statistical analysis of the droplet size distributions for emulsified acid systems used in the present study.

Emulsifier Concentration, vol%	Average Droplet Size, μm	Median Droplet Size, μm	Standard Deviation, μm
0.5	8.1 ± 0.28	7.9	1.3
1	6.9 ± 0.36	6.5	2.0
2	2.8 ± 0.17	2.7	0.9

2.3.2 Viscosity of Emulsified Acids

Pal et al. (1992) indicated that, in general, the viscosity of emulsions depends on shear rate, droplet size distribution, dispersed phase volume fraction, and temperature. Most concentrated emulsions are pseudo-plastic fluids (Pal et al. 1992). Some emulsions cannot be classified into one specific class, but stretch over a wide range of non-Newtonian behavior (Al-Mutairi et al. 2008a).

2.3.3 Effect of Shear Rate

The emulsified acids were prepared at 0.5, 1, and 2 vol% emulsifier concentrations. The additives were mixed so that the final acid concentration was 15 wt% HCl. All measurements were performed at room temperature (75°F). The samples were stable for at least 48 hours at room temperature.

The effect of increasing the shear rate on the apparent viscosity of emulsified acids, prepared using the new developed emulsifier (Emulsifier B), is shown in **Fig. 2-3.** **Fig. 2-3** represents a log-log plot of apparent viscosity vs. shear rate. The apparent viscosity of the emulsified acid decreased, as the shear rate increased. This data can be represented by a straight line on a log-log plot, indicating a non-Newtonian shear thinning behavior that can be fitted using a power-law model that can be represented by Eq. 2.1:

$$\mu_a = K\dot{\gamma}^{n-1} \quad \text{..... (2.1)}$$

where μ_a is the apparent viscosity, $\dot{\gamma}$ is the shear rate, K is the power-law constant and n is the power-law index. **Table 2-3** summarizes the values for K and n and the correlating coefficient for the different acid samples, prepared at 0.5, 1.0 and 2.0 vol% emulsifier. The correlating coefficient indicated a good correlation of the apparent viscosity and shear rate.

2.3.4 Effect of Emulsifier Concentration

The effect of emulsifier concentration on the apparent viscosity of emulsified acid formulated by Emulsifier "B" can be examined using **Fig. 2-4**. The apparent viscosity was plotted as a function of the emulsifier concentration at different shear rates, for emulsified acid formulated at an acid volume fraction of 0.7 and measured at room temperature (75°F). **Fig. 2-4** shows that the apparent viscosity of emulsified acids increased, with increasing the emulsifier concentration, and the same effect was noticed at all shear rates. Al-Mutairi et al. (2008a) indicated that increasing the emulsifier concentration offers more chemical to cover a larger surface area. This can be achieved

through splitting emulsion droplets into smaller ones, leading to the formation of fine emulsions. These fine emulsions with smaller droplet sizes have higher viscosities.

Table 2-3: Summary of power-law model parameters for emulsified acid formulated using Emulsifier B at 75°F.

Sample No.	Emulsifier Concentration (vol%)	Power-law Constant, K (mPa.s^n)	Power-law Index, n	Correlating Coefficient
1	0.5	443.59	0.549	0.9569
2	1	568.3	0.555	0.9689
3	2	709.68	0.535	0.9576

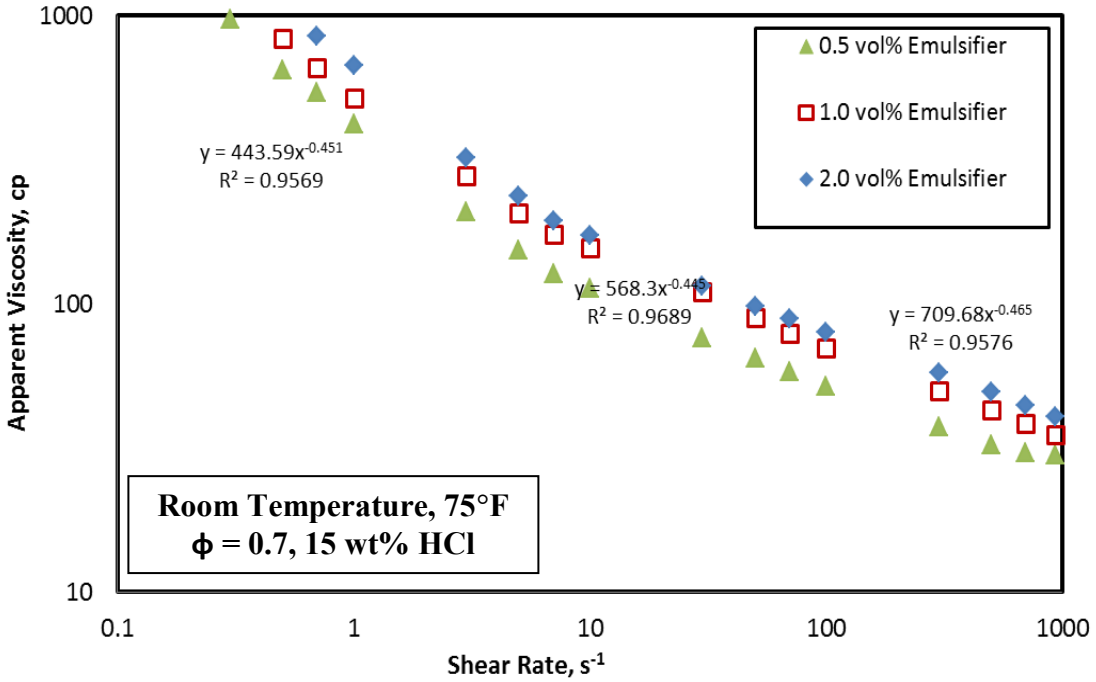

Fig. 2-3: Emulsified acid apparent viscosity vs. shear rate for different for different emulsifier concentrations.

A comparison between the rheology of emulsified acid formulated using the commercial emulsifier (Emulsifier A), and rheology of emulsified acid formulated by Emulsifier B can be represented by **Fig. 2-5**. From **Fig. 2-5**, it is apparent that, for the same emulsifier concentration, that the viscosity of emulsified acid formulated using Emulsifier B (new emulsifier) was higher than the viscosity of emulsified acid formulated using Emulsifier A (old emulsifier). This indicates that, for the same emulsifier concentration, the new emulsifier is more efficient than the commercial old emulsifier, in creating a viscous emulsified acid system.

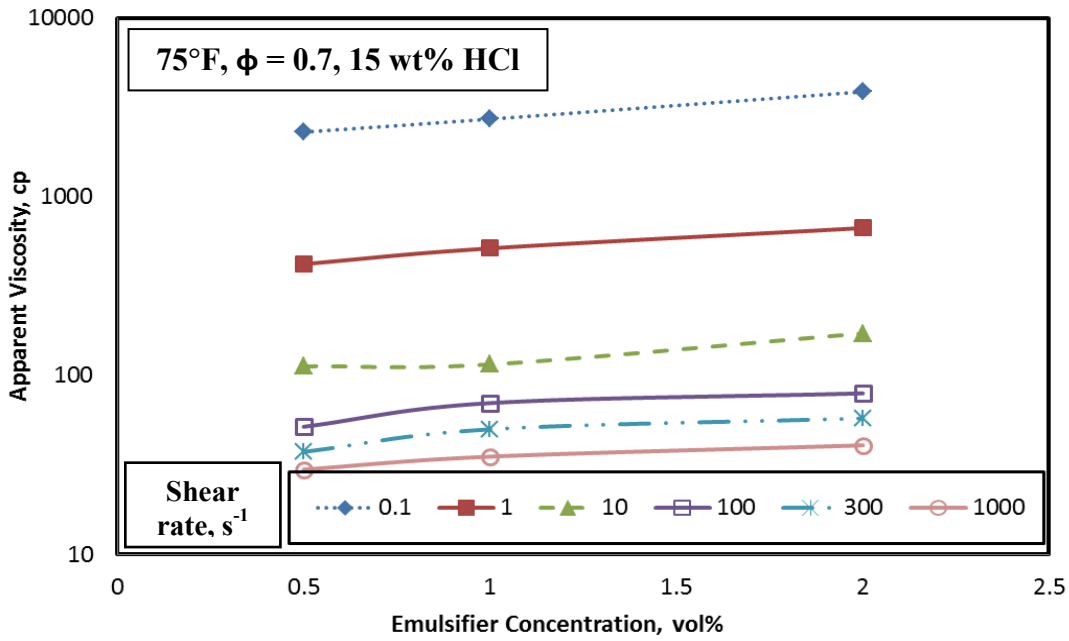

Fig. 2-4: Effect of emulsifier concentration on apparent viscosity of emulsified acids of acid volume fraction (**ϕ**) of 0.7 at different shear rates.

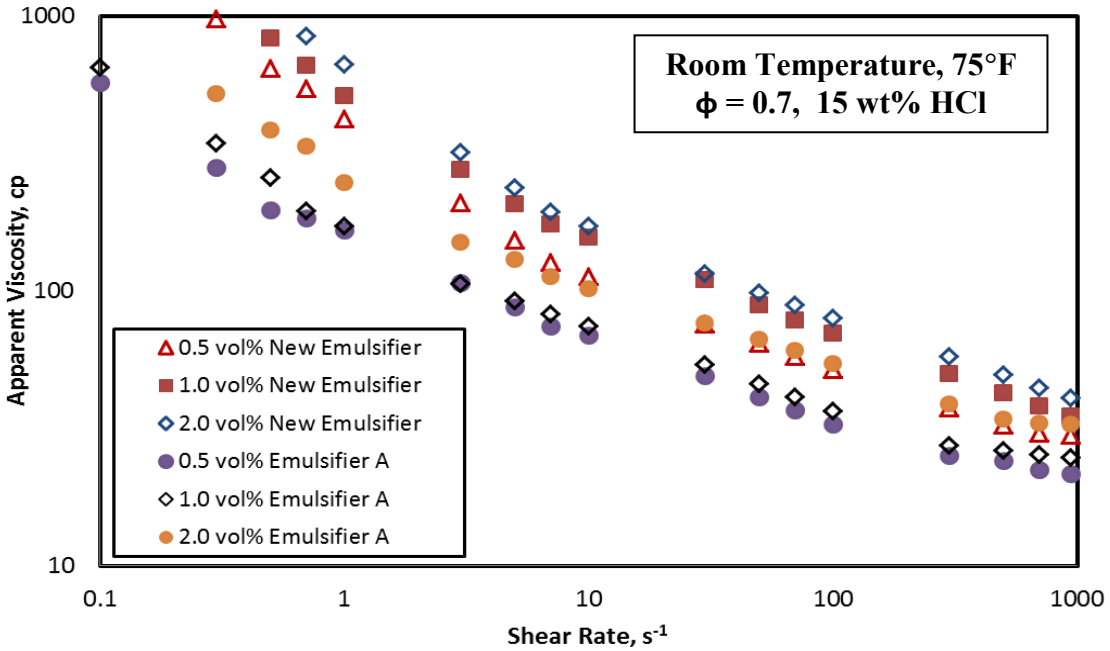

Fig. 2-5: Comparison of the apparent viscosity of emulsified acids formulated using the commercial and the new emulsifier.

2.3.5 Effect of HCl Concentration

All the viscosity measurements done were performed at room temperature, and for 15 wt% HCl concentration. The following measurements take into consideration the change in HCl concentration, through measuring the apparent viscosity of emulsified acid systems for 5, 10, 15, 20, and 28 wt% HCl concentrations at a temperature 75°F. All emulsified acid samples were prepared using the new developed emulsifier, and the emulsifier concentration was fixed at 1.0 vol% (10 gpt). **Fig. 2-6** shows the effect of changing the acid concentration on the apparent viscosity of emulsified acid prepared using 1.0 vol% emulsifier. From **Fig. 2-6**, it is apparent that, as the acid concentration increased, the apparent viscosity increased and this effect diminished at high shear rates.

Table 2-4 shows a summary of the power law model parameters as a function of acid concentration for emulsified acid prepared at 1.0 vol% new emulsifier.

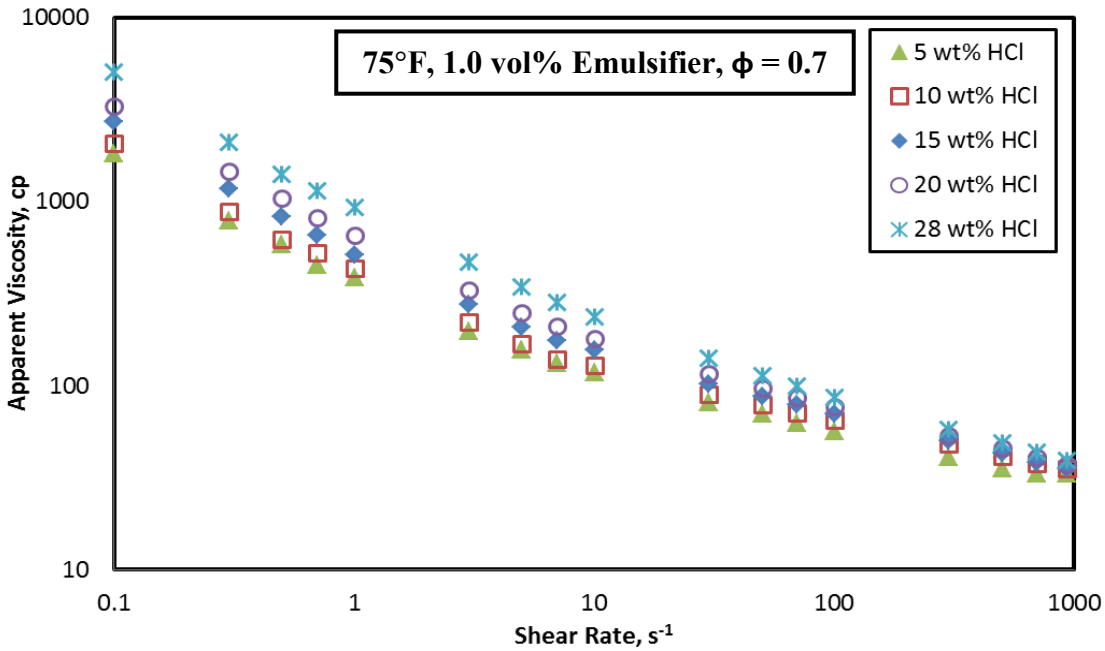

Fig. 2-6: Effect of HCl concentration of the rheology of emulsified acid formulated using the new emulsifier.

Table 2-4: Summary of power-law model parameters for emulsified acid formulated using Emulsifier B (the new emulsifier) at different HCl concentration.

HCl Concentration (wt%)	Power-law Constant, K (mPa.s^n)	Power-law Index, n	Correlating Coefficient
5	401.62	0.585	0.9612
10	447.69	0.587	0.9582
15	566.19	0.555	0.968
20	691	0.533	0.9734
28	968.65	0.491	0.9802

2.3.6 Thermal Stability of Emulsified Acids

The apparent viscosity of emulsified acid was measured at a constant shear rate (10 and 100 s^{-1}) for temperatures up to 300°F. The purpose of these measurements was to study the stability of emulsified acid prepared with different emulsifier concentrations, at high temperatures. **Figs. 2-7** and **2-8** show the effect of increasing temperature on the apparent viscosity of emulsified acid prepared using the new emulsifiers at different emulsifier concentrations (0.5, 1.0, and 2.0 vol%) at 10 and 100 s^{-1} shear rate respectively.

Fig. 2-7 shows the effect of increasing temperature on the apparent viscosity of emulsified acid, prepared using the new emulsifier, at temperature up to 300°F and 10 s^{-1} shear rate. At this low shear rate, the viscosity of the emulsified acid increased as the temperature increased, until it reached a maximum, then started to decrease again. From **Fig. 2-8**, and at 100 s^{-1} shear rate, it is clear that as the temperature increased, the apparent viscosity of emulsified acid decreased. The apparent viscosity, of the emulsified acid prepared at 2.0 vol% emulsifier concentration, slightly increased with increasing the temperature up to 164°F, and then continuously decreased up to a temperature of 300°F. This behavior was not observed at emulsifier concentrations of 0.5 and 1.0 vol%, indicating that the thermal stability of emulsified acids prepared at higher emulsifier concentrations is higher.

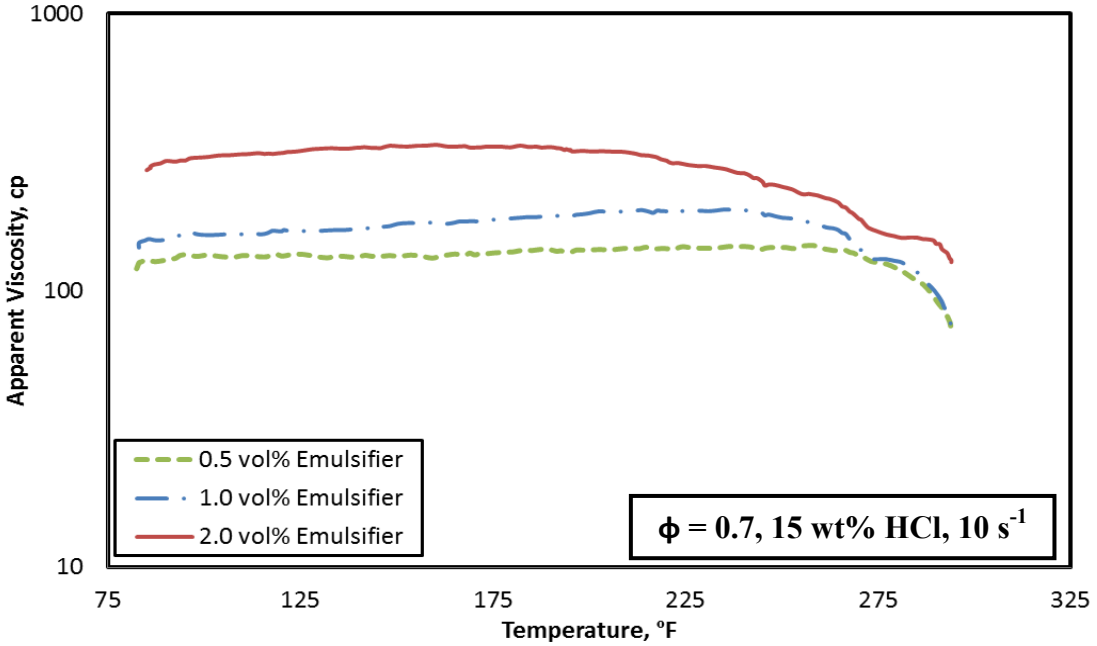

Fig. 2-7: Effect of temperature on the apparent viscosity for emulsified acid prepared using new emulsifier measured at shear rate 10 s^{-1}.

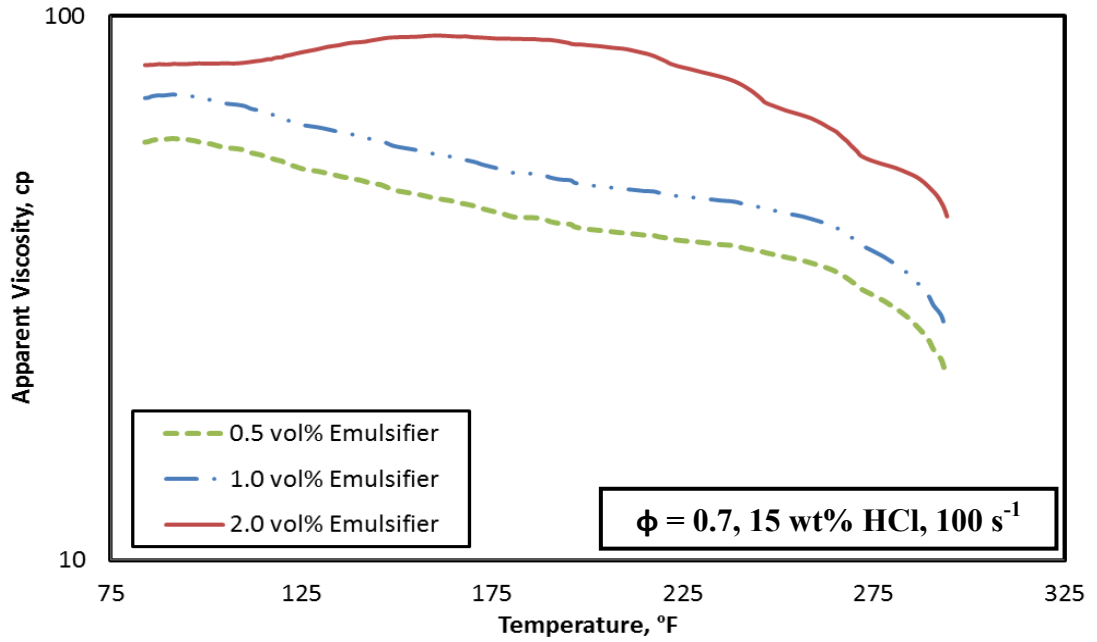

Fig. 2-8: Effect of temperature on the apparent viscosity for emulsified acid prepared using new emulsifier measured at shear rate 100 s^{-1}.

A comparison of the thermal stability of emulsified acids prepared using Emulsifiers A and B can be represented by **Fig. 2-9**. From **Fig. 2-9**, and for the same emulsifier concentration, it is apparent that the viscosity of emulsified acid prepared using the new emulsifier (emulsifier B) is higher than the viscosity of emulsified acid prepared using the commercial emulsifier (emulsifier A), and so the emulsified acid prepared using the new emulsifier is suitable for high temperature applications.

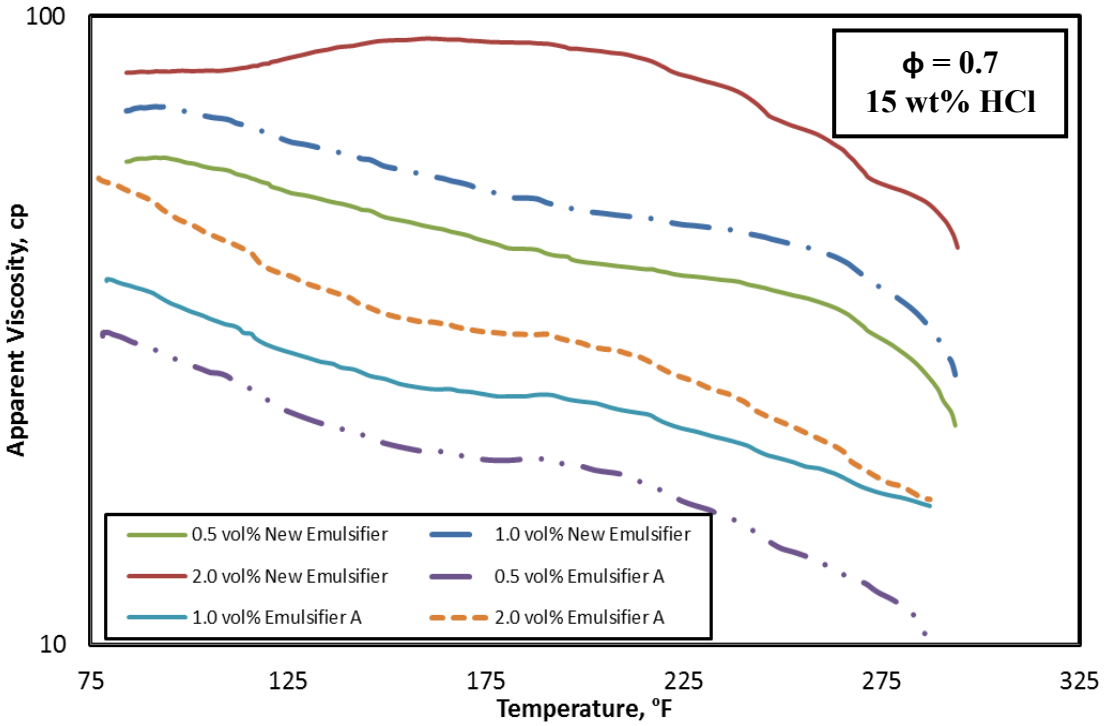

Fig. 2-9: Comparison of thermal stability of emulsified acid prepared using new and old emulsifier (Emulsifier A) measured at shear rate 100 s^{-1}.

2.3.7 Rheology of New Emulsified Acid Systems at High Temperature

The apparent viscosity of emulsified acid was measured at different shear rates (up to 1000 s^{-1}) for temperatures 150, 230, and 300°F. The purpose of these measurements is to study the effect of shear rate and temperature on the rheology of emulsified acid prepared with different emulsifier concentrations. **Figs. 2-10** through **2-12** show the effect of increasing shear rate on the apparent viscosity of new emulsified acid system at temperatures of 150, 230, and 300°F respectively. This data can be represented by a straight line indicating a non-Newtonian shear thinning behavior that can be fitted using a power law model. **Table 2-5** summarizes the values of k, n and correlating coefficient for the acid samples measured which indicates a good correlation of apparent viscosity and shear rate. This data will be used later in the interpretation and evaluation of the emulsified acid reaction kinetics.

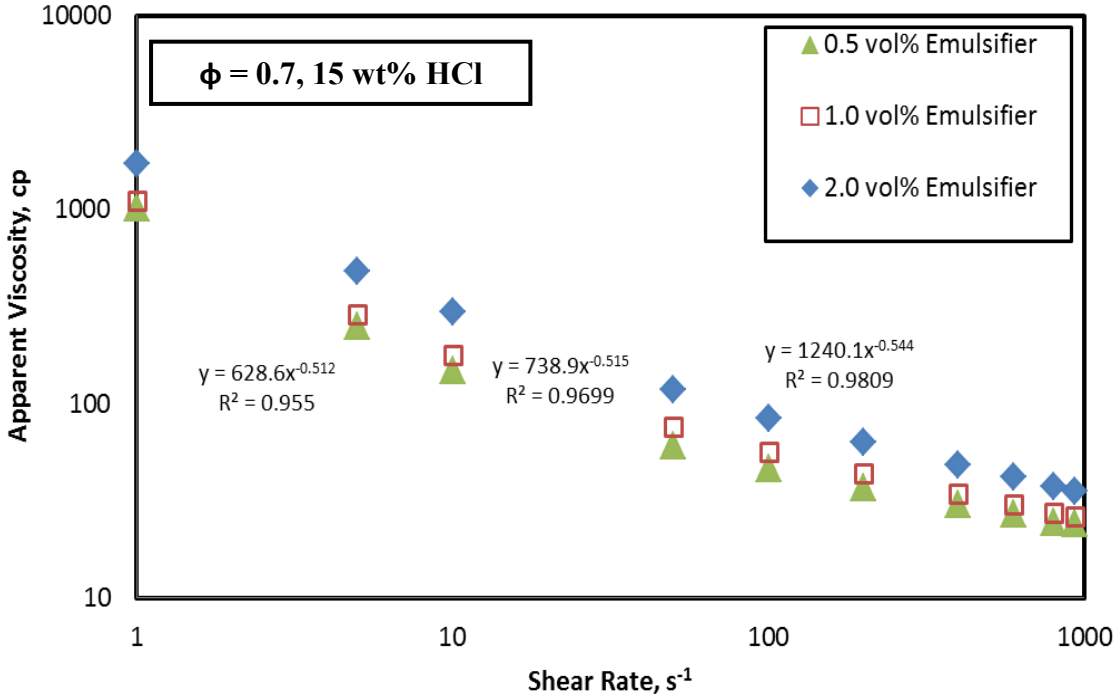

Fig. 2-10: Apparent viscosity of emulsified acids at 150°F.

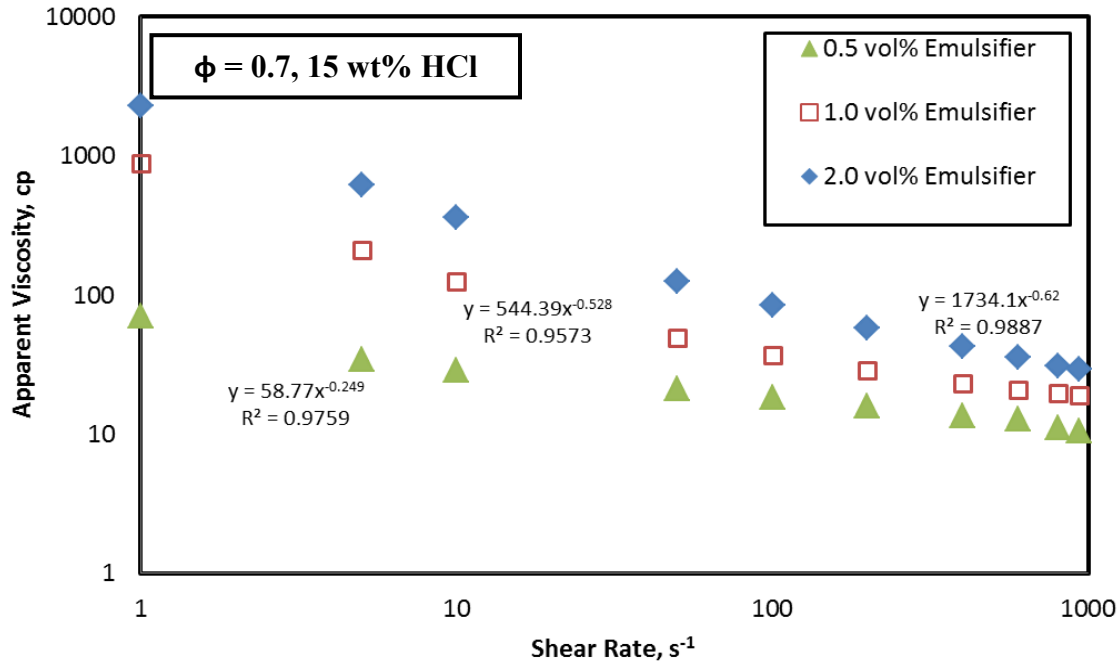

Fig. 2-11: Apparent viscosity of emulsified acids at 230°F.

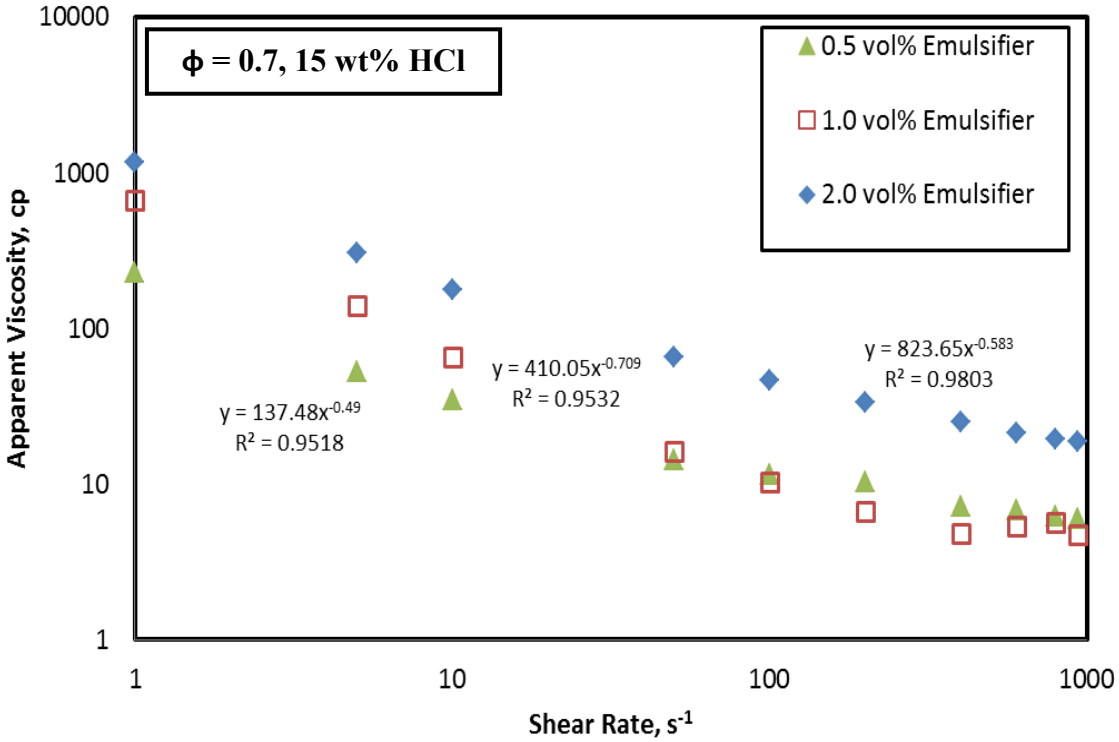

Fig. 2-12: Apparent viscosity of emulsified acids at 300°F.

Table 2-5: Summary of power-law model parameters for new emulsified acid (formulated using Emulsifier B).

Temperature	Emulsifier Concentration, (vol%)	Power-law Constant, K (mPa.s^n)	Power-law Index, n	Correlating Coefficient
150°F	0.5	628.6	0.488	0.955
	1	738.9	0.485	0.9699
	2	1240.1	0.456	0.9809
230°F	0.5	58.77	0.751	0.9759
	1	544.39	0.472	0.9573
	2	1734.1	0.38	0.9887
300°F	0.5	137.48	0.51	0.9518
	1	410.05	0.291	0.9532
	2	823.65	0.417	0.980

3. MEASUREMENT OF EMULSIFIED ACID/CALCITE REACTION RATE AND DIFFUSION COEFFICIENT

3.1 Introduction

The ability to achieve increases in productivity or injectivity by matrix acidizing in carbonate formations is strongly related to the radial distance away from the wellbore to which stimulation occurs (Hoefner et al. 1987). The enhancement in oil or water flow occurs as a result of a creation of channels that are etched in the rock by flowing acid. Stimulation efficiency is controlled by the extent to which channels propagate radially away from the wellbore and into the formation. Under certain acidizing conditions, these channels may not propagate to a significant distance or they may not form at all (Hoefner et al. 1987). Muskat (1947) showed the dependence of productivity increase on the radius of the stimulated zone.

The reaction between the emulsified acid and the rock involves three steps; the transport of acid droplets in the diesel to the rock surface, then breaking of acid droplets takes place, and as a result the actual reaction occurs on the rock surface. A number of papers have been published on the reaction kinetics of emulsified acid. These papers discussed the effect of droplet size distribution, emulsifier concentration, and temperature on the reaction of emulsified acid. The objective of this work is to examine the effect of emulsifier type and high temperature on the reaction rate of emulsified acid with carbonate rocks through the use of cores composed mainly of dolomite and calcite.

Emulsified acid was formulated so that the final acid concentration was 15 wt% HCl. The continuous phase used to disperse the acid was diesel obtained from a gas

station. The acid to diesel volume ratio was 70 to 30. The emulsifier concentration was varied from 0.5 to 2.0 vol% (5 to 20 gpt). All emulsions were characterized by measuring viscosity and thermal stability at temperatures up to 300°F and on a shear rate ranges from 0.1 to 1000 s^{-1}.

The acid/rock reaction rates and acid diffusivity coefficients were measured using the rotating disk apparatus (RDA) (Core Lab CRS Unit). The measurements were carried out at a temperature of 230°F under 1,100 psi pressure to keep CO_2 in solution. The disk rotational speeds were changed from 100 to 1500 rpm. Samples of the reacting acid were collected and analyzed for calcium concentration. Then the calcite dissolution rate was calculated using the measured calcium concentration as a function of reaction time for emulsified acids formulated at different emulsifier concentrations. From the change of dissolution rate as a function of the disk rotational speeds, the type of the reaction can be determined, and hence the effective diffusion coefficient can be predicted.

3.2 Review of Emulsified Acid / Calcite Reaction

To predict the stimulation ratio resulting from acid treatments, it is necessary to have an idea about the reaction rate between acid and rock especially under reservoir conditions (Nierode and Williams 1971). Acid-rock reaction rates can be obtained theoretically or experimentally. A number of experiments can be used to predict the acid-rock reaction rate. These experiments may include:

1. Static reaction rate test (Chamberlain and Boyer 1939; Dunlap and Hegwer 1960; Hendrickson et al. 1961; Lasater 1962; Van Poollen 1967; Van Poollen and Jargon 1968)
2. Flow experiments through parallel plates (Barron et al. 1962; Harris et al. 1966) and,
3. Dynamic tests (such as the rotating disk apparatus) (Smith et al. 1970).

It is necessary to characterize acid reaction kinetics at the rock surface, rate of acid transfer to the surface, and rate of fluid loss from the fracture or wormhole. Once reaction kinetics have been determined, field treatments can be simulated by prediction of the rate of acid transfer to the surface and fluid loss to the formation (Nierode and Williams 1971). Nierode and Williams (1971) recommended that experiments to determine reaction kinetics must be run in such a manner that the kinetic expression is the only unknown. This means that the rate of acid transfer to the surface during the reaction is predictable and does not totally control the reaction. Based on this, Nierode and Williams (1971) recommended fluid flow is laminar and acid transfer is by diffusion.

Nierode and Williams (1971) measured acid reaction rate for laminar flow through a model with the parallel plate geometry which was selected to eliminate mixing effects. Nierode and Williams (1971) concluded that reaction kinetics for the hydrochloric acid/limestone reaction can be described by a simple relation. At temperatures normally encountered in acidization treatments, reaction rate at the rock surface will not be a limiting step in the reaction process. Also, mass transport to the

rock surface is the limiting step in acid reaction in fracturing operations. Stimulation from matrix acidization treatments appears to be limited by rate of fluid loss from the wormholes to the formation rather than by acid reaction rate.

A rotating disk apparatus is used in the laboratory for studying the reaction between liquids and solid surfaces (Litt and Serad 1964; Baucke et al. 1968). Litt and Serad (1964) pointed out some of the advantages of the rotating disk over a traditional fluid flow over flat plate. Among these advantages are: no flow tunnel is required, no need for large fluid volume, minor end effects, and constant heat and mass transfer coefficients over the solid surface. Boomer et al. (1972) discussed the basis for design and gave a complete description of the rotating disk apparatus. Boomer et al. (1972) described how to use the rotating disk for studying the reaction between liquids and solid surfaces. The rotating disk can be used to study the relative importance of diffusion and reaction rate controlling effects in the reaction of a fluid with a solid.

The dissolution of calcite ($CaCO_3$) in acids is of interest to many fields of science (Langmuir 1968). The dissolution of calcite in acids is a rapid heterogeneous reaction, and the rate of dissolution will be limited both by the kinetics of the reaction at the solid-liquid interface and by the mass transfer of reactants and/or products through the fluid boundary layer. When calcite is dissolved by a weak acid, the reactants and products will form a buffer system in the boundary layer, and this affects the dissolution rate significantly. The dissolution has been proposed to be controlled by the diffusion of acid to the solid-liquid interface, the hydration rate of CO_2 in the boundary layer, the kinetic rate on the surface (Terjesen et al. 1961) and by diffusion of reaction products away

from the surface (Weyl, 1958). The problem formulation changes when calcite is dissolved in a strong acid (such as hydrochloric acid). The dissociation of the product (carbonic acid) will be suppressed by the presence of the strong acid, furthermore the reaction is considered irreversible. In this case, the dissolution will be limited by diffusion of acid to the rock surface and/or the reaction at the solid-liquid interface. The rate of dissolution of calcite with hydrochloric acid in flow systems has also been measured at different pressures which will affect the solubility of CO_2 (Barron et al. 1962; Williams et al. 1970; Nierode and Williams 1971).

In acid fracturing treatments, the injected hydrochloric acid is consumed by either reacting with the fracture walls or leaking off through the walls of the fracture then reacting with the carbonate matrix. Hendrickson et al. (1961) studied the effects of some of the variables influencing the reaction rate of HCl with carbonate. Their tests were performed under static conditions and this may limit the usefulness of their results. They found that pressure, temperature, velocity, acid concentration, area-volume ratio, physical and chemical formation structure, and the use of retarding additives affect acid spending time. Barron et al. (1962) studied acid reactivity as a function of acid flow velocity between two parallel plates of marble. Barron et al. (1962) found that HCl/carbonate reaction rate is affected by both the flow velocity and fracture width. As the flow velocity and fracture width increase, the acid penetration increases.

Boomer et al. (1972) and Lund et al. (1973) used the rotating disk apparatus to measure dissolution rate of calcite in hydrochloric acid. They used marble disks of 2” diameter in hydrochloric acid at 25°C under a nitrogen pressure of 800 psig to keep CO_2

in solution. Lund et al. (1975) studied the dissolution of calcite in hydrochloric acid with the aid of a rotating disk system at 800 psig in the temperature range of -15.6 to 25°C. They found that at 25°C the dissolution process is mass transfer limited even at high disk rotational speeds whereas at -15.6°C both mass transfer and surface reaction rates limit the dissolution rate. Lund et al. (1975) studied the dissolution of calcite using the rotating disk instrument. Their work showed that at 25°C, the dissolution of calcite is mass transfer limited even at high disk rotational speeds, while at -15.6°C, both mass transfer and surface reaction rates limit the dissolution rate. The mass transfer limited and the surface reaction limited regimes are important features of the rotating disk instrument. Fluid-solid reactions can be described by the sequence of acid diffusion to the interface, surface reaction and diffusion of reactants from the interface. The slowest step can be considered the rate-determining step. If the slowest step is the diffusion of reactants and products to and from the surface, then the reaction is mass transfer limited. If the slowest step is the surface reaction itself, then the reaction is surface reaction limited. In the rotating disk instrument, both of these regimes can occur.

Gdanski and Norman (1986) used the hollow core method to investigate simultaneously the acid-carbonate reaction rate and acid leak off rate. McLeod (1984) pointed that damage in carbonates beyond about 1 to at most 3 feet from the wellbore generally cannot be removed by matrix treatments with aqueous HCl; because HCl is completely consumed before significant penetration is achieved. This is due to the high dissolution rate of carbonates in aqueous HCl.

Hoefner et al. (1987) developed a retarded acid-in-oil micro-emulsion system. The developed micro-emulsion could exhibit acid diffusion rates two orders of magnitude lower than aqueous HCl although its viscosity was low. The decreased acid diffusion delays acid spending and allows deep acid penetration.

Mumallah (1991) mentioned that the rate of reaction between an acid and chalk is influenced by factors that can be divided into two categories; variables inherent in the chalk (cannot be controlled), and another category which can be controlled. The category of factors which can be controlled includes acid concentration, pressure, temperature, flow rate and additives in the acid solution. Mumallah (1991) indicated that the reaction rate increases as the acid concentration increases up to a concentration of about 15% HCl, then the reaction rate decreases as the acid concentration is increased to 20 and 28%.

de Rozieres et al. (1994) used the rotating disk experiments to measure diffusion coefficients. If the diffusion coefficient was accurately known, the reaction rate can be accurately calculated. The computer simulation program needs not only the diffusion coefficient for acid, but also the diffusion coefficient of the acid reaction products. Conway et al. (1999) measured the diffusion coefficients of straight acids, gelled acids, and emulsified hydrochloric acids using the diaphragm cell and the rotating disk device. Also, they developed a correlation to predict the diffusivity coefficient of hydrochloric acid, which accounts for the effect of temperature, acid concentration, and rock type with which the acid reacts. Conway et al. (1999) concluded that the diffusivity of acids

reacting with various mixtures of calcite and dolomite can be calculated by their developed correlation.

Buijse et al. (2004) proposed a new model for acid spending that can be used for strong acids (HCl) and for weak (organic) acids and also for acid mixtures. They only introduced one new element; the acid dissociation constant, describing the differences between strong and weak acids. The model was verified by comparing simulated reaction rates with rates actually measured in the laboratory with the rotating disk apparatus. Alkattan et al. (1998) showed that the dissolution rates of calcite crystals, limestone and compressed calcite powders were the same within experimental error in the bulk solution pH range of -1 to 3 and at temperatures of 25, 50, and 80°C. The limestone contained less than 1 vol% clays, but one type of limestone (St. Maximin) did contain 16 vol% quartz. This shows that the dissolution rates of pure forms of calcium carbonate are not significantly affected by different mineralogy.

Gdanski and van Domelen (1999) reported that carbonate reservoir rocks were often significantly less reactive at reservoir conditions than would be expected from reactivity data reported for pure calcite marble and dolomite marble as given by Lund et al. (1973; 1975). Taylor et al. (2006) investigated the impact of mineralogy on reservoir rock reactivity. The dissolution rate of carbonate reservoir rocks in HCl acid will generally increase as the concentration of calcite increases. Taylor et al. (2006) found that dissolution rate will significantly vary from this trend if substantial amounts of clay are present or if preferential dissolution of calcite causes mechanical loss of dolomite crystals. It was concluded that clays such as illite and mixed layer illite/smectite can

reduce dissolution rates significantly. Minor amounts (1 to 2 wt%) of naturally occurring clay in limestone appeared to reduce the dissolution rate by a factor of 25 for the reservoir rocks that were reacted with 1 M HCl at 85°C.

A few studies considered the flow pattern of non-Newtonian fluids in a rotating disk instrument. Hansford and Litt (1968) studied flow of polymer solutions (non-Newtonian) in a rotating disk and noted three flow patterns: reverse flow at low rotational speeds, toroidal flow at intermediate rotational speeds, and centrifugal flow at higher rotational speeds.

Taylor et al. (2004a) examined the effects of acidizing additives on acid reaction rates of calcite and dolomite rock. These additives were quaternary amines, polymer, surfactant, mutual solvent, iron chelating agents and dissolved iron (III). They found that trace amounts of clay impurities in limestone reservoir rocks reduced the acid dissolution rate by up to a factor of 25, to make the acid reactivity of these rocks similar to that of fully dolomitized rock. Polymer changed the acid-rock reaction from mass transfer limited to surface reaction limited with both calcite and dolomite. The presence of 5,000 mg/L iron (III) resulted in surface deposition of iron (III) hydroxide for both calcite and dolomite. At low rotational speeds, this surface layer had an inhibiting effect on the rock dissolution rate.

Al-Mutairi et al. (2009a) examined the effect of emulsified acid droplet size distribution on the acid/rock reaction rate. They found that the effect of the acid droplet size on the overall reaction rate was significant. The diffusion rate of acid droplets to the surface of the disk was found to decrease with increasing emulsifier concentration

because of higher viscosities and smaller droplet sizes. The effective diffusion coefficient of emulsified acid was found to increase linearly with the average droplet size. Emulsions with low emulsifier concentrations, large droplet sizes, were found to have high effective diffusion coefficients. While emulsions with high emulsifier concentrations had smaller average droplet sizes and low effective diffusion coefficients. The reaction kinetics between acid and limestone reservoirs is considered to be mass transfer limited under downhole conditions. The mass transfer rate is a complex, yet known, function of flow rate, fluid viscosity, and diffusion coefficient. Flow rate and fluid viscosity are readily accessible, but acid diffusivity is not an easy property to measure, especially when a heterogeneous reaction between acid and rock is taking place. Therefore, the knowledge of the diffusivity of hydrogen ions from the bulk solution to the rock surface is the key to characterizing the rate of dissolution of limestone and dolomite rocks during fracture acidizing.

The rotating disk apparatus is widely used in the petroleum industry for kinetic studies of the reaction of acidic fluids and chelating agents with reactive rocks (Levich 1962; Boomer et al. 1972; Lund et al. 1973 and 1975; Anderson 1991; Mumallah 1991; de Rozieres et al. 1994; Fredd and Fogler 1998a and b; Fredd 1998; Frenier and Hill 2002; Nasr-El-Din et al. 2002). This system allows the determination of rock dissolution rate, reaction rate constants, reaction order, and diffusion coefficients (Fredd and Fogler 1998a and b; Nasr-El-Din et al 2002).

3.3 Reaction of Calcite and Acids

The reaction of limestone with HCl proceeds according to Eq. 3.1:

$$CaCO_{3(s)} + H^{+} \text{-----> } Ca^{2+}{}_{aq} + CO_2 + H_2O \ldots\ldots \quad (3.1)$$

Lund et al. (1973 and 1975) described the rate of the surface reaction as a function of acid concentration by the power law expression that can be represented by Eq. 3.2:

$$R_{H+} = k \ C_s^m \quad \ldots\ldots \quad (3.2)$$

where

C_s = concentration of H+ on the surface (gmole/cm^3)

k = reaction rate constant (gmole/cm^2.s) (gmole/cm^3)-m

m = reaction rate order, dimensionless

R_{H+} = reaction rate in gmole/s.cm^2

The reaction rate constant, k, can be related to the temperature using Arrhenius equation:

$$k = k_o e^{\frac{-E_a}{RT}} \quad \ldots\ldots \quad (3.3)$$

where

E_a = activation energy, kcal/gmole

k_o = pre-exponential factor (frequency factor, $gmole^{(1-m)}$ $cm^{(3m-2)}s^{-1}$

($-E_a/R$) = slope of the straight line plot of k as a function of absolute temperature

The mass transfer step is represented by the diffusion rate as in Eq. 3.4:

$$J_{mt} = k_{mt} * (C_b - C_s) \ldots\ldots \quad (3.4)$$

where J_{mt} is the mass transfer rate of HCl from the bulk to the disk (gmole/cm^2.s), k_{mt} is the mass transfer coefficient (cm/s) and C_b is the concentration of H^+ in the bulk solution (gmole/cm^3).

Assuming a very rapid reaction on the rock surface, then the concentration of the hydrogen ion on the surface of the rock is negligible compared to the bulk concentration, and Eq. 3.4 reduces to

$$J_{mt} = k_{mt} * (C_b) \quad \text{..... (3.5)}$$

Newman (1966) showed that for Newtonian fluids, such as regular HCl, the rate of mass transfer, J_{mt}, to the rotating disk instrument in a laminar flow regime is given by:

$$J_{mt} = \frac{0.62048\, Sc^{-\frac{2}{3}}\, (\nu\omega)^{1/2}}{1+0.2980\, Sc^{-\frac{1}{3}}+0.1451\, Sc^{-\frac{2}{3}}} * (C_b - C_s) \quad \text{..... (3.6)}$$

where

D = Diffusion Coefficient of HCl, cm^2/s

J_{mt} = rate of mass transfer of HCl to a rotating disk, gmole/cm^2.s

S_c = Schmidt number = ν/D

ν = kinematic viscosity, cm^2/s

ω = disk rotational speed, rad/s

For non-Newtonian fluids, the viscosity of power-law model fluids, like the emulsified acid, can be given by Eq. 3.7:

$$\mu_a = K\, \gamma^{n-1} \quad \text{..... (3.7)}$$

where,

K = power law consistency index, g/cm.s$^{(n-2)}$

n = power law index

μ_a = apparent fluid viscosity, cp

γ = shear rate, s^{-1}

Hansford and Litt (1968) solved the convective diffusion equation, and the Reynolds and Schmidt numbers were modified to take into account the shear rate dependence of the power-law viscosity. The modified Reynolds and Schmidt numbers became:

$$Re = \frac{r^2 \omega^{2-n}}{N} \quad \text{..... (3.8)}$$

$$Sc = \frac{N \omega^{n-1}}{D} \quad \text{..... (3.9)}$$

where,

$N = K/\rho$, $cm^2/s^{(n+2)}$

r = radius of the disk, cm

ρ = density, g/cm^3

The final solution was introduced in the form of three dimensionless groups R_e, S_c, and S_h numbers. Eq. 3.8 can be used to define the Sherwood number (S_h),

$$S_h = \varepsilon(n) Sc^{1/3} Re^{1/3[\frac{n+2}{n+1}]} \quad \text{..... (3.10)}$$

The average mass flux to the solid surface can be determined by:

$$J_{mt} = \frac{S_h D}{r} (C_b - C_s) \quad \text{..... (3.11)}$$

where $\varepsilon(n)$ is a function that depends on the power-law index, n, and the wall radial velocity gradient.

Substituting Eq. 3.8 in Eq. 3.9 and replacing Re and Sc numbers by their definition, then the average mass flux of a solute diffuses from the bulk solution to the solid surface as a function of the rotating speed (ω), bulk concentration (C_b), diffusivity (D), and power-law index parameters (n and K) can be written in the following form:

$$J_{mt} = \left[\varepsilon(n)\left(\frac{K}{\rho}\right)^{-1/(3(n+1)}(r)^{(1-n)/3(n+1)}(\omega)^{1/(n+1)}\,D^{2/3}\right](C_b - C_s) = k_{mt}(C_b - C_s) \quad (3.12)$$

The term km is the mass transfer coefficient for non-Newtonian fluids rotating at the surface of a semi-infinite disk. It is important to note that the mass flux, for non-Newtonian fluids, is proportional to the disk rotational speed raised to the power 1/(1+n). In the case of Newtonian fluids, n is equal to 1 and the rotational speed is raised to the power 0.5.

3.3.1 Mass Transfer Limited Reaction

At low disk rotational speeds, the mass transfer of the reactant to the surface is slower than the surface reaction. The rate of reaction then can be determined from the mass flux equation. In that case, the reaction rate is proportional to the disk rotational speed raised to the power 1/(1+n). Assuming that the surface concentration of H^+ is zero, then the rate of reaction R can be determined as:

$$R_{H+} = \left[\varepsilon(n)\left(\frac{K}{\rho}\right)^{-1/(3(n+1)}(r)^{(1-n)/3(n+1)}(\omega)^{1/(n+1)}\,D^{2/3}\right](C_b) = A\,(\omega)^{1/(1+n)} \quad (3.13)$$

where

C_b = reactant concentration in the bulk solution, gmole/cm^3

C_s = reactant concentration at the surface, gmole/cm^3

D = diffusion coefficient, cm^2/s

K = power law consistency index ($g/cm.s^{n-2}$)

n = power law index

r = radius of the disk, cm

R_{H+} = the rate of reaction ($gmole/cm^2.s$)

ρ = fluid density, g/cm^3

ω = rotational speed, s^{-1}

For certain initial bulk concentrations, plotting the initial rate of reaction versus the disk rotational speed to the power 1/(1+n) should yield a straight line with a slope A, which is proportional to the diffusivity, D, raised to the power 2/3.

3.3.2 Surface Reaction Limited Reactions

If the surface reaction limits the reaction, and the rate of reaction is no longer proportional to the disk rotational speed, then acid concentration on the rock surface is assumed to be equal to the acid concentration in the bulk fluid. And in this case, the reaction rate equation can be expressed by Eq. 3.2 (Nierode and Williams 1971; Lund et al. 1973 and 1975; Alkattan et al. 1998).

3.4 Experimental Studies

3.4.1 Materials

The emulsified acids were prepared using diesel, an emulsifier, a corrosion inhibitor, and an acid solution (HCl and water). In all the emulsion preparations, the same source of diesel was used. The diesel density, viscosity and surface tension were measured at 77°F. A sample of the diesel was analyzed using a Gas Chromatograph in order to

determine the composition of the diesel. **Table 3-1** provides the specifications and results of the Gas Chromatograph analysis of the diesel used to prepare emulsified acids. De-ionized water, obtained from a water purification system, which has a resistivity of 18.2 MΩ.cm at room temperature. Hydrochloric acid (ACS grade) was titrated using 1N sodium hydroxide solution, and the HCl acid concentration was found to be 36.8 wt%. A corrosion inhibitor was added to the acid solution, while the emulsifier was added to the diesel.

3.4.2 Disk Preparation

Indiana limestone core samples (calcite - $CaCO_3$) were obtained from a local supplier and were used to study the reaction rate of emulsified acid formulated by a new developed emulsifier. Purity was determined by XRF (X-Ray Fluorescence) and elemental analysis. Elemental analysis showed that the Indiana limestone contained more than 98 wt% calcium carbonate, and the remaining was clays and quartz. **Table 3.2** summarizes the XRF results. The Indiana limestone rocks had average porosity of 17 % and average permeability of 3 md. Disks with a diameter of 1.5 in. and a thickness of 0.75 in. were cut to be used in the rotating disk apparatus. Indiana limestone core plugs were cut to the specifications described previously.

3.4.3 Preparation of Emulsified Acid

The acid solution was prepared by mixing corrosion inhibitor, di-ionized water and HCl acid. The diesel solution was prepared by adding emulsifier to diesel oil, and mixing at a high speed. Then, the acid solution was added slowly to the diesel solution and mixed at high speed (1200 rpm) for 30 min. After that, the electric conductivity of the final

mixture was measured in a conductivity cell to check the quality of the final emulsion. If the electric conductivity is nearly equal to 0, then we have a good emulsified acid. If there is some conductivity, extend mixing to 1 hour at maximum possible speed, and measure conductivity again, to be sure of the quality of the prepared emulsified acid.

Table 3-1: Properties and composition of the diesel used to prepare emulsified acids.

Density @ 77°F	0.82 g/cm^3
Viscosity @ 77°F	2.9 cp
Surface Tension @ 77°F	27.7 dyne/cm
Component	**Concentration, wt%**
Cyclobutane, ethenyl-	5.01
Decane	7.32
Undecane	6.37
Dodecane	8.18
Tridecane	9.29
Decane, 2,3,5-trimethyl-	8.58
Pentadecane	10.17
Hexadecane	10.16
Heptadecane	8.76
Octadecane	7.60
Nonadecane	6.20
Eicosane	4.98
Heneicosane	4.57
Docosane	2.15
Octacosane	0.67

Table 3-2: XRF results for Indiana limestone core plugs

Composition (wt%)	
Ca	69.12
O	29.03
Mg	0.476
Si	0.444
Fe	0.214
K	0.202
Al	0.167
S	0.157
Cl	0.12
Sr	0.04
Sn	0.02
Mn	0.01
% $CaCO_3$	98.15%

3.4.4 Equipment

Reaction rate experiments were performed using a rotating disk apparatus (**Fig. 3-1**). All acid-wetted surfaces were manufactured from acid-corrosion resistant Hastelloy. The rotating disk apparatus consists of an acid reservoir, reaction vessel, gas booster system, heaters, and associated pressure regulator, valves, temperature and pressure sensors and displays. There are two main chambers: a reservoir to hold the stimulation fluid, and a reactor to allow a contact and reaction between the rock samples and the stimulation fluids. Core plugs, which were cut in dimensions of 1.5 in. diameter and 0.75 in. thickness, were fixed in a core holder assembly in the reactor vessel using heat-shrinkable Teflon tubing. Both the reactor and the reservoir were heated up to the

desired temperature, at which the experiment takes place (230°F). After stabilizing the temperature in both vessels, acid was transferred from reservoir to reactor, and the reactor pressure was adjusted to 1100 psi, in order to keep the CO_2 in solution. Then, the disk rotation was started, and during the experiment, small samples (about 3 ml) were collected periodically from the reaction vessel through the sampling valve. Samples were collected every 1 minute for a period of 10 minutes. The samples were left to separate, and after separation, a small sample of the aqueous phase in the bottom was drawn using a syringe and diluted, in order to measure the calcium concentration using the Inductively Coupled Plasma (Optical Emission Spectrometer, Optima 7000DV).

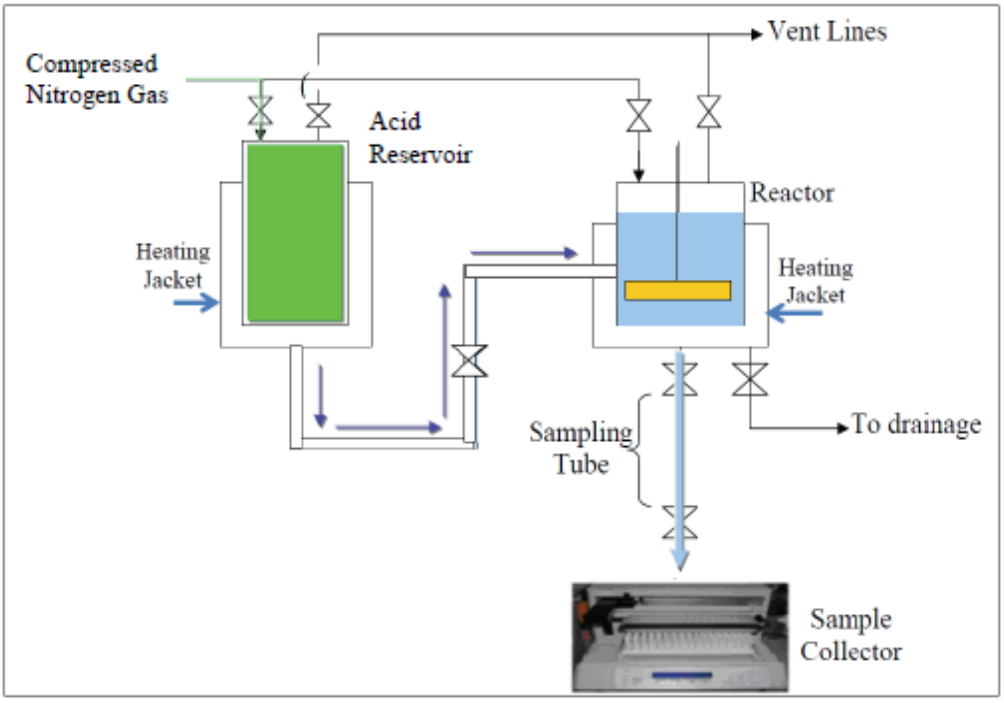

Fig. 3-1: Schematic diagram of rotating disk apparatus.

3.5 Results and Discussions

3.5.1 Viscosity of Emulsified Acids at a Temperature of 230°F

Since the emulsified acid is a non-Newtonian shear thinning fluid (Al-Mutairi et al. 2009a), the rheological parameters are important in determining and studying the acid diffusivity. The apparent viscosity of the emulsified acid was measured at shear rates up to 1000 s^{-1} and for emulsified acid prepared at different emulsifier concentrations (0.5, 1.0, and 2.0 vol%). These results were shown in Chapter 2, section 2.3.7. The effect of changing the shear rate on the apparent viscosity is shown in **Fig. 2-11. Fig. 2-11** shows the effect of increasing the shear rate on the apparent viscosity of the emulsified acid system at 230°F. This data can be represented by a straight line on the log-log plot, indicating non-Newtonian shear thinning behavior that can be fitted using a power-law model. The power-law model is given by Eq. 3.1:

$$\mu_a = K\,\dot{\gamma}^{n-1} \quad \text{(3.1)}$$

where,

K = power-law consistency factor, $g/cm.s^{(n-2)}$

n = power-law index

μ_a = apparent fluid viscosity, poise

$\dot{\gamma}$ = shear rate, s^{-1}

The power-law model parameters were summarized in **Table 2-5.**

3.5.2 Reaction of Emulsified Acid and Limestone

All the rotating disk experiments were performed at a temperature of 230°F to be consistent with the rheological measurements performed at the same temperature. All

experiments were performed using low permeability Indiana limestone core plugs. The experiments were performed at rotational speeds up to 1500 rpm. Ten fluid samples were collected in each experiment, and samples were withdrawn from the reactor every 1 minute. All experiments were performed for a 15 wt% HCl emulsified acid systems at 0.7 acid volume fraction ($\phi = 0.7$).

3.5.3 Emulsified Acid - Limestone Surface Reaction Pattern

The reaction rate and reaction patterns for limestone core samples with emulsified acids were studied using a rotating disk apparatus. The effect of the rotational speed on the dissolution pattern on the surface of the disk, at different rotational speeds 100 and 1500 rpm for 1.0 vol% emulsifier and at 230°F, is presented in **Fig. 3-2**. At 100 rpm, the reaction rate was very low and the disk almost remained uniform, indicating minimum rock/acid reaction. As the rotational speed increased to 1500 rpm, the reaction increased and the rock surface was significantly changed. The effect of the emulsifier concentration on the dissolution pattern on the surface of the disk can be studied using **Fig. 3-3**. **Fig. 3-3** shows the change of the surface pattern for a rotational speed of 500 rpm and for 0.5, 1.0 and 2.0 vol% emulsifier concentration. It appears that as the emulsifier concentration increased to 2.0, that there was not a significant change in the rock surface, indicating that the reaction is very slow.

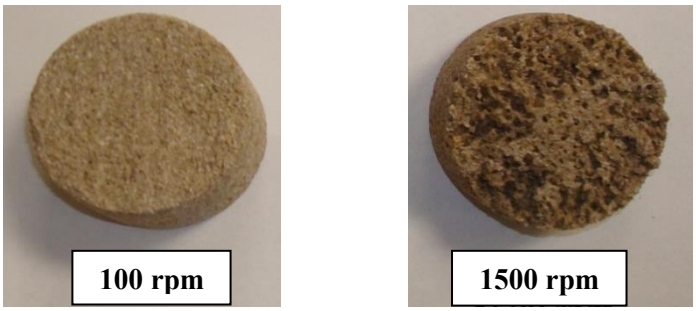

Fig. 3-2: Effect of disk rotational speed on the pattern noted on the disk surface after 10 minutes reaction with 15 wt% HCl emulsified acid prepared at 10 gpt (1.0 vol%) emulsifier at 230°F.

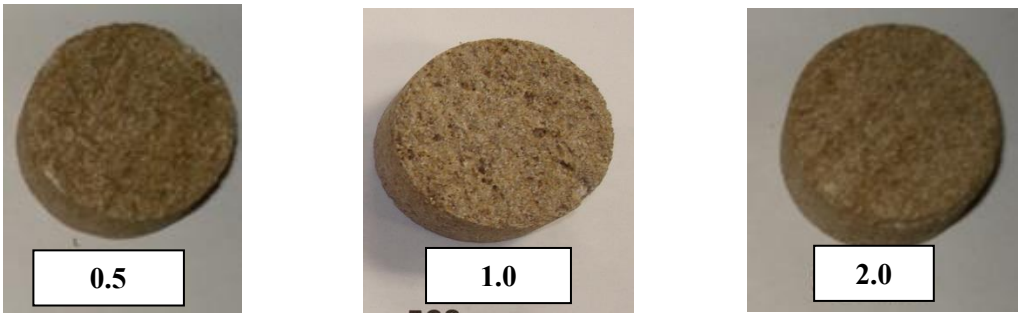

Fig. 3-3: Effect of emulsifier concentration on the pattern noted on the disk surface after 10 minutes reaction with 15 wt% HCl emulsified acid at 500 rpm at 230°F.

3.5.4 Determination of Emulsified Acid – Limestone Reaction Rate

All the experiments, for different emulsifier concentrations (0.5, 1.0, and 2.0 vol%) and at 230°F, were performed at rotational speeds up to 1500 rpm. The emulsified acid was prepared so that the final acid concentration was 15 wt% HCl and the acid volume fraction (ϕ) was 0.7. Samples were withdrawn from the reactor every 1 minute for 10 minutes, so ten fluid samples were collected from each experiment. This short test time is suitable, due to the high temperature (230°F) at which the experiments were

conducted. The concentration of calcium, in each sample, was measured using the ICP (Inductively Coupled Plasma). The amount of calcium was plotted as a function of reaction time. The dissolution rate is then obtained by dividing the slope of best fit straight line by the initial area of the core plug.

Figs. 3-4 to **3-6** show the change of calcium concentration as a function of reaction time for emulsified acid formulated at 0.5, 1.0, and 2.0 vol% emulsifier, respectively. From these plots, the calcium concentration increased, as the rotational speed increased, and decreased, as the emulsifier concentration increased. The plotted points were fitted using a straight line that passes through the zero point, and the slope of the resulting line was used to calculate the reaction (or dissolution) rate. **Table 3-3** summarizes the values of reaction rates as a function of the rotational speeds and for different emulsifier concentrations.

The rate of reaction can be directly measured from the mass flux, when mass transfer limited regime predominates. The plot of the reaction rate values versus the rotational speeds to the power (1/(1+n)), where n is the power law exponent obtained from the rheological measurements, is used in determining the boundary between the mass transfer limited regime and the surface reaction limited regime. **Fig. 3-7** shows the reaction rate vs. rotational speed to the power 1/(1+n) for emulsified acid formulated at 0.5, 1.0, and 2.0 vol% emulsifier. From **Fig. 3-7,** it is apparent that, at 230°F, the reaction of emulsified acid and limestone is mass transfer limited for all tested emulsifier concentrations.

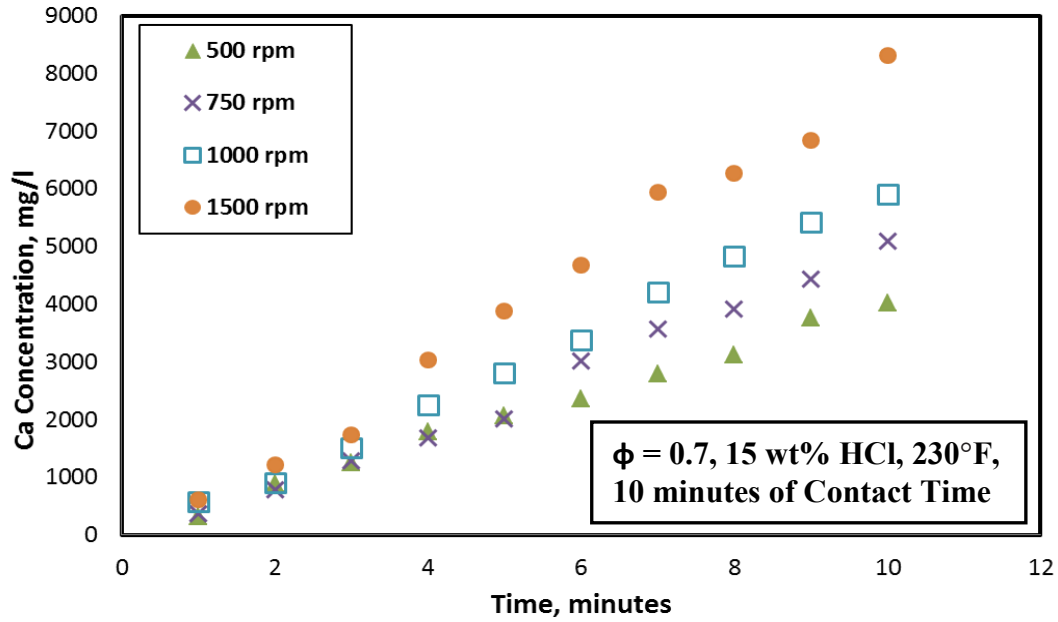

Fig. 3-4: Change of calcium concentration with time for reaction between 0.5 vol% emulsifier and 15 wt% HCl emulsified acid and limestone at 230°F.

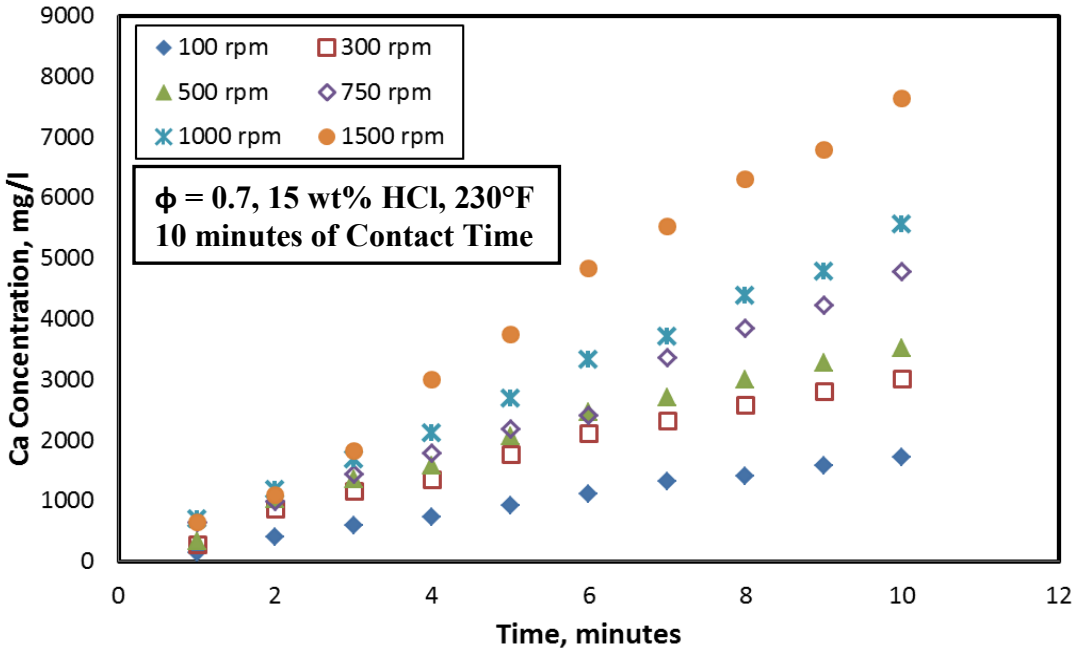

Fig. 3-5: Change of calcium concentration with time for reaction between 1 vol% emulsifier and 15 wt% HCl emulsified acid and limestone at 230°F.

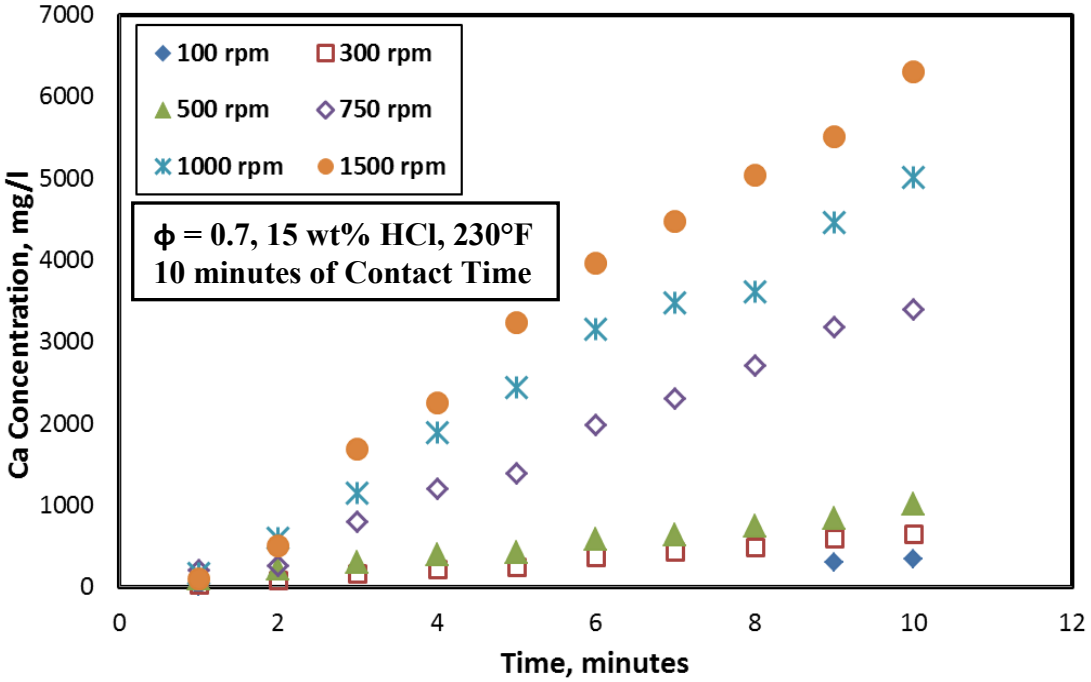

Fig. 3-6: Change of calcium concentration with time for reaction between 2.0 vol% emulsifier and 15 wt% HCl emulsified acid and limestone at 230°F.

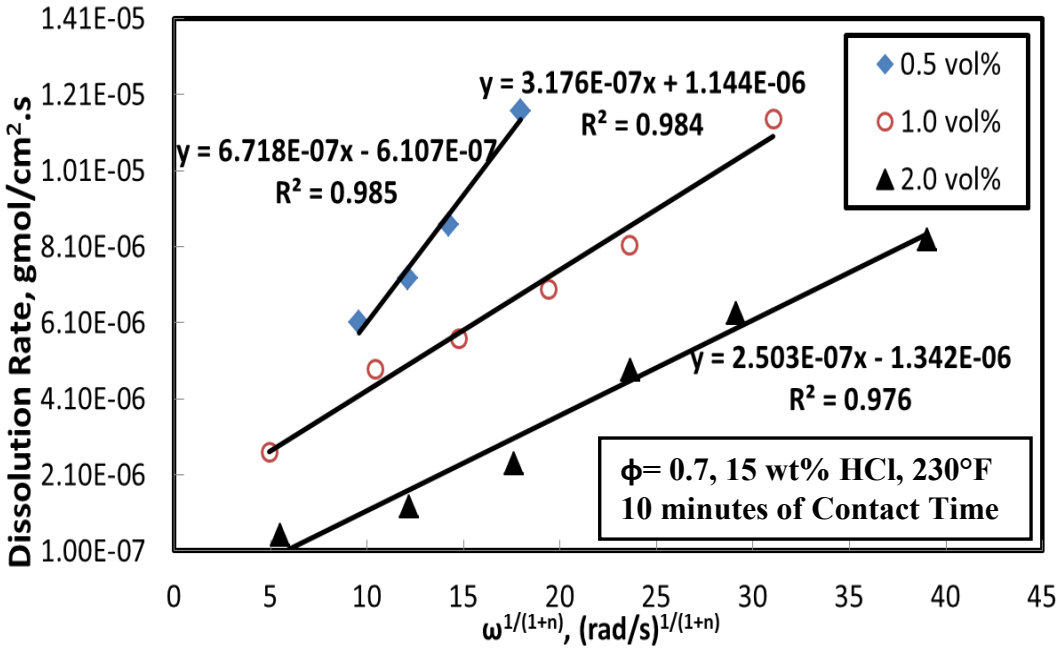

Fig. 3-7: Effect of disk rotational speed on the dissolution rate of calcite.

Table 3-3: Summary of reaction rate at different disk rotational speeds.

	Reaction rate at different ω (rpm), gmole/cm^2.s					
Emulsifier Concentration, vol%	**100**	**300**	**500**	**750**	**1000**	**1500**
0.5	---	---	6.11E-6	7.27E-6	8.69E-6	1.17E-5
1.0	2.7E-6	4.9E-6	5.7E-6	6.99E-6	8.16E-6	1.14E-5
2.0	5.2E-7	1.15E-6	2.14E-6	4.87E-6	6.4E-6	8.3E-6

3.5.5 Diffusion Coefficient of Emulsified Acid – Limestone

Hansford and Litt (1968) introduced the values for the function ε(n) at different power-law exponent values. This data is presented in **Table 3-4**. From the rheological study, values of k, n, and ε(n) were determined at 230°F. From the definition of "A" parameter in Eq. 3.13, the diffusion coefficient, D, can be estimated for each emulsified acid system. **Table 3-5** summarizes the power-law model data, values of ε(n), and the estimated diffusion coefficient (D) for 0.5, 1.0, and 2.0 vol% emulsifier concentrations. The change of diffusion coefficient as a function of the emulsifier concentration can be represented by **Fig. 3-8**. From the data shown in **Table 3-4** and **Fig. 3-8**, it is apparent that, as the emulsifier concentration increased, the diffusion coefficient decreased, and hence, the reaction rate decreased.

Table 3-4: Values of ε(n) as a function of n (Hansford and Litt 1968).

n	0.2	0.4	0.5	0.6	0.8	1.0	1.3
ε(n)	0.695	0.662	0.655	0.647	0.633	0.620	0.618

Table 3-5: Summary of diffusion rate (D) at different emulsifier concentrations.

Emulsifier Concentration (vol%)	Power-law Constant, K (mPa.s^n)	Power-law Index, n	φ(n)	D, cm^2/s
0.5	58.77	0.751	0.637212	4.73E-07
1	544.39	0.472	0.66188	2.45E-07
2	1734.1	0.38	0.67000	1.74E-07

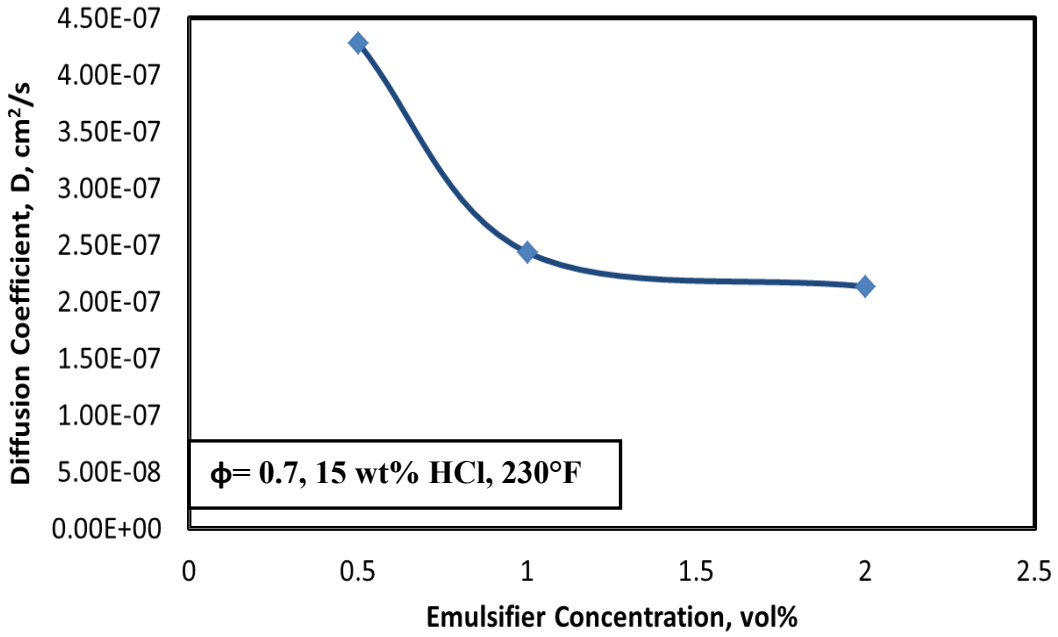

Fig. 3-8: Effect of emulsifier concentration on the diffusion coefficient of HCl in emulsified acid when reacted with calcite.

4. MEASUREMENT OF EMULSIFIED ACID /DOLOMITE REACTION AND DIFFUSION RATES

4.1 Introduction

Acid stimulation treatments in carbonate reservoirs involve injection of an acid to dissolve the rock in order to increase the productivity (or injectivity) of oil, gas, or water wells. A number of models can be used to predict the distance to which the acid penetrates and the amount of rock that will be dissolved and removed by acids (Nierode et al. 1972; Roberts and Guin 1975; Gdanski and Lee 1989; Ben-Naceur and Economides 1989; Lo and Dean 1989).

Of the two dominant carbonates present in oilfield reservoirs, calcite and dolomite, calcite dissolution has received considerable work (Nierode and Williams, 1971; Lund and Fogler, 1975; Busenberg and Plummer, 1986; Chou et al. 1989; Fredd and Fogler, 1997, 1998a, 1998b; Alkattan et al., 1998; Taylor et al., 2003, 2004a, 2006; Taylor and Nasr-El-Din 2004; Nasr-El-Din et al. 2008c; Rabie et al. 2011, 2012), while there have been fewer studies devoted to dolomite (Lund et al. 1973; Busenberg and Plummer 1982; Herman and White 1984; Chou et al. 1989; Wollast 1990; Anderson 1991; Orton and Unwin 1993). In the case of acid dissolving minerals, such as HCl with limestone and dolomite, the solid-liquid reaction process involves three steps; diffusion of liquid phase to the rock, reaction at rock surface, and diffusion of reaction products into the bulk solution (Lund and Fogler 1973). The slowest step will control the reaction. Mason and Berry (1967) indicated that the rate of dissolution of dolomite, in HCl at 25°C, is slow compared to that of marble, while at 100°C, both of them showed rapid

dissolution rates. They suggested that the dissolution of dolomite at low temperatures is surface reaction limited, while at high temperatures is diffusion limited.

Lund and Fogler (1973) used a rotating disk reactor to determine whether the dissolution of dolomite in regular HCl is reaction limited, diffusion limited, or in between. They conducted a series of experiments using dolomite at temperatures of 25 to 100°C, with an acid concentration ranging from 0.01 to 9.0 gmoles/liter, and disk rotational speeds from 50 to 500 rpm. They found that the reaction was surface reaction limited at 25 and 50°C, while at 100°C the reaction was almost diffusion limited.

Busenberg and Plummer (1982) investigated the dissolution kinetics of dolomite rocks over a range of pH (0 to 10), CO_2 pressure (0-1 atmosphere), and temperature (1.5 to 65°C). Herman and White (1984) studied the effect of lithology and fluid flow velocity on the kinetics of dolomite dissolution. They tested different stoichiometric dolomite specimens using a rotating disk. Anderson (1991) measured the reactivity of San Andres dolomite with regular HCl acid. She used different dolomite samples and a rotating disk apparatus to study rock-acid dissolution rates. The disk rotational speed was 120 rpm, test time was 5 minutes, and temperatures of 80 and 120°F. Anderson (1991) concluded that different dolomites may have drastically different surface kinetics. Li et al. (1993) used the rotating disk to measure the reaction of dolomite rocks with emulsified acid at 116°F. They measured a flux which was 10 times smaller than that obtained using regular acid. Gautelier et al. (1999) measured the dissolution rates of dolomite at 25, 50 and 80°C, for disk rotational speeds ranging from 210 to 1000 rpm, and at pH bulk between -0.39 and 4.44 using a rotating disk mixed flow reactor. The

overall dissolution process was found to be surface reaction limited at pHsurf < 1, but the effect of diffusional transport becomes increasingly significant with increasing pH.

Taylor et al. (2004b) measured acid reaction rates of a deep dolomitic gas reservoir in Saudi Arabia using a rotating disk apparatus. Measurements were made from room temperature to 85°C, at disk rotational speeds ranging from 100 to 1000 rpm, for acid concentrations of 0.05 to 5N regular HCl (0.2 to 17 wt%). They showed that dissolution rates changed as the reservoir rock varied from 3 to 100 wt% dolomite. At grain densities near 2.83 g/cm^3 (expected for pure dolomite), rock dissolution rates were higher than that observed with pure dolomitic marble. Reaction rates depended on the rock mineralogy and the presence of trace amounts of clays.

The reaction of dolomite with regular HCl was studied before at temperatures up to 100°C. Also, the reaction of emulsified acid with calcite was studied. To the best of our knowledge, only Li et al. (1993) measured the reaction rate of dolomite and emulsified acid. In this part of the study, the reaction between emulsified acid and dolomite rock was studied using a rotating disk apparatus at a temperature of 230°F and disk rotational speeds up to 1,500 rpm. A cationic emulsifier was used to prepare emulsified acids, which can be used in stimulating deep wells drilled in carbonate reservoirs. All emulsified acid systems were formulated at 0.7 acid volume fraction.

4.2 Experimental Studies

4.2.1 Materials

Material and preparation of emulsified acid was mentioned in detail in Chapter 3 section 3.3.1.

4.2.2 Disk Preparation

Dolomite cores, from a local company, were obtained as 6 in. long cores with 1.5 in. diameter. Rock composition was determined by X-ray fluorescence (XRF). Elemental analysis showed that the dolomite contained more than 98 wt% calcium, magnesium, carbon and oxygen. **Tables 4-1** and **4-2** give the XRF results of the two dolomite core samples, and the calcium to magnesium ratio, respectively. From **Table 4-2**, the calcium to magnesium molar ratio is nearly 1.20. The calcium to magnesium ratio is larger than 1, which indicates the dolomite cores may contain calcite. Disks with a diameter of 1.5 in. and a thickness of 0.75 in. were cut, and tested using the rotating disk apparatus. The porosity of all core plugs was measured and was found to be in the range of 4.2 to 6.9 vol%. The porosity was then used to calculate the initial surface area of the disk.

4.2.3 Preparation of Emulsified Acid

Preparation of the emulsified acid was accomplished in a systematic way, to warrant the reproducibility of the results. The ACS grade hydrochloric acid (36.8 wt%) was diluted to 15 wt%, by adding distilled water. Then, a corrosion inhibitor was added to the acid such that the final corrosion inhibitor concentration was 0.3 vol%. The emulsifier (at varying concentrations) was added to the diesel, and mixed using a magnetic stirrer. Then, HCl solution was added slowly to the diesel solution using a separatory funnel, and mixing was performed at a high constant speed. The final volume of the emulsion was 500 ml, at an acid-diesel volume ratio of 70:30. The electric conductivity of the final emulsion was measured in a conductivity meter (Marion L, model EP-10) to confirm the quality of the final emulsion. If the electric conductivity is nearly 0, then we have a good

emulsified acid, otherwise, the mixing time was increased to 60 minutes at the maximum possible speed.

Table 4-1: Elemental analysis of two dolomite cores using the XRF technique.

	Concentration, wt%	
Element	**Sample # 1**	**Sample # 2**
O	51.3	48.5
Ca	22.7	21.8
C	12.6	11.6
Mg	11.6	10.3
Si	0.533	3.29
Na	0.458	2.32
Al	0.235	0.837
Fe	0.204	0.489
K	0.16	0.273
Cl	0.0779	0.252
S	0.0475	0.18
Mn	0.0196	0.0155
Sn	0.0112	0.0112
Total	100.03	99.9963

Table 4-2: Calcium to magnesium molar ratio in dolomite rocks used in the study.[1]

Sample #	Element	Moles	Molar Ratio of Ca to Mg
1	Ca	0.567	**1.174**
	Mg	0.483	
2	Ca	0.545	**1.270**
	Mg	0.429	

[1] calcium to magnesium molar ratio in pure dolomite should be 1.0.

4.2.4 Equipment

Reaction rate experiments were performed using a rotating disk apparatus (**Fig. 4-1)**. All acid-wetted surfaces were manufactured from Hastelloy - C. The rotating disk apparatus

consists of an acid reservoir, reaction vessel, gas booster system, heaters, associated pressure regulators, valves, temperature and pressure sensors, and displays. The reactor and reservoir vessels were heated up to the desired temperature. After stabilizing the temperature in both vessels, the emulsified acid was transferred from the reservoir to the reactor, and the reactor pressure was adjusted to 1100 psi, in order to keep the CO_2 in solution. Then, the disk rotation was started, and during the experiment, small samples (about 3 cm^3) were collected periodically from the reaction vessel through the sampling valve. The samples which contained emulsions, were left to separate, and after separation, a small sample of the aqueous phase was drawn using a syringe and diluted, in order to measure the calcium and magnesium concentrations using the Inductively Coupled Plasma (Optical Emission Spectrometer, Optima 7000DV)

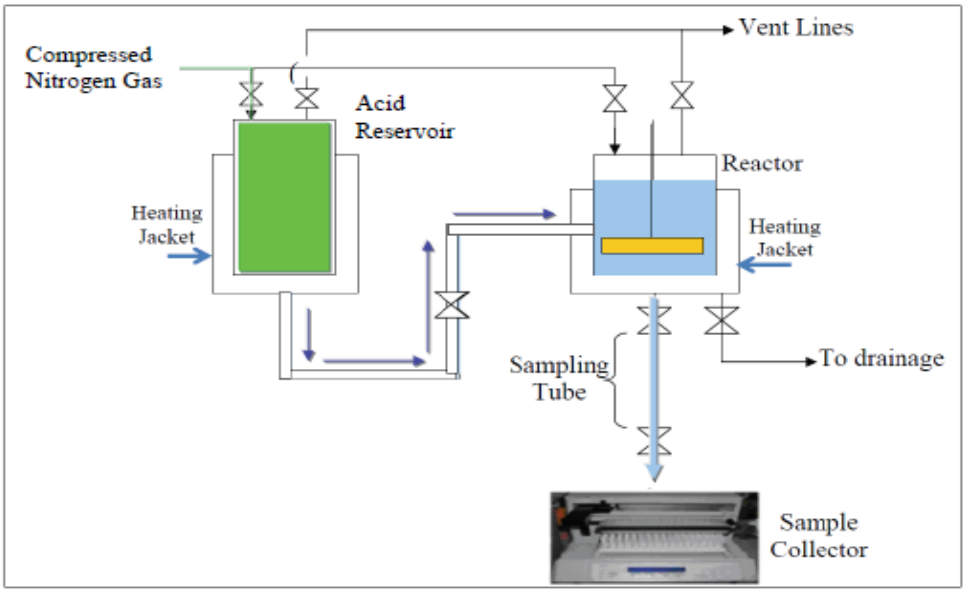

.

Fig. 4-1: A schematic diagram of the rotating disk apparatus.

Some of the reaction rate experiments were repeated several times to assess the reproducibility of the collected data. For emulsified acid formulated using 1.0 vol% emulsifier at 230°F, two experiments were performed at disk rotational speeds of 300 and 1000 rpm. The maximum relative error was calculated as the ratio of the absolute difference between the original and repeated values to the original value. The maximum relative error did not exceed 3.1 %, and this indicates good reproducibility of the data collected using the rotating disk apparatus.

An HPHT rheometer was used to measure the viscosity of live emulsified acids under different conditions. The wetted material was Hastelloy C-276, an acid-resistant alloy. The rheometer can perform measurements at various temperatures up to 500°F over shear rates of 0.00004 to 1,870 s^{-1}. A B5 bob was used in this work, which required a sample volume of 52 cm^3. The test was applied by varying the shear rate from 0.1 to 1000 s^{-1}.

4.3 Results and Discussion

4.3.1 Viscosity of Emulsified Acids at High Temperature

Since the emulsified acid is a non-Newtonian shear thinning fluid (Al-Mutairi et al. 2009a), the rheological parameters are important in determining and studying the acid diffusivity. The apparent viscosity of the emulsified acid was measured at shear rates up to 1000 s^{-1}. **Fig. 4-2** shows the effect of increasing the shear rate on the apparent viscosity of the emulsified acid system at 230°F. This data can be represented by a straight line on the log-log plot, indicating a non-Newtonian shear thinning behavior that can be fitted using a power-law model. The power-law model is given by Eq. 4.1:

$$\mu_a = K\,\dot{\gamma}^{n-1} \quad \text{..... (4.1)}$$

where,

K = power-law consistency factor, $g/cm.s^{(n-2)}$

n = power-law index

μ_a = apparent fluid viscosity, poise

$\dot{\gamma}$ = shear rate, s^{-1}

Table 4-3 gives the values of k, and n for the 15 wt% HCl emulsified acid samples prepared using 0.5, 1.0, and 2.0 vol% emulsifier and measured at 230°F.

The apparent viscosity of emulsified acid prepared using 1.0 vol% emulsifier after the reaction of emulsified acid with dolomite was studied. At the end of the rotating disk experiment performed at disk rotational speed of 1000 rpm, a sample of the remaining emulsified acid in the reactor was drawn and cooled down to 75°F. The apparent viscosity of the drawn sample was measured as a function of the shear rate. Then, the measured apparent viscosity was compared to the apparent viscosity of emulsified acid before the reaction. **Fig. 4-3** shows the comparison of the apparent viscosity of the emulsified acid measured at a temperature of 75°F before and after the reaction with dolomite. There is a good agreement between the apparent viscosity of emulsified acid after and before the reaction with dolomite, which means that there is no significant change in the emulsified acid apparent viscosity, and hence indicates the stability of the emulsified acid.

Table 4-3: Power-law parameters for emulsified acids at 230°F.

Emulsifier Concentration, vol%	Power-law Constant, K ($mPa.s^n$)	Power-law Index, n
0.5	58.77	0.751
1	544.39	0.472
2	1734.1	0.38

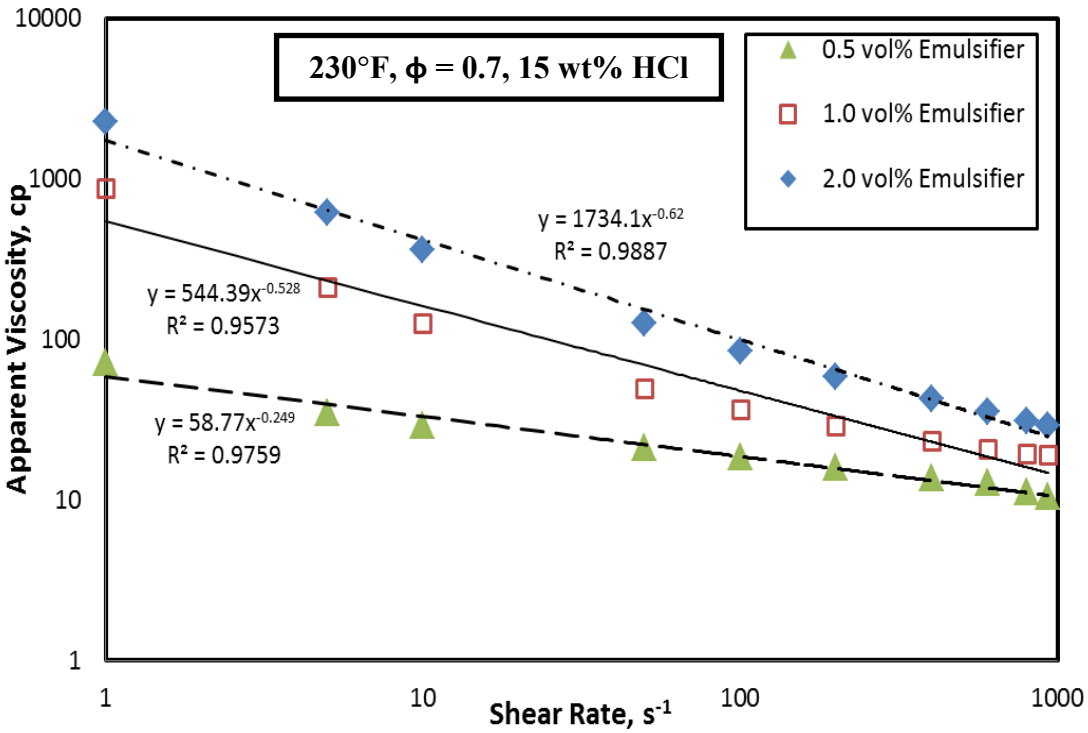

Fig. 4-2: Effect of shear rate on the apparent viscosity of emulsified acids at 230°F.

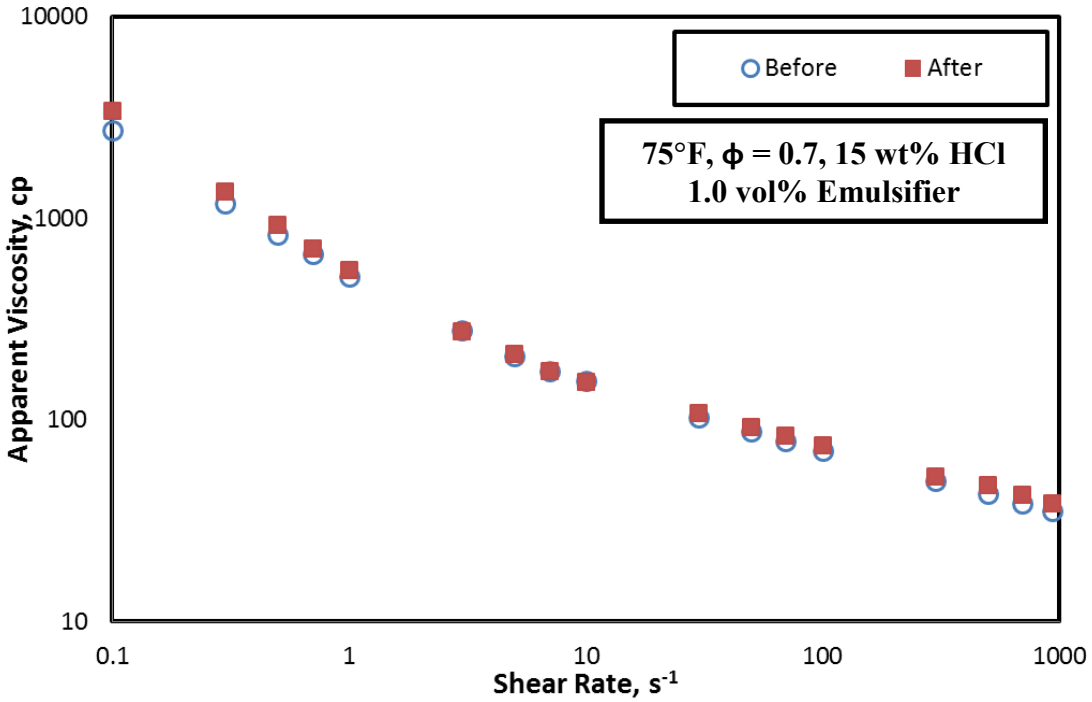

Fig. 4-3: Apparent viscosity of emulsified acid before and after the reaction with dolomite.

4.3.2 Reaction Rate of Emulsified Acid with Dolomite

Samples were withdrawn from the reactor every minute for a total time of 10 minutes. The concentrations of calcium and magnesium ions, in each sample, were measured using the ICP (Inductively Coupled Plasma). Since the XRF analysis indicated that the core samples contain calcite, the dissolution rate will be obtained using the data measured for magnesium ions. The dissolution rate is then obtained by dividing the slope of best fit straight line by the initial surface area of the disk using Eq. 4.2:

$$R_{Dh+} = \frac{1}{A_0}\frac{d(Mg)}{dt} \quad \text{..... (4.2)}$$

where R_{Dh+} is the initial dissolution rate, A_0 is the initial surface area of the disk, which equals to:

$$A_0 = \frac{A_c}{(1-\varphi)} \quad \text{..... (4.3)}$$

where A_c is the disk cross-sectional area, and φ is the initial porosity of the disk (as a volume fraction).

Figs. 4-4 and **4-5** show the change of the calcium and magnesium concentrations as a function of the reaction time, respectively, when dolomite reacted with 15 wt% HCl emulsified acid prepared using 1.0 vol% emulsifier. The calcium and magnesium concentrations increased, as the disk rotational speed was increased. As the disk rotational speed was increased, the transport of the acid droplets to the surface of the disk was enhanced, leading to faster overall reaction rate. **Fig. 4-6** shows a plot of the amount of magnesium liberated as a function of time for 15 wt% HCl emulsified acid system at 230°F, and 750 rpm disk rotational speed for different emulsifier concentrations. **Fig. 4-6** indicates that the dissolution of dolomite decreased as the emulsifier concentration increased. **Table 4-4** gives the reaction rate as a function of the disk rotational speed for different emulsifier concentrations.

Table 4-4: Dissolution rates (in gmole/cm^2.s) of dolomite with emulsified acids at various disk rotational speeds.

Emulsifier Concentration, vol%	**Dissolution rates at different ω (rpm), gmole/cm^2.s**					
	100	**300**	**500**	**750**	**1000**	**1500**
0.5	5.70E-07	8.06E-07	8.97E-07	1.03E-06	1.19E-06	1.53E-06
1.0	4.51E-07	6.73E-07	7.58E-07	9.57E-07	1.12E-06	1.23E-06
2.0	4.82E-07	5.23E-07	5.54E-07	5.94E-07	6.26E-07	7.29E-07

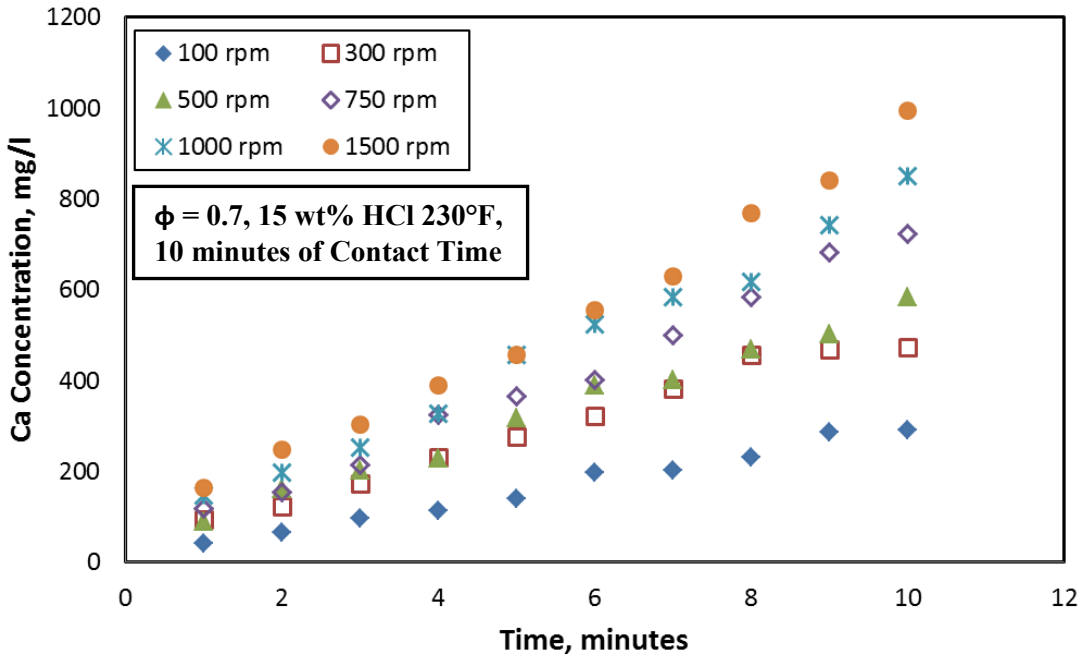

Fig. 4-4: Calcium concentration as a function of time for reaction between emulsified acid (1 vol% emulsifier) and dolomite at 230°F.

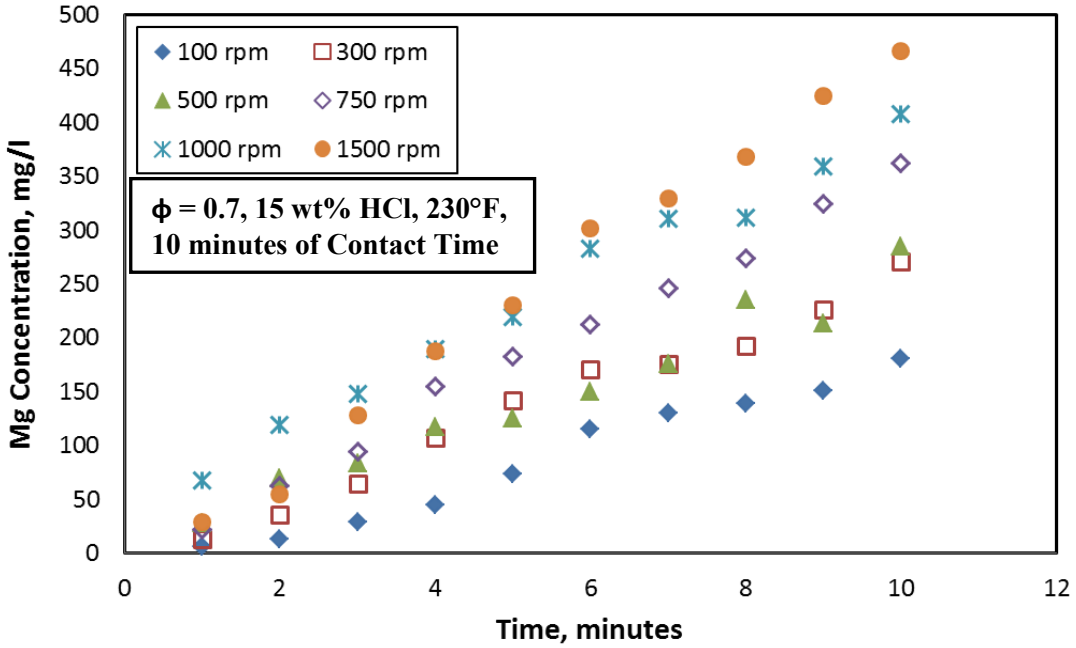

Fig. 4-5: Magnesium concentration as a function of time for reaction between emulsified acid (1 vol% emulsifier) and dolomite at 230°F.

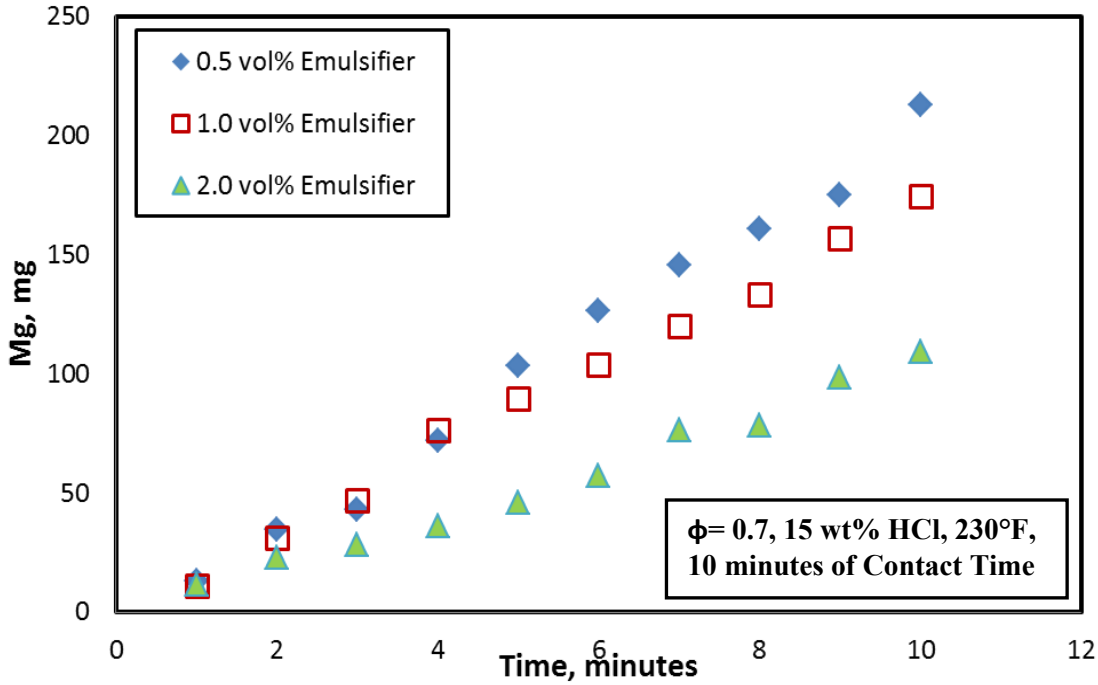

Fig. 4-6: Amount of magnesium liberated as a function of time for reaction of emulsified acid and dolomite at 750 rpm and 230°F.

The emulsified acid reaction rate experiments were repeated at disk rotational speeds of 300 and 1000 rpm to determine the reproducibility of the measured data. Two additional experiments were performed at each disk rotational speed to assess the repeatability and data reproducibility. **Fig. 4-7** shows the amount of magnesium liberated as a function of reaction time for emulsified acids formulated at 1.0 vol% emulsifier and for disk rotational speeds of 300 and 1000 rpm. **Table 4-5** shows the reaction rate obtained as a function of the disk rotational speed for the original and repeated tests. From **Table 4-5** and **Fig. 4-7**, the maximum relative difference was less than 3.1%, and the data measured shows good reproducibility of the results.

Table 4-5: Dissolution rates (in gmole/cm^2.s) of dolomite at disk rotational speeds of 300 and 1000 rpm.

ω, rpm	300	300 (1)	300 (2)	1000	1000 (1)	1000 (2)
Dissolution Rate, gmole/cm^2.s	6.73E-07	6.93E-7	6.95E-07	1.12E-06	1.12E-06	1.13E-06

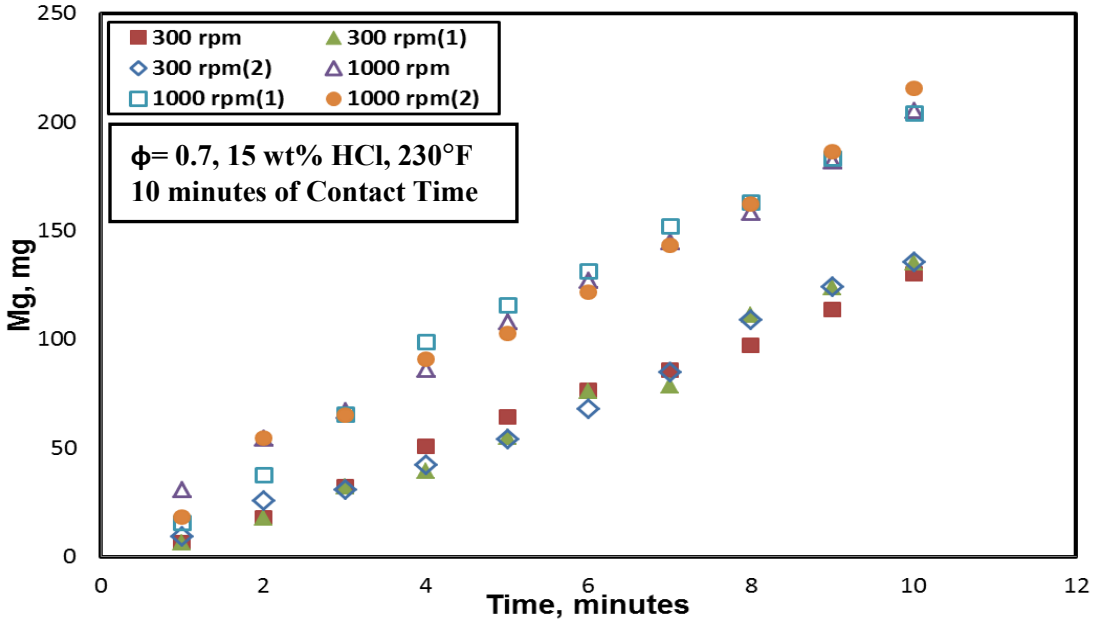

Fig. 4-7: Amount of magnesium liberated as a function of time for reaction between emulsified acid (1 vol% emulsifier) and dolomite at 230°F for disk rotational speeds 300 and 1000 rpm.

The plot of the reaction rate versus the disk rotational speed to the power (1/(1+n)), where n is the power-law index (**Table 4-3)**, is used to study the effect of the disk rotational speed on the dissolution rate, and in determining the boundary between the mass transfer limited regime and the surface reaction limited regime. **Fig. 4-8** shows the reaction rate as a function of the disk rotational speed to the power 1/(1+n). It is apparent that as the emulsifier concentration was increased, the reaction rate decreased.

This reduction in the reaction rate occurred because higher loads of emulsifier created emulsified acids with smaller acid droplet sizes (**Table 4-3)** resulting in higher viscosity (**Fig. 4**), and so lower acid mobility.

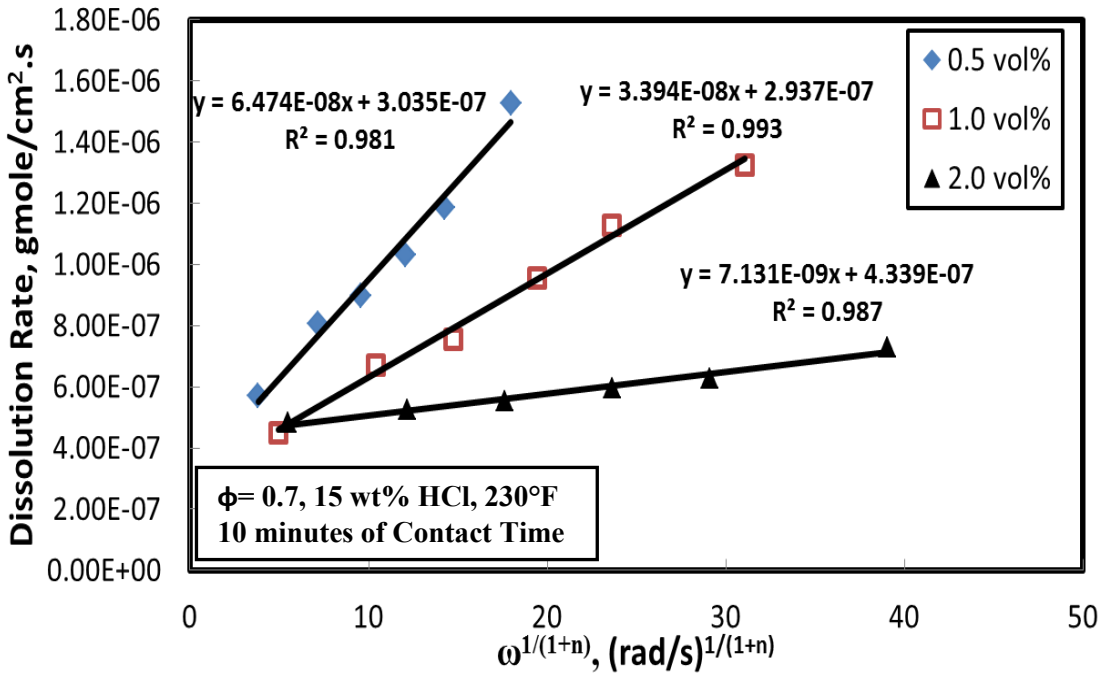

Fig. 4-8: Effect of disk rotational speed on the dissolution rate of dolomite at different emulsifier concentrations.

For emulsified acid formulated at 0.5 vol% emulsifier, the dissolution rate increased as the disk rotational speed increased up to 1500 rpm, which indicates that the reaction of emulsified acid and dolomite is mass transfer limited. The dissolution rate increased in a linear fashion with an increase in the disk rotational speed raised to the

power 1/(1+n), where n is equal to 0.751 (**Table 4-3**). Using these data, the diffusion coefficient of emulsified acid can be determined using Eq. 4.4 (de Rozieres et al. 1994):

$$R = \left[\varphi(n)\left(\frac{K}{\rho}\right)^{-1/(3(n+1)}(r)^{(1-n)/3(n+1)}(\omega)^{1/(n+1)}\,D^{2/3}\right](C_b) \quad \text{(4.4)}$$

or

$$R = A\,(\omega)^{1/(1+n)} \quad \text{(4.5)}$$

where

C_b = reactant concentration in the bulk solution, gmole/cm^3

D = diffusion coefficient, cm^2/s

K = power-law consistency factor (g/cm.s^{n-2})

n = power-law index

r = radius of the disk, cm

R = the rate of reaction (gmole/cm^2.s)

ρ = fluid density, g/cm^3

ω = disk rotational speed, s^{-1}

ε(n) = function depends on n (**Table 4-6**)

For certain initial bulk concentrations, plotting the initial rate of reaction versus the disk rotational speed to the power 1/(1+n) should yield a straight line with a slope A (Eq. 4.5), which is proportional to the diffusivity coefficient raised to the power 2/3.

With increasing the emulsifier concentration to 1.0 vol%, the reaction rate between emulsified acid and dolomite rocks decreased. From **Fig. 4-8**, the dissolution rate of dolomite rocks increased as the disk rotational speed increased up to 1500 rpm,

indicating that the reaction is diffusion (or mass transfer) limited. For emulsified acid formulated at 2.0 vol% emulsifier, the reaction rate, as a function of the disk rotational speed to the power 1/(1+n), increased as the disk rotational speed increased, which indicates that the reaction is a mass transfer limited. From **Fig. 4-8**, the reaction rate of dolomite and emulsified acid decreased with the increase in the emulsifier concentration. Also, the reaction of dolomite and emulsified acid at a temperature of 230°F is mass transfer limited.

The effect of the average droplet size of the emulsified acid systems on the dissolution rate of dolomite rocks in emulsified acid at different disk rotational speeds is shown in **Fig. 4-9**. As the average droplet size increased, the dissolution rate increased, and this was noted for both high and low disk rotational speeds.

Table 4-6: Values of ε(n) as a function of n (Hansford and Litt 1968).

n	0.2	0.4	0.5	0.6	0.8	1.0	1.3
$\boldsymbol{\varepsilon}$**(n)**	0.695	0.662	0.655	0.647	0.633	0.620	0.618

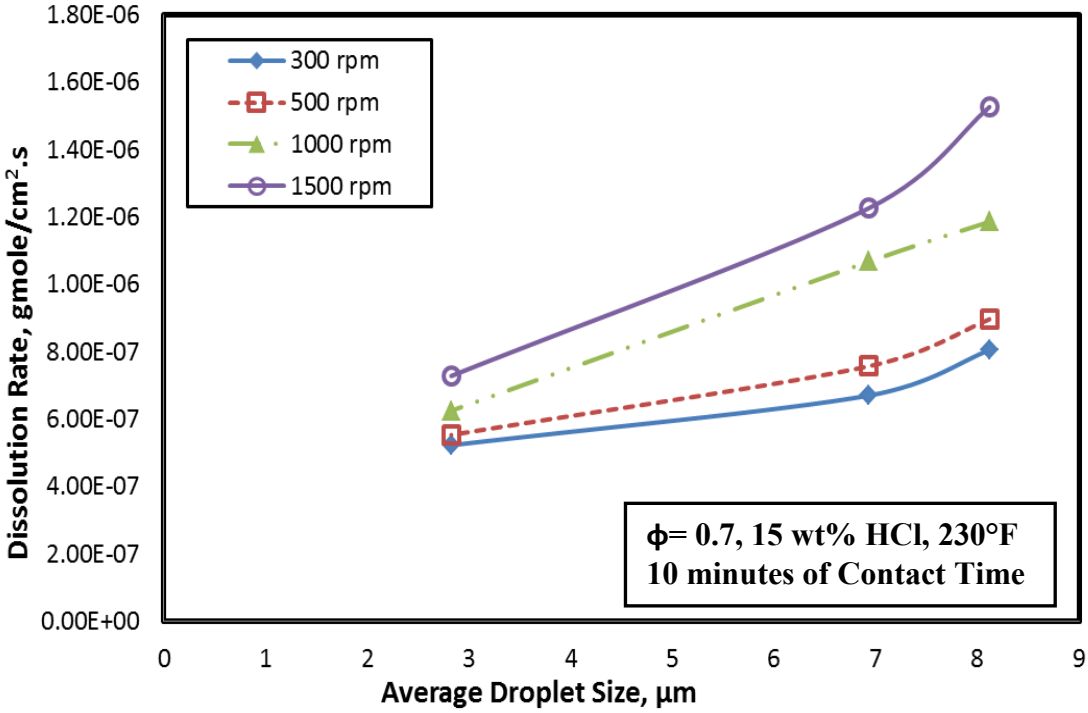

Fig. 4-9: Effect of the average droplet size of emulsified acid on the dissolution rate of dolomite.

4.3.3 Determination of Emulsified Acid Diffusion Coefficient

Hansford and Litt (1968) introduced the values for the function $\varepsilon(n)$ (**Table 4-6**). All these values were calculated assuming a mass transfer limited reaction. From the rheological study, the values of k, n, and $\varepsilon(n)$ were determined at 230°F. From the definition of "A" parameter in Eq. 4.4, the diffusion coefficient, D, can be estimated for emulsified acid systems formulated at emulsifier concentrations of 0.5, 1.0, and 2.0 vol%. **Table 4-7** gives the power-law model data, values of $\varepsilon(n)$, and the diffusion coefficient. The diffusion coefficient as a function of the emulsifier concentration is plotted in **Fig. 4-10**. It is clear that as the emulsifier concentration increased, the

diffusion coefficient decreased significantly. The diffusion coefficient for emulsified acids formulated at 0.5 vol% emulsifier was found to be 1.413E-8 cm^2/s. For emulsified acid systems prepared using emulsifier concentrations of 1.0 and 2.0 vol% emulsifier, the diffusion coefficient was found to be 6.751E-9 and 8.367E-10 cm^2/s, respectively. The diffusion coefficient decreased by 17 times, when the emulsifier concentration increased from 0.5 to 2.0 vol%. The high viscosity of emulsified acid resulted in a reduction in the mobility of acid droplets, hence reduced the reaction rate.

Table 4-7: Diffusion coefficient at different emulsifier concentrations at 230°F.

Emulsifier Concentration (vol%)	**Power-law Constant, k ($mPa.s^n$)**	**Power-law Index, n**	**ε(n)**	**D, cm^2/s**
0.5	58.77	0.751	0.637	1.414E-08
1	544.39	0.472	0.662	6.752E-09
2	1734.1	0.38	0.670	8.367E-10

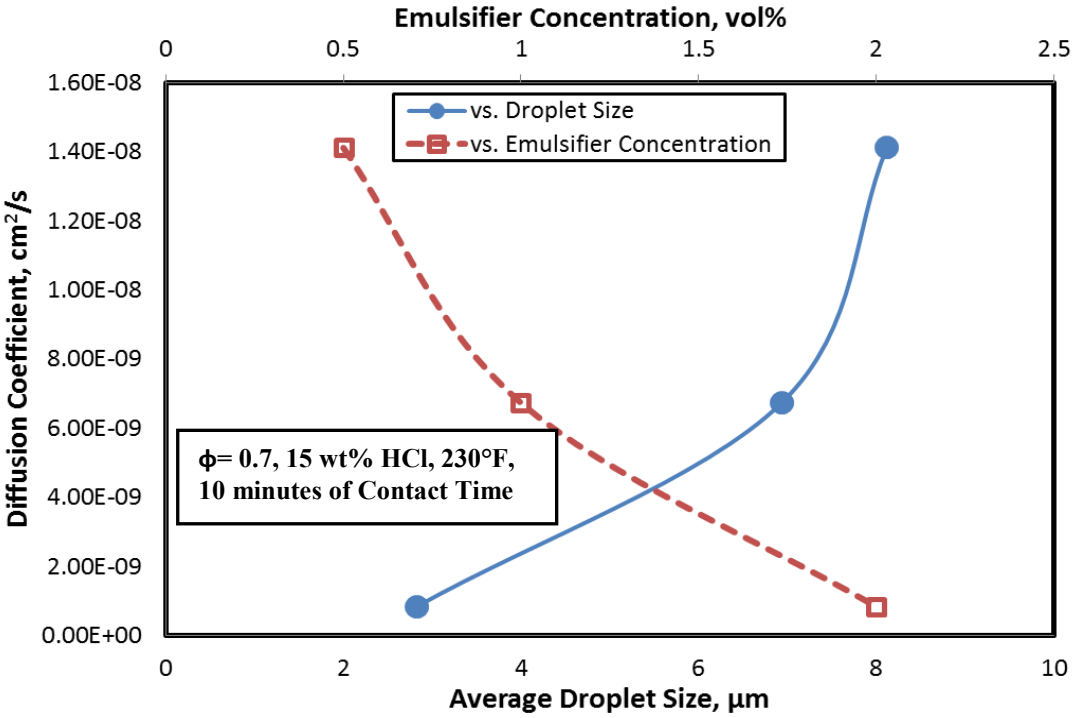

Fig. 4-10: Effect of the emulsifier concentration and average droplet size on the diffusion coefficient.

4.3.4 Comparison of Diffusion Coefficients with Dolomite

The diffusion coefficient of emulsified acid systems was measured before (Hoefner and Fogler, 1989; de Rozieres et al. 1994; Al-Mutairi et al. 2009a). **Table 4-8** lists the diffusion coefficients obtained in these studies. Hoefner and Fogler (1989) used a rotating disk technique, and measured diffusion coefficient values in the range of 10^{-8} cm^2/s for a micro-emulsified acid system. de Rozieres et al. (1994) measured the diffusion coefficients of emulsified acids with Carrara marble using both the diaphragm diffusion cell and the rotating disk at a temperature of 147°F. At a temperature of 147°F, de Rozieres et al. (1994) predicted a diffusion coefficient of 4.60E-8 cm^2/s. Al-Mutairi et

al. (2009a) measured the diffusion coefficient of emulsified acid at 85°C (185°F), and it was 2.8187E-8 cm^2/s. Comparing the acid diffusion coefficient of the emulsified acid with dolomite rocks at 230°F (D = 1.413E-8 cm^2/s) to the values obtained by Hoefner and Fogler (1989), de Rozieres et al. (1994), and Al-Mutairi et al. (2009a), the diffusion of emulsified acid in the presence of dolomite rocks was lower although the reaction rate experiments were performed at higher temperature.

Table 4-8: Diffusion coefficient of emulsified acid systems used in previous and current studies.

Authors	**Diffusion Coefficient, cm^2/s**	**Notes**
Hoefner and Fogler (1989)	10E-8	Micro-emulsion with calcite
de Rozieres et al. (1994)	4.60E-8	147°F with Carrara marble
Al-Mutairi et al. (2009a)	2.8187E-8	185°F with calcite
Present Study	1.413E-8 to 8.367E-10	230°F with dolomite rocks

Hoefner and Fogler (1989) tried to relate the measured diffusion coefficient to the particle size using the Stokes-Einstein equation for the Brownian diffusion. The Brownian diffusion coefficient of spherical particles of radius (r_D) in a fluid of a viscosity (η) is given by

$$D_B = \frac{R_g\ T}{6\ \pi\ N_A\ r_D\ \eta} \quad \text{..... (4.6)}$$

where

D_B = Brownian diffusion coefficient, m^2/s

R_g = Universal gas constant, 8.31 J/(mole.°K)

N_A = Avogadro's number, 6.022E+23 mol^{-1}

η = viscosity of the continuous phase, Pa-s

r_D = radius of the droplets of the disperse phase, m

The diffusion coefficients measured in this study fall in the range of 10^{-8} to 10^{-10} cm^2/s. The Brownian diffusion coefficient of spherical particles depends mainly on the radius of the acid droplets and the viscosity of the continuous phase (de Rozieres et al. 1994). Eq. 4.6 suggests that the diffusion coefficient is inversely proportional to the radius of the particle in the Brownian motion regime. Solving Eq. 4.6, for emulsifier concentration of 0.5 vol% and 1.413E-8 cm^2/s, a droplet size of 0.066 μm was obtained. The calculated droplet size using Eq. 4.6 is very small compared to the average size of acid droplets measured in the emulsified acid system used in the current study (8.118 μm for emulsified acid prepared using 0.5 vol% emulsifier). While, for emulsified acids prepared using 2.0 vol% emulsifier concentration, the diffusion coefficient was 8.3674E-10 cm^2/s, and the acid droplet size calculated using Eq. 4.6 was found to be 1.12 μm. The droplet size, which was predicted using Eq. 4.6, was found to be 60% less than the value measured using the microscope. Al-Mutairi et al. (2009a) mentioned that the size of the macro-emulsion is too large for Brownian motion to occur. In addition, dense emulsions exhibit droplet/droplet interactions that prevent significant Brownian motion, and the flow in the rotating disk system is centrifugal and induced by a forced convection. **Fig. 4-10** shows the diffusion coefficient of emulsified acid as a function of the measured average droplet size of emulsified acid. From **Fig. 4-10,** the acid diffusion

coefficient decreased as the average droplet size of emulsified acid decreased. This is contrary to what was mentioned in the Stokes-Einstein equation for the Brownian diffusion of spherical particles. As a result, the Stokes-Einstein equation for the Brownian diffusion is not applicable for the emulsified acids used in the present study.

4.3.5 Comparison with Previous Work

Lund et al. (1973) measured the dissolution rate of dolomite in 1 N regular HCl at 100°C (212°F). The measured dissolution rates ranged from 5.3E-6 to 1.32E-5 gmole/cm^2.s. Herman and White (1984) measured dolomite dissolution rate in regular HCl at 75°F. Anderson (1991) measured the dissolution rate of dolomite in approximately 1 to 5 N regular HCl at 120°F. She measured dissolution rates in the range of 1.8E-6 to 3.47E-6 gmole/cm^2.s. Taylor et al. (2004b) measured the reaction rate and diffusion coefficient of regular HCl using dolomite core samples and for HCl concentration up to 17 wt%. The reaction rate measured was in the range of 2E-6 to 1.6E-5 gmole/cm^2.s at 185°F. In the present work, the dissolution rate of dolomite in the emulsified acid systems was lower than the values measured previously (using regular HCl) by at least one order of magnitude. The values of the dissolution rate ranges from 4.828E-7 to 1.527E-6 gmole/cm^2.s. Although the dolomite reaction with emulsified acid was studied at a higher temperature, the dolomite dissolution rate in emulsified acid was lower than the values measured previously using regular HCl. The emulsified acid system tested in the current study achieved low reaction rates and low diffusion coefficient with dolomite cores, and this will lead to the creation of deep wormholes and etched fracture surfaces, which will increase the benefits from the stimulation treatment.

Anderson (1991) measured the diffusion coefficient of 1 to 5 N regular HCl at 120°F using dolomite core samples. Anderson (1991) measured diffusion coefficient of 6.65E-5 cm^2/s. Conway et al. (1999) measured the diffusion coefficient of regular HCl at temperatures of 110 and 150°F using dolomite cores. Conway et al. (1999) measured diffusion coefficients in the range of 1.7E-5 to 2.28 E-5 cm^2/s. Taylor et al. (2004b) measured the diffusion coefficient of regular HCl using dolomite core samples and for HCl concentrations up to 17 wt% at a temperature of 185°F. Taylor et al. (2004b) measured diffusion coefficients ranging from 6.24E-5 to 7.35E-5 cm^2/s. In the present work, the diffusion coefficient of emulsified acid systems measured using dolomite core samples was lower than the values measured previously using regular HCl by at least 3 to 5 orders of magnitude. The values of the diffusion coefficient of emulsified acid were found to be in the range of 10E-8 to 10E-10 cm^2/s.

4.3.6 Comparison of Reaction Rate and Diffusion Coefficient of Emulsified Acid with Calcite and Dolomite Rocks

In Chapter 3, the dissolution rate of calcite in emulsified acids was measured using a rotating disk apparatus. Indiana limestone core samples were used as a source for calcite. The emulsifier concentration was varied from 0.5, 1.0 and 2.0 vol%. **Fig. 4-11** gives a comparison of the dissolution rate, as a function of $\omega^{1/(1+n)}$ for an emulsified acid prepared using 1.0 vol% emulsifier, for both dolomite and calcite rocks. The dissolution rate of the dolomite was found to be lower than that of calcite, and the difference increased as the rotational speed was increased.

Fig. 4-12 gives a comparison of the diffusion coefficients of emulsified hydrochloric acids when reacted with calcite and dolomite as a function of emulsifier concentration. The diffusion coefficients of emulsified hydrochloric acids, when reacted with dolomite, were found to be at least one order of magnitude lower than the diffusion coefficients of emulsified acids when reacted with calcite. At emulsifier concentration of 2.0 vol%, the diffusion coefficients of emulsified acids when reacted with dolomite were lower by two orders of magnitude than that obtained with calcite.

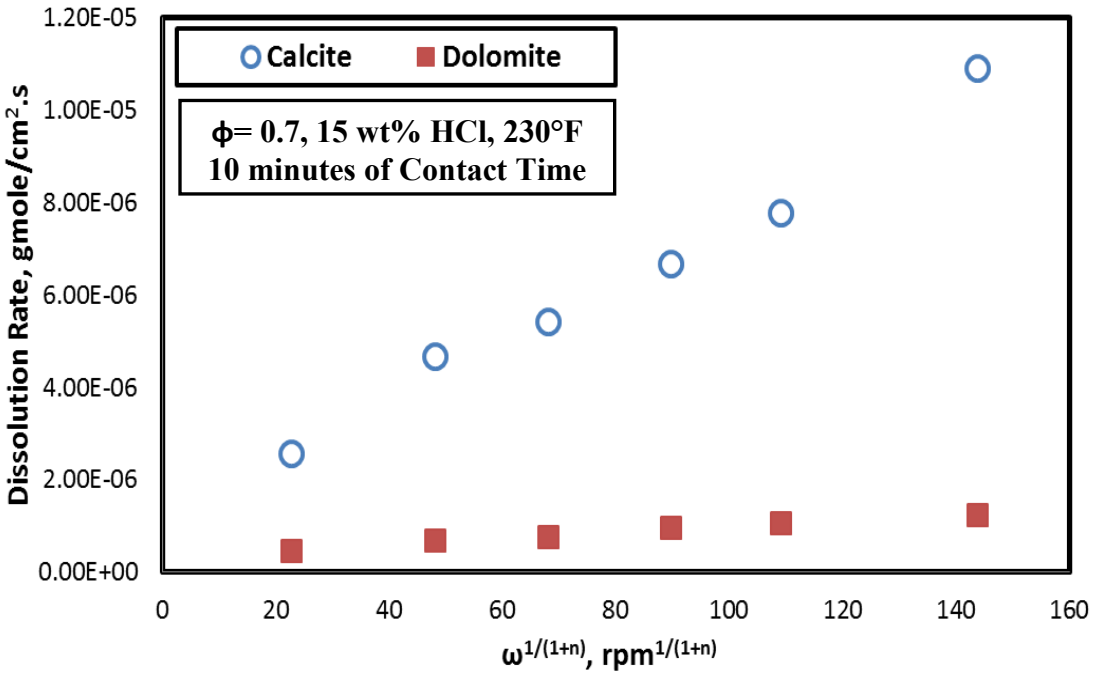

Fig. 4-11: Comparison of dissolution rate of dolomite and calcite in the emulsified acid systems formulated using 1.0 vol% emulsifier at different disk rotational speeds.

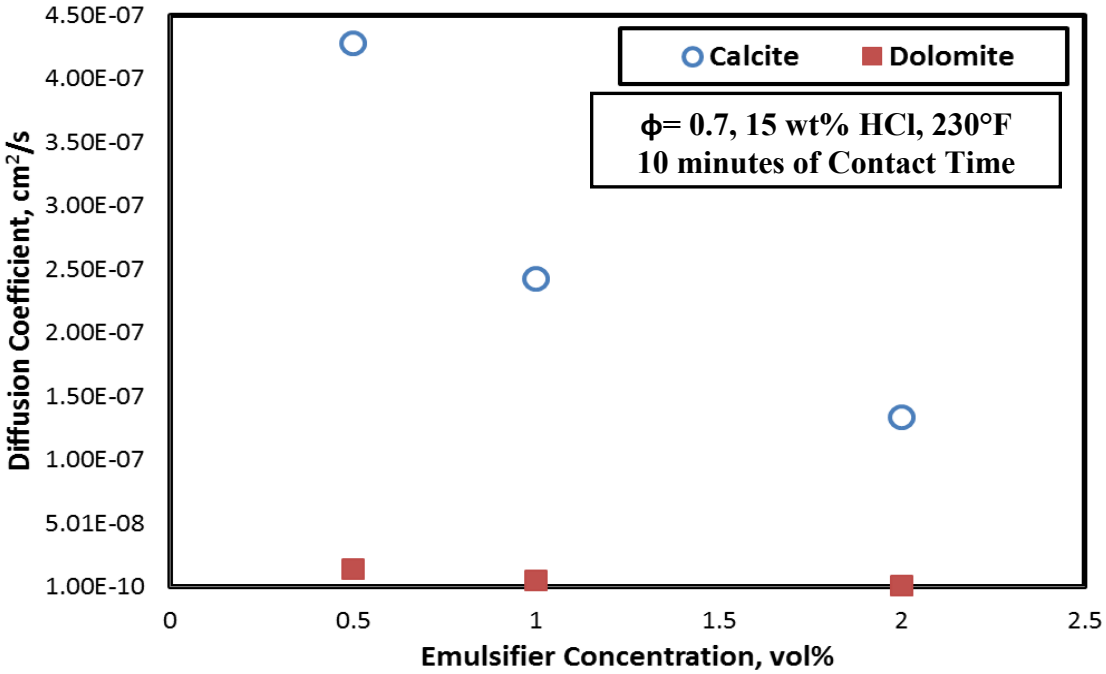

Fig. 4-12: Comparison of diffusion coefficient of emulsified acid when reacted with dolomite and calcite.

5. COREFLOOD EXPERIMENTS USING INDIANA LIMESTONE CORES

5.1 Introduction

Acids are widely used to stimulate oil and gas wells to improve the rate of hydrocarbon production (Al-Anazi et al. 1998; Kasza et al. 2006), and to stimulate disposal wells and water injection wells in order to increase the formation uptake of the injected fluids (Mohammed et al. 1999; Nasr-El-Din et al. 2000). In most carbonate-stimulation treatments, HCl is pumped as the main stimulation fluid. The reaction between HCl and calcite is very fast, and this reaction rate becomes higher at higher downhole temperatures, which results in rapid HCl spending and failure of the treatment (Allen and Roberts 1989; Nasr-El-Din et al. 2003a). Also, regular HCl can cause excessive tubing corrosion, and may form acid/oil sludge in asphaltene-rich crudes.

There are several options to lower the acid spending rate, emulsified acids is one of the most widely used alternatives (Dill 1961; Knox et al. 1964; Crenshaw and Flippen 1968; Nasr-El-Din et al. 2001). For emulsified acids, HCl acid is commonly used in these systems as the internal phase of an oil external emulsion. Emulsified acid combines a relatively high rock-dissolving power with a low acid/rock reaction rate. The most common hydrocarbon that is used as an external phase is diesel, and its main function is to act as a diffusion barrier between acid and rock (Crowe and Miller 1974; Bergstrom and Miller 1975; Hoefner and Fogler 1985; Daccord et al. 1989; Peters and Saxon 1989). This diffusion barrier will result in a reduction in the acid-rock reaction rate, which will help in the creation of deep wormholes (Williams and Nierode 1972;

Guidry et al. 1989; Navarrete et al. 1998a and b), and creation of etched fractured surfaces which enhance well performance (Navarrete et al. 1998a and b; Nasr-El-Din et al. 2006b and 2008b). An acid-diesel emulsion has several advantages (Nasr-El-Din et al. 2000). Besides its slow reaction rate with carbonate rocks, it has a relatively high viscosity. As a result, it has a better sweep efficiency that will improve acid distribution in heterogeneous reservoirs (Buijse and van Domelen 2000). Also, the live acid does not come in contact with well tubulars; therefore, the corrosion level is low.

De Groote (1933) used acid-oil emulsions to remove damage from carbonate rocks, and at the same time, protect the metallic parts of the well from corrosion that may be caused by regular acid. After that, emulsified acid systems were used for different purposes. Davis et al. (1965) used emulsified acid to test the effectiveness of their spearhead film technique.

Emulsified acid systems can be classified, based on the droplet size of the acid, as micro (Hoefner and Fogler 1985) or macro-emulsion (Al-Anazi et al. 1998). Macro emulsions have larger droplet sizes, use smaller amounts of emulsifier, and are the most widely used type in the field (Al-Anazi et al. 1998; Mohamed et al. 1999; Nasr-El-Din et al. 2000; Kasza et al. 2006).

Hoefner et al. (1987) introduced a retarded acid-in-oil micro-emulsion system that had low viscosity, and achieved acid diffusion rates two orders of magnitude lower than regular HCl. Hoefner et al. (1987) found that the decreased acid diffusion delayed the acid spending, and allowed uniform and deep acid penetration in to the formation. Al-Anazi et al. (1998) studied and applied emulsified acid with tight carbonate

reservoirs. The acid-in-diesel emulsion was evaluated for field application and the experimental tests included rheology, thermal stability, compatibility, reactivity with reservoir rocks, and coreflood experiments. Coreflood experiments were performed on reservoir cores at reservoir conditions, and for an acid injection rate range of 0.5-12.0 cm^3/min. Coreflood results showed that the emulsified acid formed deep wormholes in tight carbonate cores.

Bazin and Abdulahad (1999) compared between regular HCl and emulsified acid utilizing coreflood experiments using limestone samples. Bazin and Abdulahad (1999) showed that emulsified acid was an effective stimulation fluid at low injection rates, while at high injection rates regular HCl gave better results. Bazin and Abdulahad (1999) noted the absence of an optimum injection rate for the emulsified acid system used in their study. Lynn and Nasr-El-Din (1999) studied the formation damage associated with water-based drilling fluids and the use of emulsified acid in order to overcome this damage. They found that emulsified acid was capable of penetrating the damaged zone, and achieving negative skin factors, indicating the success of the treatment.

Mohamed et al. (1999) investigated the effectiveness of acid treatments to stimulate power water injectors and saltwater disposal wells. The study was based on conducting coreflood experiments, and analysis of collected field samples. Acid treatments were improved using emulsified acid and in-situ gelled acid as acid diverting stages. Mohamed et al. (1999) concluded that increasing the emulsified acid volume increased the efficiency of the treatment.

Nasr-El-Din et al. (2000) conducted experimental studies to evaluate the use of emulsified acid in stimulation of water disposal wells. Coreflood results showed that the emulsified acid formed deep wormholes in tight carbonate cores, and the size and distribution of wormholes was dependent on the acid injection rate, acid volume, and initial core permeability.

Buijse and van Domelen (2000) studied the application of emulsified acid in the stimulation of heterogonous carbonate reservoirs. They compared the efficiency of emulsified acid with that of regular HCl acid. Buijse and van Domelen (2000) found that acid-in-oil emulsions are effective stimulation fluids in large intervals, where streaks of high-permeability can act as thief zones. Lynn and Nasr-El-Din (2001) conducted a core-based comparison of the reaction characteristics of emulsified acid and in-situ gelled acid. The characteristics that were compared included wormhole propagation rates, volumes of carbonate consumed by acid, wormhole geometric features, and pressure response during injection. Lynn and Nasr-El-Din (2001) found that in-situ gelled acid enhanced the permeability more significantly than emulsified acid, but emulsified acid was more stable at high temperatures, utilized less volume to achieve penetration, and achieved a higher rate of wormhole propagation with no residual material in the generated wormhole.

Nasr-El-Din et al. (2001) conducted experimental studies to evaluate the influence of temperature on emulsified acid stability and retardation effect, and to study the effects of various acid additives on emulsion stability. The acid (28 wt% HCl) to diesel volume ratio was 70 to 30. Coreflood tests, conducted using tight dolomite cores,

indicated that emulsified acid created deep wormholes, which significantly increased the permeability of the treated cores.

Kasza et al. (2006) mentioned that stimulation of a high temperature dolomite formation, using straight HCl was not effective. Emulsified acid was selected to be an alternative to regular HCl, and the field results indicated that the treatments were successful. Both rotating disk and coreflood experiments indicated the retarded nature of the emulsified acid. Al-Harbi et al. (2006) evaluated acid treatments for water injection wells. These wells were stimulated using regular HCl and emulsified acid with foamed viscoelastic water (for diversion). They concluded that increasing the volume of emulsified acid in acid treatments enhanced the well's injectivity. Abdel Fatah and Nasr-El-Din (2010) utilized HCl emulsified in xylene, instead of diesel, to stimulate wells and at the same time to remove asphaltene deposition. Acid concentration was 15 wt% HCl, and the emulsified acid in xylene had a lower viscosity and was stable for shorter periods of time. The emulsified acid in xylene was applied in 4 wells with success and had no problems. Appicciutoli et al. (2010) showed that emulsified acid systems can be mixed with custom-tailored asphaltene-solving blends, and this system provided the desired benefits for matrix acidizing, such as stability, high viscosity, and slow reaction, and at the same time it was able to remove asphaltene.

5.2 Experimental Studies

5.2.1 Materials

The emulsions were prepared using diesel and an acid solution (HCl and water). The water used throughout the experiments was de-ionized water, obtained from a water

purification system that has a resistivity of 18.2 MΩ.cm at room temperature. Hydrochloric acid was titrated using 0.1 N sodium hydroxide solution, and the acid concentration was found to be 36.8 wt%. Additives, such as corrosion inhibitor and emulsifier, were added to the acid solution and the diesel, respectively. The emulsifier, which was used throughout this study, was a cationic emulsifier and consists of a blend of cationic surfactant, isopropanol, and petroleum distillate.

5.2.2 Procedures

The acid solution was prepared by mixing corrosion inhibitor, de-ionized water and HCl acid. The diesel solution was prepared by adding emulsifier to diesel oil, and mixing at a high speed. Then, the acid solution was added slowly to the diesel solution and mixed at high speed (1200 rpm) for 30 min. After that, the electric conductivity of the final mixture was measured in a conductivity cell to check the quality of the final emulsion. If the electric conductivity is nearly equal to 0, then we have a good emulsified acid. In case there is some conductivity, extend mixing to 1 hour at maximum possible speed (1200 rpm), and measure conductivity again, to be sure of the quality of the prepared emulsified acid.

5.2.3 Equipment

The coreflood setup, described in **Fig. 5-1**, was constructed to simulate a matrix stimulation treatment. A back pressure of 1100 psi was applied to keep most of the CO_2 in solution. A pressure transducer was connected to a computer to monitor the pressure drop across the core during the experiments. A Teledyne ISCO D-series D1000 precision syringe pump that had a maximum allowable working pressure of 2000 psi, was used to

inject the emulsified acid into the core. The pH values for collected effluent samples were measured using an Orion PrepHecT Ross Electrode. The calcium concentration in the core effluent samples was measured using the Inductively Coupled Plasma (ICP) technique (PerkinElmer Optical Emission Spectrometer, Optima 7000 DV) where the spectral range is 160-900 nm with resolution of < 0.009 nm @ 200 nm.

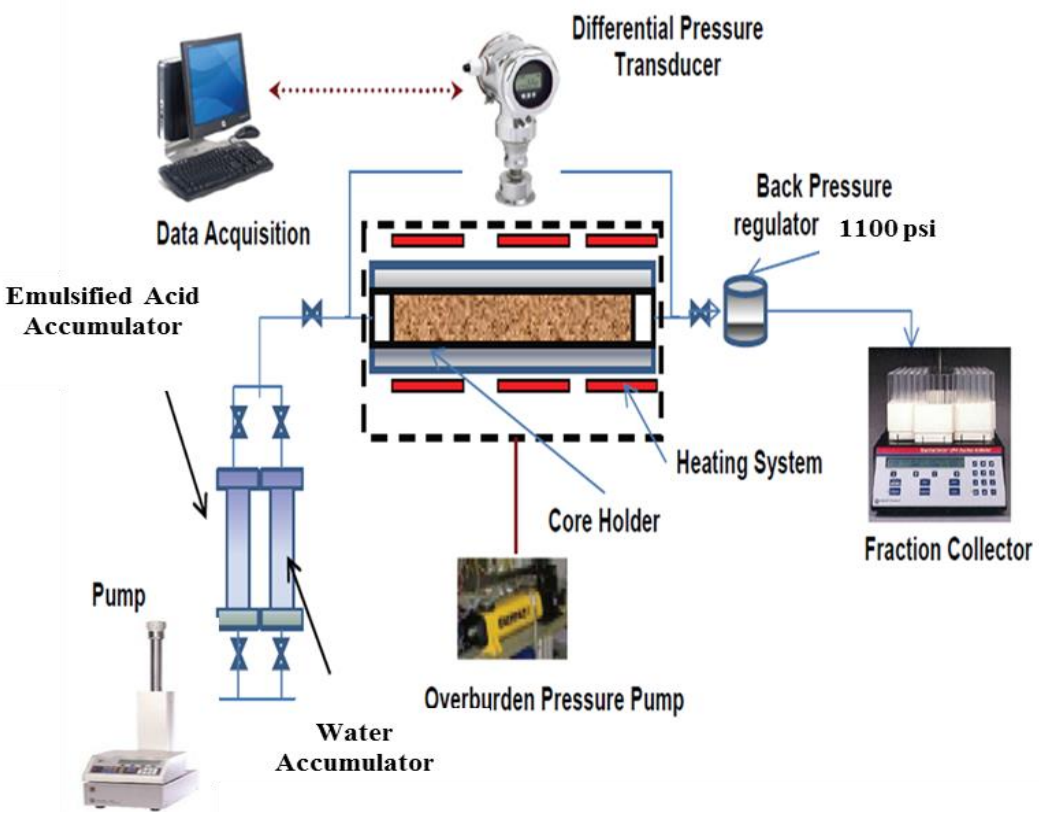

Fig. 5-1: Coreflood setup.

5.3 Results and Discussion

5.3.1 Coreflood Study

The coreflood experiments were performed using both low and high permeability Indiana limestone core samples which were fully saturated with de-ionized water. The initial permeabilities of both low and high permeability Indiana limestone core samples are represented in **Table 5-1. Table 5-1** gives a summary of all the data for the 1.5 in. diameter and 6 in. long core samples including core porosity, initial and final permeabilities, injection rate, and acid volume to achieve breakthrough. 12 coreflood runs were performed using emulsified acid formulated using 1.0 vol% emulsifier; five for high permeability core samples (initial permeability ranged from 48 to 61 md) and five for low permeability cores (initial permeability ranged from 1 to 4.5 md). These coreflood runs were performed at injection rates ranging from 0.5 to 10 cm^3/min. These runs were performed in order to test the effect of the injection rate and rock permeability on emulsified acid performance, specifically, the acid volume to breakthrough, and the resulted wormhole characteristics. The effect of changing emulsifier concentration on the performance of emulsified acid was studied using emulsifier concentrations of 0.5, 1.0 and 2.0 vol % emulsifier, with low permeability Indiana limestone cores. All coreflood runs were performed at a temperature of 300°F. For each coreflood experiment, the pressure drop across the core was plotted using Lab-View software. Samples of the coreflood effluent fluid were collected and analyzed using the ICP to measure the calcium concentration. The pH value and the density of the effluent samples were measured.

Table 5-1: Data for 6 in. long coreflood experiments.

Run #	Core Porosity, %	$K_{initial}$, md	$Q_{Injection}$, cm^3/min	Emulsifier Conc., vol%	PV to BT	K_{final}, md	$K_{final}/K_{initial}$
1	10.42	1.1	0.5	1	1.098	1092	992.7
2	12.21	3	1.0	1	0.94	2535	845
3	9.3	1.3	2.0	1	0.89	974	749.2
4	12.4	4.55	5	1	0.69	878	195.1
5	11.92	4.1	10	1	0.885	950	231.7
6	15.13	48.3	0.5	1	1.35	2885	59.7
7	13.4	49.6	1.0	1	1.304	1474	29.7
8	15	60.6	2.0	1	1.253	1285	21.2
9	14.42	47.03	5	1	1.115	1100	23.4
10	13.87	49.1	10	1	0.726	700	14.3
11	10.24	0.96	1	0.5	0.618	980	1021
12	9.35	1.03	1	2.0	1.16	1050	1019

5.3.2 Low Permeability Indiana Limestone Cores

Fig. 5-2 shows the pressure drop across the core during the injection of 1.0 vol% emulsified acid at an injection rate of 1 cm^3/min and 300°F. The pressure drop initially was constant during the injection of de-ionized water. At the instant where emulsified acid injection started, the pressure drop initially increased, then the pressure drop started to decrease as the emulsified acid penetrated the core deeper. The first increase in the pressure drop across the core can be referred to the high viscosity of emulsified acid injected into the core. As the calcite reacted with the emulsified acid, calcite dissolution started and the calcium concentration of the emulsified acid effluent started to increase. At the same time the calcite was reacting with emulsified acid, wormholes started to form and penetrate the core. These created wormholes caused the pressure drop to decrease. The increase, stabilization or decrease in pressure drop, depends mainly on the extent of dissolution in the length of the core. When the created wormholes extend from

the core inlet face to the core outlet, emulsified acid breakthrough occurs. After acid breakthrough, 10 vol% mutual solvent was injected in order to break any remaining emulsions and to remove the remaining hydrocarbon phase (diesel) from the core. After that, de-ionized water was injected for several pore volumes, the core was left to cool down and the final permeability of the core was measured using de-ionized water at room temperature. The final permeability of the core was found to be 2535 md (**Table 5-1**), while the initial core permeability was 3.0 md (**Table 5-1**). The ratio of the final to the initial permeability of the core was found to be 845, which indicates that the emulsified acid was effective in creating wormholes that extended through the core length and enhanced the permeability of the core.

Fig. 5-3 shows the calcium concentration in the core effluent samples for the experiment performed at an emulsified acid injection rate of 1.0 cm^3/min. The calcium concentration reached a maximum value of 60,750 mg/l. **Fig. 5-4** shows the density and pH of the coreflood effluent samples for the same experiment. The density of the effluent samples increased due to the presence of calcium ions in effluent samples solution. The pH was around 7 at the start of injection (injection of de-ionized water) then decreased with the injection of emulsified acid until it reached zero and increased again as injection of de-ionized water started.

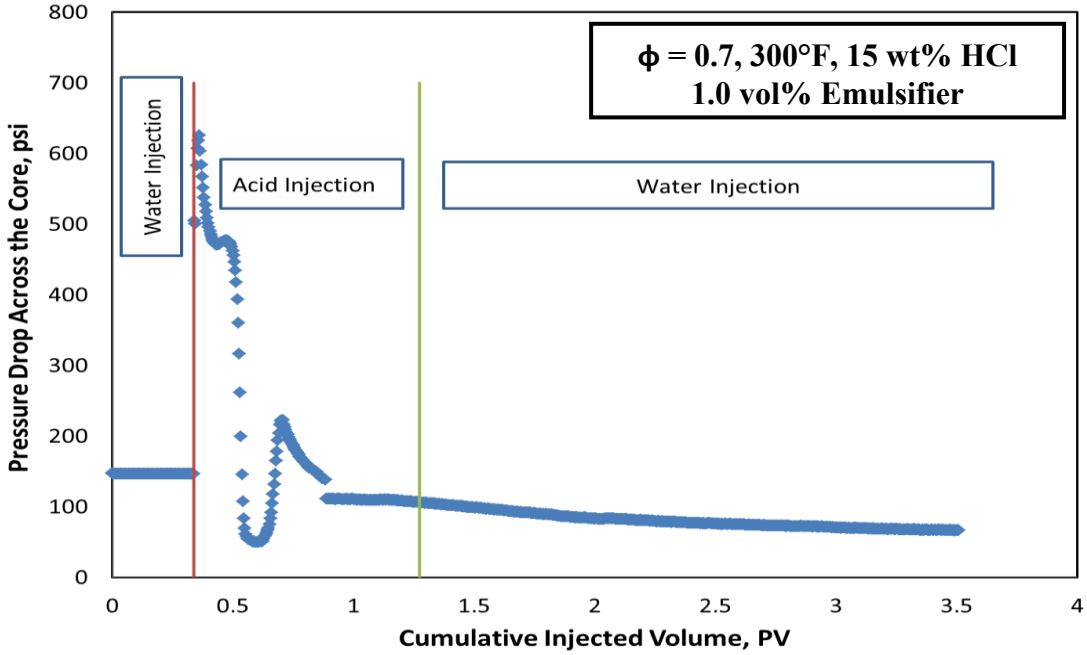

Fig. 5-2: Pressure drop across low permeability Indiana limestone core for an injection rate of 1.0 cm^3/min & 300°F.

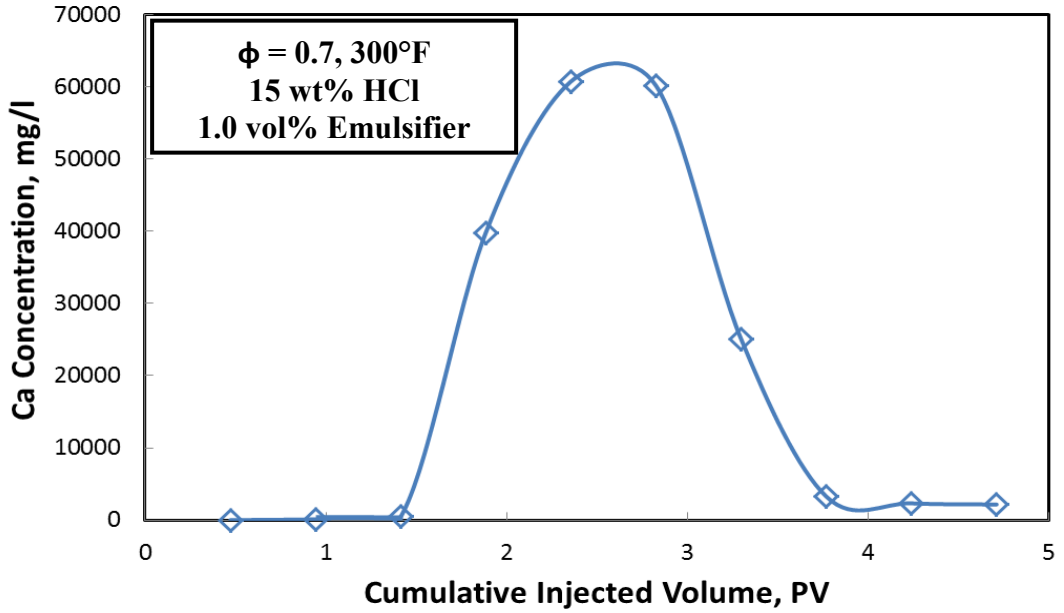

Fig. 5-3: Calcium concentration in the core effluent samples for an injection rate of 1 cm^3/min & 300°F (low permeability Indiana limestone).

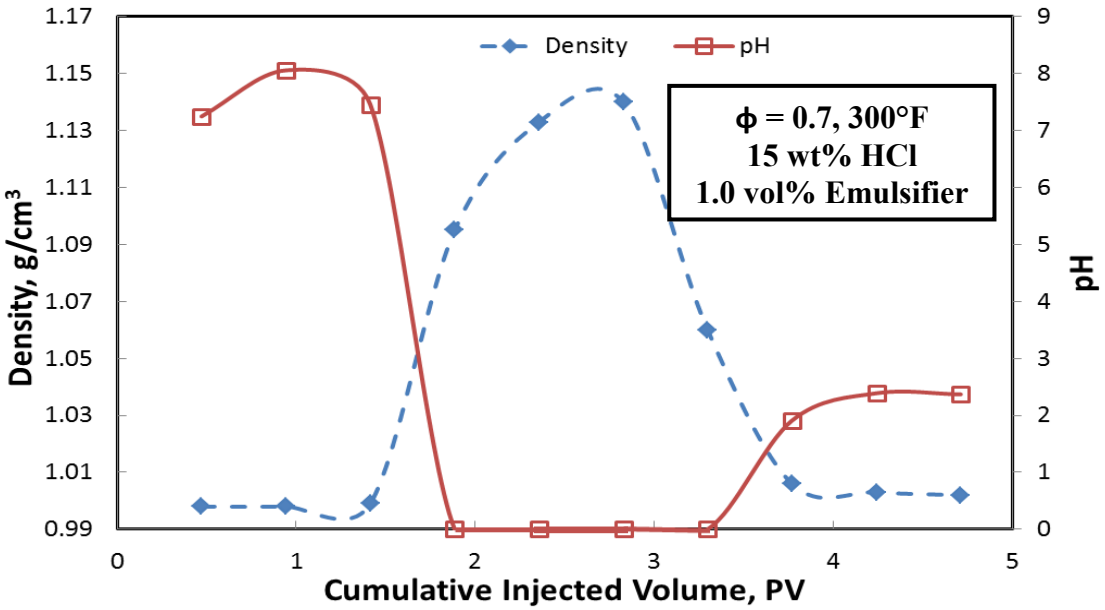

Fig. 5-4: Density and pH of the core effluent samples for an injection rate of 1.0 cm^3/min & 300°F (low permeability Indiana limestone).

Based on the volume of acid to breakthrough, emulsified acid injection rate of 5 cm^3/min achieved the minimum acid volume to breakthrough. In other words, emulsified acid injection rate of 5 cm^3/min was found to be the optimum injection rate. **Fig. 5-5** shows the pressure drop across the core during acid injection at a rate of 5 cm^3/min. At emulsified acid injection rate of 5 cm^3/min, the pressure drop across the core after starting emulsified acid injection was somewhat different from the experiment performed at an injection rate of 1.0 cm^3/min. The increase in pressure drop across the core (**Fig. 5-5**) was small compared to the pressure drop across the core in case of 1 cm^3/min emulsified acid injection rate. The pressure drop across the core reached 200 psi and then started to decrease. The reason for this less increase in the pressure drop, although the injection rate is higher, this can be related to the rheological behavior of

emulsified acid. As the injection rate increases, the shear rate increases (Gomaa and Nasr-El-Din 2010). From the rheological study, the emulsified acid was found to be a non-Newtonian shear thinning fluid. This means that as the shear rate increases, the apparent viscosity of emulsified acid decreases, resulting in less pressure drop increase at high injection rate than what was measured at the low injection rate (low shear rate). The maximum pressure drop across the core in the case of the emulsified acid injection rate of 1 cm^3/min was around 3 times the maximum pressure drop in the case of emulsified acid injection rate of 5 cm^3/min. After emulsified acid breakthrough occurred, 10 vol% mutual solvent was injected in order to break any remaining emulsions and to remove the remaining hydrocarbon phase (diesel) from the core. After that, de-ionized water was injected for several pore volumes, the core was left to cool down and the final permeability of the core was measured using de-ionized water at room temperature. The final permeability of the core was found to be 879 md (**Table 5-1**), while the initial core permeability was 4.55 md (**Table 5-1**). The ratio of the final to the initial permeability of the core was found to be 195, which indicates that the emulsified acid was effective in creating wormholes that extended through the core sample and enhanced the permeability of the core.

Fig. 5-6 shows the calcium concentration in the core effluent samples for the experiment performed at an emulsified acid injection rate of 5.0 cm^3/min. **Fig. 5-7** shows the density and pH of the coreflood effluent samples for the same experiment. As the emulsified acid penetrated and reacted with the rock, the density of the effluent samples increased due to the presence of calcium ions in solution.

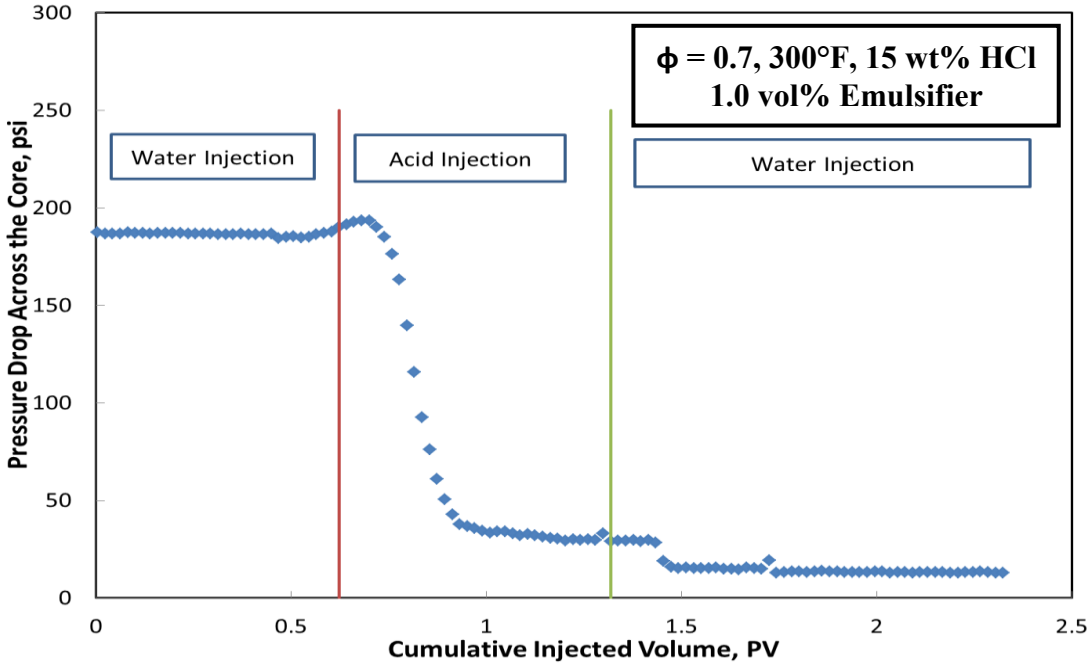

Fig. 5-5: Pressure drop across low permeability Indiana limestone core for an injection rate of 5.0 cm^3/min & 300°F.

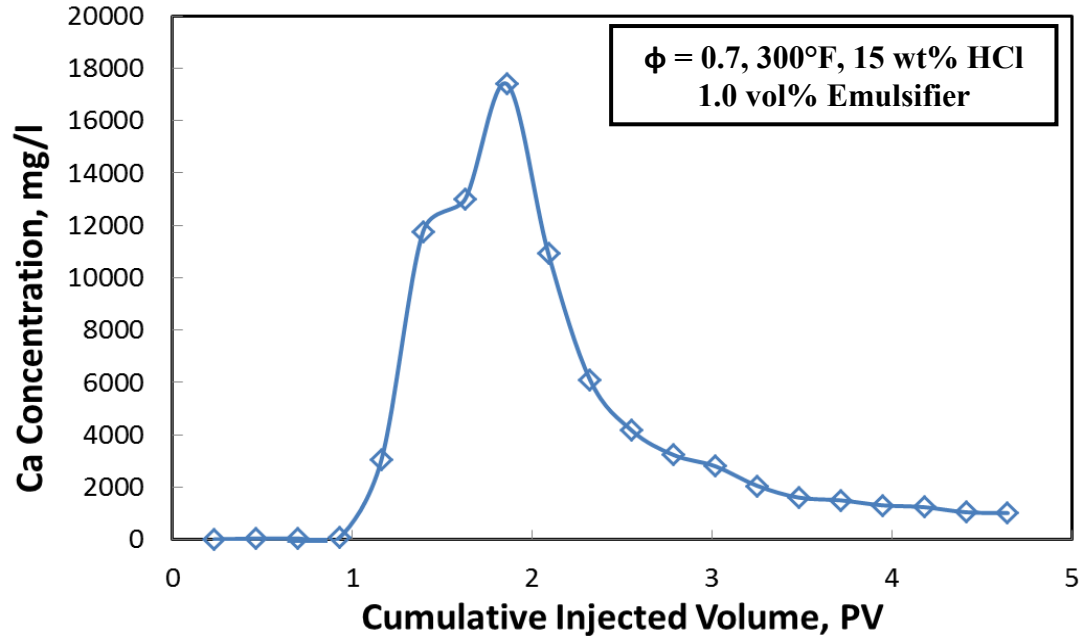

Fig. 5-6: Calcium concentration in the core effluent samples for an injection rate of 5.0 cm^3/min & 300°F ((low permeability Indiana limestone).

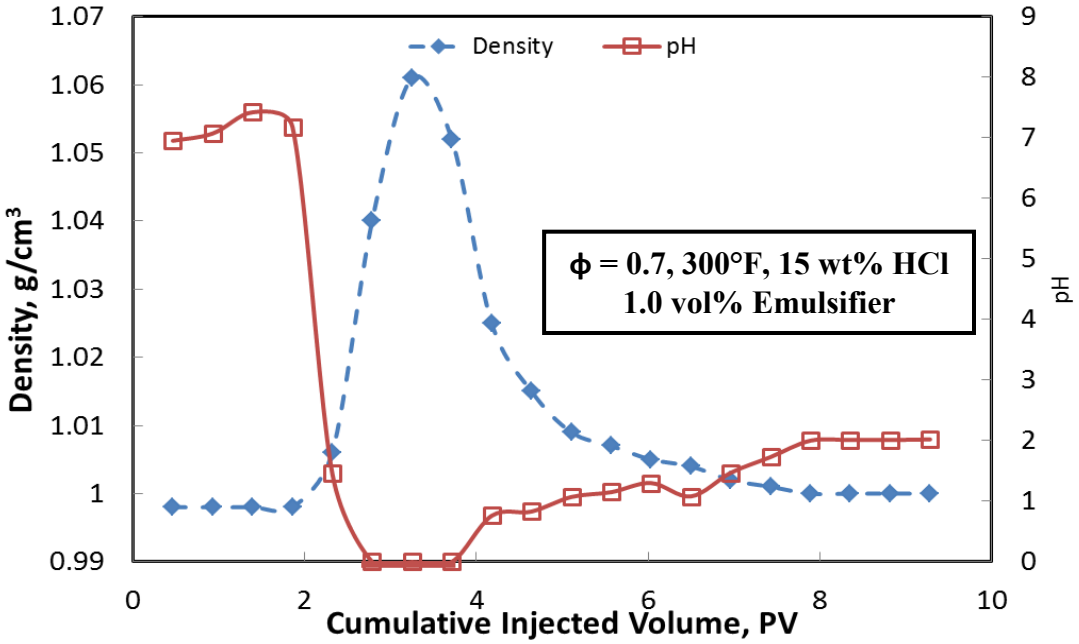

Fig. 5-7: Density and pH of the core effluent samples for an injection rate of 5.0 cm^3/min & 300°F (low permeability Indiana limestone).

A summary of all coreflood experiments performed using low permeability Indiana limestone cores, and for different emulsified acid injection rates, can be used to evaluate the performance of emulsified acid. The pressure drop encountered during emulsified acid injection at different rates is represented by **Fig. 5-8. Fig. 5-8** shows that, during the first water injection stage, the pressure drop increased as the injection rate increased, due to the increase in friction losses. Upon injection of emulsified acid, the pressure drop was dependent on the acid viscosity, which was a function of the shear rate inside the core. The shear rate itself is function of injection rate, porosity, and core permeability. In the case of 1.0 cm^3/min injection rate, the core permeability was 3 md. The combination of this low injection rate and permeability resulted in a low shear rate,

and the resulted in a higher viscosity and a higher pressure drop (upon injection of emulsified acid) than the other cases performed at higher emulsified acid injection rates. At higher injection rates (2 to 10 cm^3/min), the shear rate increases as a result of the higher injection rates, resulting in a lower viscosity and hence, a lower pressure drop than in the case of 1.0 cm^3/min injection rate.

The change in calcium concentration for all cases is represented by **Fig. 5-9**. The calcium concentration increased with the injection of acid then decreased again with the injection of water. As the injection rate affects the amount of calcium concentration in the sample effluent fluid. The calcium concentration is directly related to the amount of rock dissolved by acid, and this amount increases as the acid/rock contact time increases. The highest peak in calcium concentration curve was noticed at an injection rate of 1.0 cm^3/min, while the lowest peak was noticed at an injection rate of 5 cm^3/min.

The change in effluent fluid density and pH can be shown in **Figs. 5-10 and 5-11**. From **Fig. 5-10**, the density of effluent samples changed with the rate of fluid injected in the core. The density of effluent samples started at a value around 1.0 g/cm^3 then increased due to the dissolution of calcium upon the reaction of acid and rock. After breakthrough, and at the start of the second water injection stage, effluent sample density started to decrease to a value slightly greater than 1.0. **Fig. 5-11** shows that pH value started near 7.0, which is the pH value of the injected water. Then, the pH started to decrease with acid injection, until acid breakthrough occurred and after that water injection started again and pH started to increase.

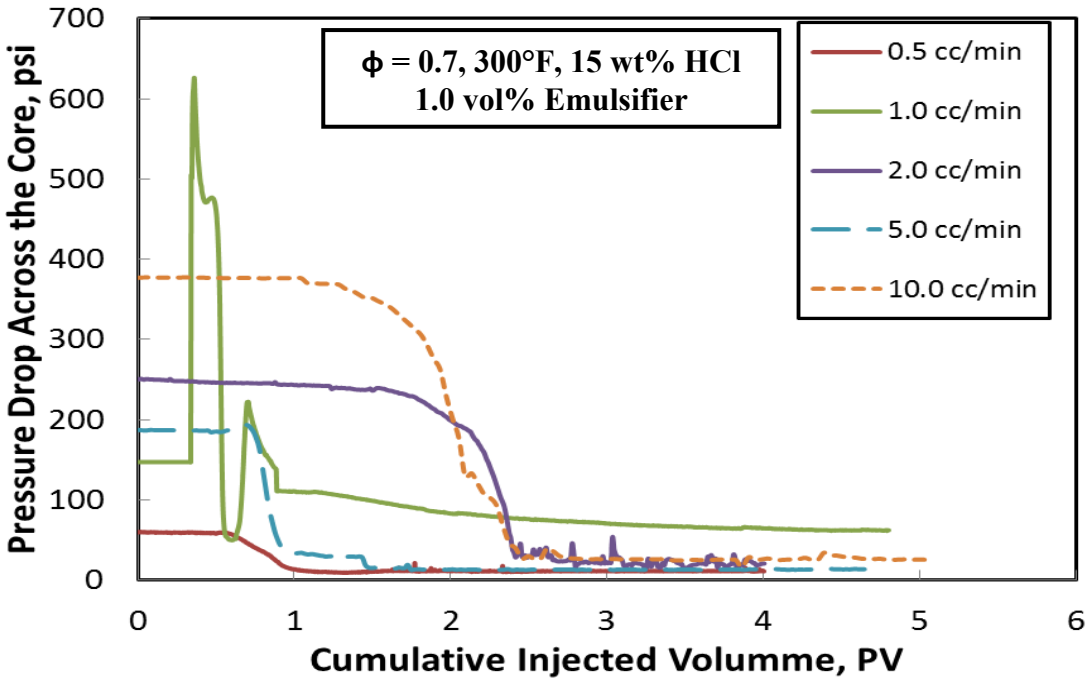

Fig. 5-8: Pressure drop for different injection rates – low permeability cores.

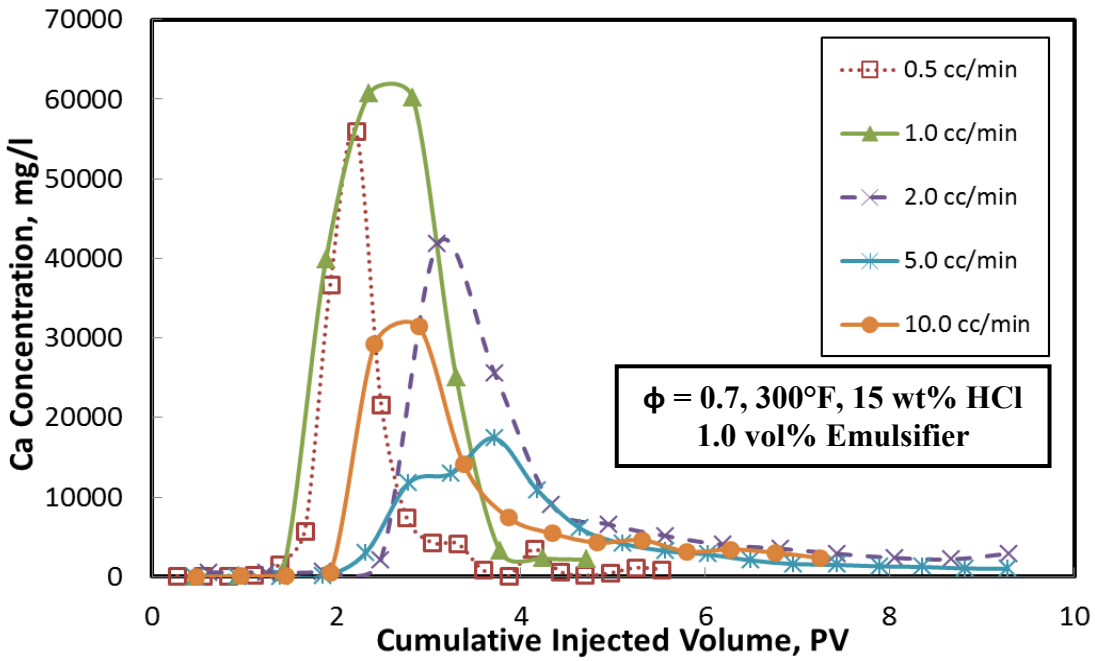

Fig. 5-9: Calcium concentration for different injection rates – low permeability cores.

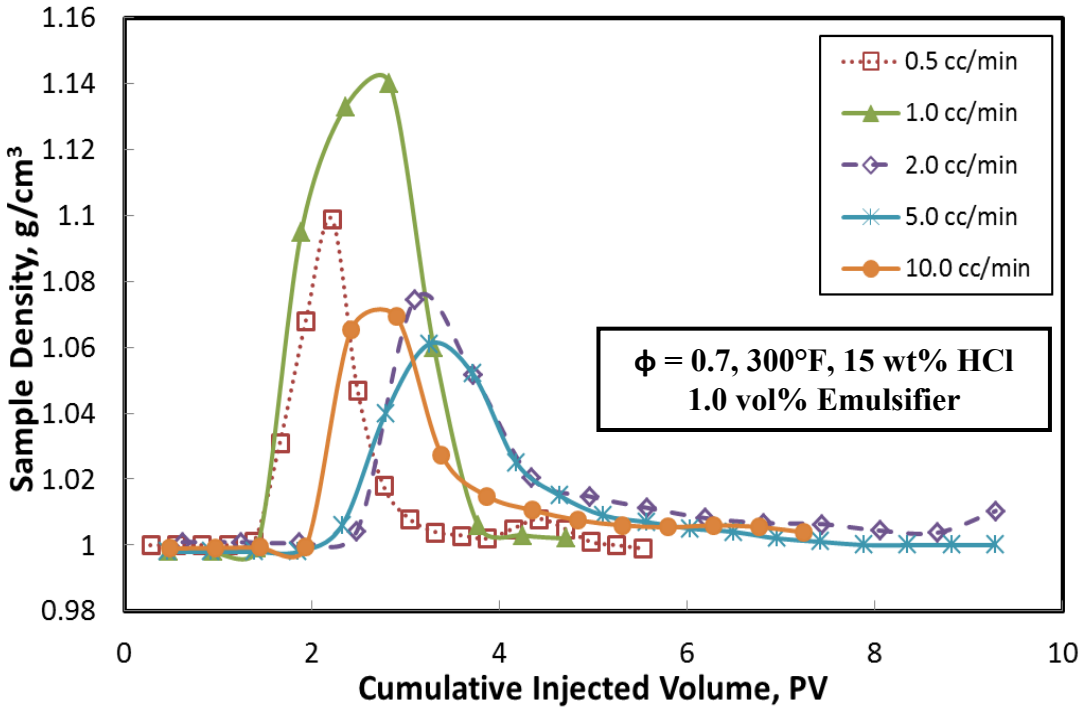

Fig. 5-10: Density of effluent samples for different injection rates – low permeability cores.

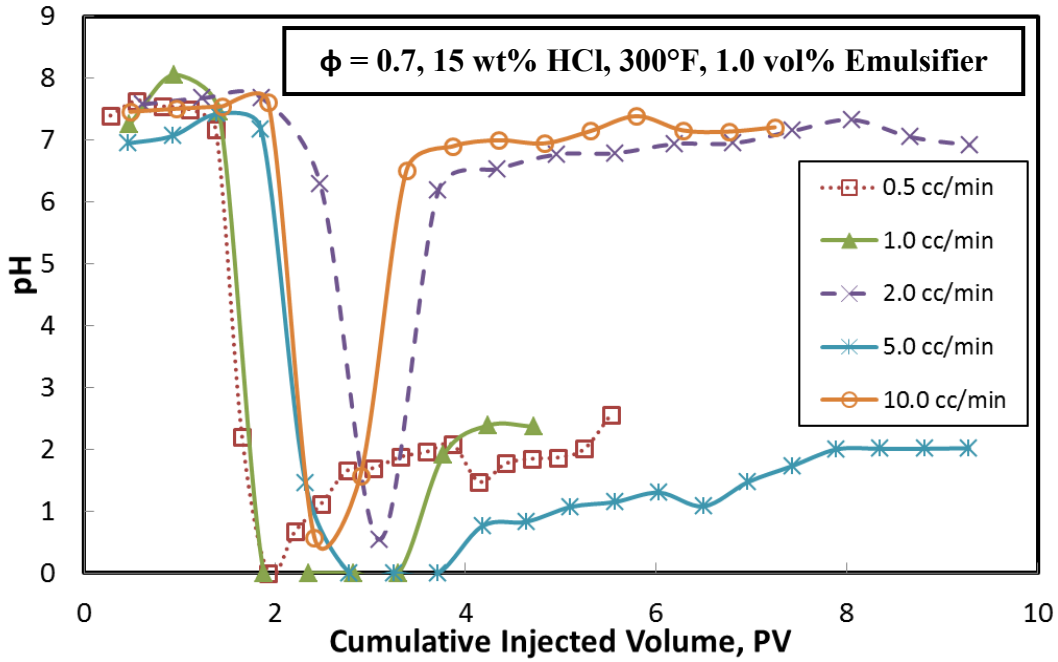

Fig. 5-11: pH of effluent samples for different injection rates – low permeability cores.

5.3.3 High Permeability Indiana Limestone Cores

The pressure drop across the core, recorded during acid injection at acid injection rates of 0.5, 1.0, 2.0, 5.0, and 10 cm^3/min can be shown in **Fig. 5-12a through 5-12e. Fig. 5-12a** shows the pressure drop across the core during the injection of 15 wt% HCl emulsified acid at an injection rate of 0.5 cm^3/min at 300°F. The pressure drop initially was constant at a value around 9.0 psi during the injection of de-ionized water. As the emulsified acid was injected into the core, the pressure drop across the core slightly increased due to the high viscosity of the injected emulsified acid. Emulsified acid breakthrough occurred after the injection of 1.35 PV of emulsified acid. As emulsified acid was injected in the core, it started to react with calcite and, as a result, the calcium concentration of the effluent fluid started to increase. At the same time, wormholes started to form and penetrated the core. These wormholes caused the pressure drop to slightly decrease, but the final pressure drop across the core was higher than the initial pressure drop recorded during de-ionized water injection. After that, de-ionized water was injected in the core, and the final pressure drop stabilized approximately at 11.6 psi. The final pressure drop was higher than the initial pressure drop before acid injection. This may be caused by the remaining diesel or emulsion inside the core. So, 10 vol% mutual solvent solution was injected in order to break down the remaining emulsion, and the core was left to cool down and the final permeability of the core was measured. The final permeability of the core sample was found to be 2885 md (**Table 5-1**). The ratio of the final permeability to the initial permeability of the core was calculated and presented in **Table 5-1**. The data presented in **Table 5-1** shows that the ratio of the final to the

initial permeability was 59.7, and this indicates that the final permeability was enhanced due to the creation of wormholes, as a result of the emulsified acid injection into the core.

Fig. 5-12e shows the pressure drop across the core during injection of emulsified acid at a rate of 10 cm^3/min. The pressure drop during initial stage of water injection was high, as a result of the pressure drop losses due to the friction losses accompanying the high injection rate. The pressure drop behavior after starting acid injection was somewhat different from experiments performed at low injection rates (0.5 and 1.0 cm^3/min). The pressure drop started to decrease with the introduction of the emulsified acid into the core sample. As the emulsified acid was injected into the core, it started to react with calcite and, as a result, calcium concentration of the effluent fluid started to increase. At the same time, wormholes started to form and deeply penetrated the core. These wormholes work as paths for the fluid to flow through with less resistance. The initial pressure drop encountered during water injection was 34 psi, while the final pressure drop after emulsified acid breakthrough was 14 psi. The final pressure drop across the core was less than the initial pressure drop recorded during the initial stage of de-ionized water injection indicating the final permeability is greater than the initial permeability. After acid breakthrough occurred, 10 vol% mutual solvent in water was injected to remove the remaining diesel and emulsion. The final permeability was measured using the coreflood setup after the core was left to cool down. The final permeability was found to be 700 md, and the ratio of the final to the initial permeability

was 14.3 (**Table 5-1**) indicating an enhancement of the core permeability through the creation of deeply penetrating wormholes.

The initial and final permeabilities for all cores, treated with emulsified acid at different injection rates, are given in **Table 5-1**. The emulsified acid was successful in creating wormholes and the final permeability was enhanced at all acid injection rates. Also, the increase in permeability was higher in cores treated with emulsified acid at low injection rates; this will be discussed with the CAT scan images of the core after acid breakthrough occurred.

Fig. 5-13 shows the calcium concentration in the core effluent samples for coreflood experiments performed using water-saturated Indiana limestone core samples. The calcium concentration increased with the injection of emulsified acid then decreased again with introduction of de-ionized water into the core. The injection rate has a significant effect on the calcium concentration in the core effluent samples, and hence the amount of rock dissolved during emulsified acid injection. This significant effect is related to the dependence of the number and size of the created wormholes on the contact time between emulsified acid and rock which depends mainly on the injection rate of the emulsified acid.

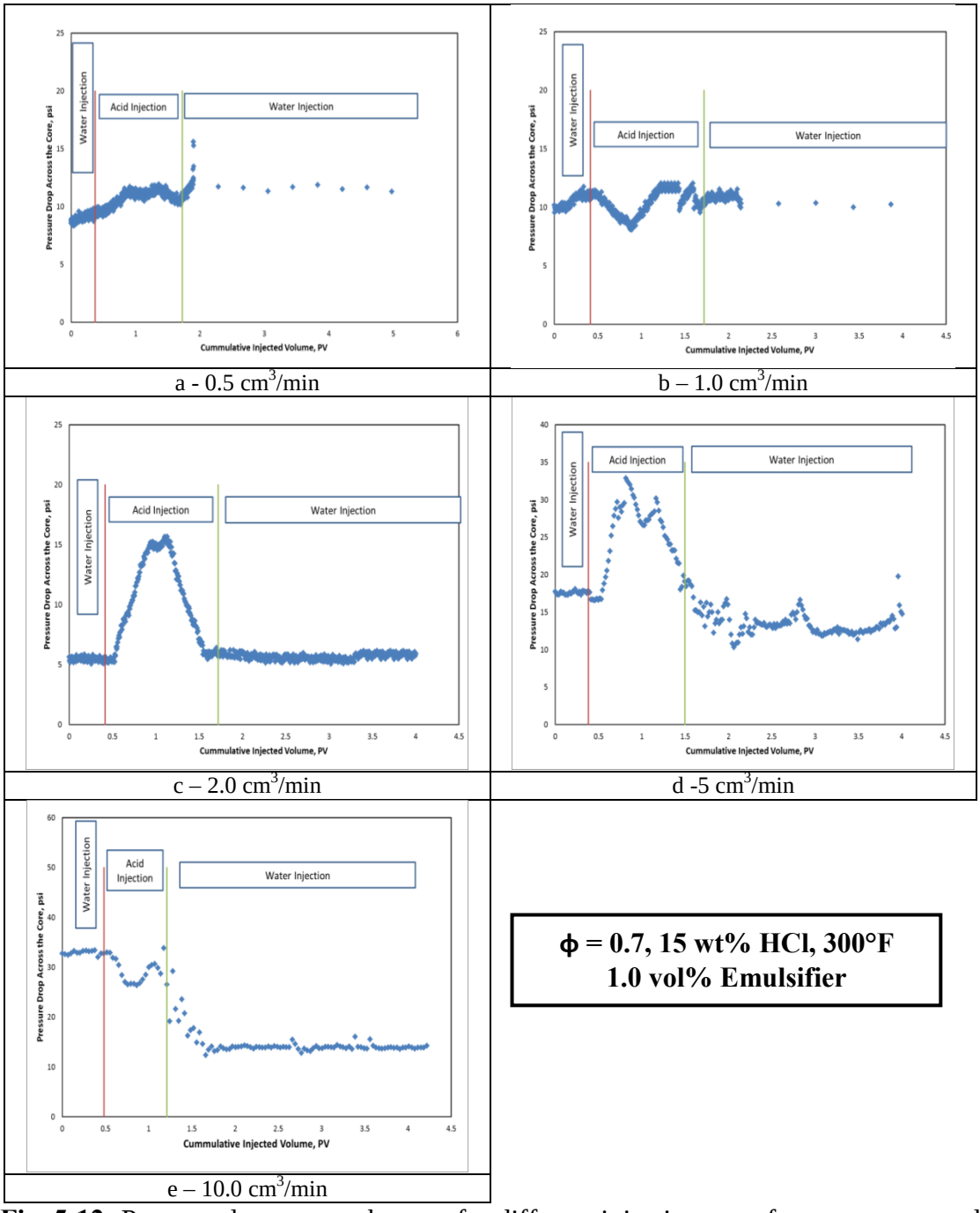

Fig. 5-12: Pressure drop across the core for different injection rates for water-saturated limestone cores.

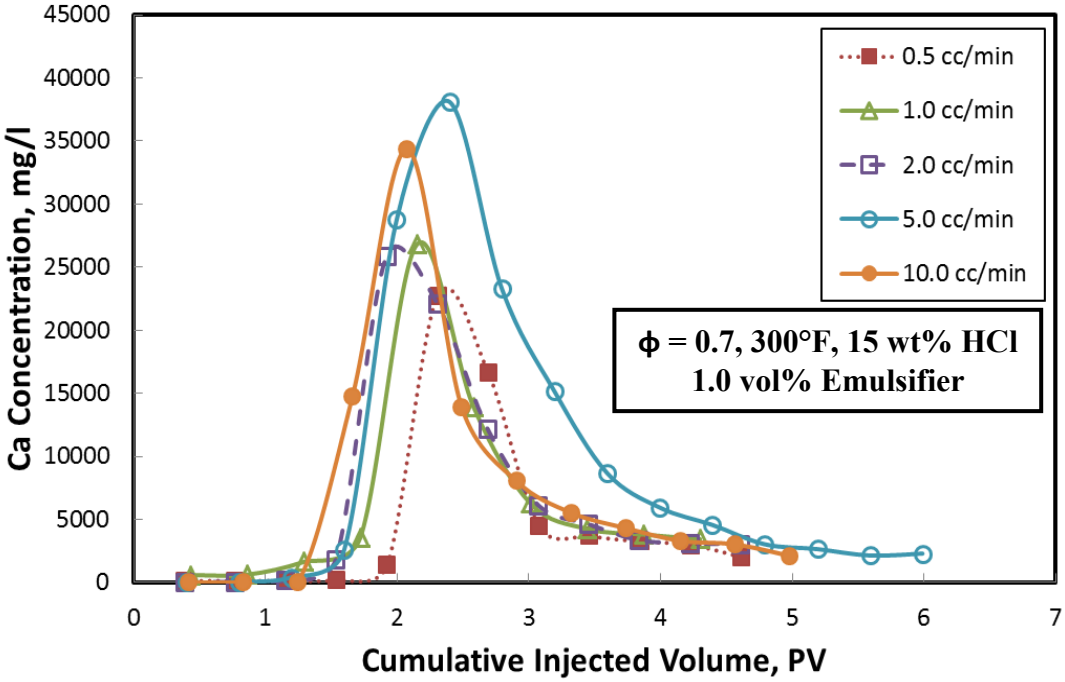

Fig. 5-13: Calcium concentration for different injection rates – high permeability cores

The change in the density and pH in the core effluent is shown in **Figs. 5-14** and **5-15,** respectively. From **Fig. 5-14**, the density of effluent samples changed with the injection rate of emulsified acid. The density of effluent samples started at value of 1.0 g/cm^3, and then increased due to the dissolution of calcite upon the reaction of emulsified acid and calcite. After emulsified acid breakthrough occurred, and with the second water injection stage, the density of the effluent fluid samples started to decrease to a value slightly greater than 1.0. **Fig. 5-15** shows that pH value started at nearly pH of 7.0, which is the pH value of the injected water. Then, the pH started to decrease with emulsified acid injection, until acid breakthrough occurred, and after that de-ionized water injection started again and pH started to increase.

The acid concentration in the effluent fluid samples was measured for effluent fluid samples collected in experiments performed using emulsified acid and cores saturated with 100% water at injection rates of 0.5 and 2.0 cm^3/min. 1M solution of sodium hydroxide (NaOH) was added to 1.0 ml of acid solution from effluent sample. For the two sets of experiments, only 1 sample in each set contained live acid. For the other samples collected in both experiments, the acid concentration was found to be zero. The acid concentration in sample No. 7 for the experiment performed at injection rate of 0.5 cm^3/min was 0.813 wt%, and in sample No. 5 for the experiment performed at injection rate of 2.0 cm^3/min was 0.582 wt%. These results indicate that the acid was consumed in the core samples and no live acid was collected in core effluent fluid samples.

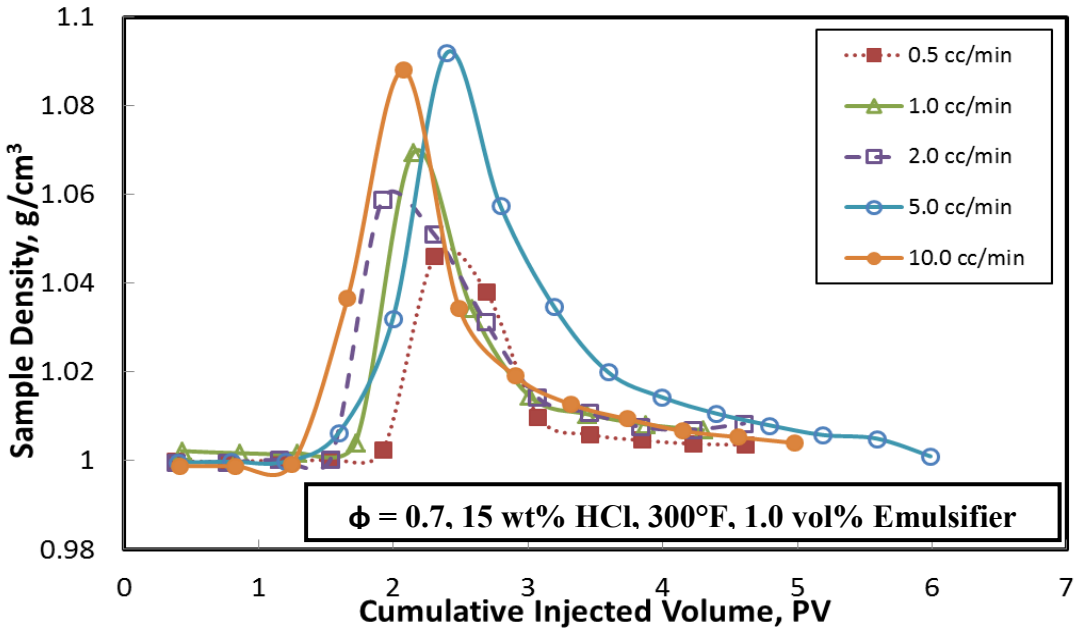

Fig. 5-14: Density of effluent samples for different injection rates – high permeability cores

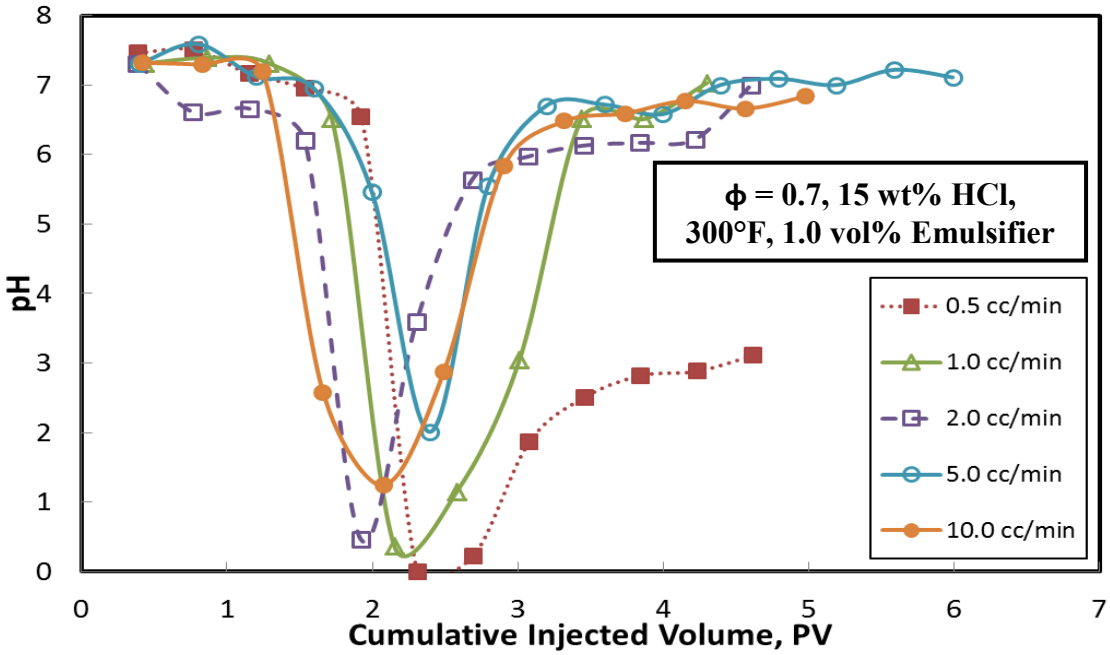

Fig. 5-15: pH of effluent samples for different injection rates – high permeability cores

5.3.4 Effect of Emulsifier Concentration on Performance of Emulsified Acid

The effect of changing the emulsifier concentration on the performance of emulsified acids was studied using low permeability Indiana limestone cores. The experiments were conducted at the same emulsified acid injection rate, 1.0 cm^3/min, but for different emulsifier concentrations of 0.5, 1.0, and 2.0 vol%.

The pressure drop encountered during emulsified acid injection at different emulsifier concentrations is represented by **Fig. 5-16.** For 0.5 vol% emulsifier, the pressure drop was lower, because of the lower viscosity of the formulated emulsified acid. While, for 2.0 vol% emulsifier, the pressure drop was lower than that of 1.0 vol% emulsifier because the core permeability was less, and so the shear rate was higher, resulting in less viscosity and less pressure drop across the core.

The change in calcium concentration for all cases is represented by **Fig. 5-17**. The highest peak was noticed for an emulsifier concentration of 1.0 vol%, while the lowest peak was noticed for an emulsifier concentration of 0.5 vol%. The change in effluent fluid density and pH can be shown in **Figs. 5-18 and 5-19**. From **Fig. 5-18**, the density of coreflood effluent samples changed with the amount of emulsifier concentration used to prepare the emulsified acid. The density of the effluent fluid samples collected during the injection of emulsified acid prepared at 1.0 vol% emulsifier, showed the highest density, indicating more dissolved calcium. **Fig. 5-19** shows that pH value started near 7.0, which is the pH value of the injected water. Then, the pH started to decrease with acid injection, until acid breakthrough occurred and after that water injection started again and pH started to increase.

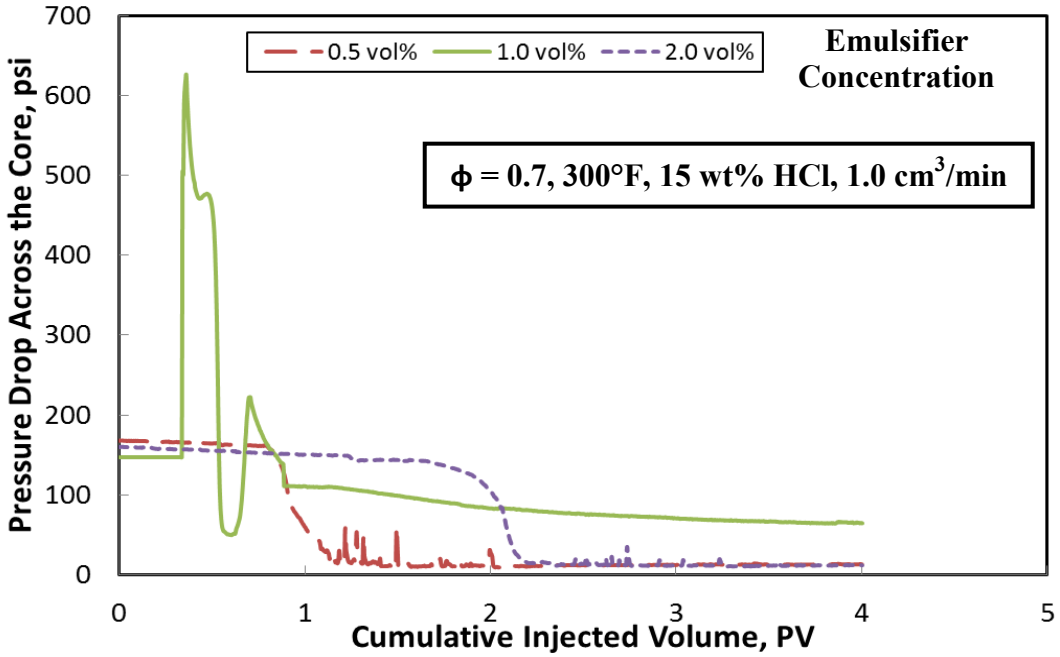

Fig. 5-16: Pressure drop across low permeability cores for an injection rate of 1.0 cm^3/min & 300°F for different emulsifier concentrations.

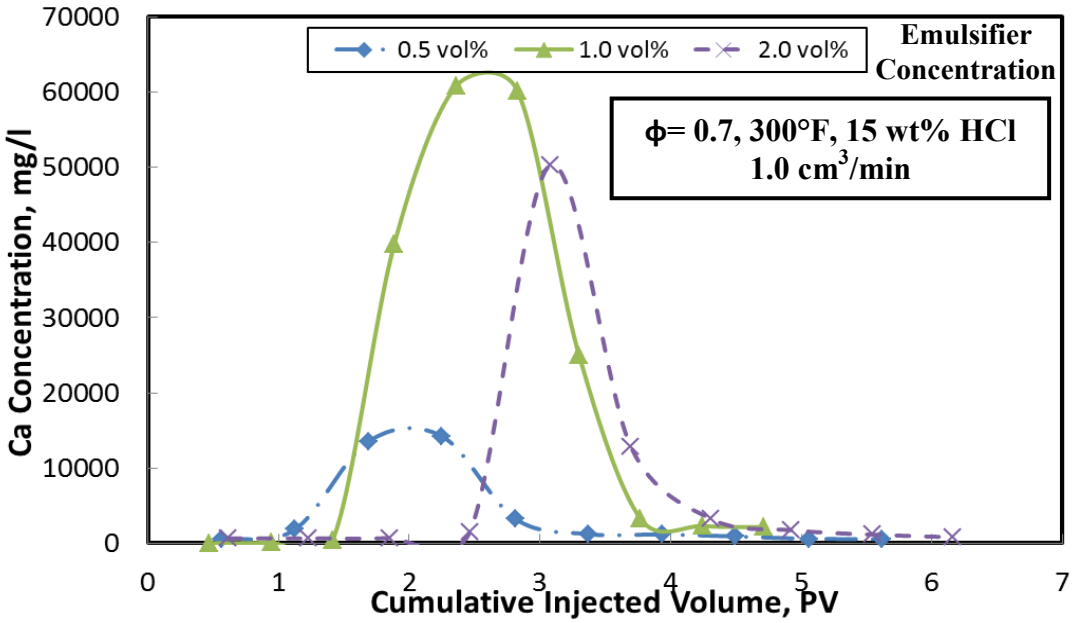

Fig. 5-17: Calcium concentration - low permeability core for an injection rate of 1.0 cm^3/min & 300°F for different emulsifier concentrations.

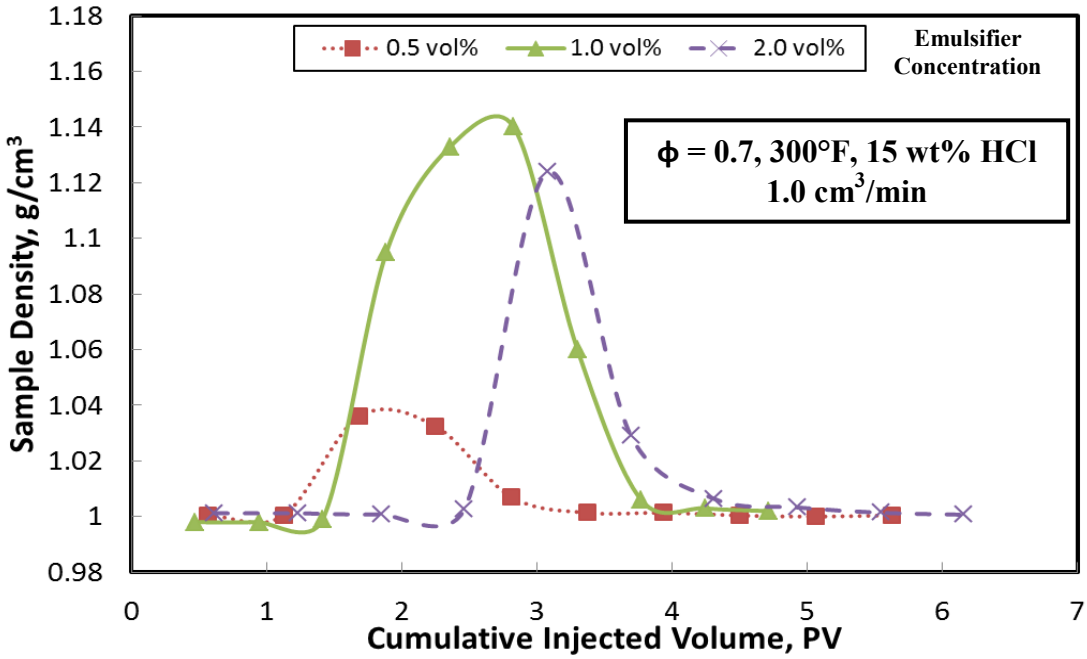

Fig. 5-18: Density of effluent samples - low permeability core for an injection rate of 1.0 cm^3/min & 300°F for different emulsifier concentrations.

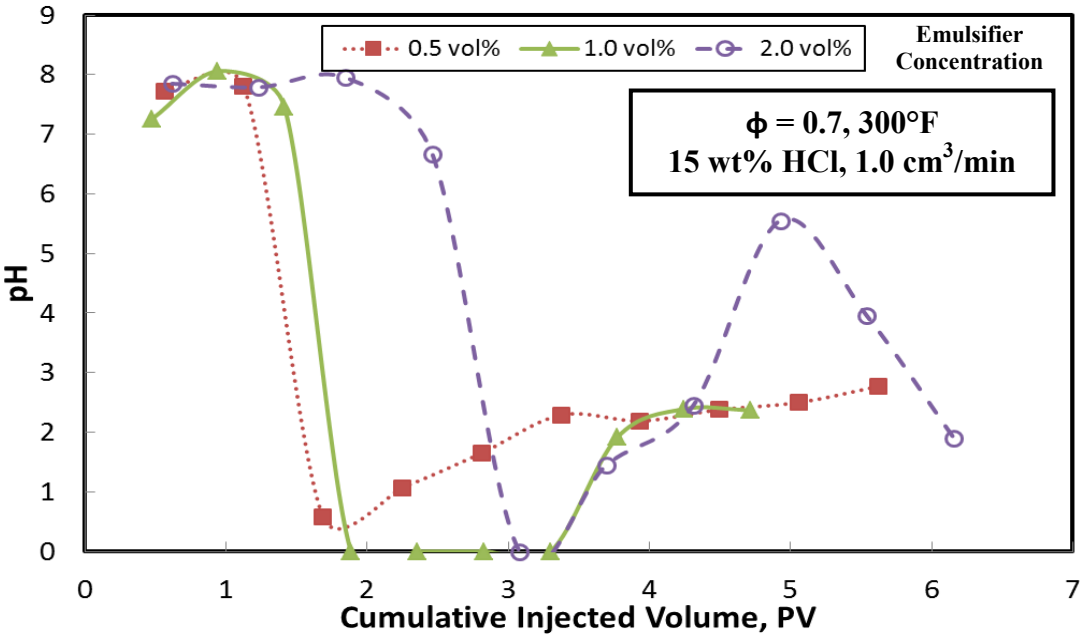

Fig. 5-19: pH of effluent samples - low permeability core for an injection rate of 1.0 cm^3/min & 300°F for different emulsifier concentrations.

5.3.5 Concept of Optimum Injection Rate

Optimum acid injection rate is the injection rate at which the volume of acid required to achieve breakthrough is minimum. Ten coreflood experiments were performed using an emulsified acid system formulated using 1.0 vol% emulsifier, and the final HCl concentration was 15 wt% and the acid to diesel volume ratio was 70-30. The volume of acid to achieve breakthrough was a function of the acid injection rate. **Fig. 5-20** shows the relationship between volume of acid to breakthrough and emulsified acid injection rate. From **Fig. 5-20**, it is apparent that, for low permeability Indiana limestone, as the injection rate increased, the volume of emulsified acid to breakthrough decreased and reached a minimum at 5.0 cm^3/min. For emulsified acid injection rates higher than 5 cm^3/min, the volume of emulsified acid to achieve breakthrough increased. This indicates that, for low permeability Indiana limestone, the optimum injection rate was 5.0 cm^3/min.

For high permeability Indiana limestone, the volume of acid to breakthrough decreased as the emulsified acid injection rate was increased. This indicates that there is no optimum acid injection rate when dealing with high permeability calcite rocks.

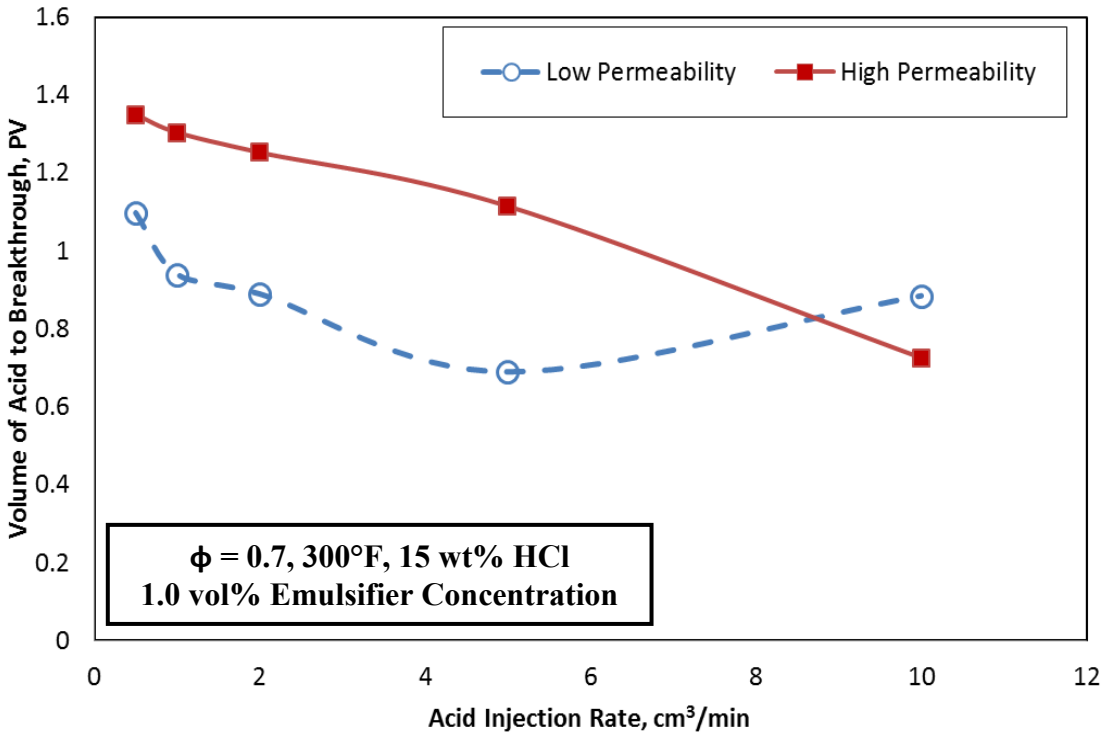

Fig. 5-20: Change of acid volume to breakthrough with acid injection rate.

5.3.6 CAT Scan Images

Fig. 5-21 shows the 2D scan images for the 6 in long, low permeability cores treated by emulsified acid, formulated at 1 vol% emulsifier, and at a temperature of 300°F. No face dissolution was noticed in the core inlet face for all the injection rates studied. Upon injection inside the core, emulsified acid started to react with the rock and create wormholes. This can be detected through inspection of the dark spots indicating a low CT number. At low injection rates, the 2D scan images revealed that the acid created more than one wormhole, with no face dissolution, and the emulsified acid was very effective, even at very low acid injection rates (0.5, and 1.0 cm^3/min).

From **Fig. 5-21**, and for an acid injection rate of 5.0 cm^3/min, there was no face dissolution and also it was noticed that the acid, at this rate, created only one main wormhole. The size of the created wormhole decreased as the acid penetrated deeply in the core until acid breakthrough occurred. At this injection rate, emulsified acid created one main wormhole that extended from the start to the end of the core.

From these 2D scan images, the new emulsified acid system is an effective stimulation fluid that can be injected in low rates and it is able to create deep wormholes, without the occurrence of face dissolution. The big difference in calcium concentration measured in both cases, at 1.0 cm^3/min and 5 cm^3/min injection rates, can be explained by the aid of the CT scan images of the core after the experiments. From the 2D scan images, at a low injection rate, the emulsified acid created many wormholes. These wormholes work as a high spot for more acid reaction with the rock, resulting in the generation of a high amount of calcium ions in the effluent fluid samples. Emulsified acid, in the second core that was treated at rate 5.0 cm^3/min, created only one main wormhole. For that reason, the calcium concentration of the effluent samples at an injection rate of 5 cm^3/min was less, compared to the same values at an injection rate of 1.0 cm^3/min. The initial and final permeabilities for the cores are summarized in **Table 5-1.** From these results, and for low permeability Indiana limestone cores, it is apparent that emulsified acid enhanced the core permeability at all injection rates tested in this study. The maximum permeability enhancement ratio occurred at the optimum acid injection rate, which was 5.0 cm^3/min.

The 2D scan images for the 6 in long, high permeability cores treated by

emulsified acid, formulated at 1 vol% emulsifier, and at a temperature of 300°F can be presented by **Fig. 5-22**. No face dissolution was noticed in the core inlet face for all injection rates studied. At all rates, the emulsified acid achieved breakthrough in all cores and the 2D images show that there is more than one wormhole created at the core face inlet. From the pressure drop recorded during acid injection, the initial and final permeabilities, and the permeability ratio were calculated. These results are shown in **Table 5-1,** and they reveal that, for high permeability limestone cores, the final permeability increased only when emulsified acid was injected with high rates (>2.0 cm^3/min). There was no enhancement for low acid injection rates (0.5 to 2.0 cm^3/min), and in the case of very low injection rates (0.5 and 1.0 cm^3/min), the final permeability was less than the initial permeability indicating that cores were damaged after the acid injection.

Fig. 5-23 shows the 2D scan images for the 6 in long, low permeability cores treated by emulsified acid, formulated at 0.5 and 2.0 vol% emulsifier, for an acid injection rate of 1.0 cm^3/min at a temperature of 300°F. No face dissolution was noticed in the core inlet face. Emulsified acid formulated using 2.0 vol% emulsifier concentration created many wormholes in the rock surface, and from the results shown in Table 1, the required volume to cause breakthrough increased with increasing the amount of emulsifier concentration. From **Table 5-1**, it can be inferred that there is not a significant permeability enhancement when changing the emulsifier concentration from 0.5 to 2.0 vol%. This indicates that the main parameter that affects the final permeability is the acid injection rate.

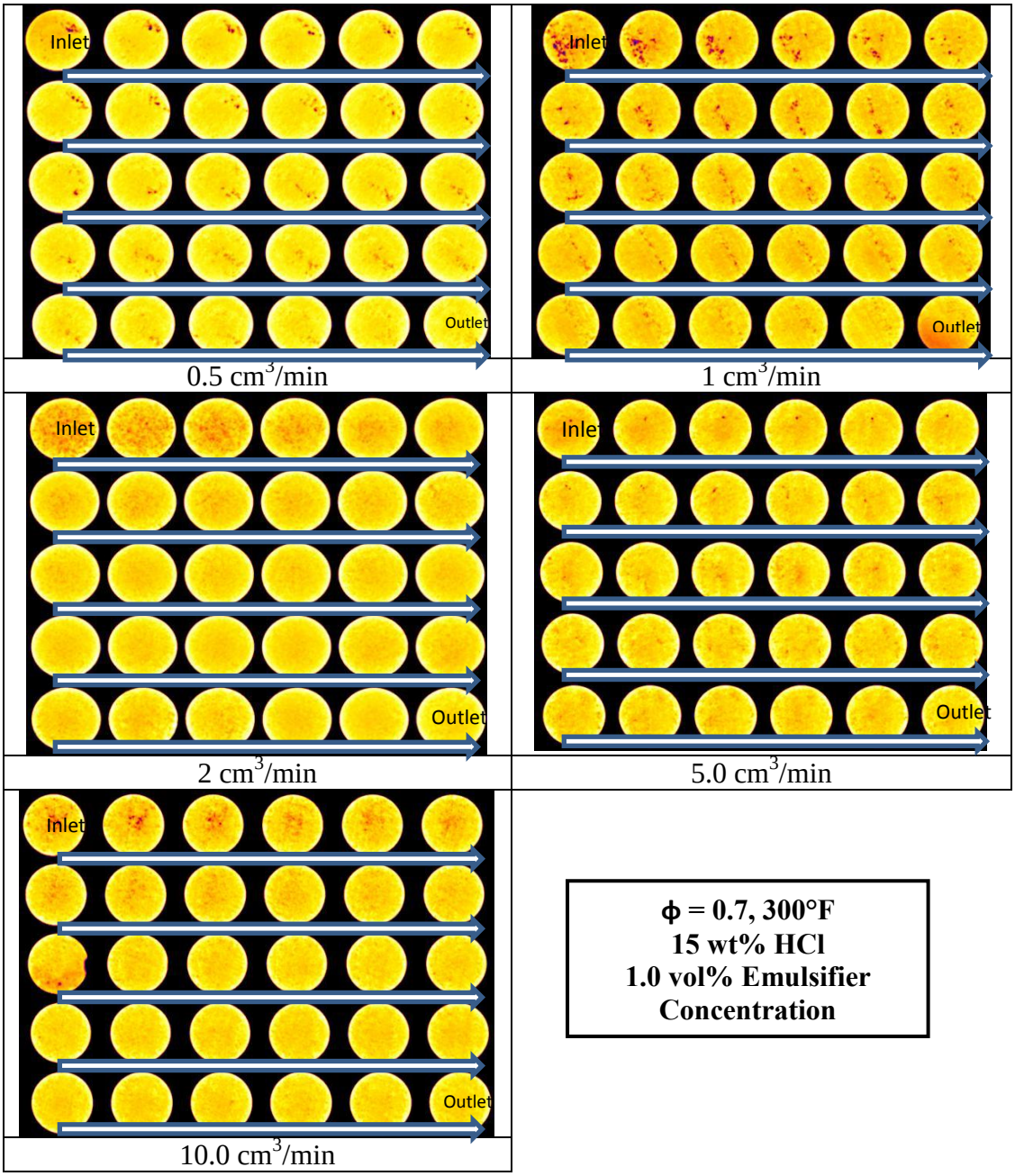

Fig. 5-21: CT scanned images for the tested low permeability Indiana limestone cores in the coreflood study.

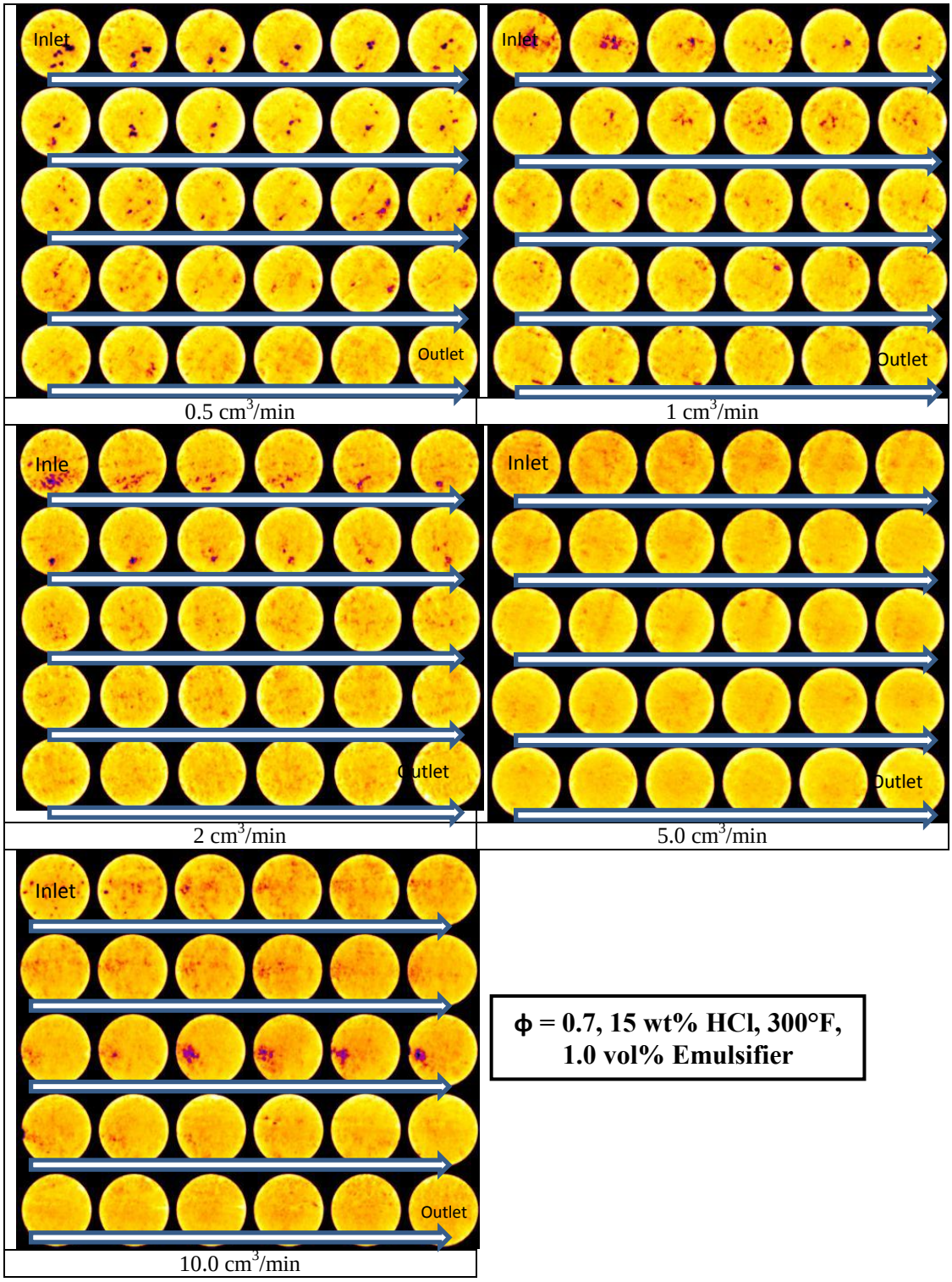

Fig. 5-22: CT scanned images for the tested high permeability Indiana limestone cores fully saturated with water.

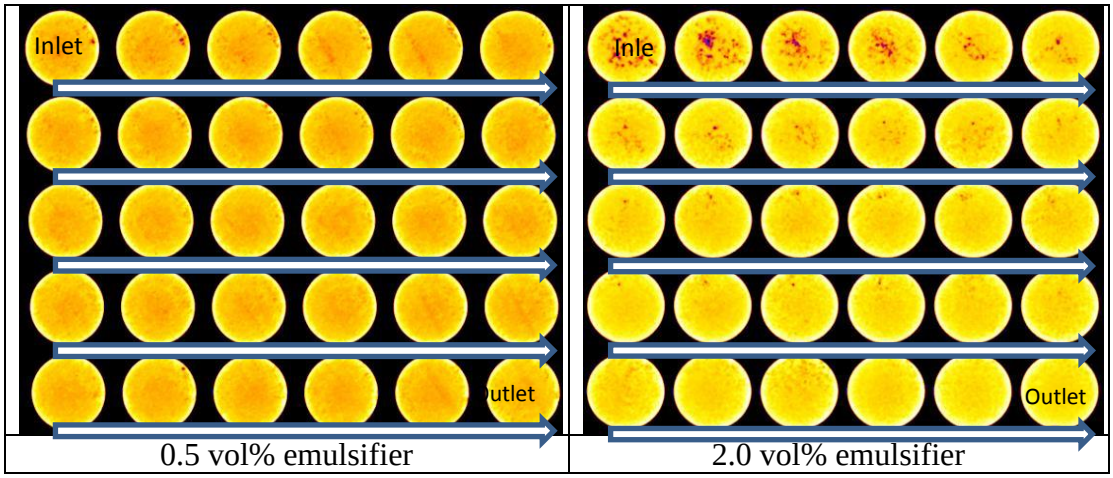

Fig. 5-23: CT scanned images for the tested low permeability Indiana limestone cores for different emulsifier concentration.

6. EFFECT OF THE PRESENCE OF CRUDE OIL IN THE CORE ON THE PERFORMANCE OF EMULSIFIED ACIDS

6.1 Introduction

Regular HCl acids are widely used to stimulate oil and gas wells to improve the rate of hydrocarbon production (Al-Anazi et al. 1998; Kasza et al. 2006), and to stimulate disposal wells and water injection wells to increase the injectivity in these wells (Mohammed et al. 1999; Nasr-El-Din et al. 2000). Regular HCl is pumped as the main stimulation fluid in carbonate stimulation treatments, but the reaction between regular HCl and calcite is very fast at high downhole temperatures. The high acid-rock reaction rates will result in rapid HCl spending, surface washout, and failure of the stimulation treatment (Nasr-El-Din et al. 2003a). Regular HCl may cause excessive tubing corrosion, and may form acid/oil sludges in asphaltene-rich crudes.

Emulsified acid is one of the most widely used alternatives for regular HCl (Dill 1961; Knox et al. 1964; Crenshaw and Flippen 1968; Nasr-El-Din et al. 2001). Emulsified acid is an acid-in-hydrocarbon emulsion. The most common hydrocarbon that is used as an external phase is diesel, and its main function is to act as a diffusion barrier between acid and rock (Crowe and Miller 1974; Bergstrom and Miller 1975; Hoefner and Fogler 1985; Daccord et al. 1989; Peters and Saxon 1989). This diffusion barrier will result in a reduction in acid-rock reaction rate, which will help in the creation of deep wormholes (Williams and Nierode 1972; Guidry et al. 1989; Navarrete et al. 1998a and b), and creation of etched fracture surfaces (Navarrete et al. 1998a and b;

Nasr-El-Din et al. 2006a, 2008b). Nasr-El-Din et al. (2000) and Buijse and van Domelen (2000) summarized the advantages and disadvantages of emulsified acid systems.

De Groote (1933) used acid-in-oil emulsions to remove damage from carbonate rocks, and protect the metallic parts of the well from corrosion that may be caused by regular acids. Based on the droplet size of the acid, emulsified acid systems can be classified as micro (Hoefner and Fogler 1985) or macro-emulsions (Al-Anazi et al. 1998). Macro emulsions have larger droplet sizes, use smaller amounts of emulsifier, and are the most widely used type in the field (Al-Anazi et al. 1998; Mohamed et al. 1999; Nasr-El-Din et al. 2000; Kasza et al. 2006).

Hoefner et al. (1987) introduced a retarded acid-in-oil micro-emulsion system. They conducted coreflood experiments that showed that the microemulsion can stimulate cores in fewer PV's and under conditions of low injection rates where aqueous HCl spent completely. Al-Anazi et al. (1998) evaluated and applied emulsified acid in stimulation of tight carbonate reservoirs. Coreflood experiments were performed on reservoir cores (calcite) at 96°C; at acid injection rates of 0.5 to 12.0 cm^3/min. Bazin and Abdulahad (1999) compared between regular HCl and emulsified acid using coreflood experiments. They showed that emulsified acid was an effective stimulation fluid at low injection rates, and noted the absence of an optimum injection rate for the emulsified acid system used in their study. Lynn and Nasr-El-Din (1999) studied the formation damage associated with water-based drilling fluids, and the use of emulsified acid in order to overcome this damage. They concluded that emulsified acid achieved negative

skin factors in the cores, and so emulsified acid was capable of achieving deep penetration in the formation.

Nasr-El-Din et al. (2000) conducted experimental studies to evaluate the use of emulsified acid in stimulation of water disposal wells. Coreflood results showed that the emulsified acid formed wormholes in tight carbonate cores (K < 50 md), and the core permeability increased after the treatment. Field application of the emulsified acid in two disposal wells indicated that both wells responded favorably to the treatment. Buijse and van Domelen (2000) found that acid-in-oil emulsions are effective stimulation fluids in large intervals, where streaks of high-permeability can act as thief zones. Al-Harbi et al. (2006) evaluated acid treatments for water injection wells. These wells were stimulated using regular HCl and emulsified acid with foamed viscoelastic water (for diversion). Their results indicated that increasing the volume of emulsified acid in acid treatments has enhanced the well's injectivity.

Shukla et al. (2006) presented laboratory results that show how wormhole propagation is affected by the presence of immiscible phases (gas or oil) when regular HCl is injected into the rock. They concluded that the efficiency of wormholing process increased when there was a high saturation of immiscible phases (either gas or oil). Also, Shukla et al. (2006) found that less branching occurred in the wormhole in presence of immiscible phases.

Abdel Fatah and Nasr-El-Din (2010) utilized HCl emulsified in xylene, instead of diesel, to stimulate wells and at the same time to remove asphaltene deposition. The emulsified acid in xylene was applied in 4 wells with success without encountering

operational problems. Appicciutoli et al. (2010) showed that emulsified acid systems can be mixed with custom-tailored asphaltene-solving blends, and this system provided the desired benefits for matrix acidizing, such as stability, high viscosity, slow reaction, and at the same time it was able to remove asphaltene. Al-Mutairi et al. (2012) discussed the effect of acid and its wormholing characteristic on tar and on carbonate rocks that were saturated with crude oil of different °API gravities. The extreme case was flooding the acid through tar saturated plugs. They showed that regular and emulsified acids produced comparable wormhole penetration in tar, and high °API crude oils consumed more emulsified acid to breakthrough compared to lower °API oils.

To the best of our knowledge, most of the previously performed coreflood experiments were conducted using cores saturated with deionized water or brine. Therefore, the main objective of the present work is to study the effect of the presence of crude oil and oil saturation on the performance of emulsified acids. A coreflood study was performed using Indiana limestone cores saturated with 100% water, 100% crude oil, or crude oil at irreducible water saturation. Emulsified acids were prepared using 1.0 vol% emulsifier, and formulated at 0.7 acid volume fraction (ϕ = 0.7). The acid concentration was 15 wt% HCl, and the coreflood study was performed at 300°F at various injection rates from 0.5 to 10.0 cm^3/min.

6.2 Experimental Studies

6.2.1 Materials

Emulsified Acid. The emulsions were prepared using diesel and an acid solution (regular HCl and deionized water). The water used throughout the experiments was

deionized water, obtained from a water purification system that has a resistivity of 18.2 MΩ.cm at room temperature. Hydrochloric acid (ACS grade) was titrated using 0.1 N sodium hydroxide solutions, and its concentration was found to be 36.8 wt%. A corrosion inhibitor was added to the acid solution, whereas the emulsifier was added to diesel. The emulsifier, which was used throughout this study, was cationic and consisted of a blend of a cationic surfactant, isopropanol, and a petroleum distillate. The diesel was obtained from a local gas station. In all the emulsions preparation, the same source of diesel was used. **Table 3-1** shows the properties of the diesel fuel used in preparation of emulsified acid.

Crude Oil. A naphthenic crude oil obtained from ConocoPhilips Company was used for saturating the cores. All oil samples were centrifuged at 5000 rpm, then filtered through a limestone core plug to separate any solids entrained in the crude oil that may cause plugging in the core samples during the coreflood experiments. The density and viscosity of this crude oil at ambient temperature was measured after filtration and were 0.828 g/cm^3 and 30.5 cp, respectively. The viscosity of crude oil at a temperature of 300°F was measured to be 3.7 cp. The acid/base number is a measure of the amount of acidic/alkaline substances in the oil. Both the total acid number (TAN) and the total base number (TBN) were measured using Potentiometric Titrators model 907 Titrando (manufactured by Metrohm). The standards ASTM D 664 and ASTM D 2896 describe two methods for the determination of TAN and TBN based on potentiometric titration of the acidic and basic constituents, respectively. The TAN and TBN for the crude oil used

in the study were found to be 0.11 (mg KOH/g of oil) and 0.6 (mg HCl/g of oil), respectively.

6.2.2 Acid Preparation

The acid solution was prepared by mixing the corrosion inhibitor, deionized water and HCl acid. The diesel solution was prepared by adding the emulsifier to diesel oil, and mixing at 1200 rpm. Then, the acid solution was added slowly to the diesel solution and mixed at 1200 rpm for 30 min. The electric conductivity of the final emulsion was measured in a conductivity meter (Marion L, model EP-10) to confirm the quality of the final emulsion. If the electric conductivity was nearly equal to 0, then we had a good emulsified acid. If the conductivity was higher than zero, we increased the mixing time to 1 hour at 1200 rpm, and measured conductivity again, to ensure the quality of the prepared emulsified acid.

6.2.3 Core Preparation

Cylindrical cores with 1.5 in. in diameter and 6.0 in. in length were cut from an Indiana limestone block. A total of nine cores were cut in order to perform the coreflood experiments. The cores were dried in an oven at temperature of 150°C (302°F) for 3 hours until the core samples were completely dried. The cores were weighed using a digital balance to obtain the dry weight of the core samples. After that, the dried cores were saturated with deionized water under vacuum for 24 hours and the weight of water-saturated cores was measured, the pore volume, and hence the core porosity were calculated (**Table 6-1**).

The core samples were put in a core holder, and water was injected at different flow rates. For each flow rate, the pressure drop after stabilization was recorded. A plot of flow rate divided by the core sectional area vs. the ratio of pressure drop to the core length was used to calculate the initial core permeability.

A set of five water-saturated cores were saturated with crude oil at irreducible water saturation. Each of the selected cores was placed in a core holder, and crude oil was injected into the core. With oil injection, water was produced from the core sample. Injection of crude oil was continued until no more water produced from the core. The amounts oil and water produced from the core were collected in a graduated cylinder, and the volume of collected water was measured. From the volume of the collected water and the previously measured pore volume, the water and oil saturations were determined (**Table 6-1)**. The porosity of the core samples ranged from 15.5 to 20.9 % and the initial core permeabilities ranged from 67.6 to 238 md.

To saturate the cores with crude oil, dry core samples were placed in the core holder in the coreflood setup (**Fig. 5-1**) and the crude oil was injected at 1.0 cm^3/min. Injection of the crude oil continued until the pressure drop across the core stabilized and steady state conditions were achieved.

6.2.4 Compatibility Tests

These tests were conducted by adding 6 cm^3 of the emulsified acid to an equal volume of the crude oil. A similar procedure was repeated with diesel, water, xylene, ethanol, and 10 vol% mutual solvent solution in water. All the compatibility tests were performed at

room temperature (78°F). The fluids were mixed very well, and then were examined for phase separation.

Table 6-1: Data for 6 in. long coreflood experiments.

Run #	S_{wi}, %	$Q_{Injection}$, cm^3/min	PV to BT	K_{final}, md	$K_{final}/K_{initial}$
1	0.64	0.5	1.80	6500	72.3
2	0.52	1.0	2.13	11500	170.1
3	0.66	2.0	1.79	7500	58.1
4	0.55	5.0	1.82	10725	61.3
5	0.53	10.0	2.11	5254	44.3
6	0	1.0	2.60	8655	68.2
7	0	2.0	2.67	3866	33.0
8	0	5.0	2.71	6678	60.7
9	0	10.0	2.84	5450	22.9

6.2.5 Equipment

The coreflood setup was described in detail in section 5.2.3 and **Fig. 5-1.** Samples of the coreflood effluent fluid were collected, and the calcium concentration of the effluent samples was measured using the ICP (Inductively Coupled Plasma) technique (PerkinElmer Optical Emission Spectrometer, Optima 7000 DV), where the spectral range is 160-900 nm with resolution of < 0.009 nm @ 200 nm.

6.3 Results and Discussion

6.3.1 Compatibility Tests

The results of compatibility tests of emulsified acid and oil, water, diesel, 10 vol% mutual solvent solution, 100% ethanol alcohol, and xylene are shown in **Figs. 6-1a** through **6-1f.** All these compatibility tests were performed at room temperature (78°F).

Fig. 6-1a shows the emulsified acid solution after mixing with water, there was no complete mixing between emulsified acid and water, and two-phases appeared. Since the continuous phase in emulsified acid is diesel, the density difference between water (more dense than diesel) resulted in the separation of the mix into two different phases. When the emulsified acid was added to diesel, xylene, or crude oil, there was only one homogeneous phase after mixing the fluids. This indicates that the emulsified acid was incompatible with water, while it was compatible with crude oil, diesel, and xylene. When emulsified acid was mixed with 100% ethanol alcohol and 10 vol% mutual solvent solutions, the emulsified acid was not stable and broke immediately into two separate phases, aqueous and diesel solutions (**Figs. 6-1d** and **6-1e**, respectively). This indicates that emulsified acid is not compatible with 100% ethanol alcohol and mutual solvent solution and the emulsified acid will not be stable in the presence of any one of them. For that reason, 10 vol% mutual solvent solution was selected to be injected to break any residual emulsified acid in the core samples after the emulsified acid injection.

6.3.2 Viscosity of the Emulsified Acid

An HPHT rheometer (Grace M5600) was used to measure the apparent viscosity of live emulsified acids under different conditions. The apparent viscosity of emulsified acid at different volume fractions of acid, and after mixing with crude oil was measured and compared to the viscosity of the neat original emulsified acid. **Fig. 6-2** shows a comparison of the apparent viscosity of emulsified acid prepared at different acid volume fractions and after mixing with crude oil, and the viscosity of the original emulsified acid system. The viscosity of emulsified acid prepared at higher acid volume

fraction was higher than the viscosity of the original emulsified acid, while the apparent viscosity of emulsified acid prepared at less acid volume fraction was less than that of original emulsified acid.

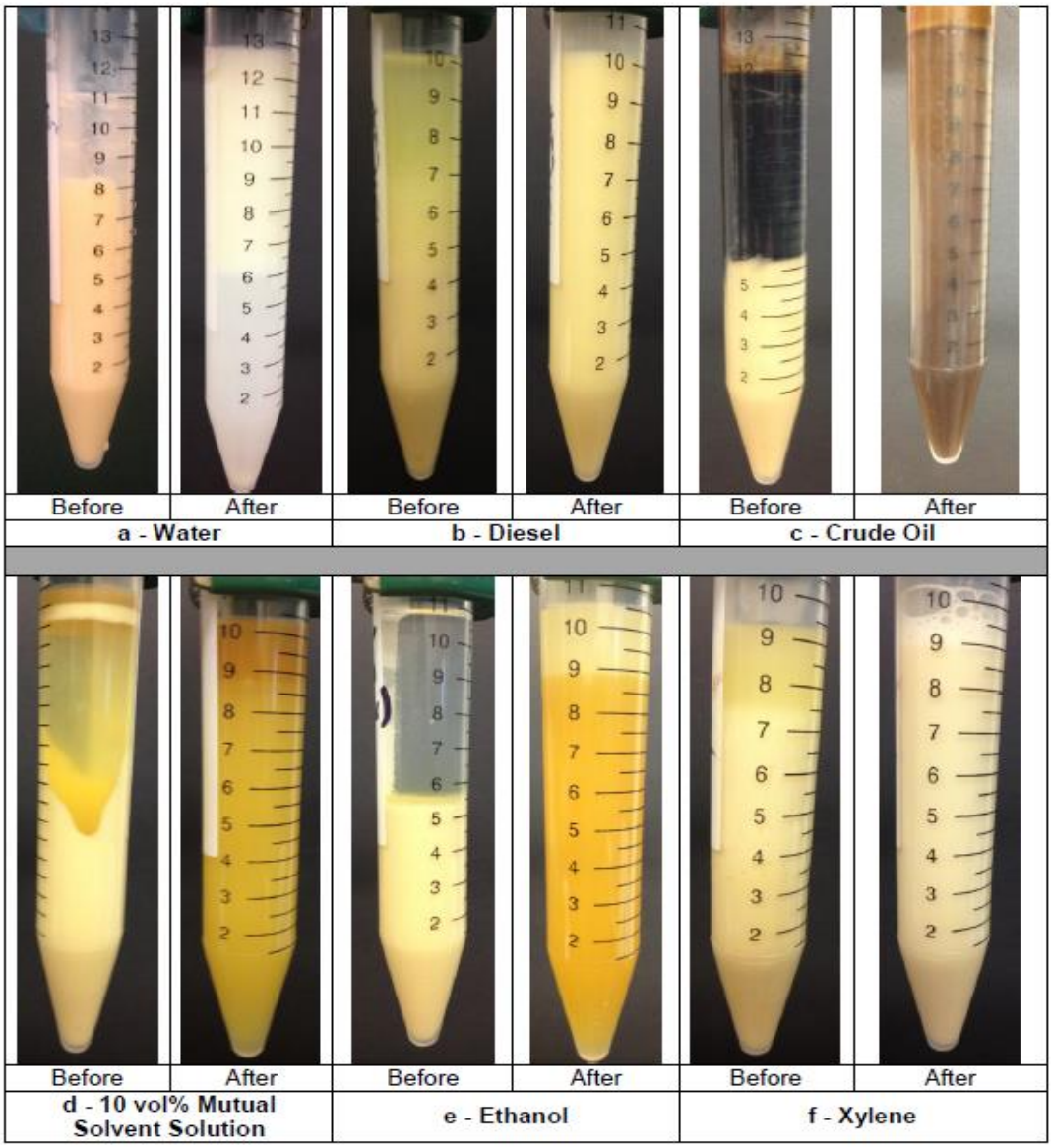

Fig. 6-1: Compatibility tests of emulsified acid systems used in the study

Einstein (1906) calculated the effective viscosity (μ") of a dilute suspension of spheres to be a function of the viscosity of the ambient fluid and the volume fraction of spheres

$$\mu'' = \mu\,(1 + \beta\,\phi) \qquad (6.3)$$

where μ is the viscosity of the continuous phase fluid, β is a coefficient to be determined and ϕ is the volume fraction of dispersed phase in the emulsion.

From Einstein's equation, it is clear that as the volume fraction of the dispersed phase increases, the viscosity of emulsion increases, and this agrees well with the results shown in **Fig. 6-2**. While the increase in the continuous phase volume fraction (diesel) will result in a reduction in the dispersed phase volume fraction and so, a reduction in the emulsified acid apparent viscosity. These results agree well with what was mentioned by Otsubo and Prud'homme (1994) and Al-Mutairi et al. (2008a) when they studied the effect of changing the volume fraction of dispersed (acid) and continuous (diesel) phases on the apparent viscosity of emulsions (or emulsified acid).

There was no significant change in the apparent viscosity of emulsified acid when it was mixed with an equal volume of crude oil when it was compared to the apparent viscosity of the neat emulsified acid. From the compatibility tests, and after adding crude oil to the emulsified acid, there was no phase separation. This is referred to as the mixing of crude oil and the diesel (continuous phase). When emulsified acid mixed with viscous crude oil, the change in the emulsified acid viscosity did not follow the Einstein equation, because of the difference in viscosity between the continuous phase (diesel) and the added phase (crude oil). Viscosity of crude oil was 30.5 cp at 78°F

compared to diesel viscosity of 2.7 cp at the same conditions. When the viscous crude oil was added to the emulsified acid, the viscosity of continuous phase increased, while the acid volume fraction decreased. As a result of these combined effects of the change in the viscosity of the continuous phase and the change in the acid volume fraction, the viscosity of the emulsified acid did not show a significant change although there was a significant change of the volume fraction of dispersed phase.

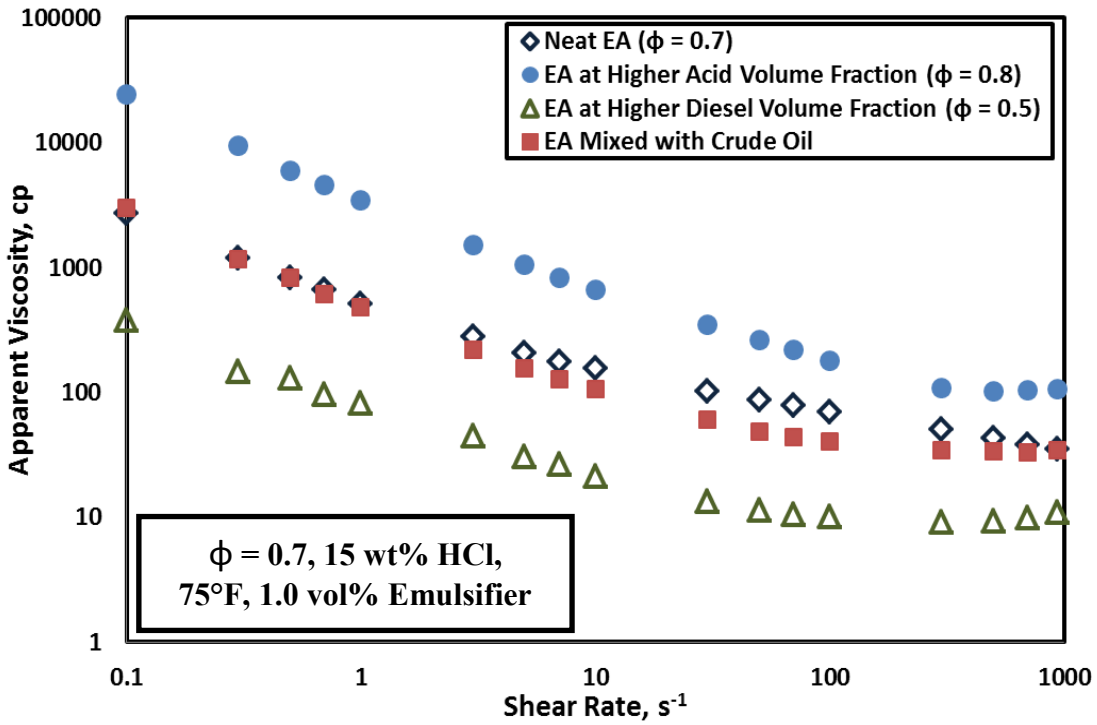

Fig. 6-2: Viscosity of emulsified acid after mixing with crude oil, water and diesel.
**EA denotes to Emulsified Acid

6.3.3 The Droplet Size Distribution of Emulsified Acids

A small sample of each emulsified acid system, after mixing with crude oil, and at higher acid volume fraction, beside a sample from the neat emulsified acid were examined using the Zeiss Axiophot microscope in order to measure the droplet size distribution of acid droplets. The photomicrographs of the different emulsified acid systems are shown in **Fig. 6-3**. The photomicrographs were analyzed using Image-J software, and the droplet size of emulsified acid was measured. The average droplet size of each emulsified acid system is presented in **Table 6-2**. The photomicrographs and droplet size measurements showed that the average droplet size decreased from 8.1 to 4.2 μm when emulsified acid was mixed with crude oil. Where, the average droplet size increased from 8.1 to 13.9 μm when the volume fraction of acid increased in the emulsified acid system. Mixing emulsified acid with crude oil resulted in an increase in the continuous phase volume and a reduction of the acid volume fraction. This agrees well with what was mentioned before by Al-Mutairi et al. (2009a) when they studied the effect of the emulsifier concentration and acid volume fraction on the droplet size distribution of acid.

Table 6-2: Statistical analysis of the droplet size distributions for emulsified acid systems used in the present study.

Emulsified Acid	Average Droplet Size, μm
Neat	8.1 ± 0.28
Higher Acid Volume Fraction (80%)	13.9 ± 2.15
Mixed With Crude Oil	4.2 ± 0.88

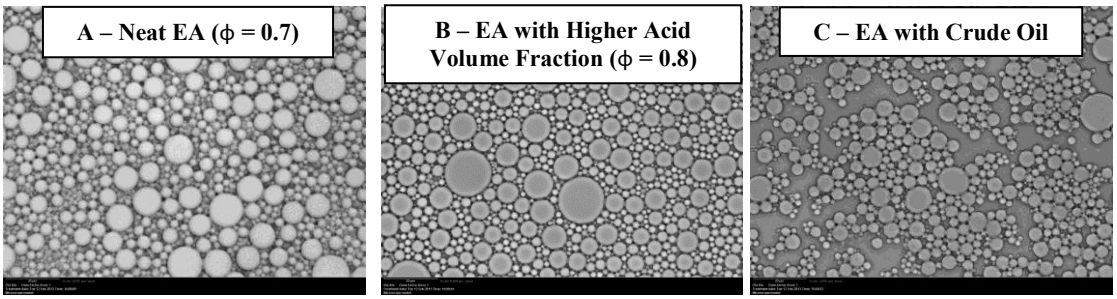

Fig. 6-3: Droplet size distributions of emulsified acid systems (40x objective: 0.0960 micrometers per pixel).

6.3.4 Coreflood Studies

Coreflood experiments with emulsified acid systems were run using the setup shown in **Fig. 5-1. Table 6-1** gives the data for the cores used in this study. These data include initial and final permeability, volume of acid to breakthrough, initial water saturation, core porosity, and injection rate. A total of nine coreflood runs were performed using emulsified acid formulated using 1.0 vol% emulsifier; five core samples were saturated with crude oil at irreducible water saturation, and four core samples were saturated with 100% crude oil. The results of these experiments were compared to those experiments performed using high permeability Indiana limestone core samples saturated with water (Chapter 5). The coreflood experiments were performed at injection rates in the range of 0.5 to 10 cm^3/min. These runs were performed in order to study the effect of the injection rate, and the presence of crude oil on the performance of emulsified acid, especially the acid volume to breakthrough, and the characteristics of created wormholes. All coreflood runs were performed at 300°F. For each coreflood experiment, the pressure drop across the core was plotted using Lab-View software. Samples of the

coreflood effluent were analyzed for calcium concentration. The pH value and the density of the effluent samples were measured for some samples.

The results of the coreflood runs performed using high permeability Indiana limestone cores saturated with water were presented in Chapter 5. Only the results of the coreflood experiments performed using high permeability Indiana limestone cores saturated with 100% crude oil and core samples saturated with crude oil at irreducible water saturation will be presented here.

6.3.5 Limestone Cores Saturated with Crude Oil at Irreducible Water

Five coreflood runs were performed using emulsified acid and high permeability Indiana limestone cores, which were saturated with crude oil at irreducible water saturation. The five experiments were performed at acid injection rates of 0.5, 1.0, 2.0, 5.0 and 10.0 cm^3/min. In general, the pressure drop increased as the emulsified acid was injected into the core. This is due to the high viscosity of emulsified acid. The emulsified acid started to react with calcite and dissolved some calcium. As a result, emulsified acid started to create wormholes, and these wormholes started to propagate deeper in the core with the continuation of the emulsified acid reaction with rock until emulsified acid achieved breakthrough. The pressure drop across the cores, after acid breakthrough, stabilized near a value of 12 psi.

Fig. 6-4 shows the pressure drop across the core for an emulsified acid injection rate of 10 cm^3/min. The pressure drop started to increase with emulsified acid injection and the pressure drop reached a value of 57 psi. With acid flow in the core, the acid reacted with calcite and wormholes started to propagate inside the core and the pressure

drop across the core had a sudden drop. The pressure drop started to increase again until acid breakthrough occurred in the core. This increase in the pressure drop can be referred to the trapping of some of the emulsions inside the core. After acid breakthrough occurred, 10 vol% mutual solvent was injected until there was no emulsion collected at the core effluent samples, and the final pressure drop was stabilized at a value of 12 psi.

A mutual solvent solution (10 vol% concentration) was injected to post flush the core, and to remove any remaining emulsions. The core samples were left to cool down to room temperature, and deionized water was injected again to saturate the core. The final permeability was measured at room temperature. The final core permeability after acid breakthrough, and the ratio of the final to the initial permeability are given in **Table 6-1**. The final permeability of the core samples after acid breakthrough was found to be in the range of few Darcies. It can be concluded that emulsified acid was successful in creating wormholes and the final permeability was enhanced at all injection rates.

The aqueous phase of the effluent fluid samples were separated from any crude oil that came out from the core. Calcium concentration, density and pH were measured for these separated aqueous phase samples. **Fig. 6-5** shows the calcium concentration in the coreflood effluent samples for experiments performed using Indiana limestone cores that were saturated with crude oil at irreducible water saturation. The calcium concentration increased with the injection of emulsified acid, until emulsified acid breakthrough occurred in the core sample. Calcium concentration then decreased again when the core was flushed with mutual solvent solution. The change in the effluent fluid density and pH can be shown in **Figs. 6-6** and **6-7**. From **Fig. 6-6**, the density of effluent

samples changed with the rate of fluid injected in the core. The density of effluent samples started at value of 1.0 g/cm^3, and then increased upon injection of emulsified acid due to the dissolution of calcite upon the reaction with emulsified acid. After breakthrough, and at the start of the mutual solvent solution and water injection stages, effluent sample density started to decrease to a value slightly greater than 1.0. **Fig. 6-7** shows that pH value started near 6.5. Then, the pH started to decrease with emulsified acid injection, until acid breakthrough occurred. After acid breakthrough, water was injected again into the core, and the pH value started to slightly increase.

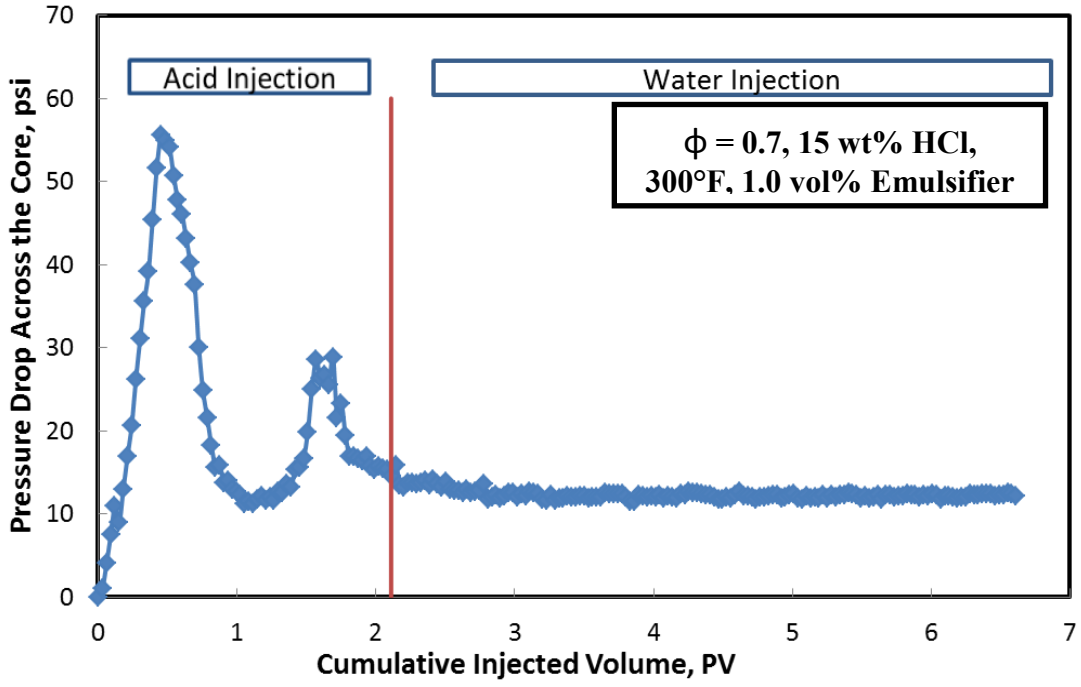

Fig. 6-4: Pressure drop across the core for and acid injection rate of 10 cm^3/min in Indiana limestone cores saturated with crude oil and irreducible water.

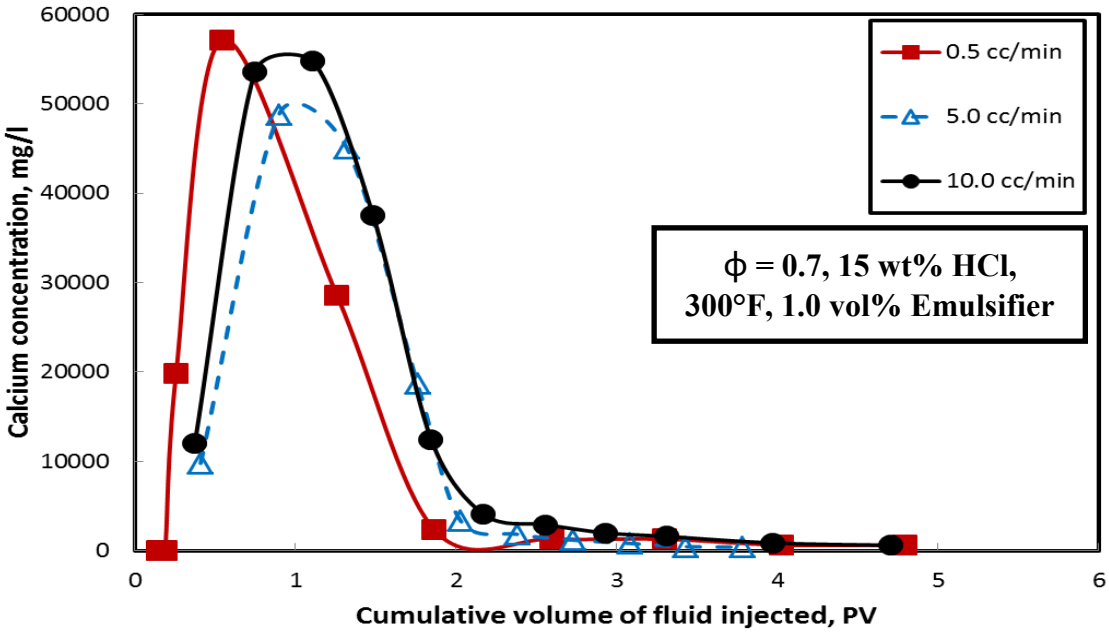

Fig. 6-5: Calcium concentration for different injection rates in Indiana limestone cores saturated with crude oil and irreducible water.

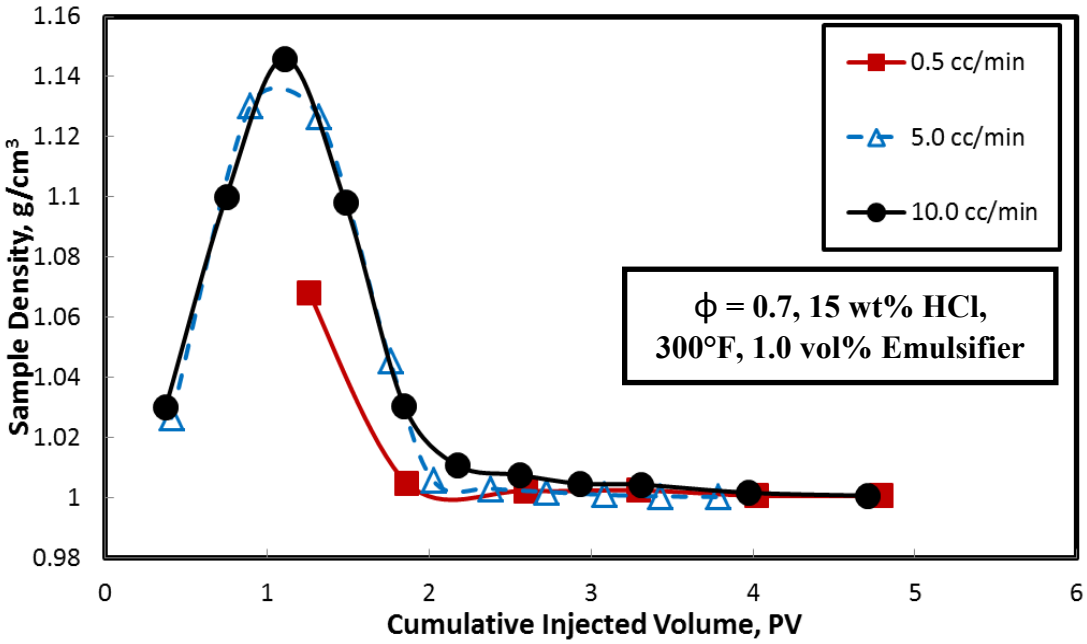

Fig. 6-6: Density of effluent samples for different injection rates – limestone cores saturated with crude oil and irreducible water.

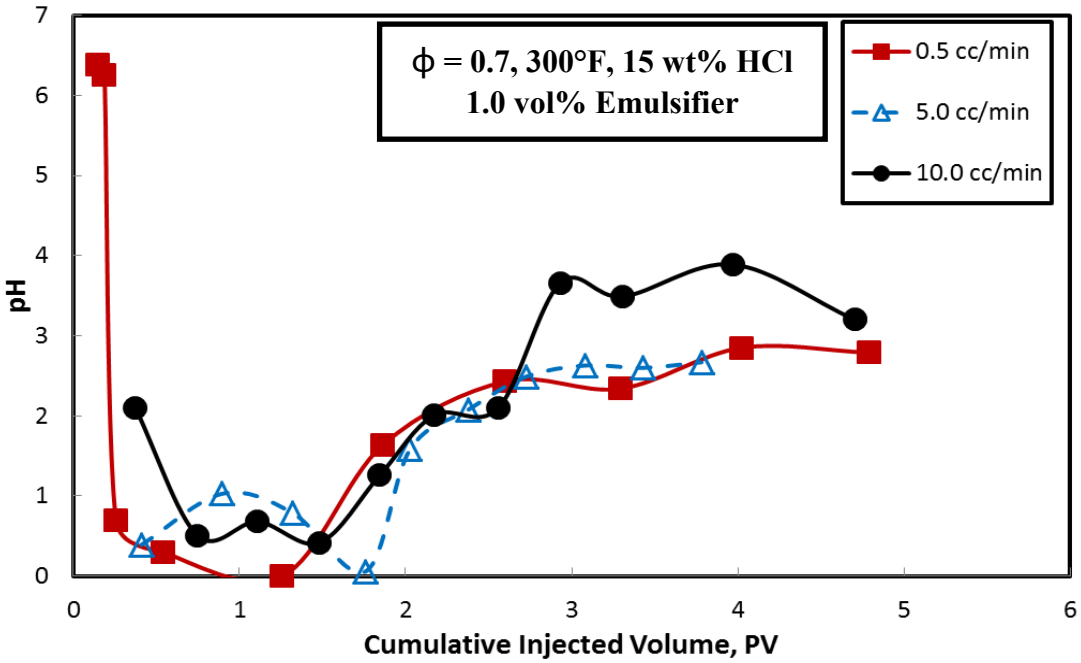

Fig. 6-7: pH of effluent samples for different injection rates – limestone cores saturated with crude oil and irreducible water.

6.3.6 Limestone Cores Fully Saturated with Crude Oil

To examine the effect of crude oil on the performance of emulsified acid, four coreflood runs were performed using emulsified acid systems and Indiana limestone cores which were saturated with 100% crude oil. The four experiments were performed at injection rates of 1.0, 2.0, 5.0 and 10.0 cm^3/min. **Fig. 6-8** shows a plot of the pressure drop across the core during emulsified acid injection at a rate of 10 cm^3/min. The pressure drop increased upon the injection of emulsified acid, then started to decrease upon the creation of wormholes. The final pressure was stabilized at 10 psi.

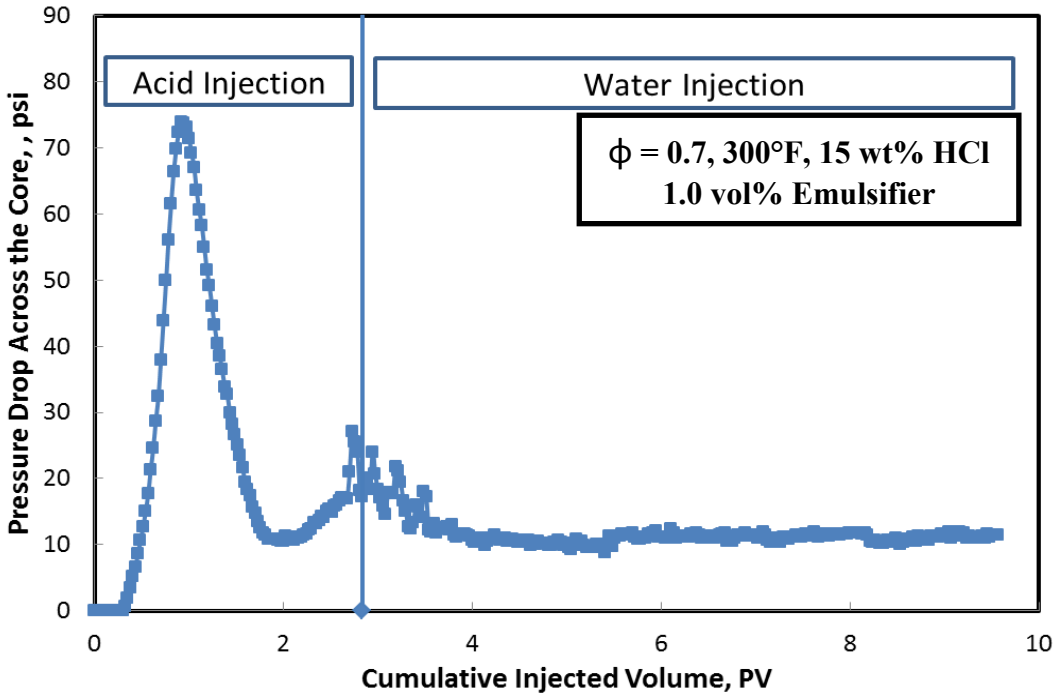

Fig. 6-8: Pressure drop across the core for emulsified acid injection rate of 10 cm^3/min in Indiana limestone cores saturated with crude oil.

All the core samples suffered some pressure drop after the emulsified acid breakthrough occurred as a result of the presence of emulsified acid and diesel in the core sample. 10 vol% mutual solvent prepared in water was injected in the reverse direction of emulsified acid injection as a backflow. The final pressure drop after injection of mutual solvent was reduced. The core was left to cool down and the final permeability was measured at room temperature using deionized water. The final permeability, and hence the ratio of the final to the initial permeability were calculated, and these values are given in **Table 6-1**. The final permeability of the core samples after acid breakthrough was found to be in the range of a few Darcies. Emulsified acid was

effective in creating wormholes in cores fully saturated with crude oil, and the final permeability was enhanced at all injection rates.

Fig. 6-9 shows the calcium concentration in the core effluent samples for coreflood experiments performed using Indiana limestone cores that were saturated with 100% crude oil. The calcium concentration increased with the injection of emulsified acid, until acid breakthrough occurred in the core, where 10 vol% mutual solvent solution was injected, and then calcium concentration started to decrease again.

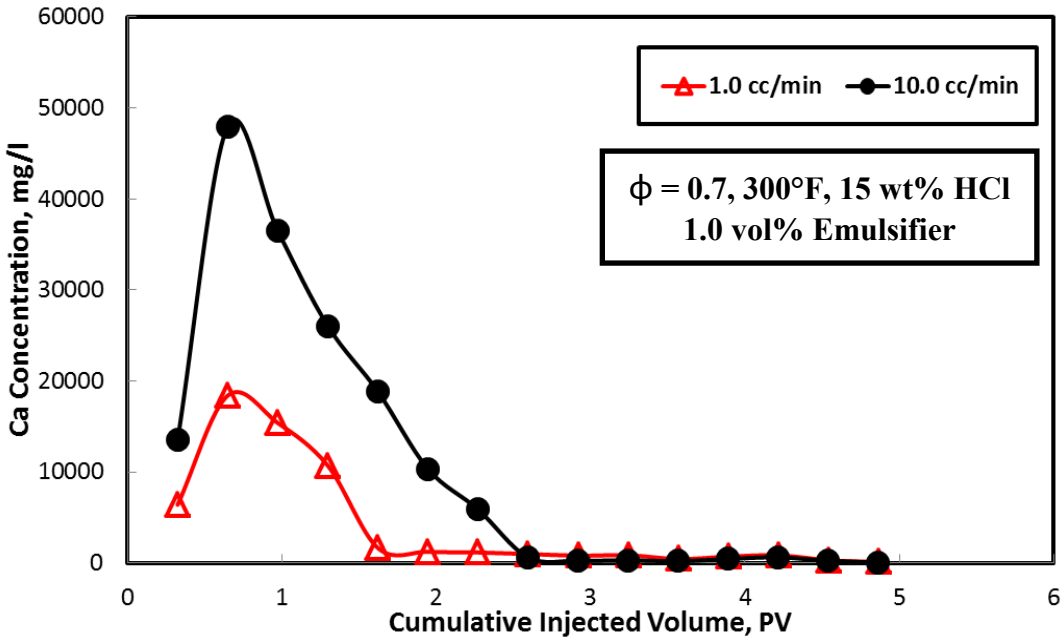

Fig. 6-9: Calcium concentration for different injection rates –limestone cores saturated with crude oil.

6.3.7 Total Amount of Calcium in the Core Effluent Samples

The total amount of calcium in effluent samples is a good and direct indication of the solubility of calcite cores in emulsified acid. The total amount of calcium in coreflood effluent fluid samples was calculated by the integration of the data like what is shown by **Figs 5-9, 6-5, and 6-9. Fig. 6-10** shows a comparison of the total calcium in coreflood effluent fluid samples in the case of injection of emulsified acid in cores saturated with 100% water (data from Chapter 5), cores saturated with crude oil at irreducible water, and cores saturated with 100% oil. The total amount of calcium in coreflood effluent fluid samples in case of cores saturated with 100% crude oil and cores saturated with crude oil at irreducible water was higher than in cores saturated with 100% water. This indicates that a greater amount of rock was dissolved, and so, a larger volume of emulsified acid was consumed in the treatment in order to achieve acid breakthrough.

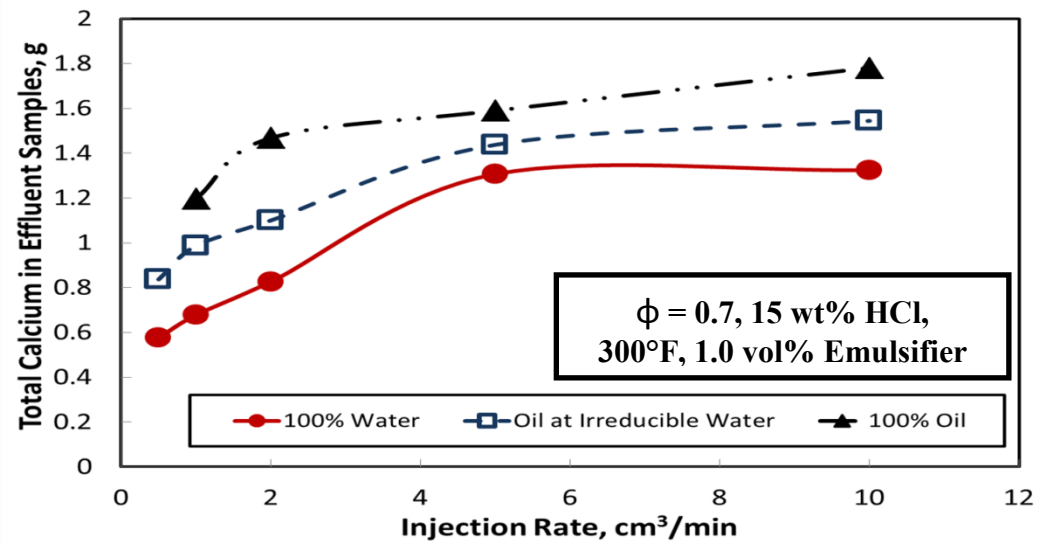

Fig. 6-10: Total amount of calcium dissolved by emulsified acid.

6.3.8 Volume of Acid to Breakthrough and Optimum Injection Rate

Optimum injection rate is the rate at which the volume of acid injected until acid breakthrough is minimum. A total of 14 coreflood experiments were performed using high permeability Indiana limestone core samples and emulsified acid systems that were formulated using 1.0 vol% emulsifier, and the HCl concentration was 15 wt%, and an acid to diesel volume ratio of 70-30. Five coreflood experiments were performed using core samples saturated with 100% water (Chapter 5) and nine coreflood experiments were performed using core samples saturated with crude oil at irreducible water saturation and core samples saturated with 100% crude oil. The volume of acid to breakthrough changed with the injection rate. **Fig. 6-11** shows the relationship between the volume of emulsified acid to achieve breakthrough and emulsified acid injection rate in all the cases studied before; limestone cores saturated with 100% water, 100% crude oil, and crude oil at irreducible water saturation. It is apparent that, for Indiana limestone cores saturated with 100% water, as the emulsified acid injection rate increased, the volume of acid to breakthrough decreased. This indicates that there is no optimum acid injection rate (for the injection rates studied in the range of 0.5 to 10.0 cm^3/min). For all injection rates studied, emulsified acid achieved breakthrough and the final permeability of the core samples was enhanced.

For the Indiana limestone cores saturated with crude oil at irreducible water saturation and cores fully saturated with crude oil, the volume of emulsified acid to achieve breakthrough increased as the injection rate of emulsified acid increased, and in the same time the volume of emulsified acid to achieve breakthrough was higher than

those in the case of Indiana limestone core samples saturated with 100% water. These results can be explained by considering the effect of the presence of crude oil in the core on the performance of emulsified acid.

From the compatibility tests, the crude oil mixed completely with the emulsified acid due to the mixing of the crude oil with the diesel (continuous phase of the emulsified acid). By adding crude oil to the emulsified acid, the volume of the continuous phase (diesel and crude oil) increased. There was no change on the volume of HCl acid solution. As a result, the volume fraction of dispersed phase (HCl solution) decreased, and so the emulsified acid system is no longer formulated at 70:30 acid to diesel volume fraction. Also, from the viscosity measurements, the apparent viscosity of emulsified acid changed with the change of the volume fraction of the dispersed phase and the viscosity of the continuous phase. **Fig. 6-12** shows the volume oil emulsified acid required to achieve breakthrough as a function of the oil saturation in the core for emulsified acid injected at 2 and 10 cm^3/min. The trend of the plotted data indicates that as the oil saturation increased, the volume of emulsified acid to achieve breakthrough increased, at both acid injection rates of 2.0 and 10.0 cm^3/min. This agrees with what was mentioned previously in **Fig. 6-10**, as there is more crude oil, larger amounts of calcium in coreflood effluent fluid samples were detected, more calcite was dissolved, and so larger volumes of emulsified acid were consumed to achieve breakthrough.

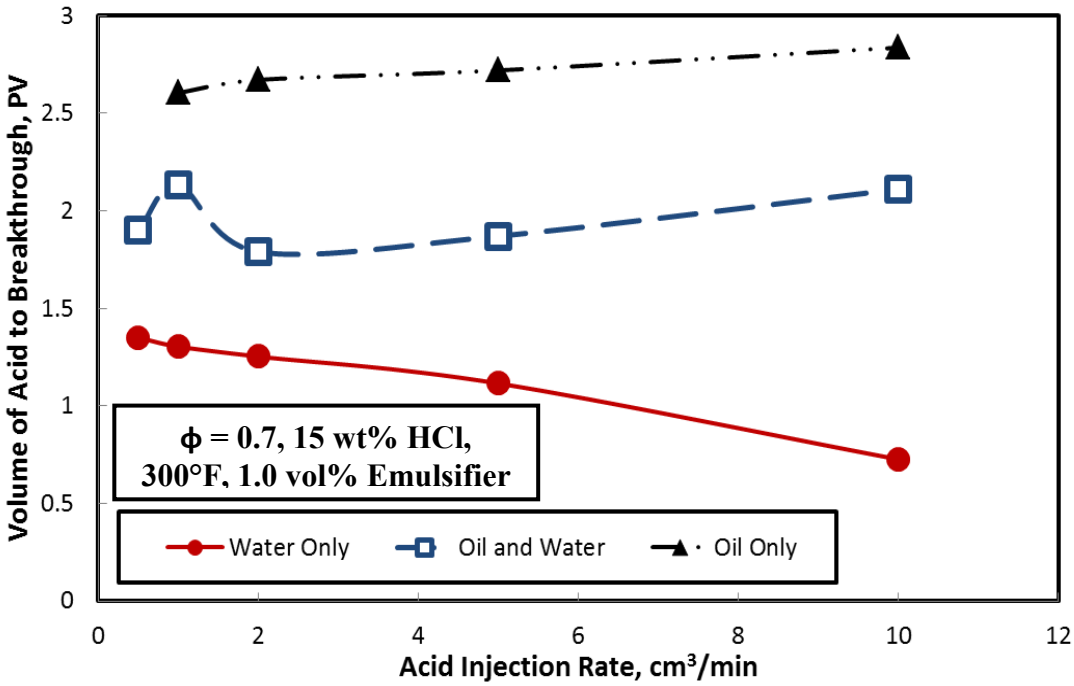

Fig. 6-11: Change of acid volume to breakthrough with acid injection rate.

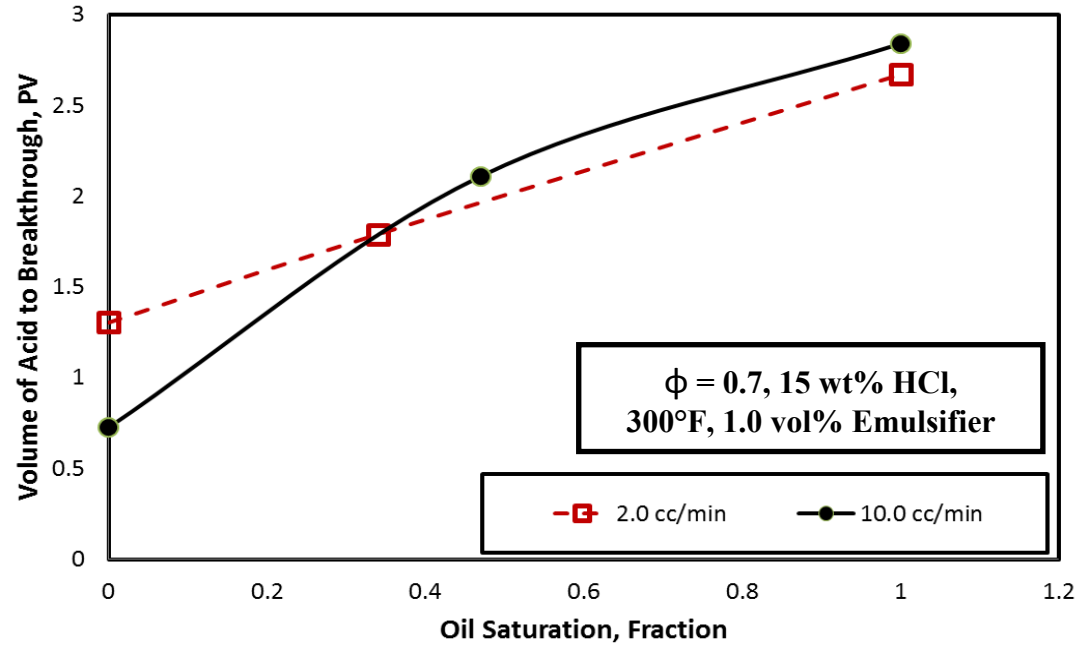

Fig. 6-12: Volume of emulsified acid to achieve breakthrough as a function of initial oil saturation in the core.

6.3.9 CAT Scan Images

Examples of the 2D images for the 6 in. long limestone cores saturated with crude oil at irreducible water, and cores saturated with 100% crude oil treated with 15 wt% HCl emulsified acid at a temperature of 300°F are shown in **Fig. 6-13** and **Fig. 6-14**, respectively. No face dissolution was noticed in the core inlet face for all injection rates studied. At all injection rates, the emulsified acid achieved breakthrough in all cores, and the 2D images show that there is more than one wormhole created at the core inlet face. Some of these wormholes extended from the core inlet face to the core outlet face. The wormholes created by emulsified acid in cores saturated with crude oil at irreducible water saturation and cores saturated with 100% crude oil were more dominant and larger in size than those created in cores saturated with 100% water. This can be referred to the fact that more emulsified acid was consumed in treating core samples. Also, more rock was dissolved in the case of treating cores saturated with crude oil at irreducible water, and cores saturated with 100% crude oil. As a result, more rock dissolved and larger wormholes were created. From the CAT scan images, the wormholes created were clear noted by the dark spots that extended from the core inlet face to the core outlet face. The wormhole size in the case of cores saturated with crude oil at irreducible water was larger than the wormhole created by emulsified acid in cores saturated with 100% water. This can be confirmed by the total amount of calcium collected in the effluent fluid samples data shown in **Fig. 6-10**. For example, the total amount of calcium in coreflood effluent fluid samples for an emulsified acid injection rate of 1.0 cm^3/min changed from 0.678 to 1.197 g when cores were saturated 100% water and 100% crude oil,

respectively. At an emulsified acid injection rate of 10.0 cm^3/min, the total amount of calcium in coreflood effluent fluid samples changed from 0.93 to 1.78 g when cores were saturated 100% water and 100% oil, respectively.

The emulsified acid was an effective stimulation fluid that can be injected at low rates (0.5 cm^3/min) or high rates (10 cm^3/min) and was able to create deep wormholes, with no face dissolution. Also, the presence of crude oil in the core samples had a significant effect on the volume of the emulsified acid consumed, the size and number of the created wormholes, and also the efficiency of the treatment. These results are very important in deciding the importance of pre-flushing the well before acid injection, since the environment of the wellbore affected the performance of the emulsified acid systems.

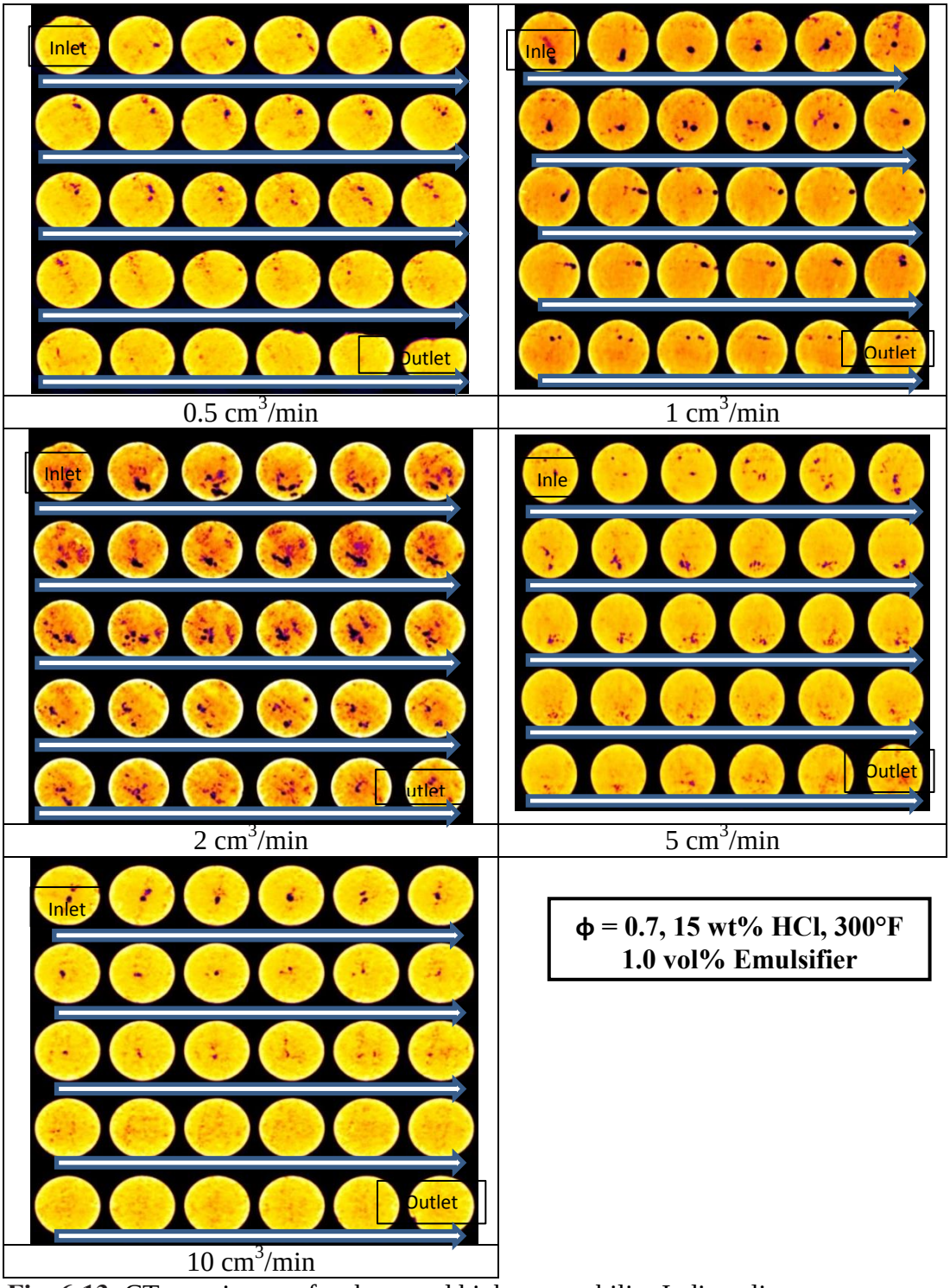

Fig. 6-13: CT scan images for the tested high permeability Indiana limestone cores saturated with naphthenic crude oil at irreducible water saturation.

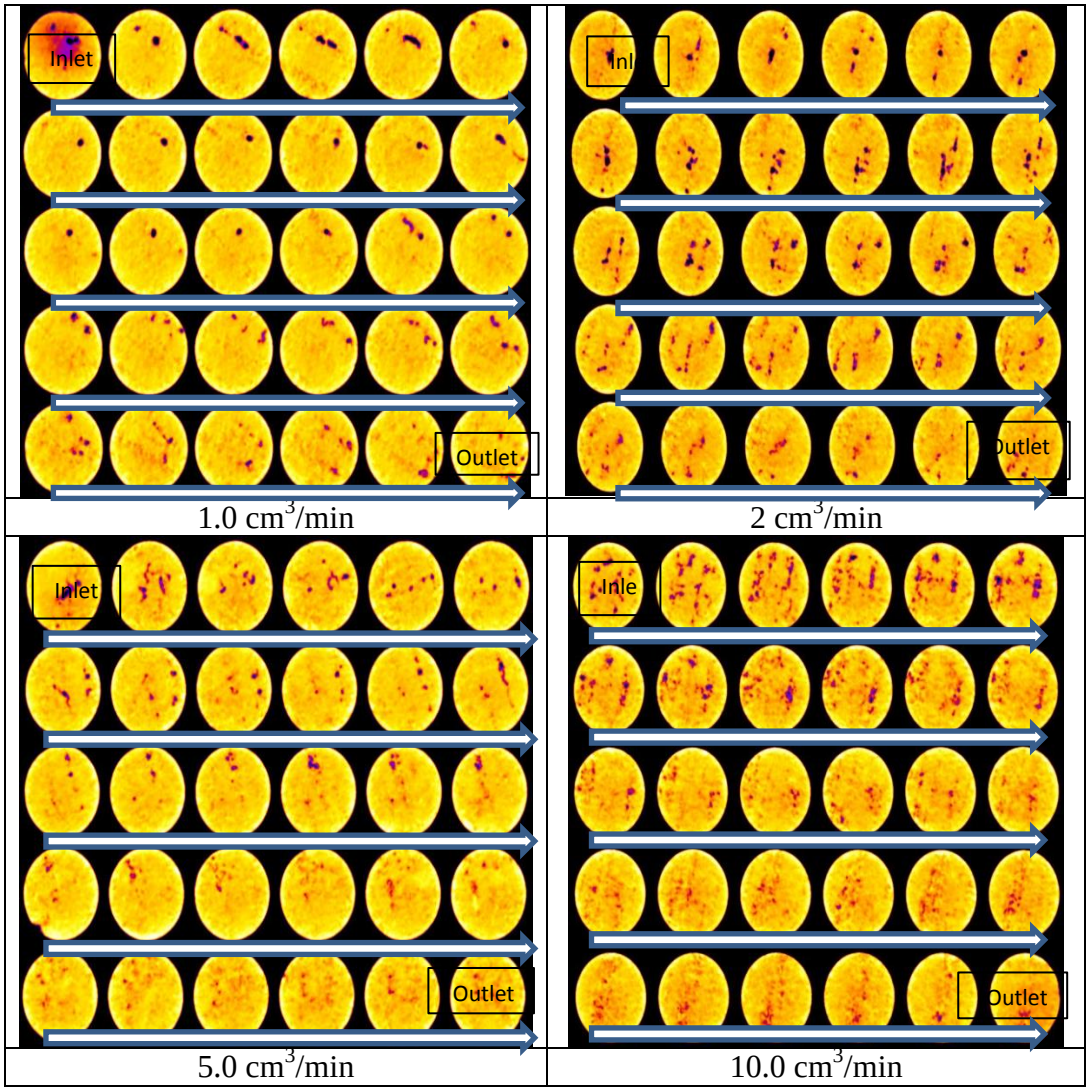

ϕ = 0.7, 15 wt% HCl, 300°F, 1.0 vol% Emulsifier

Fig. 6-14: CT scan images for the tested Indiana limestone cores saturated with crude oil.

7. EVALUATION OF THE PERFORMANCE OF EMULSIFIED ACIDS USING DOLOMITE CORE SAMPLES

7.1 Introduction

Acid stimulation treatment involves injection of acid to attack the rock, and dissolve porous and non-porous minerals in order to increase the well productivity (or injectivity) of oil, gas, and water wells. The use of different fracturing methods for stimulation of oil, gas and water wells has become a common practice in the petroleum industry. It is very important to optimize the treatment design, and to predict the post treatment performance (Anderson 1991).

Navarrete et al. (2000) presented an emulsified acid system which was stable up to 350°F, highly retarded, and more viscous than straight acid. They showed field case histories in the Smackover dolomite formation in Alabama. All tests were conducted with Phosphoria dolomite, which is 98 wt% pure dolomite, with a grain density of 2.85 g/cm^3, porosity of 11.3 vol%, and an air permeability of 0.43 md. The field case histories show the improvements of two to four times in production of oil and gas resulting from emulsified acid fracturing treatments in comparison with prior similar treatments done with straight acid. Nasr-El-Din et al. (2001) conducted a coreflood study using emulsified acid (28 wt% HCl and acid/diesel volume ratio was 70 to 30). The emulsified acid was used in stimulation of wells drilled in deep sour gas reservoir. The lithology of the formation was mainly dolomite with some calcite and streaks of anhydrite. Coreflood tests, conducted using tight dolomite cores, indicated that emulsified acid created deep wormholes, which significantly increased the permeability of the treated cores.

Lynn and Nasr-El-Din (2001) conducted a core based comparison of the reaction characteristics of emulsified acid and in-situ gelled acid. Samples were selected reflecting the nature of the reservoir. The mineralogy of the core samples was determined by X-ray diffraction (XRD) analysis. The carbonate minerals include calcite ($CaCO_3$), ankerite $\{CaMgFe\}(CO_3)_2$, dolomite $\{CaMg\}(CO_3)_2$, and siderite ($FeCO_3$). This mix of sample mineralogy is typical of the Khuff formation in the Middle East. Lynn and Nasr-El-Din (2001) concluded that emulsified acid was injected into tight cores without encountering any problems, the acid propagation rate in the core plugs was very fast, and the emulsified acid enhanced core permeability by a factor that depended on acid injection rate.

Bartko et al. (2003) studied the impact of acid type and lithology on the performance of acid fracturing treatments of a gas carbonate reservoir. They tested 28 wt% regular HCl, emulsified acid, in-situ gelled acid, and a mix of 15 wt% HCl/ 9 wt% formic gelled acids. The target zone contained calcite and dolomite. Bartko et al. (2003) evaluated the performance of the acid based on the lithology type. They found that emulsified acid was superior in a dolomitic lithology. Laws et al. (2005) described the strategy that was developed to optimize the acid stimulation treatment of the Harweel Cluster in Oman. The lithology of the Harweel Cluster is mainly dolomite with small amounts of limestone dispersed randomly throughout. The results of the treatment performed on two fields indicated that emulsified acid systems have shown superior diversion characteristics compared to gelled acid. Also, emulsified acid treatments resulted in higher negative skin and better inflow distribution compared to gelled acid.

Kasza et al. (2006) mentioned that stimulation of a high temperature dolomite formation, using straight HCl was not effective. Emulsified acid was selected to be an alternative to regular HCl. The prepared emulsified acid has to be effective for acidizing dolomite reservoirs at temperature of 120°C. The reaction rate between dolomite and emulsified acid was measured using the rotating disk apparatus. Laboratory research confirmed the efficiency of emulsified acid use for acidizing dolomite formations. A pilot test was performed on one of the oil producing wells; two fold oil production increase was obtained which indicated that the treatments were successful.

Nasr-El-Din et al. (2008a) developed and used a new emulsified acid for fracturing ten wells in a deep gas reservoir in Saudi Arabia. Lithological studies have shown that the formation is composed of dolomite intermingled with limestone and intermittent anhydrite stringers. The performance of the wells stimulated was significantly better than after the treatment. Nasr-El-Din et al. (2008b) performed laboratory work to describe the effect of various acid systems on the strength reduction of limestone and dolomite formation rock samples, and so on the production response from these formations. Neat, emulsified, gelled and cross-linked 15 wt% HCl were tested. Nasr-El-Din et al. (2008b) found that the acid-system choices made a significant difference in the degree of rock softening of limestone and dolomite formations. Also, emulsified acid caused the least softening effect on the limestone and dolomite cores, and production response from emulsified acid treatments was the best.

In the current part of this study, an emulsified acid was prepared using a cationic emulsifier at concentration of 1 vol%. The final HCl concentration of emulsified acid

was 15 wt% and the acid volume fraction was 0.7. Dolomite core samples were obtained from an outcrop and were used to study the performance of the emulsified acid using a coreflood setup. Core samples of initial permeability in the range of 1.6 to 20.9 md were used in the coreflood study.

7.2 Experimental Studies

7.2.1 Materials and Acid Preparation

The emulsions were prepared using diesel and an acid solution (HCl and water) following the same procedure described in Chapter 6, section 6.2.1.

7.2.2 Core Preparation

The porosity of all core plugs was measured using the saturation method. All cores were dried in an oven at a temperature of 302°F, and the weight of the dry core samples was measured using a digital balance. All core samples were saturated with de-ionized water under vacuum for 24 hours. The cores were re-weighed and the weight of the saturated core samples was obtained. The pore volume of the core samples, and hence the core porosity, were calculated. The core porosity was found to be in the range of 9.3 to 14.0 vol%.

The initial permeability of the dolomite cores was measured using the coreflood setup described in **Fig. 5-1**. The core permeability was measured using de-ionized water. The initial permeability of dolomite cores ranged from 1.6 to 150 md. Cores with an initial permeability falling in the range of 1.6 to 20.9 md were selected to be used to test the performance of the emulsified acid using the coreflood setup.

7.2.3 Equipment

The droplet size distribution and the apparent viscosity of the emulsified acid system which was used in the current study were measured and the results were presented in Chapter 3. All the coreflood experiments were performed using the coreflood setup, described in **Fig. 5-1**, in Chapter 5. Samples of the effluent fluids were collected, and pH values were measured using an Orion PrepHecT Ross Electrode. The calcium concentration of the effluent samples was measured using the ICP (Inductively Coupled Plasma).

7.3 Results and Discussion

7.3.1 X-Ray Fluorescence of Dolomite Samples

Dolomite cores, from a local company, were obtained as 6 in. long cores and 1.5 in. diameter. Rock composition was determined by X-ray fluorescence (XRF). Disks with a diameter of 1.5 in. and a thickness of 0.75 in. were cut, and tested using the X-ray fluorescence (XRF). Elemental analysis showed that the dolomite contained more than 94 wt% calcium, magnesium, carbon and oxygen. **Tables 7-1** and **7-2** give the XRF results of the two dolomite core samples, and the calcium to magnesium ratio, respectively. From **Table 7-2**, the average calcium to magnesium molar ratio is approximately 1.20. The calcium to magnesium ratio is larger than 1, which indicates the dolomite cores contain calcite.

Table 7-1: Elemental analysis of two dolomite cores using the XRF technique.

	Concentration, wt%	
Element	**Sample # 1**	**Sample # 2**
O	51.3	48.5
Ca	22.7	21.8
C	12.6	11.6
Mg	11.6	10.3
Si	0.533	3.29
Na	0.458	2.32
Al	0.235	0.837
Fe	0.204	0.489
K	0.16	0.273
Cl	0.0779	0.252
S	0.0475	0.18
Mn	0.0196	0.0155
Sn	0.0112	0.0112
Total	100.03	99.9963

Table 7-2: Calcium to magnesium molar ratio in dolomite rocks used in the study.[1]

Sample #	Element	Moles	Molar Ratio of Ca to Mg
1	Ca	0.567	**1.174**
	Mg	0.483	
2	Ca	0.545	**1.270**
	Mg	0.429	

[1] calcium to magnesium molar ratio in pure dolomite should be 1.0.

7.3.2 Coreflood Study

Emulsified acid was prepared using 1.0 vol% emulsifier at 0.7 acid volume fraction, and the final HCl concentration was 15 wt%. Five coreflood runs were performed, using the coreflood setup shown in **Fig. 5-1,** at emulsified acid injection rates of 0.1, 0.5, 1, 2, 5, and 10 cm^3/min. The main objective of these coreflood experiments is to test the effect

of the injection rate on the emulsified acid volume to achieve breakthrough, and on the resulted wormhole characteristics. **Table 7-3** gives the data for the core samples (6 in. in length and 1.5 in. in diameter) which were used in the coreflood study. All coreflood runs were performed at a temperature of 300°F. For each coreflood experiment, the pressure drop across the core was plotted using Lab-View software. Samples of the coreflood effluent were analyzed using the ICP technique in order to measure calcium and magnesium concentrations.

Table 7-3: Data for 6 in. long coreflood experiments.

Run #	$Q_{Injection}$, cm^3/min	PV to BT	K_{final}, md	K_{final}/ $K_{initial}$
1	0.5	1.25	1732	1082.5
2	1.0	2.29	425	47.2
3	2.0	1.94	270	117.4
4	5	2.03	530	143.2
5	10	2.37	143	7.0

7.3.3 Dolomite Cores and Emulsified Acid

Fig. 7-1 shows the pressure drop across the core during the injection of 1.0 vol% emulsified acid at an injection rate of 1 cm^3/min and at a temperature of 300°F. The initial core permeability, before acid injection, was 9.0 md. During the initial step of water injection, the pressure drop across the core was stabilized at a constant value of 25 psi. After the pressure drop across the core was stabilized at a temperature of 300°F, emulsified acid was injected into the core sample. As the emulsified acid was injected into the core sample, the pressure drop across the core started to increase. This increase

in pressure drop across the core sample is referred to the high viscosity of emulsified acid. The emulsified acid system used in the current work is a non-Newtonian shear thinning fluid, so the viscosity of emulsified acid will be affected by the shear rate inside the core. The shear rate inside the core is a function of acid injection rate, porosity, and core permeability. The shear rate increases with the increase in injection rate and reduction in core permeability (Gomaa and Nasr-El-Din 2010). The initial core permeability is low and the injection rate is low (1.0 cm^3/min), so the total effect of both parameters is that the shear rate was not high enough to cause a reduction in the emulsified acid viscosity. As a result, and with more emulsified acid injection, the pressure drop across the core continued to increase.

As the emulsified acid injection continued into the core, the reaction with dolomite started to take place, and the rock was dissolved as a result of the reaction with the emulsified acid. Both the calcium and magnesium concentrations of the coreflood effluent samples started to increase. At the same time that dolomite was reacting with emulsified acid, emulsified acid started to create wormholes and penetrate the core deeper. Due to the creation of wormholes in dolomite cores, the core permeability started to increase and then the pressure drop across the core started to decrease. The reaction of emulsified acid with dolomite continued and wormholes extended until emulsified acid achieved breakthrough. At this instant, the pressure drop across the core had a sudden drop. The final pressure drop after emulsified acid breakthrough occurred was around 5 psi. The final pressure drop was less than the initial pressure drop indicating the final permeability was greater than the initial permeability. After emulsified acid

breakthrough occurred in the core, 10 vol% mutual solvent in water was injected to remove the remaining diesel and emulsion. The final permeability was measured using the coreflood setup after the core was left to cool down. The final permeability was found to be 425 md, and the ratio of the final to the initial permeability was around 47 (**Table 7-3**) indicating an enhancement of the core permeability through the creation of deeply penetrating wormholes.

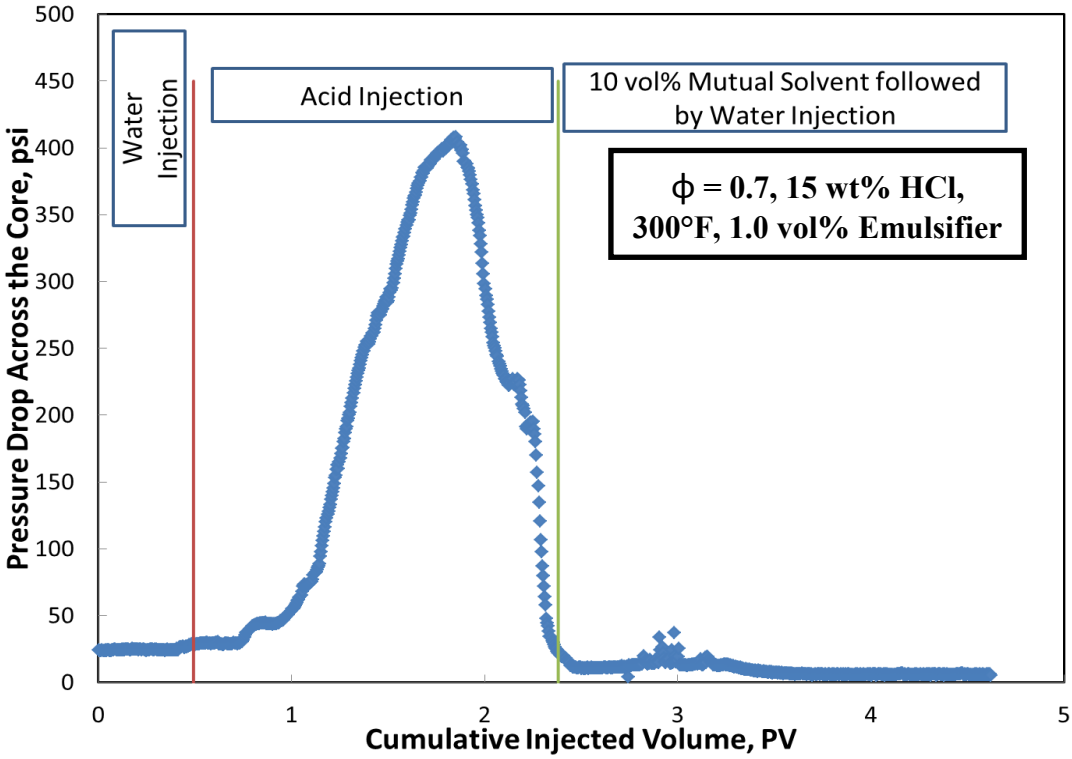

Fig. 7-1: The pressure drop across the core for emulsified acid injection rate of 1.0 cm^3/min at 300°F.

At higher emulsified acid injection rates, such as 5 cm^3/min at 300°F, the pressure drop behavior was like what was noticed at emulsified acid injection rate of 1.0 cm^3/min. The only difference is that the pressure drop increased from 175 psi to 290 psi, while in the case of an emulsified acid injection rate of 1.0 cm^3/min the pressure drop across the core increased from 25 psi to around 405 psi. This difference in pressure drop across the core is attributed to the combination effect of the core permeability and the injection rate on the shear rate inside the core, and hence on the viscosity of emulsified acids. In the case of higher injection rate, the shear rate inside the core is higher than that at lower injection rates. Since the emulsified acid is a non-Newtonian shear thinning fluid, this will result in a reduction in the emulsified acid viscosity, and so less increase in the pressure drop across the core.

In the case of injection of emulsified acid at 5 cm^3/min, the pressure drop initially was constant during the injection of water at a value around 175 psi. As emulsified acid was injected into the core, the pressure drop across the core slightly increased due to the viscosity of the emulsified acid. As the injection of the emulsified acid was continued in the core, the emulsified acid started to react with dolomite and, as a result, calcium and magnesium concentrations of the effluent fluid started to increase. With injection of acid, the pressure drop increased to a maximum value of 290 psi. Wormholes started to form and penetrated the core deeper, and these wormholes caused the pressure drop to decrease until acid breakthrough occurred in the core. The final pressure drop across the core after acid breakthrough occurred was around 20 psi, which was lower than the initial pressure drop across the core during the deionized water injection step (175 psi).

Emulsified acid breakthrough occurred after the injection of 2.0 PV's of emulsified acid. After that, 10 vol% mutual solvent solution was injected in the core to remove any remaining emulsion or diesel. The core was left to cool down and the final permeability of the core was measured. The final permeability of was found to be 530 md (**Table 7-3**). The ratio of the final permeability to the initial permeability of the core was found to be 143.2 (**Table 7-3**). This indicates that the emulsified acid was effective in the creation of conductive wormholes in dolomite rocks at a temperature of 300°F.

Fig. 7-2 shows the calcium and magnesium concentrations in the coreflood effluent samples for the experiment performed at an emulsified acid injection rate of 1.0 cm^3/min. upon injection of deionized water, the calcium and magnesium concentration were almost zero. With injection of the emulsified acid into the dolomite core samples, the reaction of dolomite and emulsified acid started, and the calcium and magnesium concentrations started to increase. The calcium concentration reached a maximum value of 19080 mg/l, while the magnesium concentration reached a maximum value of 10870 mg/l. After acid breakthrough, 10 vol% mutual solvent was injected as a back flow to remove any remaining emulsion, then followed by injection of deionized water. The calcium and magnesium concentration started to decrease until they reached a value of zero.

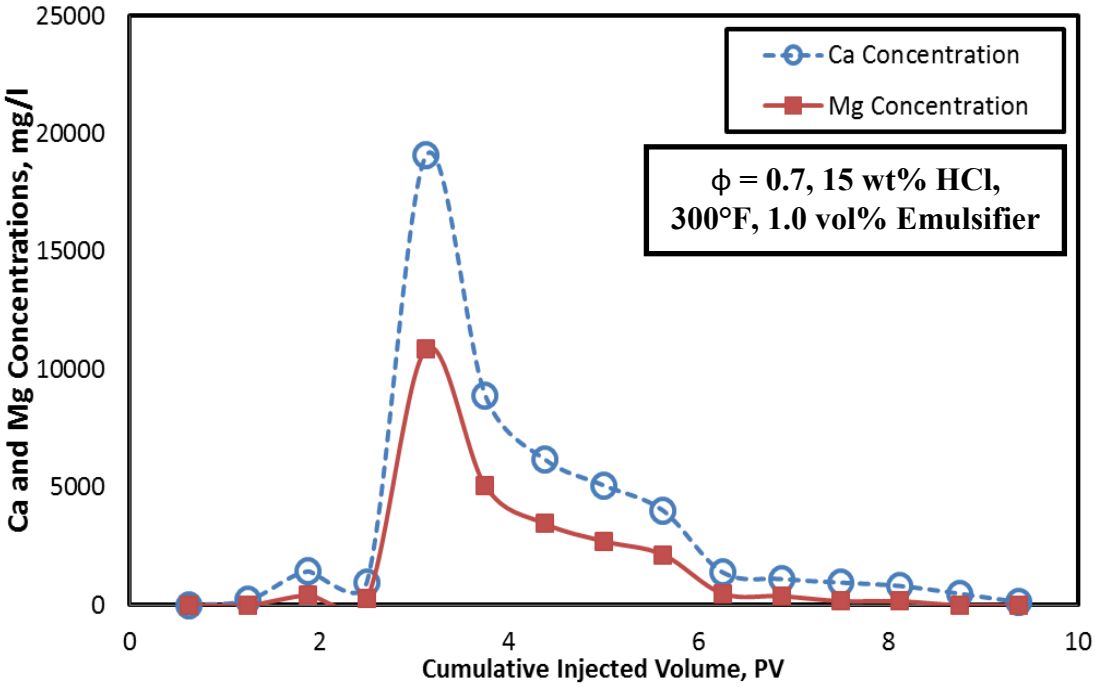

Fig. 7-2: The calcium and magnesium concentration in effluent fluid samples for emulsified acid injection rate of 1.0 cm^3/min at 300°F.

7.3.4 Total Amount of Calcium and Magnesium in Effluent Samples

The total amount of calcium and magnesium in the coreflood effluent fluid samples is a direct indication of the solubility of dolomite cores in emulsified acid. The total amount of calcium and magnesium was then calculated by the integration of the calcium and magnesium concentrations data as a function of pore volume injected (like the data shown by **Fig 7-2)**. **Fig. 7-3** shows a comparison of the total amount of calcium and magnesium in case of injection of the emulsified acid in dolomite cores saturated with 100% water. From **Fig. 7-3**, the total amount of calcium and magnesium in coreflood effluent fluid samples increased as the injection rate increased. This indicates that, with the increase in the injection rate of the emulsified acid, a greater amount of rock was

dissolved, and so a larger volume of emulsified acid was consumed in the treatment in order to achieve breakthrough.

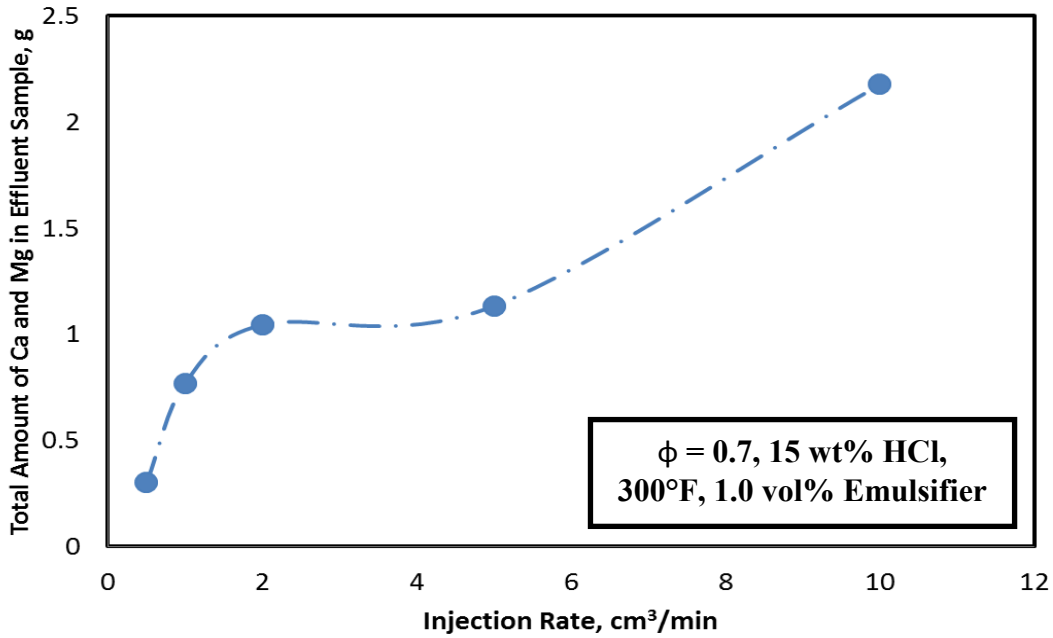

Fig. 7-3: The total amount of calcium and magnesium in the effluent fluid samples.

7.3.5 Volume of Acid to Breakthrough and Optimum Injection Rate

Optimum injection rate is the acid injection rate at which the volume of acid required to achieve breakthrough is a minimum. Five coreflood experiments were performed using emulsified acid systems formulated using 1.0 vol% emulsifier, and the final HCl concentration was 15 wt%, for an acid to diesel volume ratio of 70-30. The volume of emulsified acid to achieve breakthrough changed with the emulsified acid injection rate. **Fig. 7-4** shows the relationship between the volume of emulsified acid to achieve

breakthrough and the emulsified acid injection rates. From **Fig. 7-4**, it is apparent that, as the emulsified acid injection rate increased, the volume of emulsified acid required to achieve breakthrough increased. This can be attributed to the increase in the volume of emulsified acid consumed indicated by the increase in the total amount of calcium and magnesium detected in the coreflood effluent fluid samples. This indicates that, for the studied range of emulsified acid injection rates (0.5 to 10 cm^3/min); there is no optimum acid injection rate when dealing with dolomite cores saturated with 100% water in the permeability range studied (1.6 to 20.9 md). At all injection rates, the emulsified acid achieved breakthrough, and was found to be successful in creating wormholes extending from the core inlet face to core outlet face. The final permeability of the core samples increased at all emulsified acid injection rates.

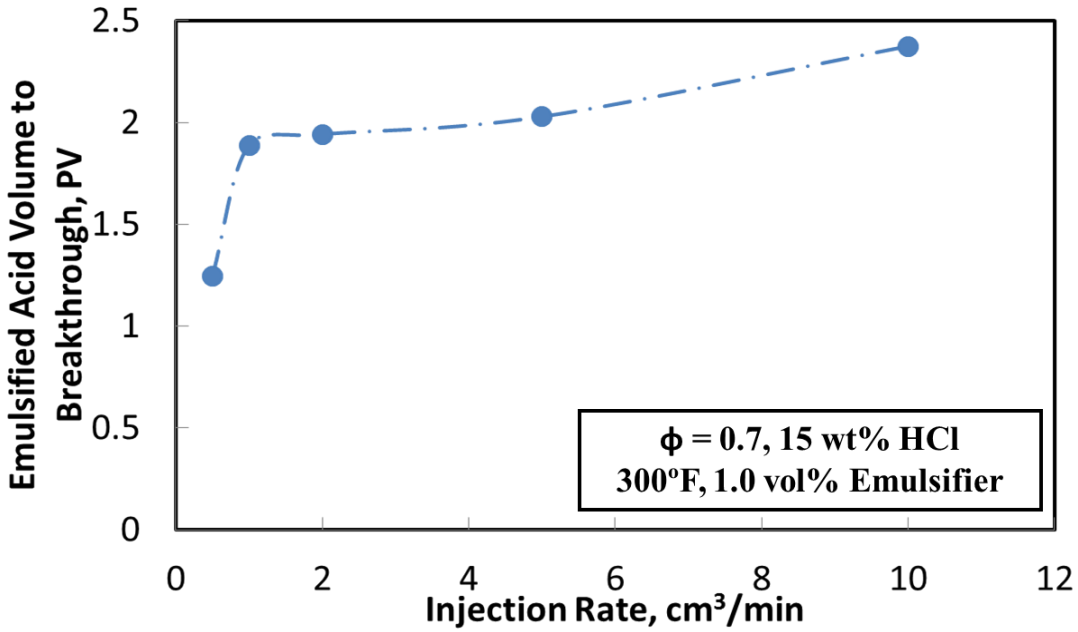

Fig. 7-4: Volume of emulsified acid required to achieve breakthrough.

7.3.6 CAT Scan Images

Figs. 7-5a and **b** shows the 2D CAT scan images for the 6 in. long core before and after it was treated by the emulsified acid systems, formulated at 1 vol% emulsifier, at an injection rate of 1.0 cm^3/min and temperature of 300°F, respectively. Before the acid treatment, the CAT scan images for the core sample show that there were no channels or vugs in the core. After the emulsified acid was injected at a temperature of 300°F and injection rate of 1.0 cm^3/min, no face dissolution was noticed in the core inlet face. The core initial permeability was 9 md. At this low emulsified acid injection rate, the 2D CAT scan images revealed that the acid created more than one wormhole, only one main wormhole continued to the outlet face of the core, and it became the main wormhole. Emulsified acid was very effective even at a low acid injection rate.

Figs. 7-6 a and **b** show the 2D CAT scan images for the 6 in long cores treated by emulsified acid, formulated at 1 vol% emulsifier, at an injection rate of 10 cm^3/min and a temperature of 300°F. The CAT scan images of the core before emulsified acid injection indicated that the core contains a channel; this channel is not connected through the whole core. After the emulsified acid was injected into the core, the emulsified acid created wormholes. At this high injection rate, the 2D scan images revealed that the acid created many wormholes; only a few of them continued to the end of the core. No face dissolution was noticed in the core inlet face.

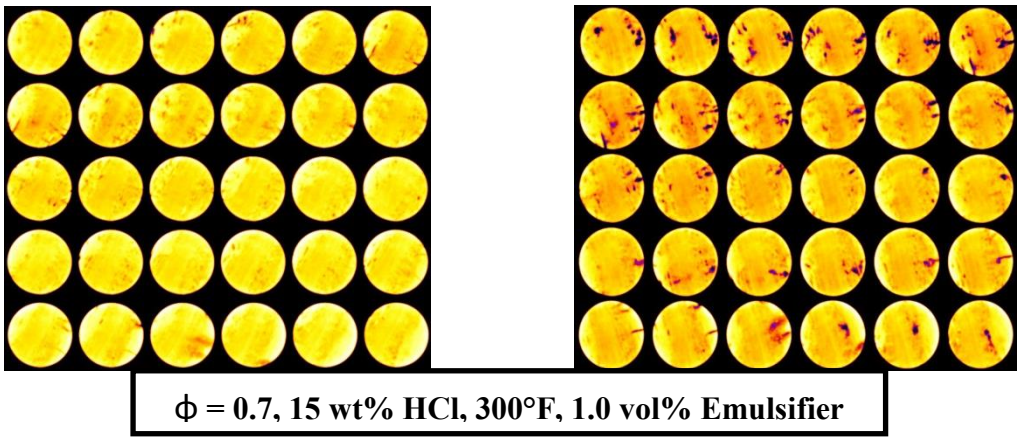

Fig. 7-5: CAT scan images for dolomite core before and after acid treatment performed at acid injection rate of 1.0 cm^3/min and 300°F.

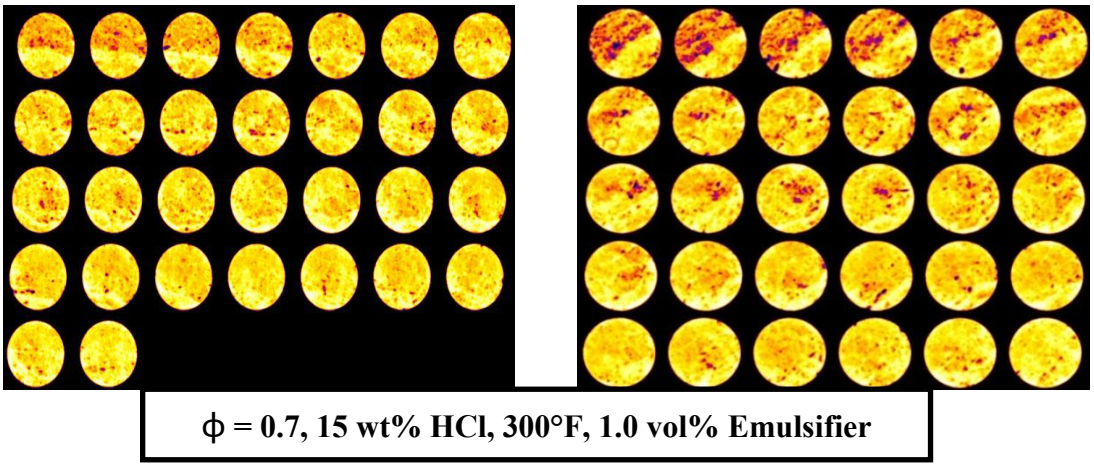

Fig. 7-6: CAT scan images for dolomite core before and after acid treatment performed at acid injection rate of 5.0 cm^3/min and 300°F.

8. EVALUATION OF THE PERFORMANCE OF EMULSIFIED ACIDS USING RESERVOIR CORE SAMPLES

8.1 Introduction

Different types of acids can be used to stimulate oil and gas production wells (Al-Anazi et al. 1998; Kasza et al. 2006), and to stimulate water injection wells and disposal wells (Mohammed et al. 1999; Nasr-El-Din et al. 2000). In most carbonate-stimulation treatments, HCl has been used as the main stimulation fluid. The reaction between HCl and calcite is very fast, and this rate becomes higher at higher downhole temperatures, which results in rapid HCl spending (Allen and Roberts 1989; Nasr-El-Din et al. 2003a). There are several alternatives to regular HCl that can be used to lower the acid spending rate; one of the most widely used alternative is the emulsified acid (Dill 1961; Knox et al. 1964; Crenshaw and Flippen 1968; Nasr-El-Din et al. 2001). The most common hydrocarbon that is used as an external phase is diesel, and it acts like a diffusion barrier between acid and rock (Crowe and Miller 1974; Bergstrom and Miller 1975; Hoefner and Fogler 1985; Daccord et al. 1989; Peters and Saxon 1989), which results in a reduction in the acid-rock reaction rate. This will help in the creation of deep wormholes and etched fractured surfaces, which in turn enhances well performance (Williams and Nierode 1972; Guidry et al. 1989; Navarrete et al. 1998a and b; Nasr-El-Din et al. 2006 and 2008b). Nasr-El-Din et al. (2000) and Buijse and van Domelen (2000) mentioned some of the advantages of an acid-diesel emulsion.

Al-Anazi et al. (1998) studied the use of the emulsified acid to stimulate tight carbonate reservoirs. The experimental tests included coreflood experiments using

reservoir cores at reservoir conditions, and they showed that the emulsified acid formed deep wormholes in tight carbonate cores. Mohamed et al. (1999) investigated the effectiveness of acid treatments to stimulate power water injectors and salt water disposal wells using emulsified acid and in-situ gelled acid as acid diverting stages. Mohamed et al. (1999) concluded that increasing the emulsified acid volume increased the efficiency of the treatment. Nasr-El-Din et al. (2000) conducted experimental studies to evaluate the use of emulsified acid in stimulation of water disposal wells. Nasr-El-Din et al. (2000) concluded that emulsified acid formed deep wormholes in tight carbonate cores, and the size and distribution of wormholes was dependent on the acid injection rate, acid volume, and initial core permeability.

Buijse and van Domelen (2000) studied the application of emulsified acid in the stimulation of heterogonous carbonate reservoirs and they found that acid-in-oil emulsions are effective stimulation fluids in large intervals, where streaks of high-permeability can act as thief zones. Laws et al. (2005) indicated that emulsified acid systems have shown superior diversion characteristics compared to gelled acid when both were applied to stimulate deep wells in the Harweel cluster in Oman. Kasza et al. (2006) mentioned that emulsified acid was selected to be an alternative to regular HCl, and the field results indicated that treatments were successful.

Al-Harbi et al. (2006) evaluated acid treatments for water injection wells. Al-Harbi et al. (2006) concluded that increasing the volume of emulsified acid in acid treatments enhanced the wells injectivity. Abdel Fatah and Nasr-El-Din (2010) utilized HCl emulsified in xylene, instead of diesel, to stimulate wells and at the same time to

remove asphaltene deposition. Appicciutoli et al. (2010) showed that emulsified acid systems can be mixed with custom-tailored asphaltene-solving blends, and this system provided the desired benefits for matrix acidizing, such as stability, high viscosity, and slow reaction, and at the same time it was able to remove asphaltene.

The main objective of the current work is to test the new emulsified acid systems used during the current study with core samples obtained from two different carbonate reservoirs located in the Middle East. All the emulsified acid systems were formulated at 0.7 acid volume fraction, and the final acid concentration was 15 wt% HCl. The emulsifier concentration was 10 gpt (1.0 vol%). A coreflood study was conducted in order to study the efficiency of the emulsified acid system to create wormholes and enhance the permeability of the rock. The coreflood study was performed at 220°F and at different injection rates. Core samples obtained from two reservoirs (Reservoir A and Reservoir Z) were used in the current study.

8.2 Experimental Studies

8.2.1 Materials and Acid Preparation

The emulsions were prepared using diesel and an acid solution (HCl and water) following the same procedure described in Chapter 6, section 6.2.1.

8.2.2 Equipment

The coreflood setup was described in detail in section 5.2.3 and **Fig. 5-1.** The pH values the collected coreflood effluent samples were measured using an Orion PrepHecT Ross Electrode. The calcium concentration in the core effluent samples was measured using the Inductively Coupled Plasma (ICP) technique (PerkinElmer Optical Emission

Spectrometer, Optima 7000 DV) where the spectral range is 160-900 nm with resolution of < 0.009 nm @ 200 nm. Reaction rate experiments were performed using a rotating disk apparatus (**Fig. 3-1**). The details of the RDA were mentioned in section 3.5.3.

8.2.3 Core Preparation

Cylindrical cores were obtained from the two reservoirs (A and Z). Cores from reservoir "A" were of a diameter of 1.0 in., while core samples obtained from reservoir "Z" were of 1.5 in. diameter. The core samples were obtained in different lengths. **Tables 8-1** and **8-2** summarize the data of the core samples used in the current study for cores obtained from reservoirs "A" and "Z", respectively. A total of 14 core samples were selected in order to be used in the coreflood experiments. The core samples were cleaned using the Dean Stark technique to remove any liquid hydrocarbon present in the core samples. Then, the core samples were dried in an oven at a temperature of 150°C (302°F) for 4 hours until the core samples were completely dry. The core samples were weighed using a digital balance to obtain the dry weight. After that, the dried core samples were saturated with deionized water under vacuum for 24 hours, and the weight of the water-saturated cores was measured, the pore volume, and hence the core porosity were calculated (**Tables 8-1** and **8-2**).

Each of the core samples were put in a core holder, and deionized water was injected at different flow rates. For each flow rate, the pressure drop after stabilization was recorded. A plot of flow rate divided by the core cross sectional area vs. the ratio of pressure drop across the core to the core length was used to calculate the initial core permeability of all core samples.

Table 8-1: Data for the cores obtained from reservoir A

Core ID	Lithology	Porosity, %	$K_{initial}$, md	Inj. Rate, cm^3/min	PV to BT	K_{final}, md	$K_{final}/K_{initial}$
1	Carbonate	9.43	4	1	9.167	2855	713.8
2	Carbonate	20.59	1.9	2	2.45	5320	2800
3	Carbonate and Anhydrite	12.51	50	2	7	2570	51.4
4	Carbonate	16.19	96	5	4.87	5500	57.3
5	Carbonate	11.04	34.5	7	4.69	1400	40.6
6	Carbonate and Anhydrite streaks	10.66	45.5	10	5.98	950	20.9

Table 8-2: Data for the cores obtained from reservoir Z and used in the coreflood experiments

Core Name	Porosity, %	$K_{initial}$, md	Inj. Rate, cm^3/min	PV to BT	K_{final}, md	$K_{final}/K_{initial}$
11	9.82	0.4	0.5	2.6	3524	8810
95	12.81	1.9	1.0	2.1	2420	1273.7
94	12.94	2	2.0	1.63	3808	1904
56	21.24	2.2	5	1.20	4600	2090.9
71	14.65	9	10	1.35	4094	454.89

8.3 Results and Discussion

8.3.1 Viscosity of Emulsified Acid

An HPHT rheometer (Grace M5600) was used to measure the viscosity of live emulsified acids under different conditions. The apparent viscosity of the emulsified acid was measured at 75 and 220°F for shear rates up to 1000 s^{-1}. **Fig. 8-1** shows the effect of increasing the shear rate on the apparent viscosity of the emulsified acid system at 75 and 220°F. These data are represented by a straight line on the log-log plot, indicating a

non-Newtonian shear thinning behavior that can be fitted using a power-law model. The power-law model is given by Eq. 8.1:

$$\mu_a = K\,\dot{\gamma}^{n-1} \quad \text{..... (8.1)}$$

where,

K = power-law consistency factor, g/cm.s$^{(n-2)}$

n = power-law index

μ_a = apparent fluid viscosity, poise

$\dot{\gamma}$ = shear rate, s^{-1}

Table 8-3 gives the values of k, and n for the 15 wt% HCl emulsified acid samples prepared using 1.0 vol% emulsifier and measured at 75 and 220°F.

Table 8-3: Power-law parameters for emulsified acids prepared at 1.0 vol% emulsifier.

Temperature, °F	Power-law Constant, K (mPa.s^n)	Power-law Index, n
75	653.29	0.573
220	499.2	0.496

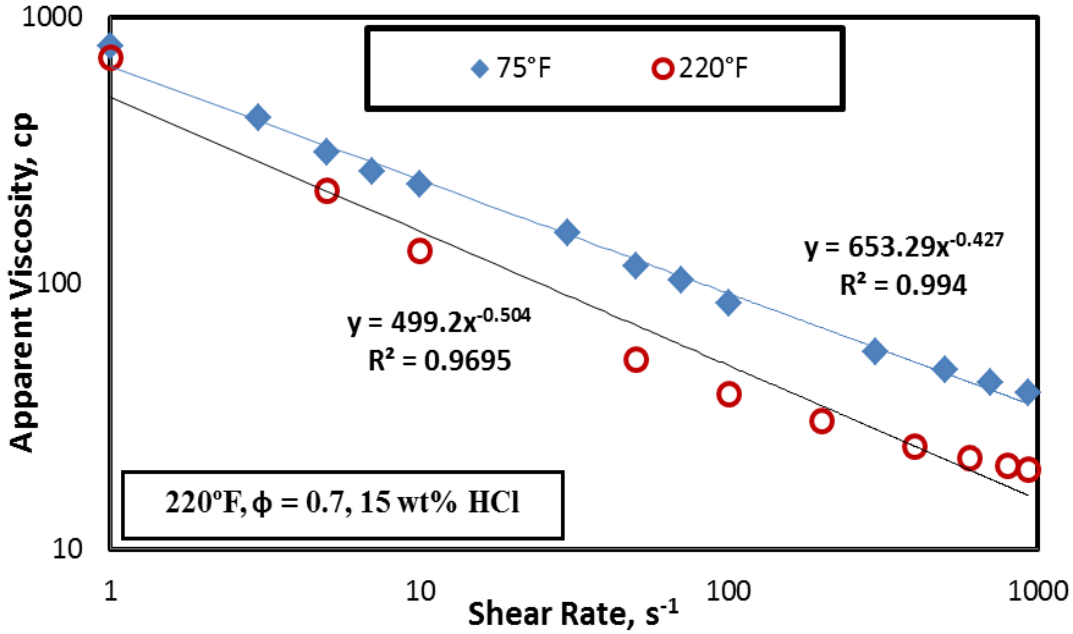

Fig. 8-1: Apparent viscosity of emulsified acid prepared at 1.0 vol% emulsifier.

8.4 Emulsified Acid and Cores Obtained from Reservoir "A"

8.4.1 CAT Scan Study of Fresh Core Samples

Thirty-six core plugs were cut from a carbonate reservoir. The plugs were screened using a computerized axial tomography (CAT) scanning. According to Nevans et al. (1996), a CT number of 2550 and above indicates the presence of extensive anhydrite. Pure dolomite has a CT number of about 2350 and the number for pure limestone is around 2250. CT numbers less than 2200 are indicative of good porosity or fracturing. After scanning the cores, the software ImageJ® was used to analyze the images obtained. To do so, the image stacking feature of this software was used to obtain a series of images in a single window to represent the core at different cuts along the length of the core. CAT scan analysis of core samples indicated that the rock was

heterogeneous. The CT numbers obtained indicated that the description of the cores varied between the following: limestone with streaks of anhydrite, limestone with anhydrite traces, mainly limestone, and vuggy limestone and anhydrite. For the coreflood study, 6 core samples were selected to test the emulsified acid systems; the cores were selected so that the rocks are mainly limestone with no vugs or channels. **Table 8-1** gives a brief description of all the selected cores used to perform the coreflood study, and **Fig. 8-2** shows a slice of the CAT scan images of the fresh core samples used in the coreflood experiments.

8.4.2 Scanning Electron Microscope (SEM) Study

A SEM analysis for 11 representative samples was performed. SEM analysis was performed in order to determine the composition of these core samples, and to compare the results with what was obtained from the CT scan analysis. The samples are mainly carbonates with some indication of a presence of anhydrite (Ca SO4) from the high CT number (spots of CT number > 2550) detected from the CT images. Based on that, the following elements were investigated: Calcium (Ca), Magnesium (Mg), Carbon (C), Oxygen (O) and Sulfur (S). The presence of sulfur indicated the presence of anhydrite, which was observed from CAT scan results. A summary of the SEM analysis for the selected 11 samples is represented in **Table 8-4**. The SEM indicates that the main lithology of the cores obtained from reservoir A is limestone carbonates. Some SEM results indicate the presence of anhydrite through the detection of sulfur. These results are in a good agreement with what was mentioned from the CAT scan study.

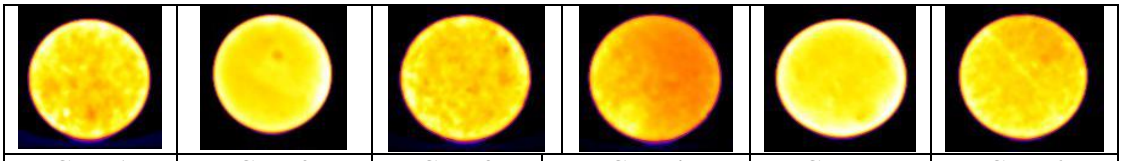

Fig. 8-2: Slice of a CAT images for selected cores before the injection of emulsified acid.

Table 8-4: SEM analysis of core samples

	Elements (wt %)							CAT Scan Results
Core ID	**C**	**O**	**Mg**	**S**	**Ca**	**Al**	**Au**	
Core 1	26.76	50.29	0.08	1.95	20.92	0	0	**CA**
Core 2	8.01	53.16	0	1.43	37.4	0	0	**C**
Core 3	15.12	54.11	0.13	0.05	29.41	1.19	0	**CTA**
Core 4	12.59	54.54	0	0.73	32.14	0	0	**C**
Core 5	25.84	51.69	6.61	0	15.86	0	0	**CSA**
Core 6	8.48	57.87	5.81	9.74	18.11	0	0	**CA**
Core 7	18.53	41.55	0	0	34.64	0	0	**C**
Core 8	14.64	51.94	11.29	0	15.04	1.07	6.02	**CSA**
Core 9	12.43	54.13	0	0.07	33.37	0	0	**CA**
Core 10	20.29	52.1	0.12	0.12	27.36	0	0	**CA**
Core 11	11.34	54.78	0	0.11	33.77	0	0	**C**

8.4.3 Solubility of Core Samples in Regular HCl Acid

The dissolution of calcite ($CaCO_3$) in acids is of interest to many fields of science, and the equilibrium relationships in the calcite-carbonic acid-water system have been studied extensively (Lund et al. 1975). The dissolution rate of calcite in acids has been measured for such purposes as the formulation of antacids, the study of secondary changes in sedimentary deposits, and the acidizing of petroleum wells. The reaction between limestone and HCl can be represented by Eq. 8.2 (Lund et al. 1975):

$$CaCO_{3(s)} + 2\ HCl_{(aq)} \rightarrow CaCl_{2(aq)} + CO_{2(g)} + H_2O_{(l)} \quad \text{..... (8.2)}$$

The solubility of carbonates (limestone and dolomite) in HCl depends on many factors; such as the acid concentration, temperature and mineralogy of the rock itself. From the CAT scan images and SEM analysis, some of the cores cut from the reservoir under consideration contain anhydrite. Anhydrite is a mineral - anhydrous calcium sulfate, $CaSO_4$.The solubility of calcium sulfate in HCl has been measured for a wide range of conditions (Delorey et al. 1996). The solubility of calcium sulfate (anhydrite) in HCl solution increases with the acid concentration up to around (2.5 to 3.0) $mol.dm^{-3}$ HCl. It decreases gradually above this value (Delorey et al. 1996).

The reactivity between the core samples and regular HCl was tested. The test was performed at static conditions and at room temperature (75°F) using 15 wt% HCl solution. The core samples were put in a beaker filled with amount of acid 20 times the weight of the core piece used in the test. The core pieces were weighed before the reaction. After a certain time of reaction, the samples were removed from the acid, rinsed by deionized water and weighed, then samples were returned back into the acid solution to continue the reaction. Eleven samples were tested with 15 wt% HCl. These samples were selected to represent different mineralogy of the rock based on the CAT scan images.

All samples were completely dissolved in acid in times ranging from 15 to 120 minutes except only one sample. The weights of this sample before and after the acid solubility test were 17.27 g and 7.45 g. The weight loss was 58% of the original weight. The remaining core was cleaned and analyzed with SEM technique and the sample was found to contain a significant amount of anhydrite. The weight loss of one of the

samples tested as a function of time is shown in **Fig. 8-4.** The weight decreased, and hence the weight loss increased, upon contact with the acid up to contact time of 9 minutes. At longer contact times, the reaction of the rock was not strong like what was noticed in the first few minutes of contact with acid. This can be referred to the acid spending. From these static simple measurements, it is clear that the core samples obtained from reservoir "A" exhibits a great solubility in regular HCl, although the tests were performed at room temperature. This also indicates that, at high bottomhole temperatures, the reaction with regular HCl acid will be very fast causing acid spending and resulting in face dissolution, and the efficiency of the treatment will be low. So it is recommended to use one of the retarding acid systems such as the emulsified acid.

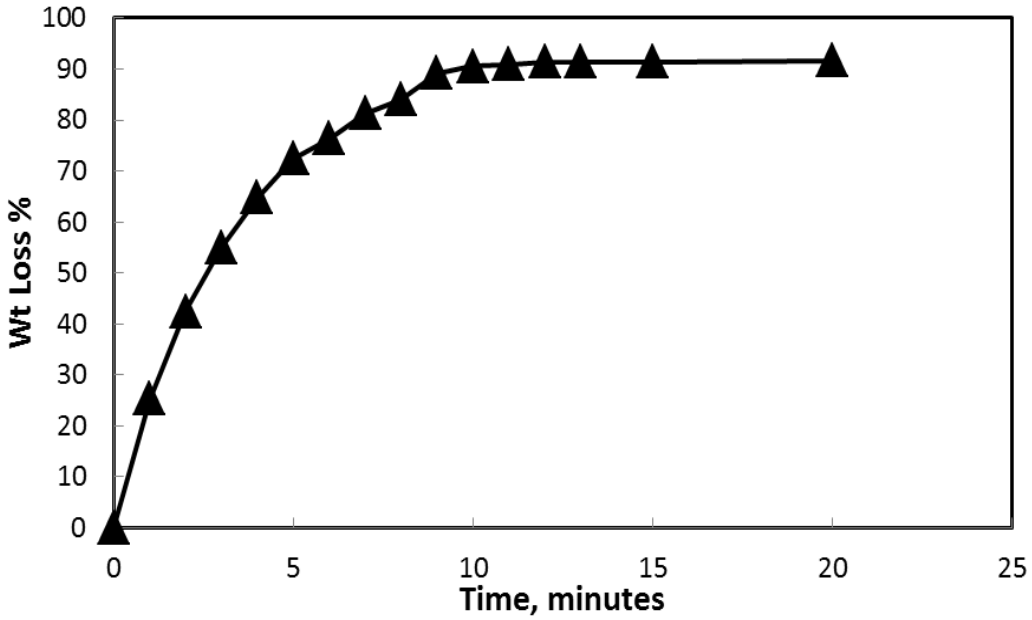

Fig. 8-3: % Weight loss of one of the core sample as a function of contact time with 15 wt% regular HCl acid at 75°F.

8.4.4 Coreflood Study

Coreflood experiments with emulsified acid systems were run using the coreflood setup shown in **Fig. 5-1**. **Table 8-1** gives the data for the 1.0 in. diameter reservoir cores which were used in this coreflood study. Five coreflood runs were performed using emulsified acid formulated using 1.0 vol% emulsifier, and at injection rates of 1, 2, 5, 7 and 10 cm^3/min to test the effect of the injection rate on the acid volume to breakthrough, and the resulted wormhole characteristics. All coreflood runs were performed at a temperature of 220°F. For each coreflood experiment, the pressure drop across the core was plotted using Lab-View software. Samples of the coreflood effluent were analyzed for calcium concentration. The pH value and the density of the effluent samples were measured.

Fig. 8-4 shows the pressure drop across the core (core #1) during the injection of 15 wt% HCl emulsified acid system at an injection rate of 1 cm^3/min and 220°F. The pressure drop initially was stabilized at 24 psi during the injection of water. At the instant where acid injection started, the pressure drop increased as a result of the high viscosity of emulsified acid, then started to decrease as the emulsified acid penetrated and reacted with the rock and started to create wormholes in the core sample. As the rock reacted with the emulsified acid and calcite started to dissolve, the calcium concentration of the coreflood effluent samples started to increase. At the same time the calcite was reacting with emulsified acid, wormholes started to form and penetrate the core. This created wormhole caused the pressure drop to decrease with time, until acid

breakthrough occurred. Nine PV's were needed for 15 wt% HCl emulsified acid to breakthrough the core when emulsified acid was injected at 1.0 cm^3/min.

Fig. 8-5 shows the calcium concentration in the core effluent samples for the experiment shown in **Fig. 8-4**. The calcium concentration increased upon the reaction of emulsified acid with calcite, and reached a maximum value of 38,780 mg/l. After emulsified acid breakthrough occurred in the core, water was injected and as a result the calcium concentration started to decrease. **Fig. 8-6** shows the density and pH of the coreflood effluent samples for the same experiment. The density of the effluent samples increased due to the presence of calcium ions in solution. The pH was around 7 at the start of injection (injection of water) then decreased with the injection of acid until it reached zero and increased again as the injection of water started.

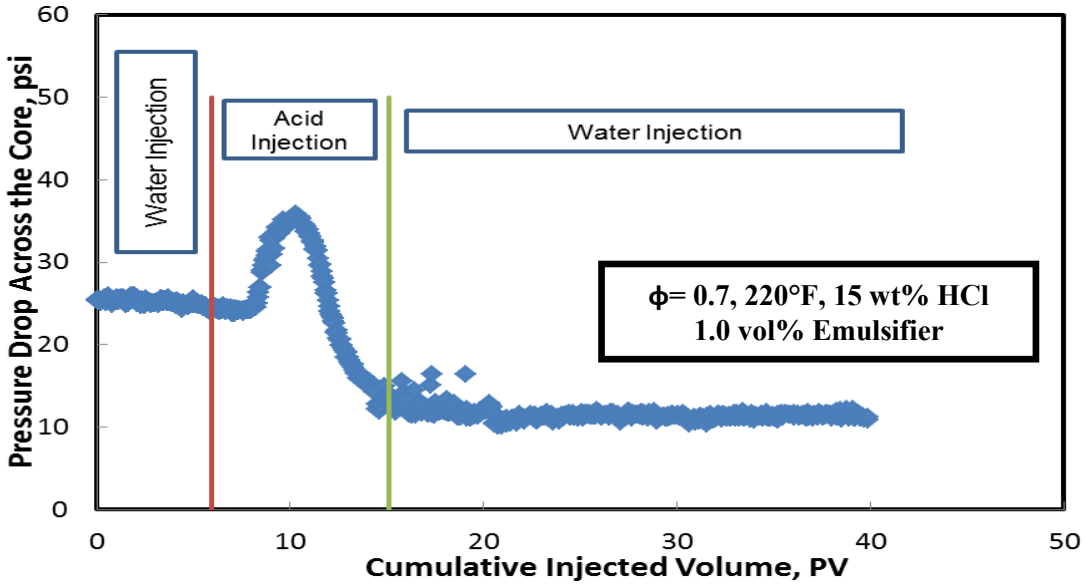

Fig. 8-4: The pressure drop across the core for an injection rate of 1.0 cm^3/min & 220°F.

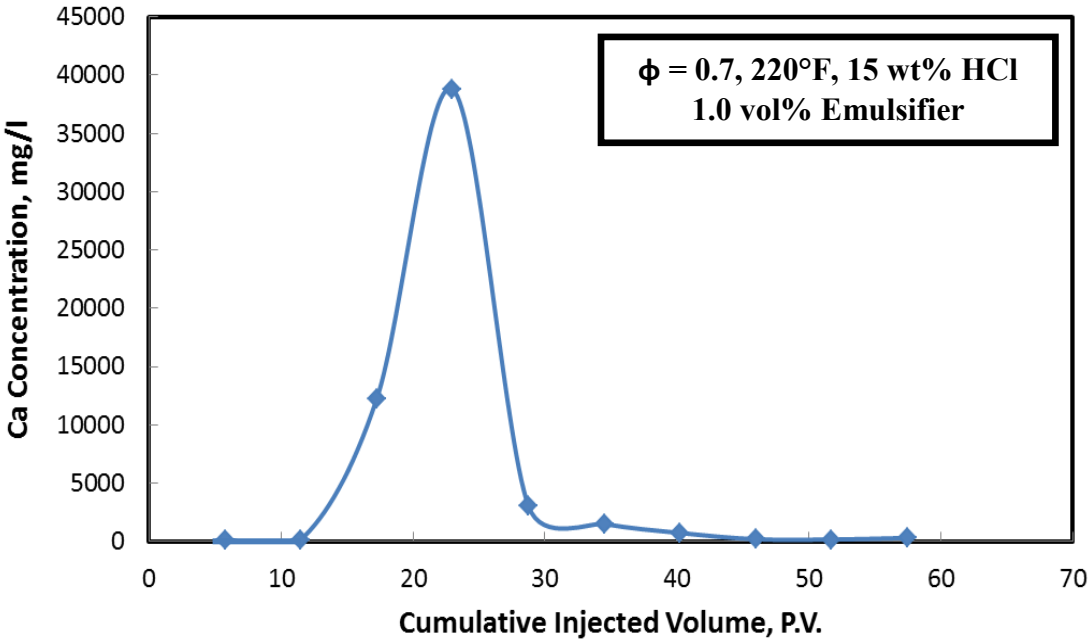

Fig. 8-5: Calcium concentration in the core effluent samples for an injection rate of 1.0 cm^3/min & 220°F.

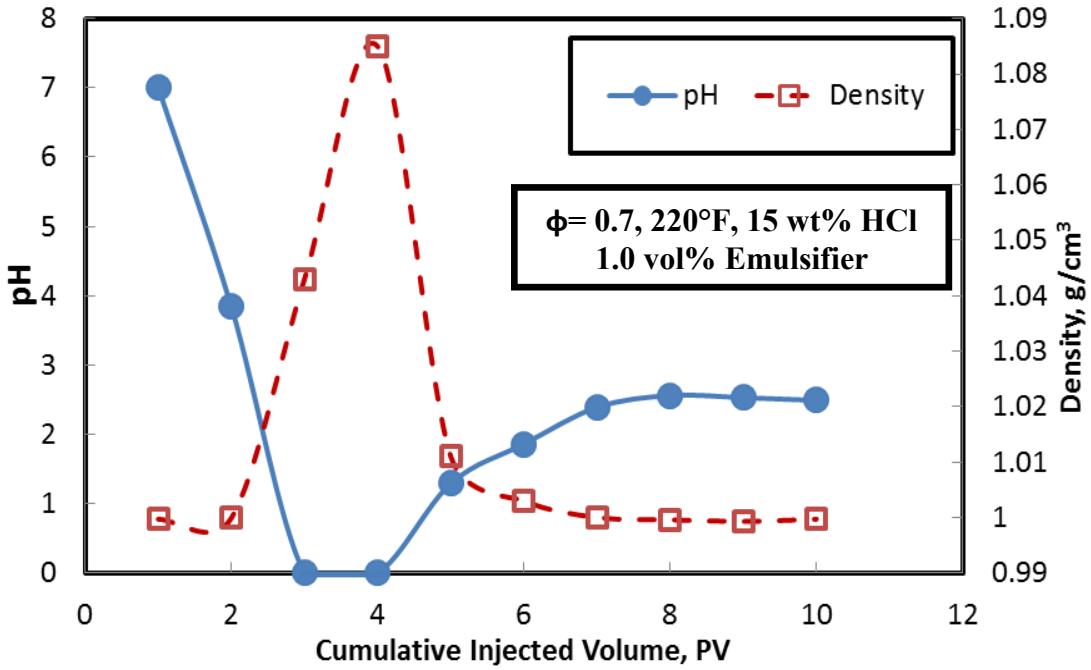

Fig. 8-6: The density and pH value of the core effluent samples for an injection rate of 1.0 cm^3/min & 220°F.

The effect of core permeability on the performance of the emulsified acid and wormhole characteristics was examined using cores # 2 and 3. The permeability of core #2 was about 1.9 md, while the permeability of core #3 was about 50 md. In both experiments, the emulsified acid was injected at a rate of 2 cm^3/min and the temperature was 220°F. **Fig 8-7** shows the pressure drop across the core during the injection of the emulsified acid at rate 2 cm^3/min, for low permeability core #2 and high permeability core #3. The pressure drop behavior was different from one experiment than other. During water injection stage before acid injection, the pressure drop stabilized at a value around 140 psi for core #2 (K = 1.9 md). While, the pressure drop in core #3 (K = 50 md) during water injection was lower than what was recorded in core #2 due to the higher core permeability. For the low permeability core (#2), and as emulsified acid was injected, the pressure drop started to decrease sharply until it reached 7 psi after acid breakthrough the core sample. 2.45 PVs were needed for the acid to breakthrough the low permeability core, while 7 PVs of emulsified acid were needed to achieve breakthrough in the high permeability core (core #3). Upon injection of emulsified acid, the pressure drop behavior was different. When emulsified acid introduced in the low permeability core, pressure drop did not start to decrease. But, when the emulsified acid system was injected inside the high permeability core, the pressure drop started to increase until it reached a peak and then started to decrease again.

The increase in the pressure in the case of injection of emulsified acid into the permeable core (core #3) is attributed to the high viscosity of emulsified acid. From the rheological study, the emulsified acid is a non-Newtonian shear thinning fluid, where the

apparent viscosity decreases with the increase in the shear rate. The shear rate inside the core is function of core permeability and porosity, and the injection rate. The shear rate inside the core increases with the decrease in the core permeability. So, for low permeability cores, the shear rate is high and so the apparent viscosity of emulsified acid will be low, while for high permeability cores, the shear rate will be low and the so the apparent viscosity of emulsified acid will be high resulting in an increase in the pressure drop. The reduction in pressure drop in both cases is attributed to the reaction of emulsified acid with the rock and the creation of wormholes. The same pressure drop behavior was noted in all cores at all injection rates. **Fig. 8-8** shows the calcium concentration in the core effluent samples for both experiments. As shown the calcium concentration for the high permeability core was higher than the calcium concentration in the effluent samples for the low permeability core. This may explain why more PV was needed by the acid to breakthrough in high permeability core.

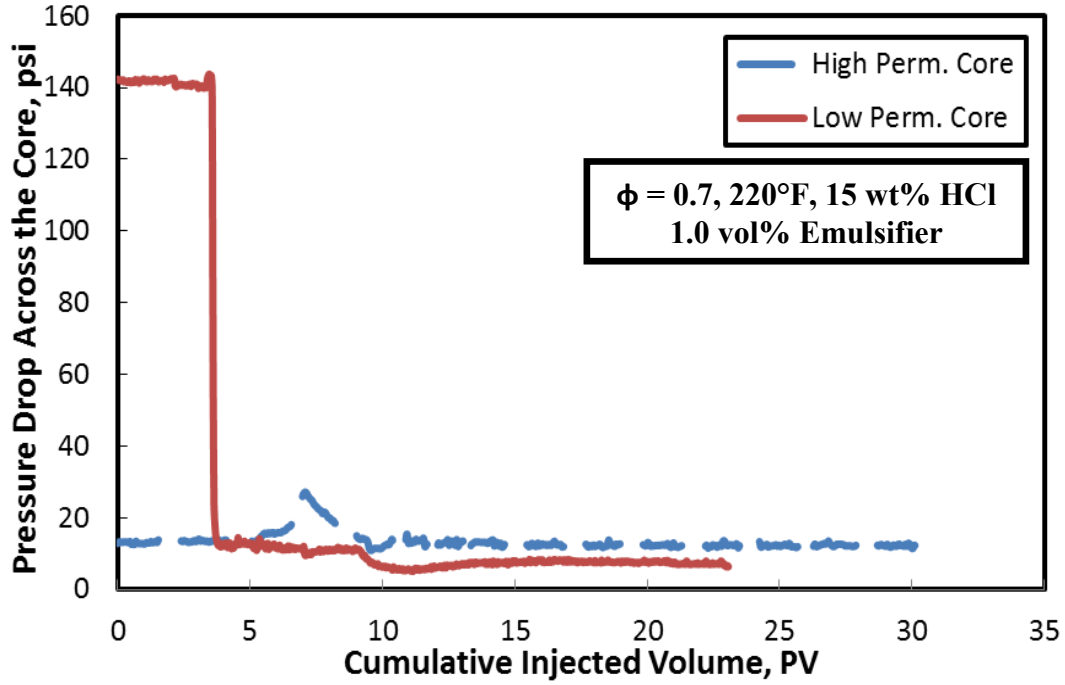

Fig. 8-7: Comparison of the pressure drop across cores # 4 and 5 for an injection rate of 2.0 cm^3/min & 220°F.

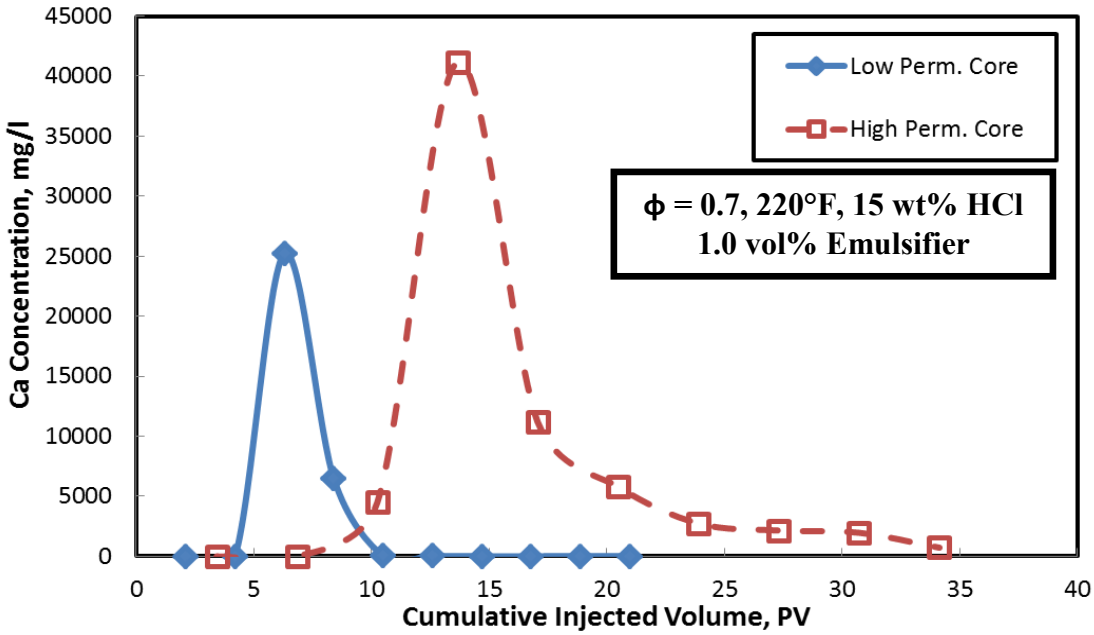

Fig. 8-8: Calcium concentration for low permeability (1.9 md) and high permeability (50 md) cases.

8.4.5 Total Amount of Calcium in the Effluent Samples

The total amount of calcium in coreflood effluent samples is a good and direct indication of the solubility of calcite cores in emulsified acid. The total amount of calcium was calculated by the integration of the calcium concentration as a function of injected volume such as the data shown by **Fig 8-5**. **Fig. 8-9** shows a comparison of the total calcium in effluent fluid samples in case of injection of emulsified acid in cores saturated with 100% water obtained from reservoir "A". The total amount of calcium in the coreflood effluent fluid samples decreased with the increase in injection rate from 1 to 7 cm^3/min. At emulsified acid injection rates higher than 7 cm^3/min, the total amount of calcium in coreflood effluent samples started to increase again. The total amount of calcium in the effluent sample is a direct indication of the amount of rock dissolved, and hence the amount of emulsified acid consumed. A higher amount of total calcium in effluent samples means more amount of rock was dissolved, and so more amount of emulsified acid was consumed in the treatment in order to achieve acid breakthrough.

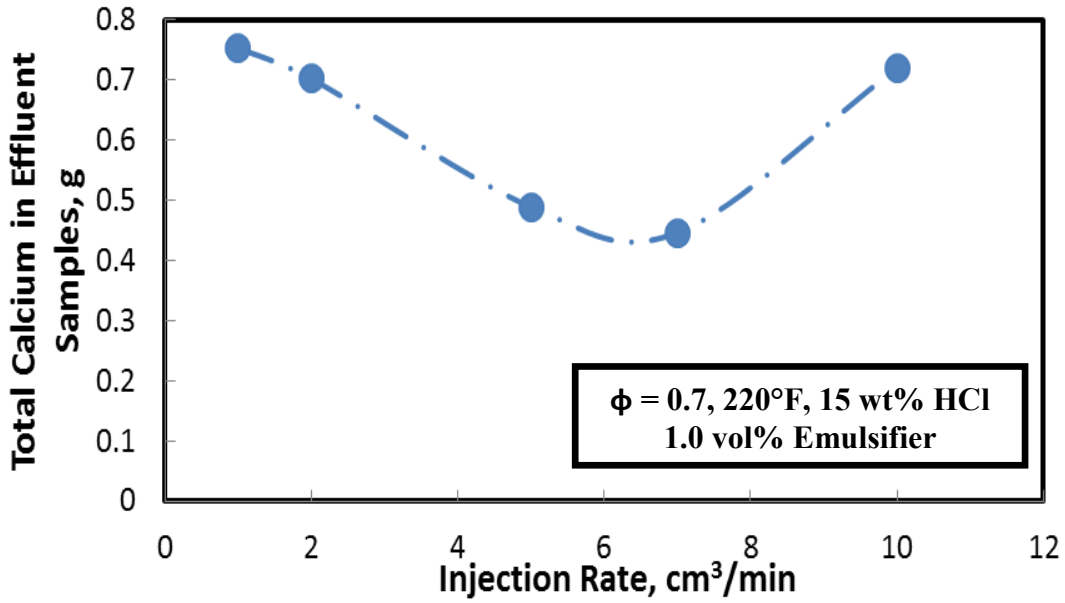

Fig. 8-9: Total amount of calcium in effluent fluid samples.

8.4.6 Concept of Optimum Injection Rate

Optimum injection rate is the rate at which the volume of acid injected until acid breakthrough is minimum. Six coreflood experiments were performed using emulsified acid systems formulated using 1.0 vol% emulsifier, and the HCl concentration was 15 wt%, for an acid to diesel volume ratio of 70-30. The volume of acid to achieve breakthrough as a function of acid injection rate is shown in **Fig. 8-10.** Based on pore volume of emulsified acid to achieve breakthrough, one can see that as the injection rate increased, the volume required to breakthrough decreased, and reached a minimum at a rate of between 5 and 7 cm^3/min. At higher injection rates, the volume of acid to achieve breakthrough increased with the increase in emulsified acid injection rate.

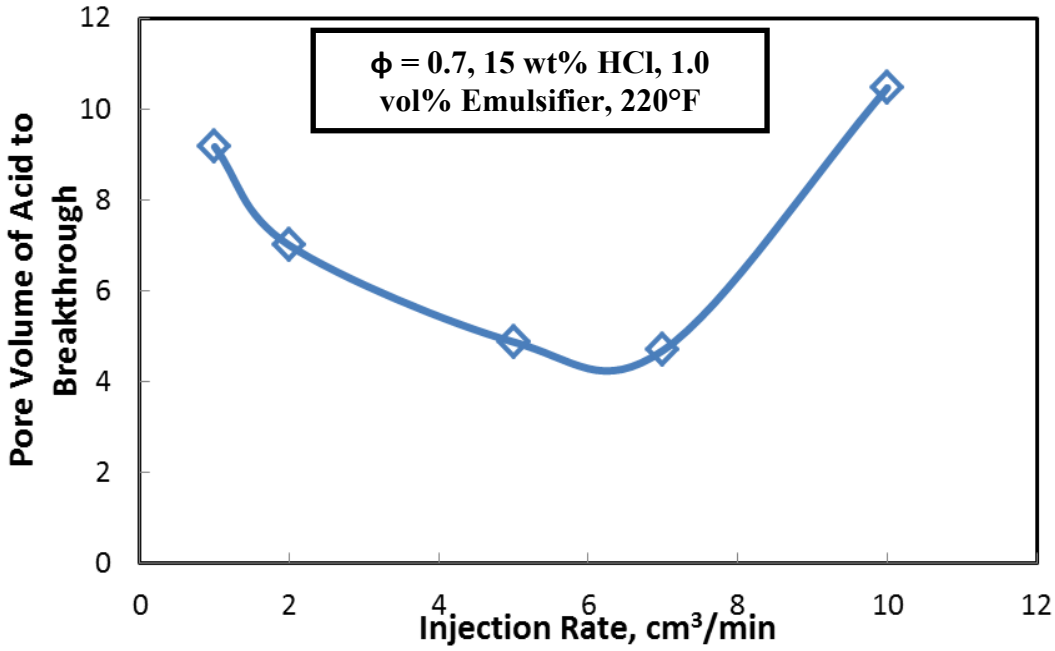

Fig. 8-10: Pore volume breakthrough vs. emulsified acid injection rate.

8.4.7 CAT Scan Images

Fig. 8-11 shows the 2D scan images for the core samples treated by emulsified acid, formulated at 1 vol% emulsifier, and at a temperature of 220°F. No face dissolution was noticed in the core inlet face for all cores obtained from reservoir A which were used in the current study. Upon injection inside the core, emulsified acid started to react with the rock and create wormholes. This can be detected through inspection of the dark spots, indicating a low CT number.

At low injection rates, 1 cm^3/min (core #1), the 2D scan images revealed that the acid created more than one wormhole, with no face dissolution, and the emulsified acid was very effective even at this low acid injection rate. Two different cores were treated with emulsified acid at the same injection rate of 2.0 cm^3/min (cores #2 and 3). From

Fig. 8-11, and for the low permeability core treated with an emulsified acid at injection rate of 2.0 cm^3/min (core #2), there was no face dissolution and emulsified acid created only one main wormhole that extends from the inlet to the outlet of the core. For the high permeability core treated with an emulsified acid at injection rate of 2.0 cm^3/min (core #3), there was no face dissolution and emulsified acid created many wormholes on the core inlet face. Some of these wormholes extended from the inlet to the outlet of the core and most of the wormholes terminated inside the core.

Fig. 8-11, and for cores treated at high injection rates (7.0 and 10.0 cm^3/min), the emulsified acid created different wormholes that extended from the core inlet to the core outlet. From **Fig. 8-11**, the emulsified acid was an effective stimulation fluid that can be injected at both low and high rates, and it had the ability to create deep wormholes without the occurrence of face dissolution. The cores obtained from the carbonate reservoir described in the current study showed a high reactivity and solubility in regular HCl although the tests were performed at room temperature. This gives an indication of the importance of the use of one of the retarding acid systems to treat wells drilled in these carbonate reservoirs. The emulsified acid system was tested using these cores at a temperature simulating the bottomhole temperature of the reservoir. The results of the CAT scan images reveal the effectiveness of the emulsified acid in treating these cores with no face dissolution at all injection rates and for different initial core permeability.

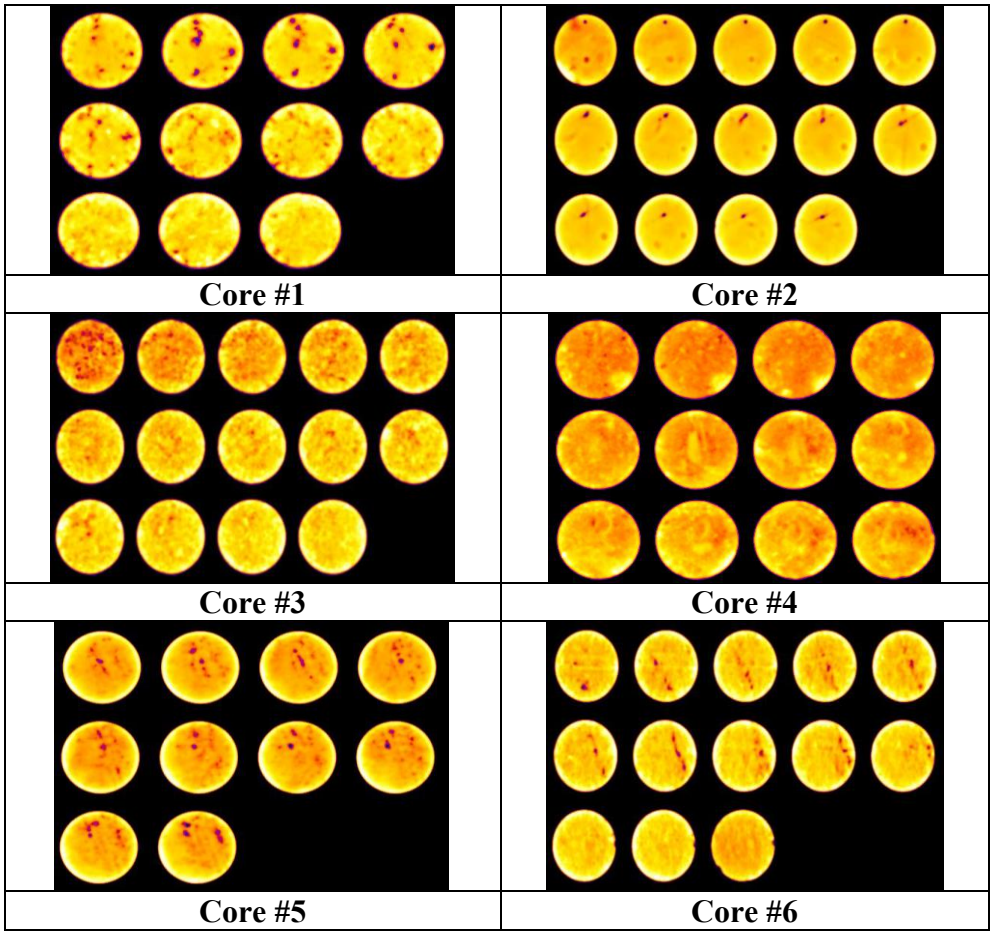

Fig. 8-11: CAT images for some core samples obtained from reservoir "A" after treatment with emulsified acid.

8.5 Emulsified Acid and Cores Obtained from Reservoir Z

Core samples were obtained from reservoir "Z" with a diameter of 1.5 in. and of different core lengths. The main objective of this part is to study the performance of the emulsified acid using reservoir cores obtained from reservoir "Z" through performing a coreflood study. Also, to measure the reaction rate of the emulsified acid and the reservoir core samples. Core samples will be CAT scanned before and after acid injection to study the creation and propagation of the wormhole.

8.5.1 CAT Scan Study of Fresh Core Samples

Thirty-six core plugs were cut from a carbonate reservoir. The plugs were screened using a computerized axial tomography (CAT) scanning. CAT scan analysis of core samples selected for the coreflood study indicated that the rock was homogeneous; it composed mainly of calcite. Also, the CAT scan images for the cores selected did not show the presence of vugs or channels in the core samples. For the coreflood study, five core samples were selected to test the emulsified acid systems; the cores were selected based on the initial core permeability, so cores of low permeability were tested via the emulsified acid. **Table 8-2** gives a brief description of all the selected cores used to perform the coreflood study and CAT scan images of the fresh cores are presented by **Fig. 8-12**.

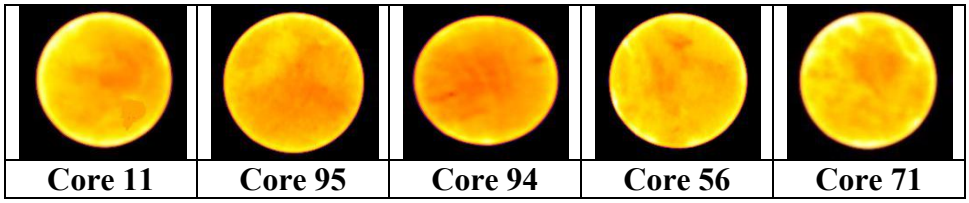

Fig. 8-12: Slice of the CAT images of the selected core samples obtained from reservoir "Z" before the injection of emulsified acid.

8.5.2 XRF of Rock Samples

An X-ray fluorescence technique was used to examine eight core samples obtained from reservoir "Z". The XRF analysis was performed in order to determine the elemental composition of these core samples, and to determine the presence of any dolomite in the

core samples. The XRF of the samples is shown in **Table 8-5** for sample #11. The main composition of the sample is calcite with traces of other elements such as magnesium, silicon, sulfur, aluminum, iron and potassium. A summary of the calcium and magnesium concentration, and hence the molar ratio of calcium to magnesium, as obtained from the XRF analysis for the selected seven samples is represented in **Table 8-6**. The XRF analysis indicates that all cores consist mainly of calcite with small trace amounts of dolomite and clays.

8.5.3 Coreflood Study Using Emulsified Acids

Coreflood experiments with emulsified acid systems were run using the setup shown in **Fig. 5-1**. **Table 8-2** gives the data for the core samples obtained from reservoir "Z" which were used in the coreflood experiments. These data include initial and final permeability, volume of emulsified acid to achieve breakthrough, core porosity, and injection rate. A total of five coreflood runs were performed using emulsified acid formulated using 1.0 vol% emulsifier and using core samples which were saturated with 100% water. The coreflood experiments were performed at injection rates in the range of 0.5 to 10 cm^3/min. These runs were performed in order to study the effect of the injection rate on the performance of emulsified acid, especially the volume of emulsified acid to achieve breakthrough and the characteristics of created wormholes. All coreflood runs were performed at 220°F. For each coreflood experiment, the pressure drop across the core was plotted using Lab-View software. Samples of the coreflood effluent were analyzed for calcium concentration.

Table 8-5: Summary of XRF analysis for core sample #11 obtained from reservoir "Z"

Element	Concentration, wt%
Ca	65.5
O	29.8
Mg	1.37
Si	1.04
S	0.621
Al	0.563
Cl	0.515
Fe	0.258
K	0.181
Sr	0.039
Ti	0.0304

Table 8-6: Summary of calcium and magnesium concentration in the selected core samples (obtained from reservoir "Z") as obtained from the XRF analysis

Sample	Ca, wt%	Mg, wt%	Mole Ca	Mole Mg	Ca/Mg
116	62.6	3.75	1.565	0.1563	10.02
55	66.3	2.8	1.6575	0.1167	14.21
21	66.2	1.13	1.655	0.0471	35.15
11	65.5	1.37	1.6375	0.0571	28.69
71	63.9	4.69	1.5975	0.1954	8.17
4	65.6	1.22	1.64	0.0508	32.26
17	66.7	1.1	1.6675	0.0458	36.38

8.5.4 Coreflood Study

Fig. 8-13 shows the pressure drop across the core during the injection of emulsified acid at 0.5 cm^3/min. The pressure drop during initial water injection stabilized at 65 psi, as a result of the pressure drop due to the friction losses accompanying the injection of water due to the low core permeability (0.4 md). The pressure drop behavior after starting

emulsified acid injection slightly increased to 70 psi, and then pressure drop started to slightly decrease with introduction of the emulsified acid into the core sample. As injection of emulsified acid was continued, it started to react with calcite and, as a result, wormholes started to form and propagate through the core. These wormholes work as paths for the fluid to flow with less resistance. The initial pressure drop across the core during water injection stage was 65 psi, while the final pressure drop across the core after emulsified acid breakthrough occurred was 15 psi. The final pressure drop was less than the initial pressure drop indicating the final permeability is greater than the initial permeability. 2.6 PVs of emulsified acid were required to achieve the breakthrough. After acid breakthrough occurred, 10 vol% mutual solvent in water was injected in to the core in order to remove the remaining diesel and emulsion. The final permeability was measured using the coreflood setup after the core was left to cool down. The final permeability was found to be 3,524 md, and the ratio of the final to the initial permeability was 8810 (**Table 8-2**) indicating an enhancement of the core permeability as a result of the creation of deeply penetrating wormholes.

At higher injection rates, such as 5.0 cm^3/min at a temperature of 220°F, the pressure drop during water injection was higher due to the friction losses encountered as a result of the high injection rates (**Fig. 8-14**). At emulsified acid injection rate of 5.0 cm^3/min, the pressure drop was initially constant during the injection of water at a value of 170 psi. As emulsified acid was injected into the core, the pressure drop across the core slightly decreased. Upon the reaction of calcite with emulsified acid, wormholes were created and the pressure drop across the core sharply decreased. Emulsified acid

breakthrough occurred after the injection of 1.2 PVs of emulsified acid. The final pressure drop stabilized at 15.7 psi, and the final permeability of the core was found to be 4600 md (**Table 8-2**). The ratio of the final permeability to the initial permeability of the core was calculated and presented in **Table 8-2**, and it shows that the final permeability was enhanced due to the creation of wormholes as a result of the emulsified acid injection into the core.

The initial and final permeability for all cores, treated with emulsified acid at different injection rates, are given in **Table 8-2**. The emulsified acid was successful in creating wormholes and the final permeability was enhanced at all acid injection rates. Also, the increase in permeability was higher in cores treated with emulsified acid at low injection rates; this will be discussed with the CAT scan images of the core after acid breakthrough occurred.

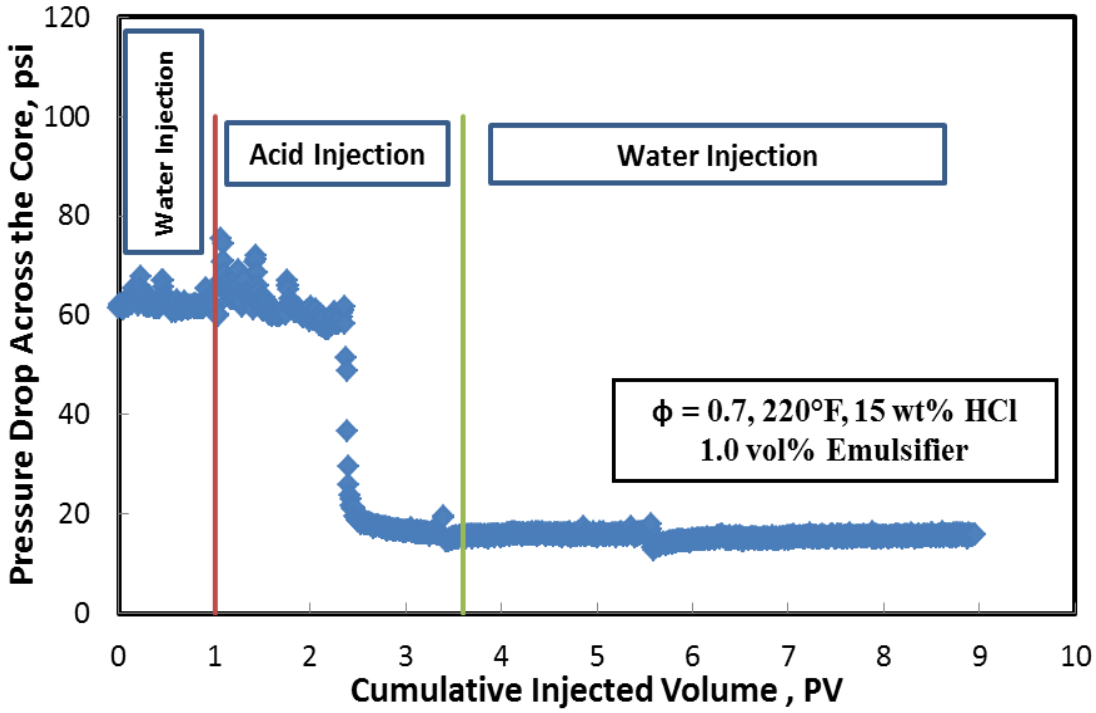

Fig. 8-13: The pressure drop across the core#1 (reservoir Z) for an injection rate of 0.5 cm^3/min & 220°F.

8.5.5 Total Amount of Calcium in the Effluent Samples

Fig. 8-15 shows the calcium concentration in the coreflood effluent samples for coreflood experiments performed using core samples obtained from reservoir "Z" and for emulsified acid injection rates of 1, 5 and 10 cm^3/min. The calcium concentration increased with the injection of emulsified acid as a result of the reaction with calcite, then the calcium concentration in coreflood effluent samples decreased again with introduction of water into the core after emulsified acid breakthrough occurred. The injection rate has a significant effect on the calcium concentration in the core effluent samples, and hence the amount of rock dissolved during emulsified acid injection. This

significant effect is related to the dependence of the number and size of the created wormholes on the injection rate of emulsified acid. The data shown in **Fig. 8-15** will be used to calculate the total amount of calcium in the effluent fluid samples. **Fig. 8-16** shows the change of the total amount of calcium in coreflood effluent fluid samples in case of injection of emulsified acid in core samples obtained from reservoir "Z". The total amount of calcium in effluent fluid samples decreased with the increase in emulsified acid injection rate until it reached minimum at an injection rate of 5 cm^3/min, then increased at higher injection rates. This is a direct indication of the amount of rock dissolved and the volume of emulsified acid consumed during the creation of wormholes.

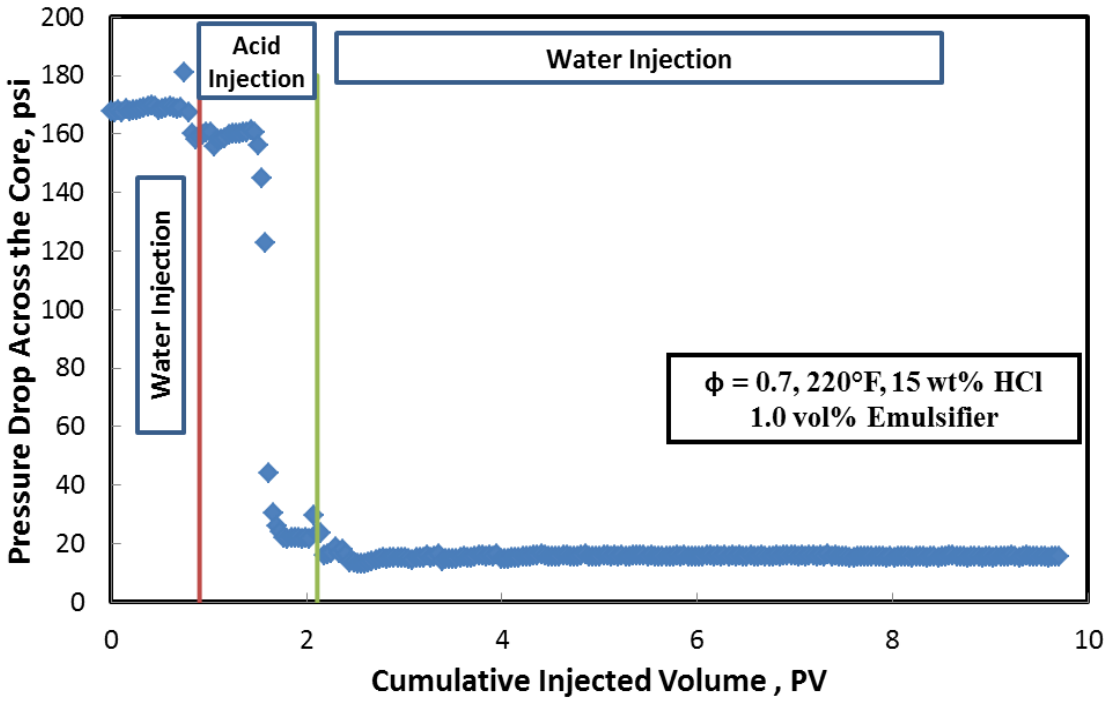

Fig. 8-14: The pressure drop across the core#4 (reservoir "Z") for an injection rate of 5 cm^3/min & 220°F.

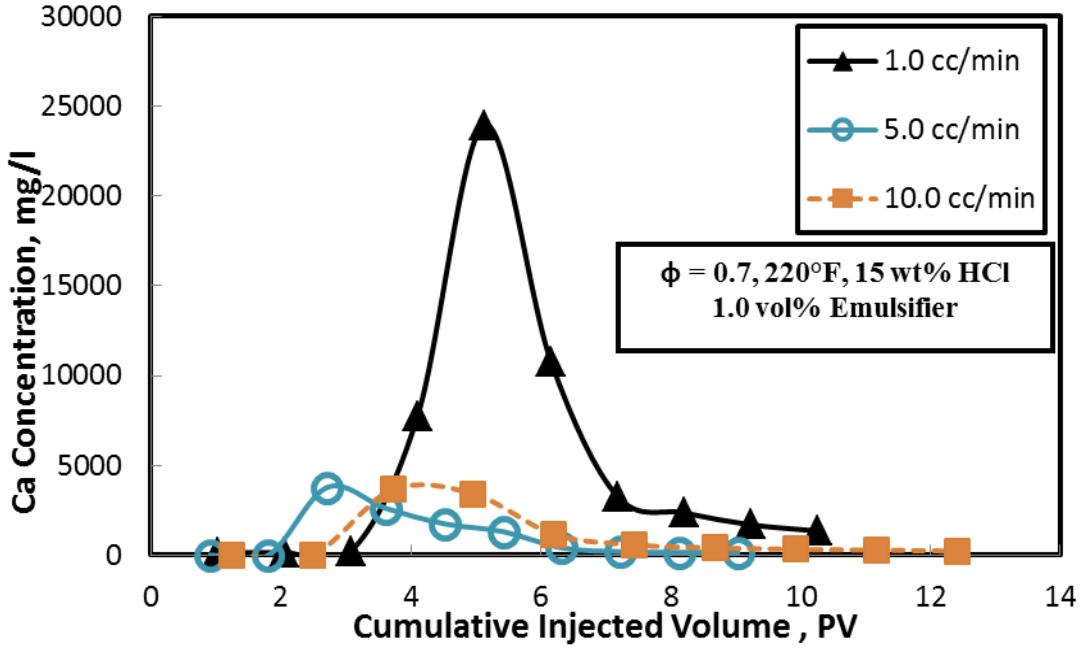

Fig. 8-15: Calcium concentration in the core effluent samples for cores obtained from reservoir "Z".

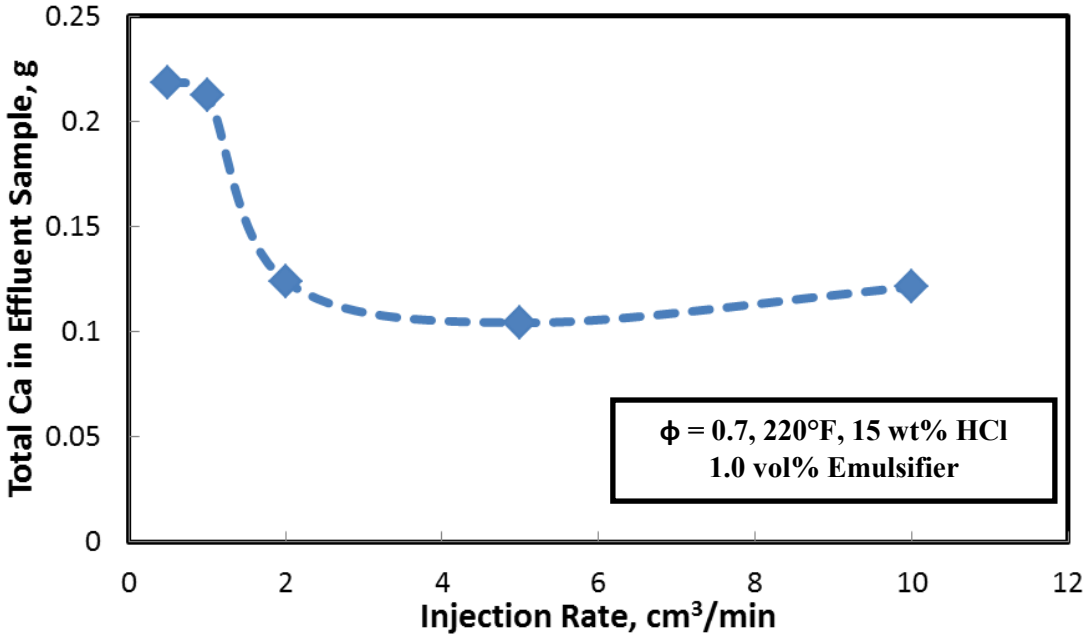

Fig. 8-16: Total amount of calcium in the core effluent samples for cores obtained from reservoir "Z".

8.5.6 Volume of Acid to Breakthrough and Optimum Injection Rate

Fig. 8-17 shows the relationship between the volume of acid to breakthrough and emulsified acid injection rate. As the emulsified acid injection rate increased, the volume of acid to breakthrough decreased until it achieved a minimum at an injection rate of 5 cm^3/min. At higher injection rates, the volume of acid to breakthrough increased again. This indicates that there is an optimum acid injection rate (for the injection rates studied of 0.5 to 10.0 cm^3/min), and it was found to be at 5 cm^3/min. For all injection rates studied, emulsified acid achieved breakthrough and was found to be successful in creating wormholes extending from the core inlet face to core outlet. The final permeability of the core was enhanced at all injection rates.

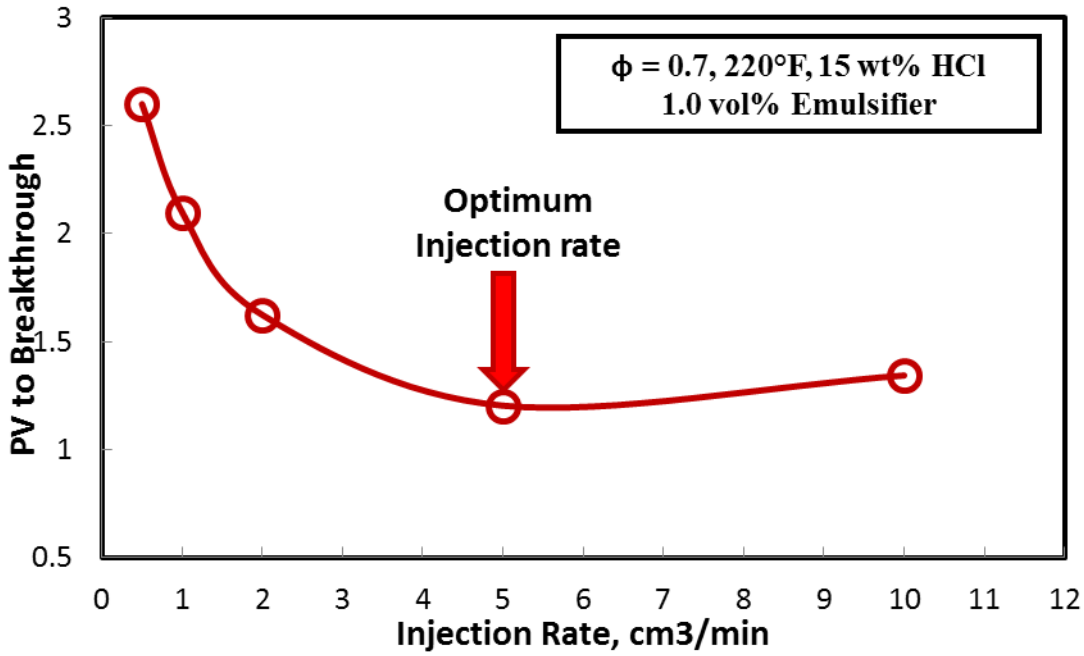

Fig. 8-17: Pore volume breakthrough vs. emulsified acid injection rate for cores obtained from reservoir "Z".

8.5.7 CAT Scan of Core Samples after Acid Injection

Fig. 8-18 shows the 2D images for the core samples obtained from reservoir Z after the injection of emulsified acid at 220°F. No face dissolution was noticed in the core inlet face for all the injection rates studied. Upon injection inside the core, emulsified acid started to react with the rock and create wormholes, which is indicated by presence of the dark spots indicating a low CT number. Emulsified acid was very effective even at low acid injection rates (0.5 and 1.0 cm^3/min). The size of the created wormhole decreased as the acid penetrated deeply in the core until acid breakthrough occurred. The final permeability was higher than the initial, which indicates that the emulsified acid created a conductive wormhole as can be detected from the CAT images in **Fig. 8-18**.

The emulsified acid was an effective stimulation fluid that can be injected at low rates (0.5 cm^3/min) or high rates (10 cm^3/min) and was able to create deep wormholes, with no face dissolution. The emulsified acid injection rate had a significant effect on the volume of the emulsified acid consumed, and the size and number of the created wormholes.

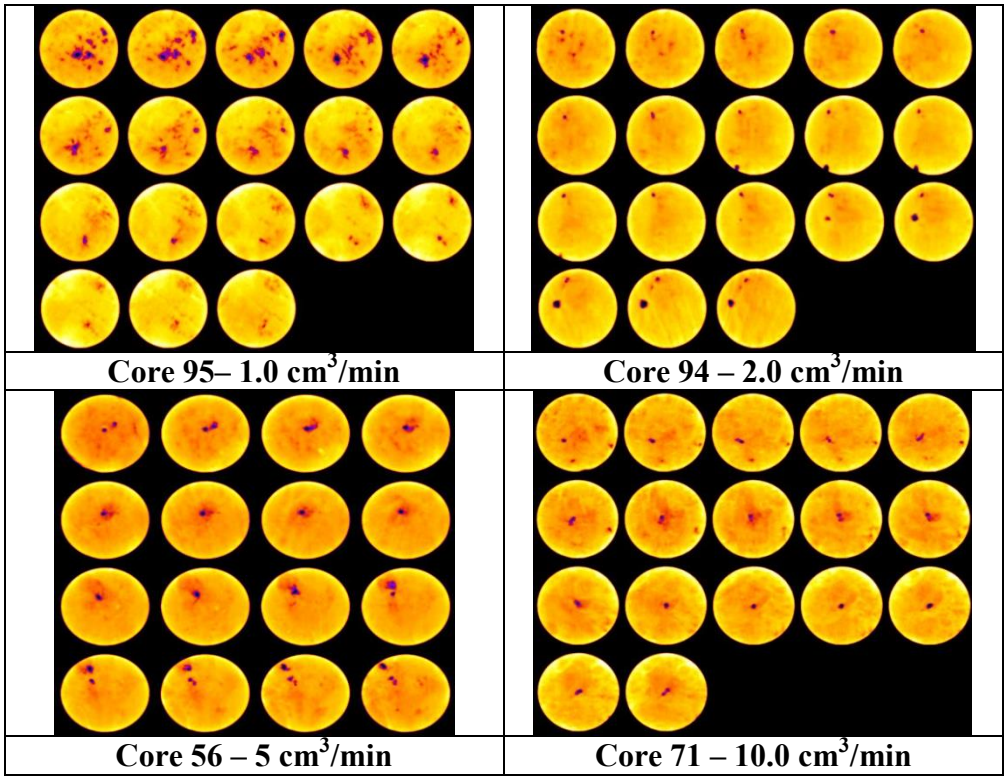

Fig. 8-18: CAT images for some core samples obtained from reservoir Z after the injection of emulsified acid.

8.5.8 Reaction of Emulsified Acid and Reservoir Core

All the rotating disk experiments were performed at a temperature of 220°F to be consistent with the reservoir temperature. All experiments were performed using reservoir core samples obtained from reservoir "Z". The rotating disk experiments were performed at disk rotational speeds up to 1000 rpm. Samples were withdrawn from the reactor every 1 minute for 10 minutes, so ten fluid samples were collected from each experiment. The calcium concentration in each sample was measured using the ICP (Inductively Coupled Plasma). The amount of calcium was plotted as a function of

reaction time. The dissolution rate was then obtained by dividing the slope of the best fit straight line by the initial area of the core plug.

Fig. 8-19 shows the change of calcium concentration as a function of reaction time, for emulsified acid formulated at 1.0 vol% emulsifier and 15 wt% HCl at 220°F and all experiments. The plotted points were fitted using a straight line and the slope of the resulted line was used to calculate the reaction (or dissolution) rate. The dissolution rate varied between 9.32E-07 gmol/cm^2.s at 200 rpm and 6.41E-06 gmol/cm^2.s at 1000 rpm. **Table 8-7** summarizes the reaction rate calculation at different rotational speeds.

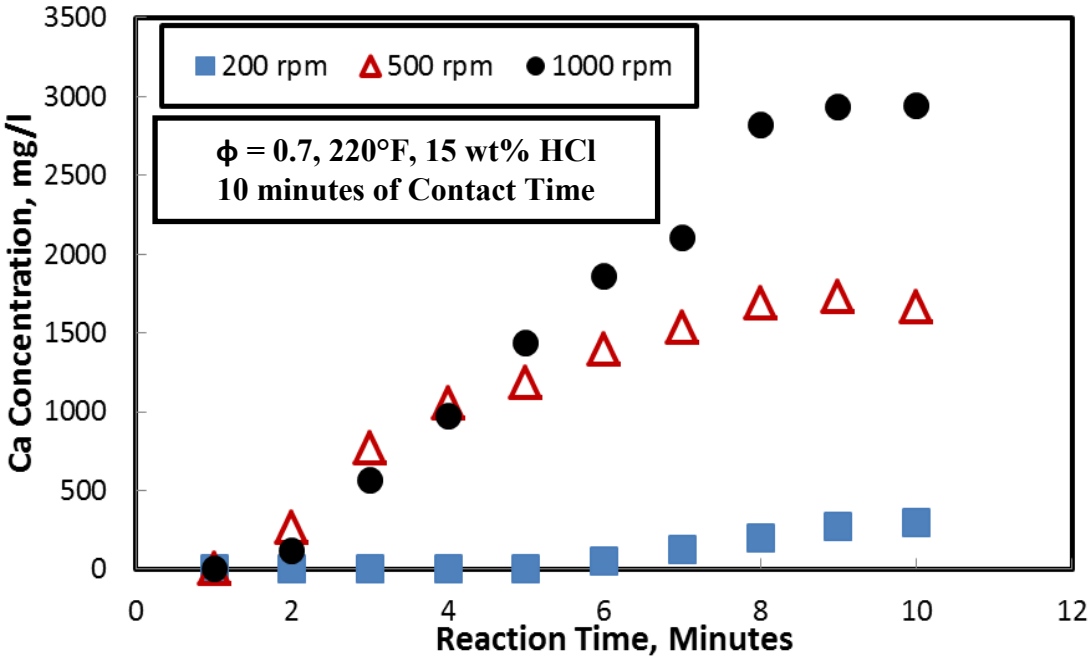

Fig. 8-19: Change of calcium concentration with time for reaction between 1 vol% emulsifier and 15 wt% HCl emulsified acid and reservoir core samples at 220°F.

Table 8-7: Summary of reaction rate constant at different rotational speeds at 220°F.

ω, rpm	200	500	1000
Dissolution Rate, R, gmol/cm^2.s	9.32E-07	3.61E-6	6.41E-6

The rate of reaction can be directly measured from the mass flux when the mass transfer limited regime predominates. Plotting the reaction rate versus rotational speed to the power (1/(1+n)), where n is the power law exponent obtained from the rheological measurements, can be helpful in determining the boundary between the mass transfer limited regime and the surface reaction limited regime. **Fig. 8-20** shows the plot of reaction rate vs. rotational speed to the power 1/(1+n). From **Fig. 8-20**, the reaction of emulsified acid and limestone is mass transfer limited for rotational speeds up to 1500 rpm, which is the range of rpm speed studied in this work. The effective diffusion coefficient (D) of HCl in emulsified acid at 220°F can be determined using Eq. 8.3:

$$R = \left[\varepsilon(n)\left(\frac{K}{\rho}\right)^{\frac{-1}{3(1+n)}}(r)^{\frac{1-n}{3(1+n)}}(\omega)^{\frac{1}{(1+n)}}(D)^{\frac{2}{3}}\right](C_b) = A\,(\omega)^{\frac{1}{(1+n)}} \quad \text{..... (8.3)}$$

where

C_b = reactant concentration in the bulk solution, gmole/cm^3

D = diffusion coefficient, cm^2/s

K = power-law consistency factor (g/cm.s^{n-2})

n = power-law index

r = radius of the disk, cm

R = the rate of reaction (gmole/cm^2.s)

ρ = fluid density, g/cm^3

ω = disk rotational speed, s^{-1}

$\varepsilon(n)$ = function depends on n (**Table 8-8**)

Hansford and Litt (1968) introduced the values for the function $\varphi(n)$ at different power law exponent values. This data is represented by **Table 8-8**. From the rheological study, values of k, n and $\varepsilon(n)$ were determined to be 499.2 ($mPa.s^n$), 0.496 and 0.6685 respectively at 220°F. From the definition of (A) parameter in the previous equation, the diffusion coefficient D can be estimated to be 2.75E-7 cm^2/s.

Table 8-8: Values of $\varphi(n)$ as a function of n (Hansford and Litt 1968).

n	0.2	0.4	0.5	0.6	0.8	1.0	1.3
***ε*(n)**	0.695	0.662	0.655	0.647	0.633	0.620	0.618

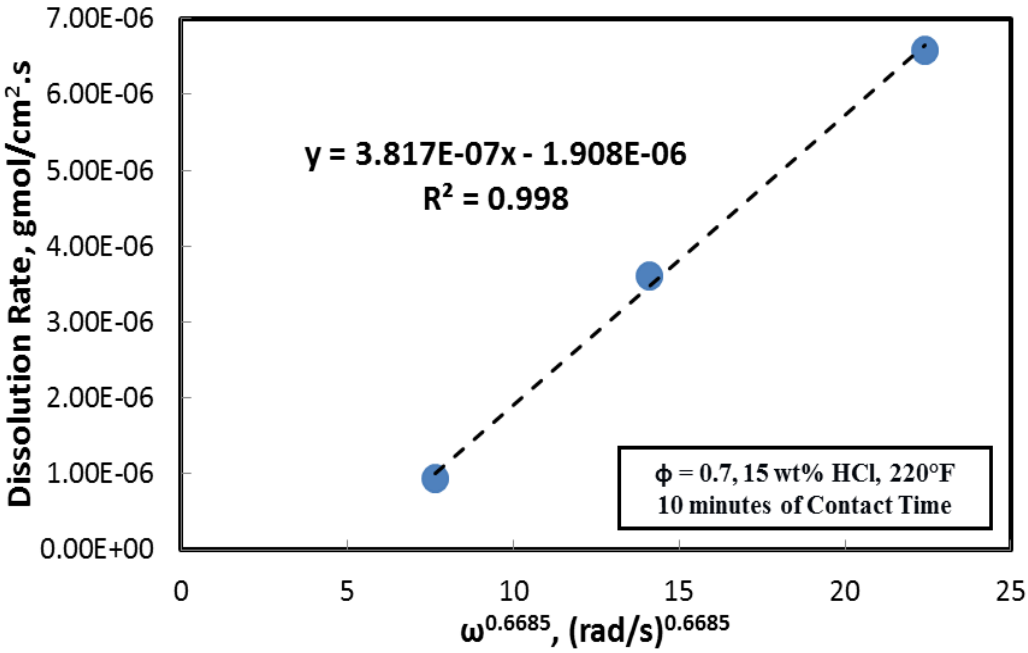

Fig. 8-20: Effect of disk rotational speed on the dissolution rate of core samples obtained from reservoir Z in 1 vol% emulsifier and 15 wt% HCl emulsified acid at 220°F.

9. EMULSIFIED CHELATING AGENT: EVALUATION OF A NEW INNOVATIVE TECHNIQUE

9.1 Introduction

Acidizing treatments are commonly used to remove near-wellbore damage or to create conductive permeable flow channels in carbonate formations (Fredd and Fogler, 1998a). Acids are widely used to stimulate oil and gas wells to improve the rate of hydrocarbon production (Al-Anazi et al. 1998; Kasza et al. 2006), and to stimulate disposal wells and water injection wells, in order to increase the formation uptake of the injected fluids (Mohammed et al. 1999; Nasr-El-Din et al. 2000). HCl is pumped as the main stimulation fluid in most of the stimulation treatments. At high temperatures, the reaction between HCl and carbonates is very fast, and for low acid injection rates this will result in rapid HCl spending and face dissolution (Allen and Roberts 1989; Nasr-El-Din et al. 2003). Also, HCl can cause excessive tubing corrosion and formation of acid/oil sludge in asphaltene-rich crudes.

Various acid systems have been used to reduce the limitations of rapid acid spending at high temperature and low injection rates. These alternatives include: organic acids (Harris 1961; Abrams et al. 1983) such as acetic and formic acid, chemically retarded acids such as emulsified acid (Dill 1961; Knox et al. 1964; Crenshaw and Flippen 1968; Nasr-El-Din et al. 2001) and foamed acid (Bernadiner et al. 1992), viscosified acids like gelled acid (Pabley et al. 1982; Deysarkar et al. 1984; Crowe et al. 1989) or in-situ gelled acid (Johnson et al. 1988; Yeager and Shuchart 1997; Saxon et al. 2000).

A variety of acid additives such as antisludging agents, corrosion inhibitors, and iron-reducing agents have been used to prevent the sludging and corrosion problems (Fredd and Fogler 1998c). However, their effectiveness is limited by the need to obtain a compatible combination of additives and a lack of understanding of the complex chemistries involved in the precipitation reactions. These limitations demonstrate the need for an alternative stimulation fluid that combines the ability to stimulate at low injection rates with fluid properties that are not conducive to asphaltic sludge precipitation or corrosion problems (Fredd and Fogler, 1998a).

Chelating agents have been used for the dissolution of metal-containing materials in a variety of applications (Moore et al. 1972; Bodine and Fernalld 1973; Jamialahmadi and Mullersteinhagen 1977; Fredd and Fogler 1998c). Chang and Matijević (1983) studied the dissolution of hematite in the presence of EDTA, and of related aminocarboxylic acids as a function of different parameters. They found that the leaching of ferric species from this oxide depends greatly on the pH, temperature, and nature of the chelating agents. Tyler et al. (1985) first used the EDTA to remove the carbonate scale from the sandstone reservoir at the Prudhoe Bay field. Chelating agents are negatively charged organic molecules that have the ability to combine with metal ions through coordination bonds. The process of chelation, or sequestering, results in the formation of stable ring-like structures which surround the metal ions and occupy all of their coordination sites, thus preventing their interaction with other ions in the solution. The stability of the metal/ligand complex depends on the properties of the metal ion and of the chelating agent (Fredd and Fogler, 1998b).

Fredd and Fogler (1997) studied the use of 1,2-cyclohexanediaminetetraacetic acid (CDTA) and diethylenetriamineepentaacetic acid (DTPA) to create wormholes and stimulate limestone cores. They performed a rotating disk study to investigate the reaction between chelating agents and calcite at a temperature of 22°C. The dissolution of calcite by chelating agents was not a fully mass transfer limited reaction (at 22°C).

Fredd and Fogler (1998a) studied the use of ethylenediamineteraacetic acid (EDTA) as an alternative fluid that is capable of stimulating wells drilled in carbonate formations. They performed a coreflood study at room temperature using Texas cream chalk and Indiana limestone cores of diameters 1.5 inch and 2.5, 4, and 5 inch in length. They used 0.25M EDTA, and 0.5M acetic acid and HCl. 0.25M EDTA solution was injected at different pH values ranging from 4 to 13, and it was effective in forming wormholes in limestone cores even at low injection rates, and without the formation of oil sludges. Fredd and Fogler (1998b) studied the kinetics of calcite dissolution in the presence of chelating agents over the pH range of 3.3 – 12 using the rotating disk apparatus. CDTA, DTPA and EDTA were prepared so that the final concentration was 0.25M. Fredd and Fogler (1998b) found that the reaction that dominates the dissolution was dependent on the pH value and the concentration and type of the chelating agent.

Frenier et al. (2001a) described the development and testing of hydroxyaminocarboxylic acid chelating agents (HACA) as components of matrix acidizing formulations for stimulating carbonate formations. Linear coreflood tests were used to study wormhole formation using Indiana limestone cores (1.0 in. diameter and about 6 in. long). The temperature of the tests was maintained at 150 and 250°F. Both

HACA chemicals were studied, HEDTA and HEIDA produced wormholes in limestone cores when tested at 150°F. The pore volume to achieve breakthrough decreased with the decrease in pH value. The rotating disk tests using HEDTA and EDTA (0.25 m, pH 12) with marble samples were employed to interpret the kinetics and mechanisms of the dissolution processes over a temperature range of 20 to 100°C. The reaction of HEDTA increased with the decrease in the pH value of the solution. Frenier et al. (2001a) indicated that there is some degree of surface reaction controlled kinetics, and that the reaction rates are the same for the two chelating agents. Frenier et al. (2001b) continued testing of HACA materials as components of matrix acidizing formulations for stimulating carbonate formations at very high temperatures (400°F). These fluids did not require iron control agents to be added and are easily inhibited to high temperatures (up to 400°F) using minimal amounts of corrosion inhibitors. Frenier et al. (2001b) concluded that dominant wormholes were produced at temperatures as high as 400°F. Huang et al. (2003) studied the effectiveness of EDTA, acetic acid and long chained carboxylic acid (LCA) for matrix acidizing of carbonate formations at a temperature of 250°F. Huang et al. (2003) found that all the fluids were able to create wormholes in limestone cores.

Mahmoud et al. (2010) investigated the efficiency of GLDA to stimulate calcite and dolomite cores. Indiana limestone cores (1.5 in. in diameter and 6 and 20 in. in length) and dolomite cores (1.5 in. in diameter and 6 in. in length) were used to test GLDA at various pH (1.7 – 13) and temperature range (180 – 300°F). Mahmoud et al. (2010) concluded that higher temperatures enhanced the reaction rate and created larger

wormholes with less pore volumes of GLDA at different pH values. GLDA was successful in stimulating calcite cores (6 and 20 in. in length) and dolomite cores.

LePage et al. (2011) discussed the use of a chelating agent, L-glutamic acid, N,N –diacetic acid (GLDA). They compared the GLDA chelating agent to the old chelating agents like EDTA, HEDTA, NTA and EDG. GLDA showed better solubility in HCl over a wide range of pH and GLDA was effective in dissolving the calcium carbonate (1.5 lb. calcite / gallon of 20 wt% GLDA). LePage et al. (2011) found that the thermal stability of GLDA was very good at high temperature.

Mahmoud et al. (2011a) performed a study to examine the ability of GLDA to dissolve calcite and form wormholes in long cores. They compared the performance of GLDA to that of HEDTA, and EDG. Mahmoud et al. (2011a) noted that calcite dissolution increased with the decrease in the pH, and there are two reaction regimes; complexation at high pH and dissolution at low pH. Also, GLDA was able to form wormholes at low injection rates (2 cm^3/min at 200°F and 3 cm^3/min at 220°F).

Mahmoud et al. (2011b) studied the optimum injection rate of GLDA over different pH ranges and temperatures. They found that for pH 1.7 and 3.0 and a temperature of 180°F, the optimum injection rate was 1.0 cm^3/min. Also, for different pH values, there was no effect of temperature on the value of optimum injection rate.

Mahmoud et al. (2011c, and d) used GLDA to stimulate sandstone cores and dolomite cores. For both Berea sandstone and dolomite cores, GLDA at different pH values was able to enhance the core permeability. Mahmoud et al. (2011e) investigated the effect of fluid type on the performance of chelating agents. They (2011e) found that

the cores saturated with crude oil consumed a smaller volume of GLDA to achieve breakthrough and the performance was enhanced through the creation of dominant wormhole.

Rabie et al. (2011) investigated the reaction of GLDA with calcite by measuring the rate of dissolution using the rotating disk apparatus. The effect of initial pH (1.7, 3.8, and 13) and disk rotational speed (100-1800 rpm) on the rate of reaction was studied at 150, 220 and 300°F. Pink Desert limestone cores 1.5 in. diameter and 0.65 in. length were utilized. Rabie et al. (2011) found that the calcite dissolution rate was a strong function of temperature and increased significantly by increasing the temperature from 80 to 300°F. Increasing the pH from 1.7 to 13 resulted in a reduction in the rate of dissolution. GLDA reacted with calcite by one of two mechanisms; hydrogen ion attack or calcium complexation reaction. The GLDA chelation ability (expressed as a percentage of the total rate of dissolution) decreased by increasing temperature, but was not greatly affected by changing the disk rotational speed.

Nasr-El-Din et al. (2012) evaluated the results of the first field application of GLDA to acidize a sour, high temperature, tight gas well completed with high chrome content tubulars. The treatment was applied in the field without encountering any operational problems. Improved productivity and longer term performance results confirm the effectiveness of the new chelate as a versatile stimulation fluid.

The main objective of the current work is to evaluate an innovative technique to formulate a new emulsified chelating agent for high temperature applications. GLDA with a pH value of 3.8 and an initial concentration of 38 wt% was selected to formulate

the emulsified GLDA (EGLDA). The EGLDA was formulated using a cationic emulsifier, with a final GLDA concentration and volume fraction of 20 wt% and 0.7, respectively. The viscosity of the new EGLDA is measured at temperatures up to 300°F using an HPHT rheometer. The reaction of the EGLDA with the limestone disks is studied using a rotating disk apparatus at temperatures of 230, 250 and 300°F. Effluent fluid samples are analyzed using the Inductively Coupled Plasma mass spectrometer (ICP) to measure the calcium concentration, and hence predict the reaction rate data.

9.2 Chelation Chemistry

Chelating agents have the ability to combine with metal ions by surrounding them with one or more ringed structures. The process of chelation results in the formation of metal/ligand chelates with exceptionally high stability. Chelates of transition metals (such as iron) typically have the highest stability, while many chelates of alkaline-earth metals (such as calcium) have low stability with most chelating agents. The distribution of ionic species is dependent upon the equilibrium constants for each of the dissociation reactions and on the pH of the solution.

GLDA is a member of the aminopolycarboxlic acids which has the ability to form metal complex with different ions. The chemical structure of GLDA is shown in **Fig. 9-1.** GLDA as a member of the aminopolycarboxlic acid group undergo dissociation reactions in which acid loses hydrogen ions and changes from a totally acidic form at low pH to a totally protonated form at high pH (Rabie et al. 2011). The dissociation reactions, dissociation coefficient and stability constants were mentioned in detail in Rabie et al. (2011).

Also, the reaction of GLDA with calcite was discussed by Rabie et al. (2011). Beside the hydrogen attack, reaction of GLDA and calcite may take place in the form of chelation based on the pH value of the solution. For equations and more details, refer to Rabie et al. (2011).

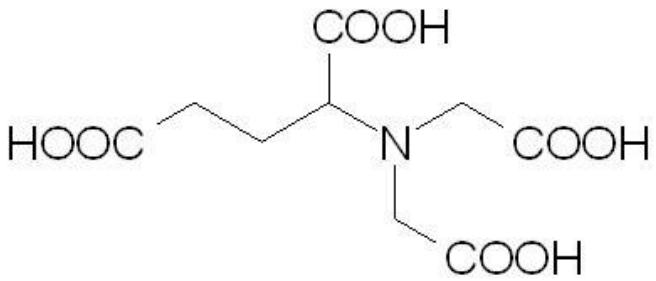

Fig. 9-1: Chemical structure of GLDA.

9.3 Experimental Studies

9.3.1 Materials

GLDA solutions of concentration 20 wt% and pH of 3.8 were prepared from original solution that was obtained from AkzoNobel. The original GLDA concentration was 38 wt%. De-ionized water, obtained from a water purification system, which has a resistivity of 18.2 MΩ.cm at room temperature, was used to prepare the 20 wt% GLDA solutions. The emulsified GLDA solutions were prepared using diesel, an emulsifier and 20 wt% GLDA solution. In all the emulsion preparations, the same source of diesel was used. A cationic emulsifier was added to the diesel to create the emulsion.

9.3.2 Disk Preparation

An Indiana limestone block was obtained from a local company. Core samples were cut as 6 in. long cores and 1.5 in. diameter. Rock composition was determined by X-ray fluorescence (XRF). Elemental analysis showed that the limestone core samples contained more than 98 wt% calcite with some traces of clays. **Table 9-1** gives the XRF results of two limestone core samples. The cores were dried in an oven at a temperature of 150°C (302°F) for 3 hours until the cores were completely dry. The cores were weighed using a digital balance to obtain the dry weight of the core samples. After that, the dried cores were saturated with deionized water under vacuum for 24 hours and the weight of the water-saturated cores was measured, as well as the pore volume, and hence the core porosity was calculated (**Table 9-2**). The cores were put in a core holder, and water was injected at different flow rates. For each flow rate, the pressure drop after stabilization was recorded. A plot of flow rate divided by the core cross sectional area vs. the ratio of pressure drop to the core length was used calculate the initial core permeability.

Disks with a diameter of 1.5 in. and a thickness of 0.75 in. were cut, and tested using the rotating disk apparatus. The porosity of all the core plugs was measured and found to be in the range of 13.2 to 13.5 vol%. The porosity was then used to calculate the initial surface area of the disk. Disk preparation was identical for all experiments and the procedure suggested by Fredd (1998) was followed. Disks were soaked in 0.1N HCl solution for 30 to 35 minutes. After that, the disks were thoroughly rinsed with deionized water before mounting them to the rotating disk apparatus. The main objective of

following this procedure is increase the reproducibility of the dissolution rate data with the rotating disk apparatus (Fredd 1998).

Table 9-1: Elemental analysis of two limestone cores using the XRF technique.

	Concentration, wt%	
Element	**Sample # 1**	**Sample # 2**
Ca	69.2	67.6
O	29	29.5
Mg	0.657	1.39
Si	0.412	0.592
Al	0.221	0.328
Fe	0.202	0.224
K	0.109	0.143
S	0.0753	0.0594
Sr	0.0471	0.046
Cl	0.0323	0.0284
Sn	0.0293	0.0298
Mn	0.011	0.0239
Total	99.996	99.9645

Table 9-2: Data for 6 in. long coreflood experiments.

Run #	**φ, vol%**	**$K_{initial}$, md**	**Q_{inj}, cm^3/min**	**Temperature, °F**	**PV Injected**	**K_{final}, md**	**$K_{final}/K_{initial}$**
1	13.2	5	2	300	5	15	3.0
2	13.2	15	2	300	2.3	55	3.7
3	13.5	4.8	1	350	2.08	14.5	3.0

9.3.3 Emulsified GLDA Preparation

Preparation of the emulsified GLDA was accomplished in a systematic way, to warrant the reproducibility of the results. The original GLDA solution was diluted to 20 wt%, by

adding deionized water. The cationic emulsifier (at varying concentrations) was added to the diesel, and mixed using a mixer. Then, the 20 wt% GLDA solution was added to the diesel solution, and mixing was performed at a high constant speed (600 rpm). The final volume fraction of the emulsion was 70% GLDA in 30% diesel solution. The electric conductivity of the final emulsified GLDA was measured in a conductivity meter (Marion L, model EP-10) to confirm the quality of the final emulsion. If the electric conductivity is nearly 0, then we have a good emulsified GLDA, otherwise, the mixing time was increased to the maximum possible speed to ensure the creation of a good emulsion.

9.3.4 Equipment

The droplet size distribution was measured using a Zeiss Axiophot microscope. Images were analyzed using Image-J software. An HPHT rheometer was used to measure the apparent viscosity of live emulsified GLDA under different conditions of shear rate and temperature. The test was applied by varying the shear rate from 0.1 to 1000 s^{-1}, and for different temperatures up to 300°F. Reaction rate experiments were performed using a rotating disk apparatus (**Fig. 3-1)**.

The coreflood setup described in **Fig. 5-1** and section 5.2.3 was constructed to simulate a matrix stimulation treatment. Coreflood experiments were performed at temperatures of 300 and 350°F. The calcium concentration of the effluent samples was measured using the ICP.

9.3.5 Compatibility Tests

These tests were conducted by adding 6 cm^3 of the emulsified GLDA to an equal volume of water, diesel, crude oil, 100% ethanol alcohol and 10 vol% mutual solvent in water. All the compatibility tests were performed at room temperature (77°F). The fluids were mixed very well, and then were examined for phase separation.

9.4 Results and Discussion

9.4.1 Droplet Size Distribution of Emulsified GLDA

Emulsified GLDA was prepared so the GLDA volume fraction was 0.7 and the emulsifier concentration was varied from 0.5 to 2.0 vol% (5 to 20 gpt). A small sample of each emulsified GLDA system was examined using the Zeiss Axiophot microscope in order to measure the droplet size distribution of the GLDA droplets. The photomicrographs of the emulsified GLDA prepared using emulsifier concentrations of 0.5, 1.0, and 2.0 vol% are shown in **Figs. 9-2a to 9-2c**, respectively. The droplet size of the GLDA decreased as the emulsifier concentration was increased from 0.5 to 2.0 vol%. The photomicrographs were analyzed using Image-J software, and the droplet size of emulsified GLDA was measured. The droplet size distributions of the three emulsified GLDA systems studied are shown in **Fig.9-3.**

The average, median, standard deviation and errors with 95% confidence limits of these distributions are presented in **Table 9-3.** The photomicrographs and droplet size measurements showed that as the emulsifier concentration increased from 0.5 vol% to 2.0 vol%, the average droplet size decreased from 1.91 to 0.63 μm. The droplet size distribution curve for emulsified GLDA formulated at 2.0 vol% emulsifier concentration

was narrower, indicating that the emulsion was more homogeneous than emulsified GLDA systems formulated with less emulsifier concentrations.

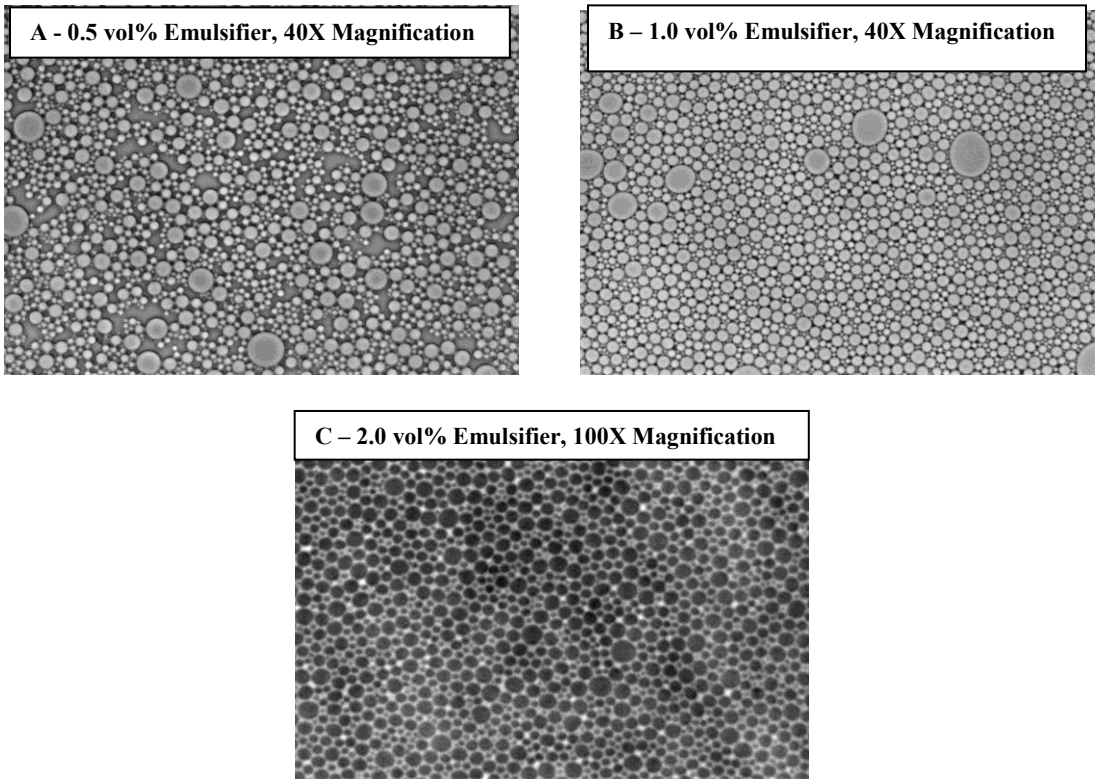

Fig. 9-2: Droplet size distributions of emulsified GLDA systems (40x objective: 0.0960 micrometer per pixel, and 100x objective: 0.0383 micrometer per pixel).

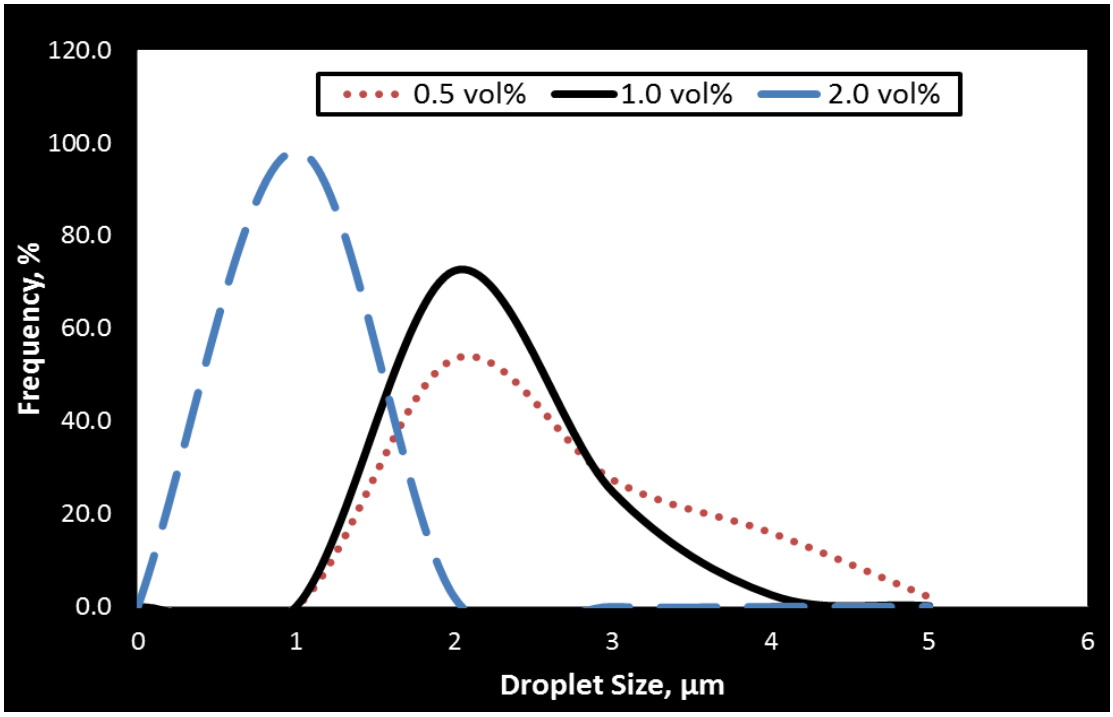

Fig. 9-3: Droplet size distributions of emulsified GLDA prepared at three emulsifier concentrations.

Table 9-3: Statistical analysis of droplet size distributions for emulsified GLDA systems used in the present study.

Emulsifier Concentration, vol%	Average Droplet Size, µm	Standard Deviation, µm
0.5	1.91	0.96
1	1.69	0.47
2	0.63	0.14

9.4.2 Viscosity of Emulsified GLDA

Emulsified GLDA is an emulsion of GLDA as an internal (or dispersed) phase in a diesel external (or continuous) phase. The flow properties of an emulsion are obviously among some of its more important physical attributes in either technical or aesthetic

terms. Hence the ability to measure, adjust, and, if possible, predict such properties is very important (Barnes, 1994). The basic rheology-determining parameters of an emulsion are: continuous phase rheology and the nature of the drops (size distribution, deformability, internal viscosity, concentration and nature of particle - particle interaction) (Barnes, 1994). Extensive work was done before to study the rheology of emulsions. Pal et al. (1992) indicated that, in general, the viscosity of emulsions depends on shear rate, droplet size distribution, dispersed phase volume fraction, and temperature. Most concentrated emulsions are pseudo-plastic fluids (Pal et al. 1992). Some emulsions cannot be classified into one specific class, but stretch over a wide range of non-Newtonian behavior (Al-Mutairi et al. 2008a).

9.4.3 Effect of Shear Rate

The emulsified GLDA systems were prepared using different emulsifier concentrations of 5, 10, and 20 gpt (0.5, 1.0 and 2.0 vol%, respectively). The apparent viscosity of the emulsified GLDA was measured at room temperature (75°F) and for a shear rate range of 1.0 to 1000 s^{-1}. The emulsified GLDA samples were stable for at least 48 hours at room temperature with no phase separation encountered.

The effect of increasing the shear rate on the apparent viscosity of emulsified GLDA is shown in **Fig. 9-4**. **Fig. 9-4** represents a log-log plot of apparent viscosity of emulsified GLDA as a function of the shear rate. As the shear rate increased from 1.0 to 300 s^{-1}, the apparent viscosity of the emulsified EGLDA decreased. At higher shear rates (> 300 s^{-1}), the apparent viscosity of emulsified GLDA showed a non-dependency on the shear rate applied. The apparent viscosity of emulsified GLDA as a function the shear

rate up to 300 s^{-1} is represented by a straight line on a log-log plot, indicating that emulsified GLDA is a non-Newtonian shear thinning fluid. The change in the apparent viscosity of emulsified GLDA as a function of the shear rate can be represented using a power-law model expressed by Eq. 1:

$$\mu_a = K\dot{\gamma}^{n-1} \quad \text{..... (1)}$$

where μ_a is the apparent viscosity of the emulsified chelating agent (GLDA), $\dot{\gamma}$ is the shear rate, K is the power-law constant and n is the power-law index. **Table 9-4** summarizes the values for K and n and the correlating coefficient for the different emulsified GLDA systems, prepared at 0.5, 1.0 and 2.0 vol% emulsifier. The correlating coefficient (0.98) indicated a good correlation of the apparent viscosity and shear rate.

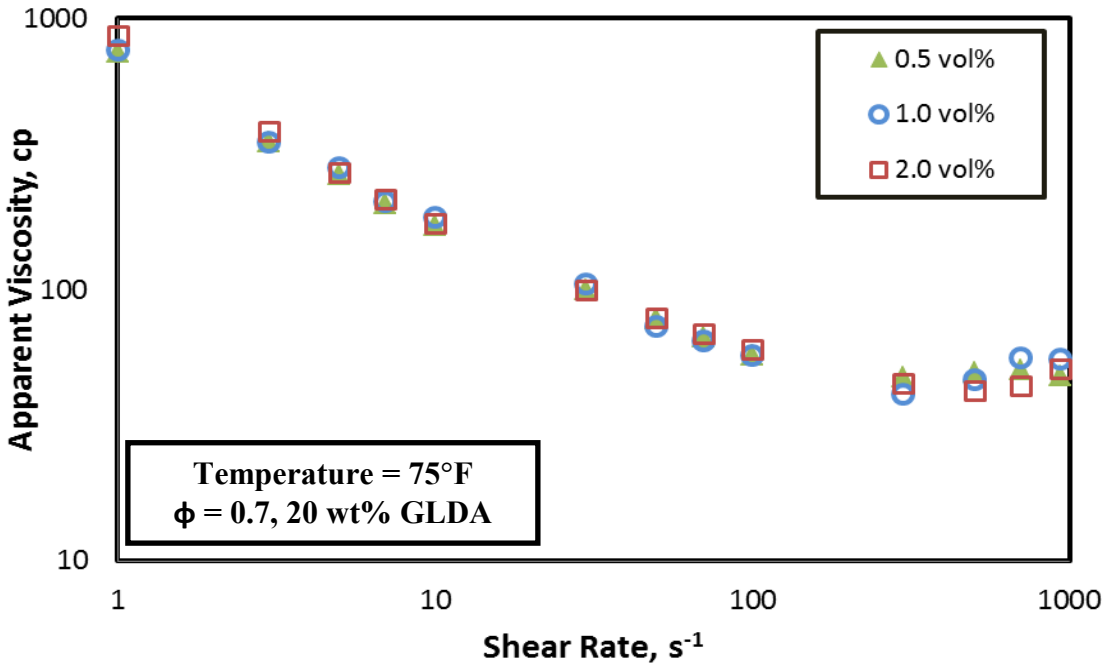

Fig. 9-4: Apparent viscosity of emulsified GLDA as a function of shear rate and different emulsifier concentrations.

Table 9-4: Power-law parameters for emulsified GLDA at 75°F.

Emulsifier Concentration, vol%	Power-law Constant, K (mPa.s^n)	Power-law Index, n
0.5	597.12	0.503
1	637.76	0.479
2	661.54	0.48

9.4.4 Effect of Emulsifier Concentration

The effect of emulsifier concentration on the apparent viscosity of emulsified GLDA was examined using **Fig. 9-4.** The apparent viscosity was plotted as a function of the shear rate for emulsified GLDA formulated at different emulsifier concentrations. **Fig. 9-4** shows that there was no significant effect of the emulsifier concentration on the apparent viscosity of emulsified GLDA. With increasing the emulsifier concentration from 5 to 20 gpt, there was no significant change in the apparent viscosity at all shear rates. Al-Mutairi et al. (2008a) studied the effect of increasing the emulsifier concentration on the apparent viscosity of emulsified acid. They found that, as the emulsifier concentration increased, the apparent viscosity of emulsified acid increased. This was not the same behavior for emulsified GLDA, as there was no significant change in the apparent viscosity of the emulsified GLDA with changing the emulsifier concentration from 5 to 20 gpt.

9.4.5 Thermal Stability of Emulsified GLDAs

The apparent viscosity of emulsified GLDA was measured at a constant shear rate of 10 s^{-1} and for temperatures up to 300°F. The main objective of these measurements was to study the thermal stability of emulsified GLDA at high temperatures. Three emulsified

GLDA systems were prepared at emulsifier concentrations of 5, 10 and 20 gpt. The results of the thermal stability tests are presented in **Fig. 9-5**, where the effect of increasing the temperature on the apparent viscosity of emulsified GLDA at 10 s^{-1} shear rate is shown. From **Fig. 9-5,** and at 10 s^{-1} shear rate, it is clear that as the temperature was increased; the apparent viscosity of emulsified GLDA slightly increased (for emulsifier concentration of 20 gpt) or almost stayed the same (for emulsifier concentrations of 5 and 10 gpt) up to a temperature of 160°F. The apparent viscosity, of the emulsified GLDA prepared at 2.0 vol% emulsifier concentration, slightly increased with increasing the temperature up to 164°F, and then continuously decreased up to a temperature of 300°F. With the increase in temperature, the viscosity of the three emulsified GLDA systems started to decrease, and at a temperature of 285°F the apparent viscosity was the same for the three systems. The viscosity of the emulsified GLDA at 300°F and 10 s^{-1} was around 43 cp.

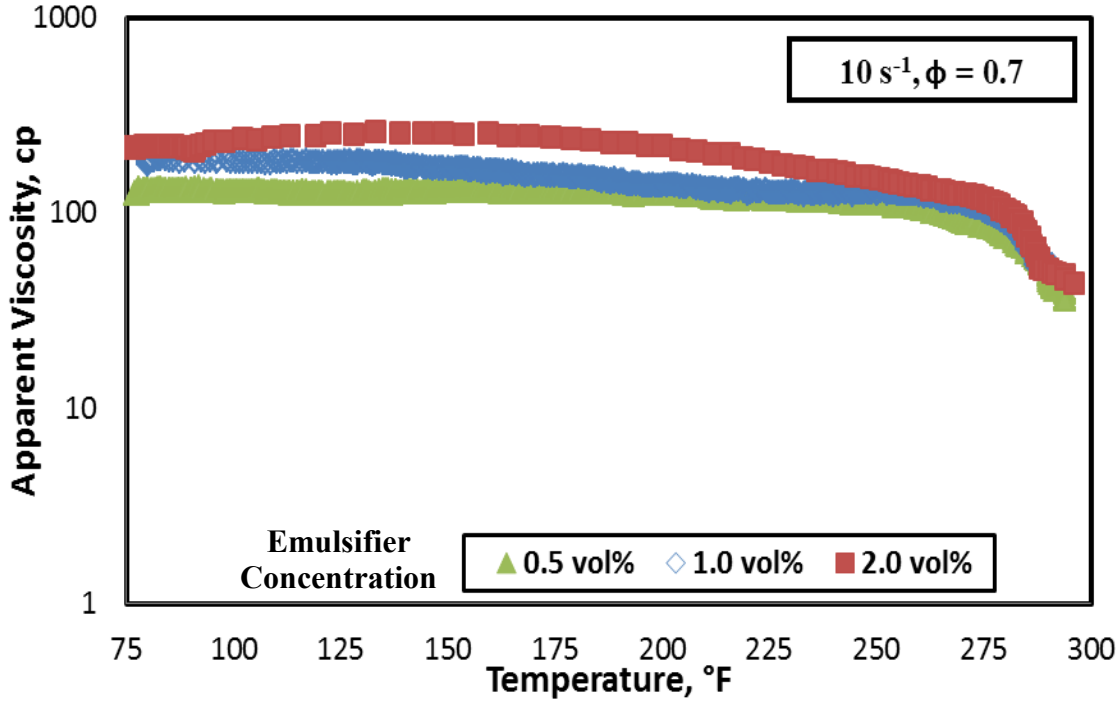

Fig. 9-5: Apparent viscosity of emulsified GLDA at 10 s^{-1} shear rate and for temperatures up to 300°F.

9.4.6 Rheology of Emulsified GLDA Systems at High Temperature

The apparent viscosity of emulsified GLDA was measured at different shear rates (up to 1000 s^{-1}) for temperatures 150, 230, and 300°F. The purpose of these measurements is to study the effect of shear rate and temperature on the rheology of emulsified GLDA prepared with different emulsifier concentrations. **Figs. 9-6** through **9-8** show the effect of increasing the shear rate on the apparent viscosity of the emulsified GLDA system at temperatures of 150, 230, and 300°F, respectively. At temperatures of 150 and 230°F, there was no significant effect of changing the emulsifier concentration on the apparent viscosity of emulsified GLDA. At a temperature of 300°F, the apparent viscosity of

emulsified GLDA prepared at 10 gpt (1.0 vol%) emulsifier was higher than that for emulsified GLDA prepared using 5 and 20 gpt (0.5 and 2.0 vol%) emulsifier concentration. Also, at a temperature of 300°F, the apparent viscosity decreased with the increase in shear rate up to a shear rate of 300 s^{-1}, and then the apparent viscosity showed a shear independency for shear rates higher than 300 s^{-1}. The change of the apparent viscosity as a function of shear rate on log-log scale coordinates can be represented by a straight line indicating a non-Newtonian shear thinning behavior that can be fitted using a power-law model. **Table 9-5** summarizes the values of k, n and the correlating coefficient for the emulsified GLDA samples measured, which indicates a good correlation of apparent viscosity and shear rate. This data will be used later in the interpretation and evaluation of the emulsified GLDA reaction kinetics.

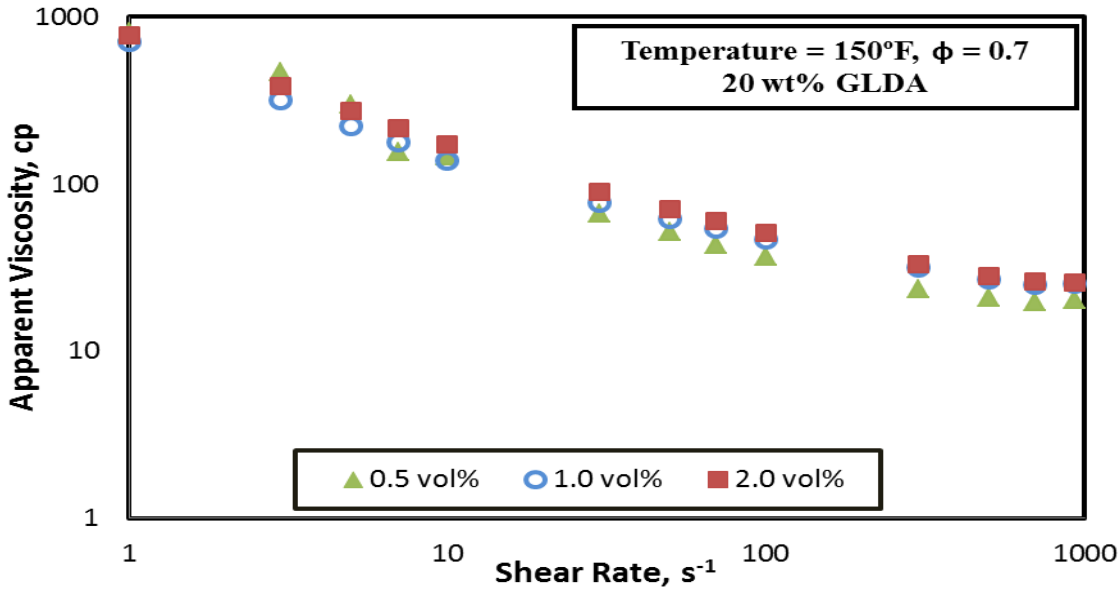

Fig. 9-6: Effect of changing shear rate on the apparent viscosity of emulsified GLDA at 150°F.

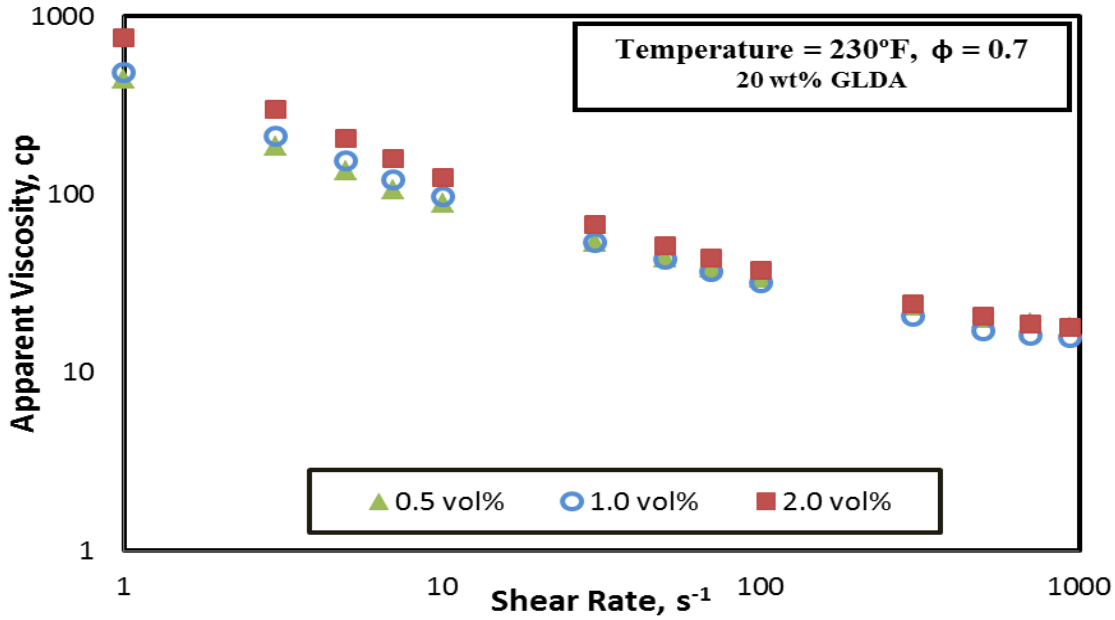

Fig. 9-7: Effect of changing shear rate on the apparent viscosity of emulsified GLDA at 230°F.

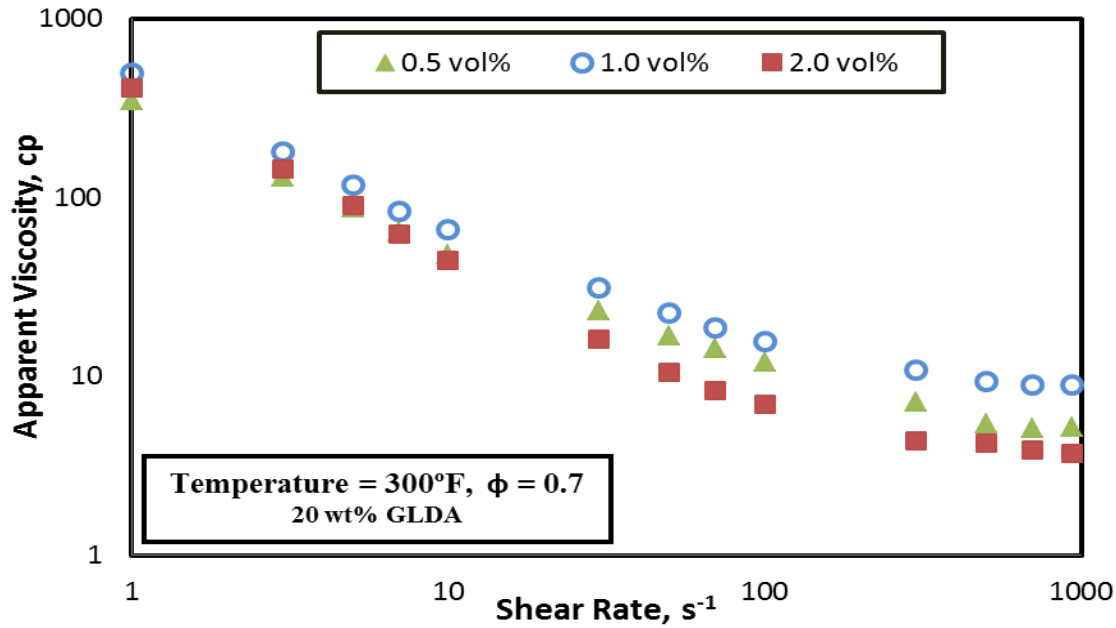

Fig. 9-8: Effect of changing shear rate on the apparent viscosity of emulsified GLDA at 300°F.

Table 9-5: Summary of power-law model parameters for the emulsified GLDA systems.

Temperature	Emulsifier Concentration (vol%)	Power-law Constant, K ($mPa.s^n$)	Power-law Index, n	Correlating Coefficient
150°F	0.5	603.9	0.443	0.96
	1	481.8	0.525	0.97
	2	597.6	0.5	0.98
230°F	0.5	287.5	0.567	0.96
	1	340.5	0.512	0.98
	2	493.3	0.474	0.97
300°F	0.5	268.4	0.32	0.99
	1	365.3	0.32	0.98
	2	335.0	0.165	0.98

9.4.7 Compatibility Tests

The results of compatibility tests of emulsified GLDA and water, diesel, crude oil, 100% ethanol alcohol and 10 vol% mutual solvent solution are shown in **Fig. 9-9**. All these compatibility tests were performed at room temperature (75°F). **Fig. 9-9** shows the emulsified GLDA solution after mixing with water; there was no mixing between emulsified GLDA and water, and two-phases appeared. When emulsified GLDA was added to diesel and crude oil, there was only one homogeneous phase after mixing the fluids. This indicates that emulsified GLDA was incompatible with water, while it was compatible with diesel and crude oil. When emulsified GLDA was mixed with methanol alcohol and 10 vol% mutual solvent solutions, the emulsified GLDA was not stable and broke immediately into two separate phases, aqueous and diesel. This indicates that emulsified GLDA is not compatible with ethanol and mutual solvent solution and it will not be stable in the presence of it. For that reason, 10 vol% mutual solvent solution was

selected to be injected to break any residual emulsified GLDA in the formation after the treatment.

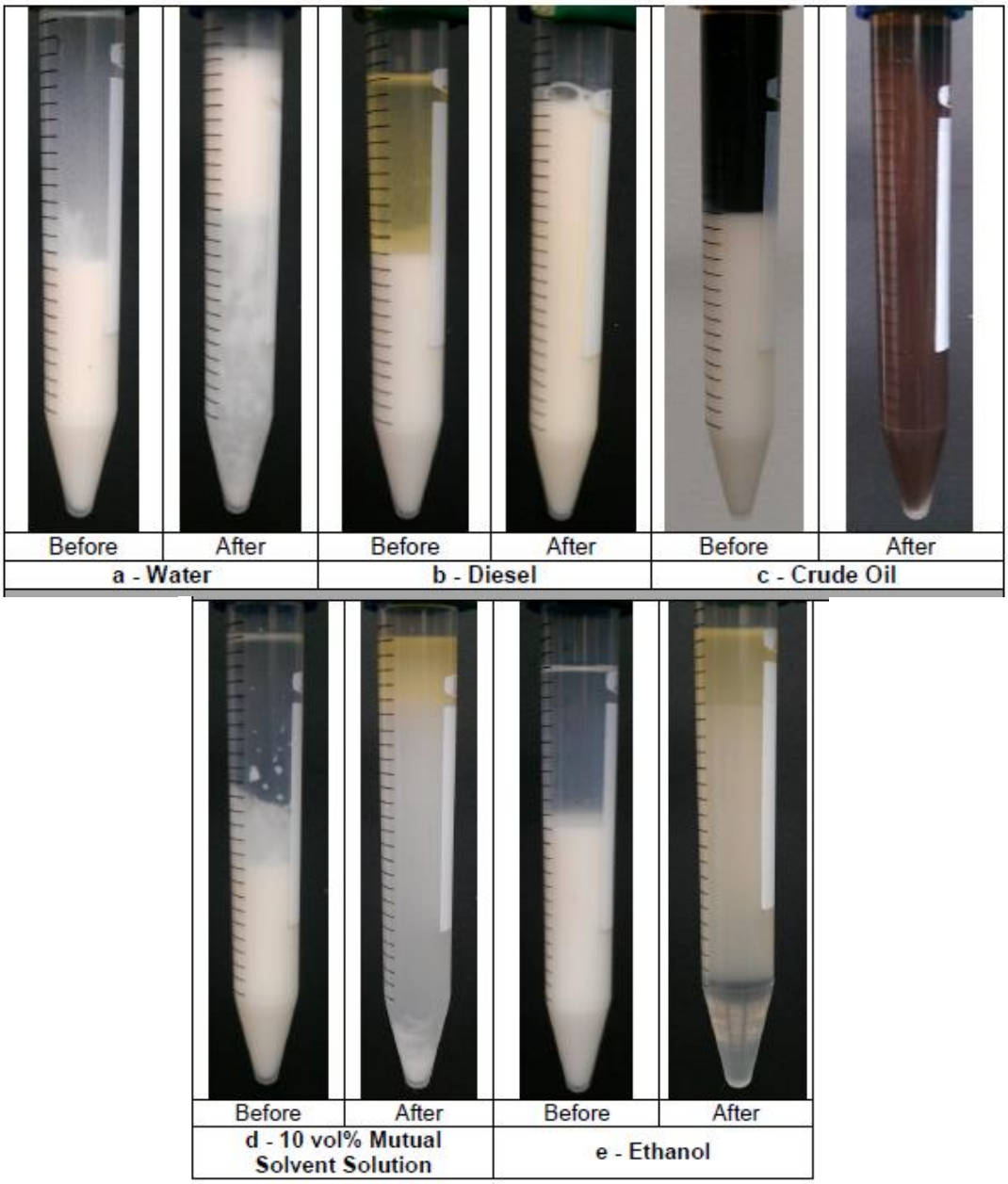

Fig. 9-9: Compatibility tests of emulsified acid systems used in the study.

9.4.8 Reaction Rate of Emulsified GLDA Systems with Calcite

The rotating disk apparatus has been used in the oil industry to measure the rate of calcite and dolomite dissolution in the presence of acids. Different types of acids were used by many researchers (Lund et al. 1973 and 1975; Fredd and Fogler 1998b). The dissolution rate of calcite in the emulsified GLDA was studied using the rotating disk apparatus. The reaction rate experiments were performed at 230°F and covered a disk rotational speed range from 100 to 1500 rpm. Also, the dissolution rate of calcite in emulsified GLDA was measured at temperatures of 250 and 300°F and disk rotational speed of 1000 rpm, and these data were compared to the work done by Rabie et al. (2011). These measurements were performed using emulsified GLDA prepared using 1.0 vol% emulsifier (10 gpt). Indiana limestone core samples were cut into disks sized 0.7 in. in thickness and 1.5 in. in diameter and were used as the main source of calcite that reacts with the emulsified GLDA.

Four rotating disk experiments were performed at a temperature of 230°F and at disk rotational speeds up to 1500 rpm. Samples were withdrawn from the reactor every 2 minute for 20 minutes, so ten fluid samples were collected from each experiment. The calcium concentration in each sample was measured using the ICP. The calcium concentration was plotted as a function of reaction time, and the dissolution rate was obtained by dividing the slope of the best fit straight line by the initial area of the core plug.

Fig. 9-10 shows the change of calcium concentration as a function of reaction time, for emulsified GLDA formulated at 1.0 vol% emulsifier for all experiments. The

plotted points were fitted using a straight line and the slope of the resulted line was used to calculate the reaction (or dissolution) rate. The dissolution rate varied between $6.2X10^{-8}$ gmol/cm^2.s at 100 rpm to $1.214X10^{-7}$ gmol/cm^2.s at 1500 rpm. **Table 9-6** summarizes the reaction rate calculation at different disk rotational speeds.

Table 9-6: Summary of reaction rate constant at different rotational speeds for emulsified GLDA formulated at 1.0 vol% emulsifier and 20 wt% GLDA at 230°F.

ω, rpm	100	500	1000	1500
Dissolution Rate, R, gmol/cm^2.s	6.218E-8	7.941E-8	9.161E-8	1.214E-7

The rate of reaction can be directly measured from the mass flux when the mass transfer limited regime predominates. Plotting the reaction rate versus the disk rotational speed (ω) to the power (1/(1+n)), where n is the power-law exponent obtained from the rheological measurements, can be helpful in determining the boundary between the mass transfer limited regime and the surface reaction limited regime. **Fig. 9-11** shows the plot of reaction rate vs. disk rotational speed to the power 1/(1+n). From **Fig. 9-11**, the reaction of emulsified GLDA and limestone is mass transfer limited for disk rotational speeds up to 1500 rpm, which is the range of rpm speed studied in this work. The effective diffusion coefficient (D) of GLDA in emulsified GLDA at 230°F can be determined using Eq. 9-2 (de Rozieres et al. 1994):

$$R = \left[\varepsilon(n)\left(\frac{K}{\rho}\right)^{\frac{-1}{3(1+n)}}(r)^{\frac{1-n}{3(1+n)}}(\omega)^{\frac{1}{(1+n)}}(D)^{\frac{2}{3}}\right](C_b) = A\,(\omega)^{\frac{1}{(1+n)}} \quad \text{..... (9-2)}$$

where

C_b = reactant concentration in the bulk solution, gmole/cm^3

D = diffusion coefficient, cm^2/s

K = power-law consistency factor ($g/cm.s^{n-2}$)

n = power-law index

r = radius of the disk, cm

R = rate of reaction ($gmole/cm^2.s$)

ρ = fluid density, g/cm^3

ω = disk rotational speed, (rad/s)

ε(n) = function depends on n (**Table 9-7**)

Hansford and Litt (1968) introduced the values for the function ε(n) at different power-law exponent values. These data are represented by **Table 9-7**. From the rheological study, the values of k, n and ε(n) were determined to be 340.5 ($mPa.s^n$), 0.512 and 0.654 respectively at 230°F. From the definition of "A" parameter in the previous equation, the diffusion coefficient D can be estimated to be 1.281E-09 cm^2/s. The diffusion coefficient of 15 wt% HCl emulsified acid prepared at 1.0 vol% emulsifier when reacted with calcite was measured and presented in chapter 3. The value of the diffusion coefficient "D" was 2.73E-7 cm^2/s. From the data obtained from the current work, the emulsified GLDA achieved a diffusion coefficient with calcite that is two orders of magnitude less than that of 15 wt% HCl emulsified acid at the same conditions.

Table 9-7: Values of ε(n) as a function of n (Hansford and Litt 1968).

n	0.2	0.4	0.5	0.6	0.8	1.0	1.3
ε(n)	0.695	0.662	0.655	0.647	0.633	0.620	0.618

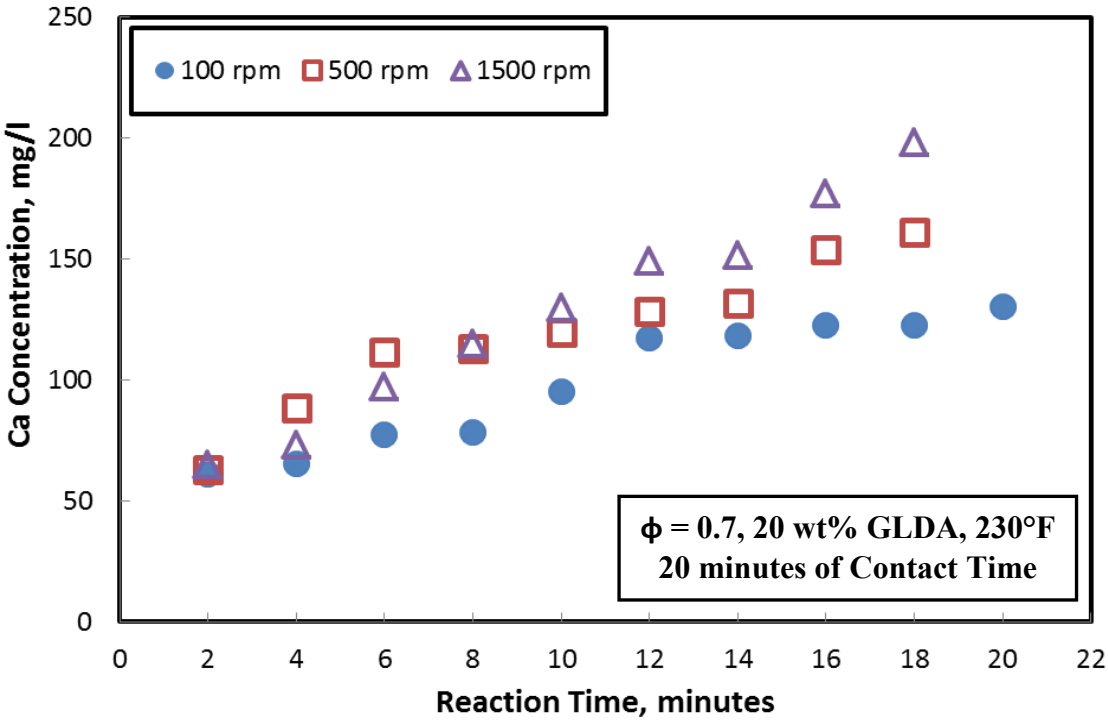

Fig. 9-10: Calcium concentration as a function of time for reaction between emulsified GLDA (1 vol% emulsifier) and calcite at 230°F.

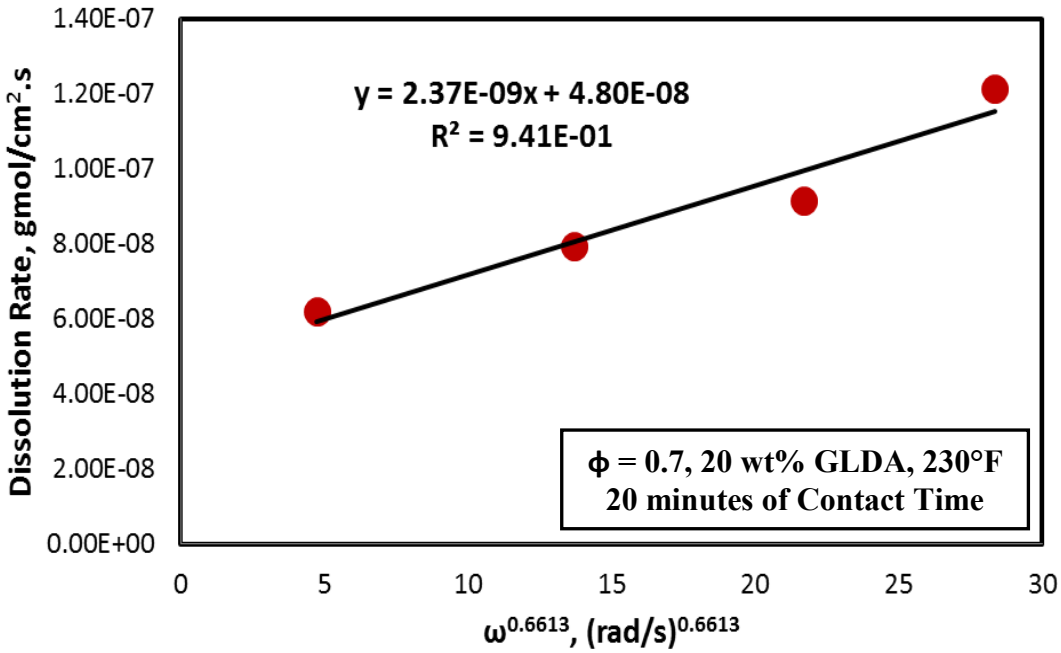

Fig. 9-11: Effect of disk rotational speed on the dissolution rate of calcite in emulsified GLDA.

9.4.9 Comparison of Reaction Rates of Regular and Emulsified GLDA

The dissolution rate of calcite in emulsified GLDA was measured at temperatures of 250 and 300°F and at a disk rotational speed of 1000 rpm. Samples were withdrawn from the reactor every 2 minute for 20 minutes at a temperature of 250°F, and every 1 minute for 10 minutes at a temperature of 300°F. The calcium concentration in each sample was measured using the ICP, the calcium concentration was plotted as a function of the reaction time and the dissolution rate was obtained. These results were compared to what was shown by Rabie et al. (2011).

The dissolution rate of calcite in emulsified GLDA at temperatures of 250 and 300°F and disk rotational speed of 1000 rpm were found to be $1.13X10^{-7}$ and $2.37X10^{-7}$

gmol/cm^2.s, respectively. Rabie et al. (2011) measured dissolution rates of calcite in 20 wt% GLDA solution at temperatures of 250 and 300°F and 1000 rpm disk rotational speed of 4.83X10^{-6} and 7.67X10^{-6} gmol/cm^2.s, respectively. From these results, it is obvious that emulsified GLDA achieved dissolution rates one order of magnitude less than that of regular GLDA solutions.

9.4.10 Coreflood Studies

Coreflood experiments were performed using the emulsified GLDA systems formulated using 1.0 vol% emulsifier. Two coreflood experiments were performed at a temperature of 300°F and injection rate of 2.0 cm^3/min using low permeability Indiana limestone cores (5 and 15 md). **Table 9-2** gives the data for the 6 in. long cores which were used in this coreflood study. The main objective of these coreflood experiments is to test the ability of the emulsified GLDA to enhance the permeability of calcite rocks. For each coreflood experiment, the pressure drop across the core was plotted using Lab-View software. Samples of the coreflood effluent were analyzed for calcium concentration. In the first experiment, emulsified GLDA was injected continuously. The pump pressure started to increase as a result of the high viscosity of emulsified GLDA. The pump pressure continued to increase until the maximum pumping pressure was reached and the pump stopped the injection of the emulsified GLDA. The injection of emulsified GLDA was stopped after injecting 2.8 pore volumes, and 10 vol% mutual solvent was injected to break any remaining emulsion. The core sample was left to cool down and the final permeability of the core was measured and found to 15 md. The initial core permeability was 5 md, and the final to initial permeability ratio was 3, indicating that the

permeability enhanced by just a factor of 3. This can be attributed to the stability of the emulsified GLDA, and so the lower reaction with the rock indicated by the data obtained from the rheological and reaction rate studies shown in the previous sections. As a result, a decision was made to try injecting the emulsified GLDA and soaking the core sample at 300°F to simulate what happens in the field and to give enough time for emulsified GLDA to react with the rock.

In the second coreflood experiment, 2.3 pore volumes of the emulsified GLDA were injected in the core sample and left for a soaking time of 4 hours at 300°F. **Fig. 9-12** shows the pressure drop across the core during the injection of 1.0 vol% emulsified GLDA at an injection rate of 2 cm^3/min and 300°F. The initial permeability of the core was 15 md. The pressure drop initially was constant during the injection of deionized water and stabilized at a value of 24 psi. At the instant where GLDA injection started, the pressure drop increased and continued to increase until it reached 800 psi. This large increase in the pressure drop is attributed to the viscosity of emulsified GLDA injected into the core. After injecting 2.3 pore volumes of emulsified GLDA, injection was stopped and the emulsified GLDA was left soaking in the core sample for 4 hours. With time and at this high temperature, calcite reacted with the emulsified GLDA, and the calcium concentration of the emulsified GLDA effluent started to increase. After 4 hours of soaking, 10 vol% mutual solvent solution was injected to remove any remaining emulsified GLDA or diesel from the core. After injecting of 2 pore volumes of mutual solvent, deionized water was injected. The core sample was left to cool down and the final permeability was measured using deionized water at room temperature (75°F). The

final permeability was found to be 55 md and the ratio of the final to the initial permeability was found to be 3.7. This indicates that emulsified GLDA was successful in stimulating limestone core samples at such a temperature of 300°F.

Fig. 9-13 shows the calcium concentration in the core effluent samples for the experiment shown in **Fig. 9-12**. The calcium concentration reached a maximum value of 9533 mg/l. These data were used to calculate the total amount of calcium collected in the effluent fluid samples, and it was found to be 0.4 grams.

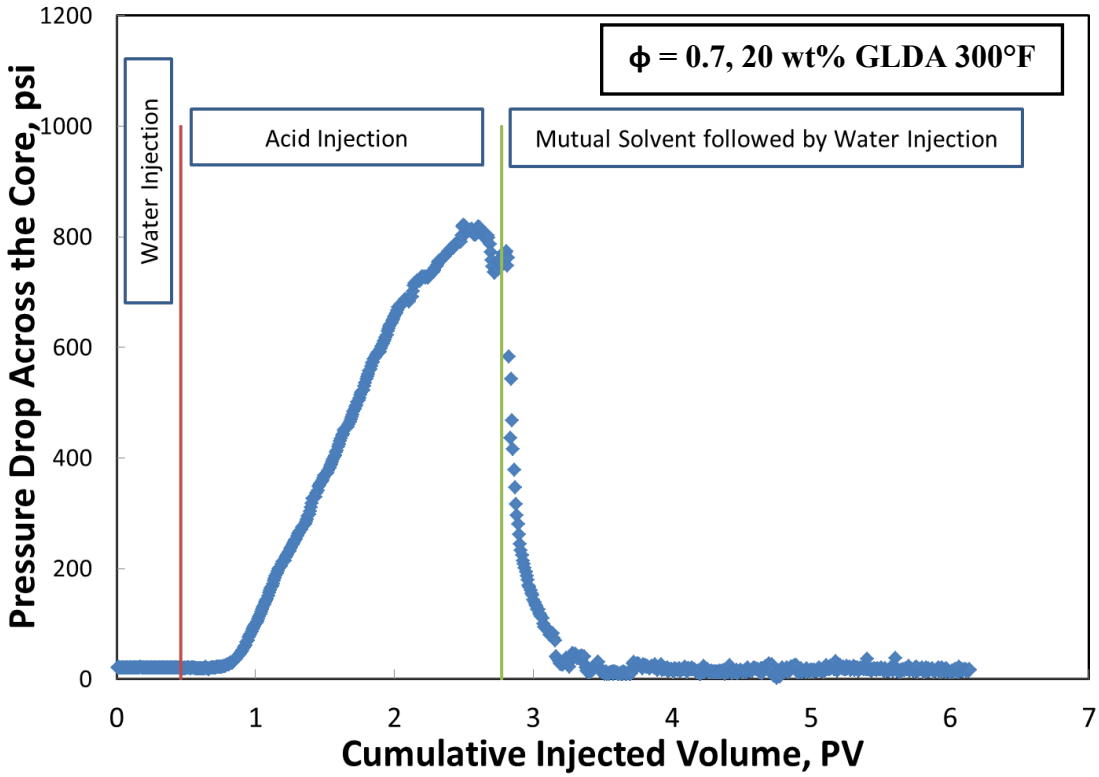

Fig. 9-12: The pressure drop across the core during the injection of 1.0 vol% emulsified GLDA at an injection rate of 2 cm^3/min and 300°F.

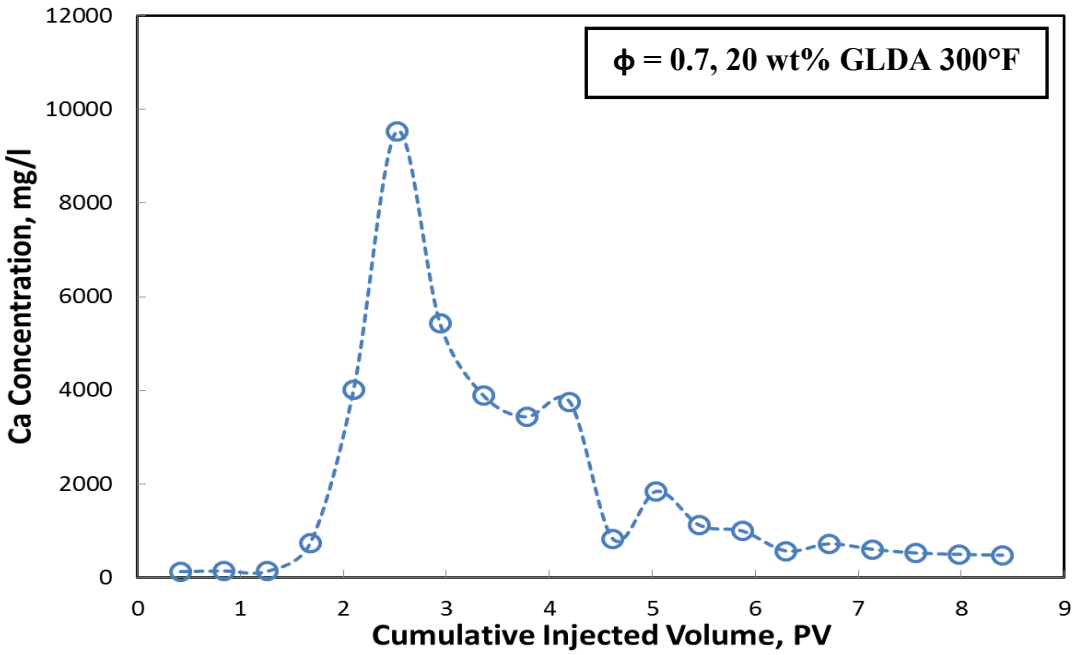

Fig. 9-13: The calcium concentration in the effluent fluid samples during the injection of 1.0 vol% emulsified GLDA at an injection rate of 2 cm^3/min and 300°F.

In the third coreflood experiment, 2.0 pore volumes of the emulsified GLDA were injected in the core sample at an injection rate of 1.0 cm^3/min, and left for soaking for 3 hours at a temperature of 350°F. The initial permeability of the core was 4.8 md. The pressure drop initially was constant during the injection of deionized water and stabilized at a value of 44 psi. At the instant where GLDA injection started, the pressure drop increased and continued to increase until it reached 980 psi. This large increase in the pressure drop is attributed to the viscosity of emulsified GLDA injected into the core. After injecting 2.0 pore volumes of emulsified GLDA, injection was stopped and the emulsified GLDA was left soaking in the core sample for 3 hours at a temperature of 350°F. With time and at this high temperature, calcite reacted with the emulsified

GLDA, the calcium concentration of the emulsified GLDA effluent started to increase. After 3 hours of soaking, 10 vol% mutual solvent solution was injected, and the core sample was left to cool down, and the final permeability was measured using deionized water at room temperature (75°F). The final permeability was found to 14.8 md and the ratio of the final to the initial permeability was found to be 3. This indicates that emulsified GLDA was successful in stimulating limestone core samples at a temperature of 350°F. After examining the core inlet face, there was no face dissolution observed. The calcium concentration of the coreflood effluent samples was measured using the ICP. The maximum calcium concentration was 19300 mg/l. These data were used to calculate the total amount of calcium collected in the effluent fluid samples, and it was found to be 0.764 grams.

10. CONCLUSIONS AND RECOMMENDATIONS

A new cationic emulsifier was used to formulate emulsified acid systems that can be used for high temperature stimulation treatments. The new emulsified acids will be used to retard the acid/rock reaction rate during matrix acidizing of carbonate formations. The rheology of the new emulsified acid system was examined under different emulsifier concentrations, acid concentrations and different temperatures. Based on the results obtained, the following conclusions can be drawn:

- Diesel viscosity decreased with increasing the temperature.
- The apparent viscosity of the new emulsified acid increased with increasing emulsifier concentration.
- The apparent viscosity of emulsified acid decreased with increasing the temperature due to the reduction in the continuous phase viscosity (diesel).
- At a low emulsifier concentration, 0.5 vol%, the emulsion breakdown occurred at high temperature and high shear rate, while this behavior was less severe for emulsified acid systems prepared at higher emulsifier concentrations.
- Emulsified acids are non-Newtonian shear thinning fluids that follow the power-law model.

Emulsified acids have been used to retard the acid/rock reaction rate during matrix acidizing of carbonate formations. These acids were examined under different emulsifier concentrations. The reaction rate of the emulsified acid with limestone core samples was studied using a rotating disk apparatus at 230°F, and disk rotational speeds ranging from 100 to 1500 rpm. The acid diffusivity in emulsified acid with calcite rocks

was determined using the reaction kinetics data at different disk rotational speeds. Based on the results obtained, the following conclusions can be drawn:

- From the reaction kinetics measurements, the new emulsified acid showed a low reaction rate with limestone, and also low diffusion rates.
- For the tested emulsifier concentrations (0.5, 1.0, and 2.0 vol%), the reaction rate increased proportionally with the disk rotational speed to the power 1/(1+n), where n is the power-law index from the rheology measurements, which indicated that the reaction of emulsified acid with limestone, at 230°F, is a mass transfer limited reaction.
- At higher emulsifier concentrations, the emulsified acid-limestone reaction was slower and achieved low acid diffusion rates.

The reaction of dolomite with regular HCl was studied before, while reaction of dolomite with emulsified acids did not get the same attention. The reaction of 15 wt% HCl emulsified acid with dolomite disks was examined using the rotating disk apparatus at disk rotational speeds in the range of 100 to 1500 rpm. Based on the results obtained, the following conclusions can be drawn:

- At 230°F, the reaction of dolomite with emulsified acid is a mass transfer limited reaction.
- The dissolution rate and diffusion coefficient decreased as the emulsifier concentration was increased.
- The reaction rate of emulsified acids with dolomite is lower by an order of magnitude than that of calcite.

- The diffusion coefficient of emulsified acid in the presence of dolomite is two orders of magnitude less than that obtained using calcite disks.
- The dissolution rate of dolomite in emulsified acids is lower by one or two orders of magnitude than that measured previously using regular HCl acids.
- Diffusion coefficients of emulsified acid in the presence of dolomite rock were found to be lower by 3 to 5 orders of magnitude than that measured previously using regular HCl.
- The emulsified acid system achieved a low diffusion coefficient and dissolution rate. This low diffusion coefficient and dissolution rate will retard acid-rock reaction, and enhance the outcome of the stimulation treatment by creating deep wormholes (matrix acidizing) or etched fracture surface (acid fracturing).

Emulsified acids have been used to retard acid/rock reaction rate during matrix acidizing of carbonate formations. A coreflood study was performed using both low and high permeability Indiana limestone core samples obtained from an outcrop. All acids were formulated using 1.0 vol% emulsifier and the final acid concentration was 15 wt% HCl. The injection rate of emulsified acid covered a range from 0.5 to 10 cm^3/min, and all coreflood experiments were performed at a temperature of 300°F. Based on the results obtained from the coreflood study; the following conclusions can be drawn:

- From the coreflood study, there is an optimum injection rate for an emulsified acid system when it was tested using low permeability Indiana limestone cores, and it was found to be 5 cm^3/min.
- When emulsified acid systems were used to stimulate high permeability Indiana

limestone, the volume acid to cause breakthrough decreased with increasing the acid injection rate, indicating that there is no optimum acid injection rate in this case.

- The emulsified acid system can be used effectively, with no face dissolution, at low and high injection rates for both high and low permeability cores.
- For both low and high permeability Indiana limestone cores, the new emulsified acid enhanced the permeability of core indicating the effectiveness of the new emulsified acid in stimulating calcite rocks at 300°F.

The flow of emulsified acids in Indiana limestone cores was examined. The cores were saturated with 100% water, 100% oil, or crude oil at irreducible water saturation (Swir). All acids were formulated using 1.0 vol% emulsifier and the final acid concentration was 15 wt% HCl. Based on the results obtained, the following conclusions can be drawn:

- Emulsified acid was compatible with diesel, xylene, and crude oil, and it was not compatible with water and broke in the presence of ethanol alcohol and 10 vol% mutual solvent solution.
- Droplet size of the emulsified acid decreased when the emulsified acid was mixed with crude oil.
- The viscosity of emulsified mixed with crude oil is affected by both the viscosity of the crude oil and the change of the acid volume fraction.
- The volume of emulsified acid to achieve breakthrough in cores saturated with a crude oil was greater by 2 to 3.9 times than that needed for cores fully saturated

with water, while in cores saturated with crude oil at irreducible water saturation, the volume of emulsified acid to achieve breakthrough was 1.3 to 2.9 times greater than that needed for cores fully saturated with water.

- At the same emulsified acid injection rate, the permeability enhancement in cores saturated with 100% crude oil was 1.3 to 2.5 times higher than what was noticed with core samples saturated with 100% water.
- Within the emulsified acid injection rate studied (0.5 to 10.0 cm^3/min), there was no optimum injection rate noticed when emulsified acids were injected into limestone cores saturated with 100% water, saturated with 100% crude oil, or saturated with crude oil at irreducible water saturation.

The new emulsified acids were used to stimulate dolomite cores at high temperature using a coreflood setup. All acids were formulated using 1.0 vol% emulsifier and the final acid concentration was 15 wt% HCl. Based on the results obtained, the following conclusions can be drawn:

- From the coreflood study, and for the emulsified acid injection rates covered in the current study, there was no optimum injection rate for an emulsified acid system when it was used to stimulate dolomite cores.
- In general, the volume of emulsified acid to achieve breakthrough increased with the increase in emulsified acid injection rate (for emulsified acid injection rates ranging from 0.5 to 10 cm^3/min).
- The emulsified acid system was used effectively, with no face dissolution, at low and high injection rates.

The new emulsified acids have been used to retard acid/rock reaction rate during matrix acidizing of carbonate formations. A coreflood study was conducted using core samples obtained from two different carbonate reservoirs (A and Z) in order to test the performance of the emulsified acid. All acids were formulated using 1.0 vol% emulsifier and the final acid concentration was 15 wt% HCl. Based on the results obtained, the following conclusions can be drawn:

- The solubility of the reservoir core samples in 15 wt% regular HCl at 75°F was very high indicating the need for an effective retarding acid system.
- Emulsified acid was formulated and used to stimulate the cores obtained from two carbonate reservoirs. The rheological measurements of this acid indicated that the emulsified acid is a non-Newtonian shear thinning fluid.
- From the coreflood study, there is an optimum injection rate for an emulsified acid system when it was tested with reservoir cores, and it was found to be 5 cm^3/min.
- The emulsified acid system can be used effectively, with no face dissolution, at low and high injection rates.
- The reaction of emulsified acid and reservoir core samples obtained from reservoir "Z" was mass transfer limited at 220°F.
- Emulsified acid achieved both low reaction rates (9.32E-07 to 6.41E-06 gmol/cm^2.s) and a diffusion coefficient (2.75E-7 cm^2/s) at a temperature of 220°F.
- The new emulsified acid system tested in the current study was effective in

stimulating wells drilled in carbonate reservoir cores, at different acid injection rates, it is recommended to be used in stimulation of low or high permeability carbonate reservoirs.

An innovative technique of emulsifying the chelating agents was evaluated. Emulsified GLDA systems were formulated using a cationic emulsifier and 20 wt% GLDA solutions. The viscosity of the emulsified GLDA systems was examined under different emulsifier concentrations, and temperatures. Coreflood and reaction rate studies were performed to evaluate the performance of the emulsified GLDA. Based on the results obtained, the following conclusions can be drawn:

- The emulsified GLDA was a non-Newtonian shear thinning fluid.
- There was no significant effect of changing the emulsifier concentration on the apparent viscosity of emulsified GLDA.
- From the coreflood study, the emulsified GLDA was able to enhance the permeability of Indiana limestone core samples by a factor of 3 to 3.7
- The emulsified GLDA was used effectively, with no face dissolution, at very low injection rates (1.0 cm^3/min) and at high temperatures (350°F).
- Emulsified GLDA achieved dissolution rates one order of magnitude less than that of regular GLDA solutions with calcite.
- Emulsified GLDA achieved reaction (dissolution) rates and diffusion coefficient that are less by two orders of magnitude than those with emulsified acid at the same conditions.

Emulsified acids are used for matrix acidizing and acid fracturing at acid concentrations up to 28 wt% HCl. The new cationic emulsifier was effective in formulating emulsified acid systems that was stable at temperatures up to 300°F.

Acid injection rate should be determined based on the coreflood study which will be performed using the core samples from the reservoir that will be stimulated. Also, acid injection rate should be determined based the expected shear rate in the formation. A coreflood experiment is recommended to confirm the optimum injected rate. The newly developed emulsified acid achieved both low reaction and diffusion rates. This new emulsified acid is recommended to be used in stimulation of low permeability, deep carbonate reservoirs.

The type and concentration of the fluids in the reservoir has a great influence on the performance of the emulsified acid, and it is recommended to study this effect using the coreflood setup. Also, the use of a mutual solvent solution is very important to remove any remaining emulsion and to clean the formation from the diesel hydrocarbon phase. Measuring the reaction rate of emulsified acid and the reservoir cores is recommended in order to better design the acid stimulation treatment.

REFERENCES

Abdel Fatah, W., and Nasr-El-Din, H.A. 2010. Acid Emulsified in Xylene: A Cost-Effective Treatment to Remove Asphalting Deposition and Enhance Well Productivity. *SPE Production & Operations* **25**(2): 151-154.

Abramoff, M.D., Magalhaes, P.J., and Ram, S.J. 2004. Image Processing with ImageJ. *Biophtonics International* **11**: 36-42.

Abrams, A. Scheuerman, R.F., Templeton, C.C., and Richardson, E.A. 1983. Higher-pH Acid Stimulation Systems. *JPT* **35**(12): 2175-2184.

Al-Anazi, H.A., Nasr-El-Din, H.A. and Mohamed, S.K. 1998. Stimulation of Tight Carbonate Reservoirs Using Acid-in-Diesel Emulsions - Field Application. Paper SPE 39418 presented at the SPE International Symposium and Exhibition on Formation Damage Control, Lafayette, Louisiana, USA, 18-19 February.

Al-Harbi, M.S., Al-Dhafeeri, A.M., Al-Rufaie, Y.A, and Mohammed, S.K. 2006. Evaluation of Acid Treatment Results for Water-Injection Wells in Saudi Arabia. Paper SPE 101344 presented in the SPE Annual Technical Conference and Exhibition, San Antonio, Texas, USA, 24-27 September.

Al-Muhareb, M.A., Nasr-El-Din, H.A., Samuel, E., P. Marcinew, R.P., and Samuel, M. 2003. Acid Fracturing of Power Water Injectors: A New Field Application Using Polymer-free Fluids. Paper SPE 82210 presented at the SPE European Formation Damage Conference, The Hague, Netherlands, 13-14 May.

Al-Mutairi, S.H., Hill, A.D., and Nasr-EI-Din, H.A. 2008a. Effect of Droplet Size, Emulsifier Concentration, and Acid Volume Fraction on the Rheological Properties and Stability of Emulsified Acids. *SPE Production and Operations* **23**(4): 484-497.

Al-Mutairi, S.H., Hill, A.D., and Nasr-EI-Din, H.A. 2008b. Fracture Conductivity Using Emulsified Acids: Effects of Emulsifier Concentration and Acid Volume Fraction. Paper IPTC 12186 presented at the International Petroleum Technology Conference, Kuala Lumpur, Malaysia, 3-5 December.

Al-Mutairi, S.H., Nasr-El-Din, H.A., and Hill, A.D., Al-Aamri, A.D. 2009a. Effect of Droplet Size on the Reaction Kinetics of Emulsified Acid with Calcite. *SPE Journal* **14**(4): 606-616.

Al-Mutairi, S.H., Hill, A.D., and Nasr-EI-Din, H.A. 2009b. Droplet Size Analysis of Emulsified Acid. SPE 126155 presented at the SPE Saudi Arabia Section Technical Symposium and Exhibition, Al-Khobar, Saudi Arabia, 09-11 May.

Al-Mutairi, S.H., Al-Obied, M.A., Al-Yami, I.S., Shebatalhamd, A.M., and Al-Shehri, D.A. 2012. Wormhole Propagation in Tar During Matrix Acidizing of Carbonate Formations. Paper SPE presented at the SPE International Symposium and Exhibition on Formation Damage Control, Lafayette, Louisiana, USA, 15-17 February.

Alkattan, M., Oelkers, E.H., Dandurand, J.L., and Schott, J. 1998. An Experimental Study of Calcite and Limestone Dissolution Rates as a Function of pH from –1 to 3 and Temperature from 25 to 80°C. *Chemical Geology* **151**(1): 199-214.

Allen, T.O., and Roberts, A.P. 1989. Production Operations: Volume1 & 2. Penn Well Books; Tulsa, Oklahoma, USA.

Anderson, M.S. 1991. Reactivity of San Andres Dolomite. *SPEPE* **6**(2): 227-232.

Appicciutoli, D, Maier, R., Strippoli, D.P., Tiani, A., and Mauri, L. 2010. Novel Emulsified Acid Boosts Production in a Major Carbonate Oil Field with Asphaltene Problems. Paper SPE 135076 presented in the SPE Annual Technical Conference and Exhibition, Florence, Italy, 19-22 September.

Barron, A.N., Hendrickson, A.R. and Wieland, D.R. 1962. The Effect of Flow on Acid Reactivity in a Carbonate Fracture. *J. Pet. Tech* **14**(4): 409-415.

Barnes, H.A. 1994. Rheology of Emulsions - *A Review. Colloids Surfaces* A: *Physicochemical and Engineering Aspects*, **91**: 89-95.

Bartko, K.M., Nasr-El-Din, H.A., Rahim, Z., and Al-Muntasheri, G.A. 2003. Acid Fracturing of a Gas Carbonate Reservoir: The Impact of Acid Type and Lithology on Fracture Half Length and Width. Paper SPE 84130 presented at the SPE Annual Conference and Exhibition, Denver, Colorado, USA, 5-8 October.

Baucke, F.G., Landolt, D. and Tobias, C.W. 1968. Rotating Disk System for the Study of Metal Deposition from Non-aqueous Solvents. *The review of Scientific Instruments* **39**(11): 1753-1754.

Bazin, B. and Abdulahad, G. 1999. Experimental Investigation of Some Properties of Emulsified Acid Systems for Stimulation of Carbonate Formations. Paper SPE 53237 presented at the SPE Middle East Oil Show, Bahrain, 20-23 February.

Becher, P. (ed.). 1985. Encyclopedia of Emulsion Technology, II. Marcel Dekker; New York, USA.

Beenakker, C.W.J. 1984. The Effective Viscosity of a Concentrated Suspension of Spheres. *Physica A* **128**: 48-81.

Ben-Naceur, K., and Economides, M.J. 1989. Design and Evaluation of Acid Fracturing Treatments. Paper SPE 18978 presented in the Low Permeability Reservoirs Symposium, Denver, Colorado, USA, 6-8 March.

Bergstrom, J.M. and Miller, B.D. 1975. Results of Acid-in-Oil Emulsion Stimulations of Carbonate Formations. Paper SPE 5648 presented at the SPE Annual Fall Meeting of SPE AIME, Dallas, Texas, USA, 28 September-1 October.

Bernadiner, M.G., Thompson, K.E., and Fogler, H.S. 1992. Effect of Foams Used During Carbonate Acidizing. *SPEPE* **7**(4): 350-356.

Bibette, J. and Leal-Calderon, F. 1996. Surfactant-Stabilized Emulsions. *Current Opinion in Colloid & Interface Science* **1**: 746-751.

Bodine, M.W., and Fernalld, T.H. 1973. EDTA Dissolution of Gypsum, Anhydrite, and Ca-Mg Carbonates: *J. Sediment. Petrol.* **43**(4): 1152-1156.

Boomer, D.R., McCune, C.C., and Fogler, H.S. 1972. Rotating Disk Apparatus for Reaction Rate Studies in Corrosive Liquid Environment. *The Review of Scientific Instruments* **43**(2): 225-229.

Borwankar, R.P. 1997. Case SE. Rheology of Emulsions, Foams, and Gels. *Curr Opin Colloid Interface Sci*. **2**: 584-589.

Broaddus, G.C., Knox, J.A., and Fredrickson, S.E. 1968. Dynamic Etching Tests and Their Use in Planning Acid Treatments. Paper SPE 2362 presented at the SPE Oklahoma Regional Meeting, Stillwater, Oklahoma, USA, 25 October.

Buijse, M.A. 2000. Understanding Wormholing Mechanisms Can Improve Acid Treatments in Carbonate Formations. *SPEPF* **15**(3): 168-175.

Buijse, M.A. and van Domelen, M.S. 2000. Novel Application of Emulsified Acids to Matrix Stimulation of Heterogeneous Formations. *SPEPF* **15**(3): 208-213.

Buijse, M., Boer, P., Breukel, B., and Burgos, G. 2004. Organic Acids in Carbonate Acidizing. *SPEPF* **19**(3): 128-134.

Busenberg, E., and Plummer L.N. 1982. The Kinetics of Dissolution of Dolomite in CO_2-H_2O Systems at 1.5 to 65°C and 0 to 1 atm P_{CO2}. *Amer. J. Sci.* **282**: 45-78.

Busenberg, E., and Plummer, L.N., 1986. A Comparative Study of the Dissolution and Crystal Growth Kinetics of Calcite and Aragonite. In: Mumptom, F.A. (Ed.), Studies in Diagenesis. U. S. Geological Survey Bulletin **1578:** 139–168.

Cannan, W.L., Jennings, A.R., Huseini, S., Bordelon, T.P. and Sardjono, S. 1992. Increasing Arun Well Deliverability Through Effective Acid Fracturing. Paper SPE 22397 presented at the SPE International Meeting on Petroleum Engineering, Beijing, China, 24-27 March.

Chamberlain, L.C., and Boyer, R.F. 1939. Acid Solvents for Oil Wells Physicochemical Adapted to Various Production Conditions. *Industrial & Engineering Chemistry* **73** (4): 400-406.

Chang, H., and Matijevic, E. 1983. Interactions of Metal Hydrous Oxides with Chelating Agents: IV. Dissolution of Hematite. *J. Colloid Interface Sci.* **92**(2): 479-488.

Chou, L., Garrels, R.M., and Wollast, R. 1989. Comparative Study of the Kinetics and Mechanisms of Dissolution of Carbonate Minerals. *Chemical Geology* **78**: 269-282.

Clayton, W. (ed.). 1923. Theory of Emulsions and Emulsification, Churchill, London.

Conway, M.W., Asadi, M., Penny, G., and Chang, F. 1999. A Comparative Study of Straight/Gelled/Emulsified Hydrochloric Acid Diffusivity Coefficient Using Diaphragm Cell and Rotating Disk. Paper SPE 56532 presented at the SPE Annual Technical Conference and Exhibition, Houston, Texas, USA, 3-6 October.

Crenshaw, P.L. and Flippen, F.F. 1968. Stimulation of the Deep Ellenburger in the Delaware Basin. *JPT* **20**(12): 1361-1370.

Crowe, C.W. 1971. Acidizing Composition. US Patent 3,779,916, November 4.

Crowe, C.W. and Miller, B.D. 1974. New, Low-Viscosity Acid-in-Oil Emulsions Provide High Degree of Retardation at High Temperature. Paper SPE 4937 presented at the SPE Rocky Mountains Regional Meeting of SPE-AIME, Billings, Montana, USA, 15-17 May.

Crowe, C.W., Hutchinson, B.H., and Trittipo, B.L. 1989. Fluid-Loss Control: The Key to Successful Acid Fracturing. *SPE Production Engineering* **4**(2): 215-220.

Daccord, G., Touboul, E., and Lenormand, R. 1989. Carbonate Acidizing: Toward a Quantitative Study of the Wormholing Phenomenon. *SPE Production Engineering* **4**(1): 63-68.

Davis, J.J., Mancillas, G. and Melnyk, J.D. 1965. Improved Acid Treatments by Use of the Spearhead Film Technique. Paper SPE 1164 presented at the SPE Rocky Mountains Regional Meeting of SPE-AIME, Billings, Montana, USA, 10-11 June.

De Groote, M. 1933. Process for Increasing the Output of Oil Wells. US Patent No. 1,922,154, April 15.

de Rozieres, J., Chang, F.F. and Sullivan, R.B. 1994. Measuring Diffusion Coefficients in Acid Fracturing Fluids and Their Application to Gelled and Emulsified Acids. Paper SPE 28552 presented at the SPE 69th Annual Technical Conference and Exhibition, New Orleans, Louisiana, USA, 25-28 September.

Delorey, J.R., Allen, S., and McMaster, L. 1996. Precipitation of Calcium Sulphate During Carbonate Acidizing: Minimizing the Risk. Document ID 96-84. Annual Technical Meeting, Calgary, Alberta, Canada, 10-12 June.

Deysarkar, A.K., Dawson, J.C., Sedillo, L.P., and Knoll-Davis, S. 1984. Crosslinked Acid Gel. *J. Canadian Petroleum Technology* **23**(1): 26-32.

Dill, W.R. 1961. Reaction Times of Hydrochloric Acetic Acid Solutions on Limestone. Paper SPE 211 presented at the Southwest Regional Meeting of the American Chemical Society, Oklahoma City, Oklahoma, USA, 1-3 December.

Dnistryansky, V., Mokshaev, A., Bogatyrev, O., Ilgildin, R., Kayumov, R., Burdin, K., and Lobov, M. 2012. Comprehensive Approach to Production Stimulation of Massive Cold Heterogeneous Carbonate Formation Using Coiled Tubing. Paper SPE 152351 presented at SPE Middle East Unconventional Gas Conference and Exhibition, Abu Dhabi, UAE, 23-25 January.

Dunlap, P.M. and Hegwer, J.S. 1960. An Improved Acid for Calcium Sulfate-Bearing Formations. *J. Pet. Tech*. **12**(1): 67-70.

Einstein, A. 1906. Eine Neue Bestimmung der Molek¨uldimensionen. *Ann. Physik*. **19**: 289-306.

Fredd, C.N. and Fogler, H.S. 1996. Alternative Stimulation Fluids and Their Impact on Carbonate Acidizing. Paper SPE 31074 presented at the SPE Formation Damage Control Symposium, Lafayette, Louisiana, USA, 14-15 February.

Fredd, C.N. and Fogler, H.S. 1997. Chelating Agents as Effective Matrix Stimulation Fluids for Carbonate Formations. Paper SPE 37212 presented at the SPE International Symposium on Oil field Chemistry, Houston, Texas, USA, 18-21 February.

Fredd, C.N. 1998. The Influence of Transport and Reaction on Wormhole Formation in Carbonate Porous Media: A Study of Alternative Stimulation Fluids. PhD. Thesis, University of Michigan.

Fredd, C.N., and Fogler, H.S. 1998a. The Kinetics of Calcite Dissolution in Acetic Acid Solutions. *Chem. Eng. Sci.* **53**(22): 3863 -3874.

Fredd, C.N., and Fogler, H.S. 1998b. The Influence of Chelating Agents on the Kinetics of Calcite Dissolution. *Journal of Colloid and Interface Science* **204**(1): 187-197.

Fredd, C.N., and Fogler, H.S. 1998c. Alternative Stimulation Fluids and Their Impact on Carbonate Acidizing. *SPE Journal* **3**(1): 34-41.

Frenier, W.W., Fredd, C.N., and Chang, F. 2001a. Hydroxyaminocarboxylic Acids Produce Superior Formulations for Matrix Stimulation of Carbonates. Paper SPE

68924 presented at the SPE European Formation Damage Conference, The Hague, Netherlands, 21-22 May.

Frenier, W.W., Fredd, C.N., and Chang, F. 2001b. Hydroxyaminocarboxylic Acids Produce Superior Formulations for Matrix Stimulation of Carbonates at High Temperatures. Paper SPE 71696 presented at the SPE Annual Technical Conference and Exhibition, New Orleans, Louisiana, USA, 30 September - 3 October.

Frenier, W.W., and Hill, D.G. 2002. Effect of Acidizing Additives on Formation Permeability During Matrix Treatments. Paper SPE 73705 presented at the SPE International Symposium and Exhibition on Formation Damage Control, Lafayette, Louisiana, USA, 20-21 February.

Gautelier, M., Oelkers, E.H., and Schott, J. 1999. An Experimental Study of Dolomite Dissolution Rates as a Function of pH from -0.5 to 5 and Temperature from 25 to 80ºC. *Chemical Geology* **157**: 13-26.

Gdanski, R.D., and Norman, L.R. 1986. Using the Hollow-Core Test to Determine Acid Reaction Rates. *SPE Production Engineering* **1**(2): 111-116.

Gdanski, R.D., and Lee, W.S. 1989. On the Design of Fracture Acidizing Treatments. Paper SPE 18885 presented in the SPE Production Operations Symposium, Oklahoma City, Oklahoma, USA, 13-14 March.

Gdanski, R. and van Domlen, M.S. 1999. Slaying the Myth of Infinite Reactivity of Carbonates. Paper SPE 50730 presented at the SPE International Symposium on Oilfield Chemistry, Houston, Texas, USA, 16-19 February.

Gilchrist, J.M., and Lietard, O.M.N. 1994. Use of High-Angle, Acid-Fractured Wells on the Machar Field Development. Paper SPE 28917 presented at the European Petroleum Conference, London, U.K., 25-27 October.

Gomaa, A.M., and Nasr-El-Din, H.A. 2010. Propagation of Regular HCl Acids in Carbonate Rocks: The Impact of an In-Situ Gelled Acid Stage. Paper SPE 130586 presented at the CPS/SPE International Oil & Gas Conference and Exhibition, Beijing, China, 8-10 June.

Guidry, G.S., Ruiz, G.A. and Saxon, A. 1989. SXE/N2 Matrix Acidizing. Paper SPE 17951 presented at the SPE Middle East Oil Technical Conference and Exhibition, Manama, Bahrain, 11-14 March.

Hansford, G.S. and Litt, M. 1968. Mass Transport from a Rotating Disk into Power-Law Liquids. *Chem. Eng. Sci*. **23**(8): 849-864.

Harris, F.N. 1961. Applications of Acetic Acid to Well Completion, Stimulation and Reconditioning. *JPT* **13**(7): 637-639.

Harris, O.E., Hendrickson, A.R. and Coulter, A.W. 1966. High-Concentration Hydrochloric Acid Aids Stimulation Results in Carbonate Formations. *J. Pet. Tech,* **18**(10): 1291-1296.

Hendrickson, A.R., Rosene, R.B. and Wieland, D.R. 1961. Acid Reaction Parameters and Reservoir Characteristics Used in the Design of Acid Treatments. Paper presented at the 137th ACS Meeting, Cleveland, Ohio, USA, 5-14 April.

Hendrickson, A.R., Crowe, C.W. and Horton, H.L. 1965. Matrix Acidizing of Limestone Reservoirs. Paper No. 906-10-F presented at Southwestern API, Division of Production, Dallas, Texas, USA, 10-12 March.

Herman, J.S. and White, W.B. 1984. Dissolution Kinetics of Dolomite: Effect of Lithology and Fluid Flow Velocity. *Geochemica et Cosmochemica Acta* **49**: 2017-2026.

Hoefner, M.L. and Fogler, H.S. 1985. Effective Matrix Acidizing in Carbonates Using Microemulsions. *Chem. Eng. Prog.* **81**: 40-44.

Hoefner, M.L., Fogler, H.S, Stenius, P., and Sjoblom, J. 1987. Role of Acid Diffusion in Matrix Acidizing of Carbonates. *JPT* **39**(2): 203-208.

Hoefner, M.L. and Fogler, H.S. 1989. Fluid Velocity and Reaction Rate Effects During Carbonate Acidizing: Application of Network Model. *SPE Production Engineering* **4**(1): 56–62.

Huang, T., McElfresh, P.M., and Gabrysch, A.D. 2003. Carbonate Matrix Acidizing Fluids at High Temperatures: Acetic Acid, Chelating Agents or Long-Chained Carboxylic Acids? Paper SPE 82268 presented at the SPE European Formation Damage Conference, The Hague, Netherlands, 13-14 May.

Jamialahmadi, M., and Mullersteinhagen, H., 1991. Reduction of Calcium Sulfate Scale Formation during Nucleate Boiling by Addition of EDTA. *Heat Transfer Eng.* **12**(4): 19-26.

Johnson, D.E., Fox, K.B., Burns, L.D., and O'Mara, E.M. 1988. Carbonate Production Decline Rates Are Reduced Through Improvements in Gelled Acid Technology.

Paper SPE 17297 presented at the Permian Basin Oil and Gas Recovery Conference, Midland, Texas, USA, 10-11 March.

Jones, A.T., Doyle, M., and Davies, D.R. 1995. Using Acids Viscosified With Succinoglycan Could Improve the Efficiency of Matrix Acidizing Treatments. Paper SPE 30122 presented at the SPE European Formation Damage Conference, The Hague, The Netherlands, 15-16 May.

Jones, A.T. and Davies, D.R. 1998. Quantifying Acid Placement: The Key to Understanding Damage Removal in Horizontal Wells. *SPEPF* **13**(3): 163-169.

Kalfayan, L.J. 2007. Fracture Acidizing: History, Present State, and Future. Paper SPE 106371 presented at the SPE Hydraulic Fracturing Technology Conference, College Station, Texas, USA, 29-31 January.

Kasza, P., Dziadkiewicz, M. and Czupski, M. 2006. From Laboratory Research to Successful Practice: A Case Study of Carbonate Formation Emulsified Acid Treatments. Paper SPE 98261 presented at the SPE International Symposium and Exhibition on Formation Damage Control, Lafayette, Louisiana, USA, 15-17 February.

Knox, J.A., Lasater, R.M. and Dill, W.R. 1964. A New Concept in Acidizing Utilizing Chemical Retardation. Paper SPE 975 presented in the Fall Meeting of the Society of Petroleum Engineers of AIME, Houston, Texas, USA, 11-14 October.

Ladd, A.J.C. 1990. Hydrodynamic Transport Coefficients of Random Dispersions of Hard Spheres. *J. Chem. Phys.* **93**:3484-3494.

Langmuir D. 1968. Stability Of Calcite Based on Aqueous Solubility Measurements. *Geochimica et Cosmochimica Acta* **32**(8): 835 – 851.

Lasater, R. 1962. Kinetic Studies of the HCl-$CaCO_3$ Reaction. Paper presented at the 18th Southwest ACS Meeting, Dallas, Texas, USA, 19 December.

Laws, M.S., Al-Riyami, A.M.N., Soek, H.F. and Abdulkadir, R. 2005. Optimization of Stimulation Techniques for HP, Deep Wells in the Harweel Cluster, Oman. Paper SPE 93494 presented at the 14th SPE Middle East Oil and Gas Show and Conference, Bahrain International Exhibition Centre, Bahrain, 12-15 March.

LePage, J.N., De Wolf, C.A., Bemelaar, J.H., and Nasr-El-Din, H.A. 2011. An Environmentally Friendly Stimulation Fluid for High-Temperature Applications. *SPE Journal* **16**(1): 104-110.

Lequeux, F. 1998. Emulsion Rheology. *Curr. Opin. in Colloid Interface Sci.* **3**: 408-411.

Levich, V.G.1962. Physicochemical Hydrodynamics, Prentice-Hall Inc., Englewood Cliffs, New Jersey, USA, pp.78.

Li, Y., Sullivan, R.B., de Rozieres, J., Gaz, G.L., and Hinkel, J.J. 1993. An Overview of Current Acid Fracturing Technology with Recent Implications for Emulsified Acids. SPE paper 26581 presented at the SPE Annual Technical Conference and Exhibition, Houston, Texas, USA, 3-6 October.

Lietard, O., 1997. Matrix Treatment in Horizontal Openhole Wells: Design of Viscous Diverter Slugs and Treatment Fluid Placement Optimization. Paper SPE 38201 presented at the SPE European Formation Damage Conference, The Hague, The Netherlands, 2-3 June.

Litt, M. and Serad, M. 1964. Chemical Reactions on a Rotating Disk. *Chemical Engineering Science,* **19**(11): 867-884.

Lo, K.K. and Dean, R.H. 1989. Modeling of Acid Fracturing. *SPEPE* **4**(2): 194-200.

Lowenberg, M., and Hinch, E.J. 1996. Numerical Simulation of a Concentrated Emulsion in Shear Flow. *J Fluid Mech.* **321**:395-419.

Lund, K., Fogler, H.S., and McCune, C.C. 1973. Acidization I: The Dissolution of Dolomite in Hydrochloric Acid. *Chemical Engineering Science* **28**(3): 691 - 700.

Lund, K., Fogler, H.S., McCune, C.C., and Ault, J.W. 1975. Acidization-II. The Dissolution of Calcite in Hydrochloric Acid. *Chem. Eng. Sci.* **30**(8): 825-835.

Lynn, J.D., and Nasr-El-Din, H.A. 1999. Formation Damage Associated with Water-Based Drilling Fluids and Emulsified Acid Study. Paper SPE 54718 presented in the SPE European Formation Damage Conference, The Hague, Netherlands, 31 May-1 June.

Lynn, J.D and Nasr-El-Din, H.A. 2001. A Core Based Comparison of the Reaction Characteristics of Emulsified and in-situ Gelled Acids in Low Permeability, High Temperature, Gas Bearing Carbonates. Paper SPE 65386 presented at the SPE International Symposium on Oilfield Chemistry, Houston, Texas, USA, 13-16 February.

Madyanova, M., Hezmela, R., Artola, P., Guimaraes, C. R., and Iriyanto, B. 2012. Effective Matrix Stimulation of High-Temperature Carbonate Formations in South Sumatra Through the Combination of Emulsified and Viscoelastic Self- Diverting Acids. Paper SPE 151070 presented at the SPE International Symposium and

Exhibition on Formation Damage Control, Lafayette, Louisiana, USA, 15-17 February.

Mahmoud, M.A., Nasr-El-Din, H.A., De Wolf, C.A., and LePage, J.N. 2010. An Effective Stimulation Fluid for Deep Carbonate Reservoirs: A Core Flood Study. Paper SPE 131626 presented at the International Oil and Gas Conference and Exhibition in China, Beijing, China, 8-10 June.

Mahmoud, M.A., Nasr-El-Din, H.A., De Wolf, C.A., and LePage, J.N., and Bemelaar, J.H. 2011a. Evaluation of a New Environmentally Friendly Chelating Agent for High-Temperature Applications. *SPE Journal* **16**(3): 559-574.

Mahmoud, M.A., Nasr-El-Din, H.A., De Wolf, C.A., and LePage, J.N. 2011b. Optimum Injection Rate of a New Chelate That Can Be Used To Stimulate Carbonate Reservoirs. *SPE Journal* **16**(4): 968-980.

Mahmoud, M.A., Nasr-El-Din, H.A., De Wolf, C.A., and Alex, A.K. 2011c. Sandstone Acidizing Using A New Class of Chelating Agents. Paper SPE 139815 presented at the SPE International Symposium on Oilfield Chemistry, The Woodlands, Texas, USA, 11-13 April.

Mahmoud, M.A., Nasr-El-Din, H.A., De Wolf, C.A., and Alex, A.K. 2011d. Effect of Lithology on the Flow of Chelating Agents in Porous Media during Matrix Acid Treatments Paper SPE 140149 presented at the SPE Production and Operations Symposium, Oklahoma City, Oklahoma, USA, 27-29 March.

Mahmoud, M.A., Nasr-El-Din, H.A., De Wolf, C.A., and Alex, A.K. 2011e. Effect of Reservoir Fluid Type on the Stimulation of Carbonate Reservoirs Using Chelating

Agents. Paper SPE 143086 presented at the Brazil Offshore Conference and Exhibition, Macaé, Brazil, 14-17 June.

Maier, R., Appicciutoli, D., and Tedeschi, P. 2011. Innovative Fluid Storage and Blending Applications of Solvents, Acids, and Emulsified Acids Lead to Three-Year Spill-Free Operations in an Environmentally Sensitive Area. Paper SPE 140763 presented at the SPE European Health, Safety and Environmental Conference in Oil and Gas Exploration and Production, Vienna, Austria, 22-24 February.

Mason B., and Berry L. G. 1967. Elements of Mineralogy, W.H. Freeman, San Francisco, USA.

Mason, T.G., and Weitz, D.A. 1995. Optical Measurements of the Linear Viscoelastic Moduli of Complex Fluids. *Phys Rev Lett* **74**: 1250-1253.

Mason, T.G., Bibette, J., and Weitz, D.A. 1995. Elasticity of Compressed Emulsions. *Phys Rev Lett.***75**:2051-2054.

Mason, T.G., Krall, A.H., Gang, H., Bibette J., and Weitz D.A. 1996a. Monodisperse Emulsions: Properties and Uses. In: P. Becher, editor. Encyclopedia of Emulsion Technology, Marcel Dekker Inc.; New York, USA, pp: 299-336.

Mason, T.G., Bibette, J., and Weitz, D.A. 1996b. Yielding and Flow of Monodisperse Emulsions. *J Colloid Interface Sci.* **179**: 439-448.

Mason, T.G., Lacasse, M.D., Grest, G.S., Levine, D., Bibette, J., and Weitz, D.A. 1997a. Osmotic Pressure Viscoelastic Shear Moduli of Concentrated Emulsions. *Phys Rev E* **56**: 3150-3166.

Mason, T.G., Gang, H., and Weitz, D.A. 1997b. Diffusing-Wave-Spectroscopy Measurements of Viscoelasticity of Complex Fluids. *J. Opt. Soc. Am. A* **14**: 139-149.

Mason, T.G. 1999. New Fundamental Concepts in Emulsion Rheology. *Current Opinion in Colloid & Interface Science* **4**: 231-238.

McLeod, H.O. 1984. Matrix Acidizing. *J. Pet. Tech,* **36** (12): 2055-2069.

Mohamed, S.K., Nasr-El-Din, H.A. and Al-Furaidan, Y.A. 1999. Acid Stimulation of Power Water Injectors and Saltwater Disposal Wells in a Carbonate Reservoir in Saudi Arabia: Laboratory Testing and Field Results. Paper SPE 56533 presented at the SPE Annual Technical Conference and Exhibition, Houston, Texas, USA, 3-6 October.

Moore, R.E., Brenneman, D.R., Bischof, A.E., and Robins, J.D., 1972. One Step Anhydrite Scale Removal. *Mater. Prot. Perform.* **11**(3): 41–48.

Mumallah, N.A. 1991. Factors Influencing the Reaction Rate of Hydrochloric Acid and Carbonate Rock. Paper SPE 21036 presented at the SPE International Symposium on Oilfield Chemistry, Anaheim, California, USA, 20-22 February.

Muskat, M. 1947. Physical Principles of Oil Production, McGraw-Hill Book Co. Inc.; New York City, USA, pp. 242.

Nasr-El-Din, H.A., Al-Anazi, H.A. and Mohamed, S.K. 2000. Stimulation of Water Disposal Wells Using Acid-in-Diesel Emulsions - Case Histories. *SPEPF* **15**(3): 176-182.

Nasr-El-Din, H.A., Solares, J.R., Al-Mutairi, S.H., and Mahoney, M.D. 2001. Field Application of Emulsified Acid-Based System to Stimulate Deep Sour Gas Reservoirs in Saudi Arabia. Paper SPE 71693 presented at the SPE Annual Technical Conference and Exhibition, New Orleans, Louisiana, USA, 30 September – 3 October.

Nasr-El-Din, H.A., Al-Mutairi, S.H., Al-Jari, M., Metcalf, A.S., and Walters, W. 2002. Stimulation of a Deep Sour Gas Reservoir Using Gelled Acid. Paper SPE 75501 presented at the SPE Gas Technology Symposium, Calgary, Alberta, Canada, 30 April – 2 May.

Nasr-El-Din, H.A., Al-Driweesh, S., Al-Muntasheri, G.A., Marcinew, R., Daniels, J., and Samuel, M. 2003a. Acid Fracturing HT/HP Gas Wells Using a Novel Surfactant Based Fluid System. Paper SPE 84516 presented at the SPE Annual Technical Conference and Exhibition, Denver, Colorado, USA, 5-8 October.

Nasr-El-Din, H.A., Samuel, E., and Samuel, M. 2003b. Application of a New Class of Surfactants in Stimulation Treatments. Paper SPE 84898 presented at the SPE International Improved Oil Recovery Conference in Asia Pacific, Kuala Lumpur, Malaysia, 20-21 October.

Nasr-El-Din, H.A., Al-Driweesh, S. M., Metcalf, A. S., and Chesson, J. 2006a. Fracture Acidizing: What Role Does Formation Softening Play in Production Response?. Paper SPE 103344 presented at the SPE Annual Technical Conference and Exhibition, San Antonio, Texas, USA, 24-27 September.

Nasr-El-Din, H.A., Al-Driweesh, S., Bartko, K.M., Al-Ghadhban, H.H., Ramanathan, V., Kelkar, S.K., and Samuel, M. 2006b. Acid Fracturing of Deep Gas Wells Using a Surfactant-Based Acid: Long-Term Effects on Gas Production Rate. Paper SPE 102469 presented at the SPE Annual Technical Conference and Exhibition, San Antonio, Texas, USA, 24-27 September.

Nasr-EI-Din, H.A., Al-Dirweesh, S., and Samuel, M. 2008a. Development and Field Application of a New, Highly Stable Emulsified Acid. Paper SPE 115926 presented at the SPE Annual Technical Conference and Exhibition, Denver, Colorado, USA, 21 -24 September.

Nasr-El-Din, H.A., Al-Driweesh, S.M., Metcalf, A.S., and Chesson, J.B. 2008b. Fracture Acidizing: What Role Does Formation Softening Play in Production Response?. *SPEPO* **23**(2): 184-191.

Nasr-El-Din, H.A., Al-Mohammed, A.M., Al-Aamri, A.M., and Al-Fuwaires, O. 2008c. Reaction of Gelled Acids with Calcite. *SPEPO* **23**(3): 353-361.

Nasr-El-Din, H.A., de Wolf, C.A. , Stanitzek, T. , Alex, A., Gerdes, S., and Lummer, N.R. 2012. Field Treatment To Stimulate A Deep, Sour, Tight Gas Well Using A New, Low Corrosive And Environmentally Friendly Fluid. Paper SPE 163332 presented at the 2012 SPE Kuwait International Petroleum Conference and Exhibition, Kuwait City, Kuwait, 10 – 12 December.

Navarrete, R.C., Miller, M.J. and Gordon, J.E. 1998a. Laboratory and Theoretical Studies for Optimization of Acid Fracture Stimulation. Paper SPE 39776 presented

at the SPE Permian Basin Oil and Gas Recovery Conference, Midland, Texas, USA, 23-26 March.

Navarrete, R.C., Holms, B.A., McConnell, S.B. and Linton, D.E. 1998b. Emulsified Acid Enhances Well Production in High Temperature Carbonate Formations. Paper SPE 50612 presented at SPE European Petroleum Conference, The Hague, The Netherlands, 20-22 October.

Navarrete, R.C., Holms, B.A., McConnell, S.B. and Linton, D.E. 2000. Laboratory, Theoretical, and Field Studies of Emulsified Acid Treatments in High-Temperature Carbonate Formation. *SPEPF* **15**(2): 96-106

Newman, J. 1966. Schmidt Number Correction for the Rotating Disk. *Journal of Physical Chemistry* **70**(4): 1327-1328.

Nierode, D. E. and Williams, B. B. 1971. Characteristics of Acid Reaction in Limestone Formations. *SPEJ* **11**(4): 406-418.

Nierode, D.E., Williams, B.B., and Bombardieri, C.C. 1972. Prediction of Stimulation from Acid Fracturing Treatments. *Journal of Canadian Petroleum Technology* **11**(4): 31-41.

Orton, R., and Unwin, P.R. 1993. Dolomite Dissolution Kinetics at Low pH: A Channel-Flow Study. *J. Chem. Soc., Faraday Trans*. **89**: 3947–3954.

Otsubo, Y. and Prud'homme, R.K. 1994. Rheology of oil-in-water emulsions. *Rheol. Acta.* **33**(1): 29-37.

Pabley, A.S., Ewing, B.C., and Callaway, R.E. 1982. Performance of Crosslinked Hydrochloric Acid in the Rocky Mountain Region. Paper SPE 10877 presented at the SPE Rocky Mountain Regional Meeting, Billings, Montana, USA, 19–21 May.

Pal, R., Yan, Y., and Masliyah, J. 1992. Rheology of Emulsions. In Emulsions: Fundamentals and Applications in the Petroleum Industry, ed. L.L. Schramm, Chap. 4, 131-170. Washington, DC: Advances in Chemistry Series, ACS.

Pal, R. 1996. Multiple O/W/O Emulsion Rheology. *Langmuir* **12**(9): 2220-2225.

Peters, F.W. and Saxon, A. 1989. Nitrified Emulsion Provides Dramatic Improvements in Live Acid Penetration. Paper SPE 19496 presented at the SPE Asia-Pacific Conference, Sydney, Australia, 13–15 September.

Pournik, M., Gomaa, A., and Nasr-EI-Din, H.A. 2010. Influence of Acid-Fracture Fluid Properties on Acid-Etched Surfaces and Resulting Fracture Conductivity. Paper SPE 128070 presented at the 2010 SPE International Symposium and Exhibition on Formation Damage Control, Lafayette, Louisiana, USA, 10-12 February.

Princen, H.M. 1985. Rheology of Foams and Highly Concentrated Emulsions: Experimental Study of the Yield Stress And Wall Effects For Concentrated Oil In Water Emulsions. *J Colloid Interface Sci*. **105**: 150-171.

Princen, H.M. 1986a. Rheology of Foams and Highly Concentrated Emulsions: Static Shear Modulus. *J Colloid Interface Sci.* **112**: 427 – 437.

Princen, H.M. 1986b. Osmotic Pressure of Foams and Highly Concentrated Emulsions Theoretical Considerations. *Langmuir* **2**: 519-524.

Princen, H.M., and Kiss, A.D. 1987. Osmotic Pressure of Foams and Highly Concentrated Emulsions Determination from the Variation in Volume Fraction with Height in an Equilibrated Column. *Langmuir* **3**: 36-41.

Princen, H.M. 1989. Rheology of Foams and Concentrated Emulsions An Experimental Study of the Shear Viscosity and Yield Stress of Concentrated Emulsions. *J Colloid Interface Sci.***128**: 176-187.

Rabie, A.I., Gomaa, A.M., and Nasr-El-Din, H.A. 2012. Reaction of In-Situ-Gelled Acids with Calcite: Reaction-Rate Study. *SPEJ* **16**(4): 981-992.

Rabie, A.I., Gomaa, A.M., and Nasr-El-Din, H.A. 2012. HCl/Formic In-Situ-Gelled Acids as Diverting Agents for Carbonate Acidizing. *SPEPO* **27**(2): 170-184.

Rabie, A.I., Mahmoud, M.A., and Nasr-El-Din, H.A. 2011. Reaction of GLDA with Calcite: Reaction Kinetics and Transport Study. Paper SPE 139816 presented at the SPE International Symposium on Oilfield Chemistry, The Woodlands, Texas, USA, 11-13 April.

Roberts, L.D., and Guin, J.A. 1975. A New Method for Predicting Acid Penetration Distance. *SPEJ* **15**(4): 277-286.

Sabhapondit, A., Vielma Guillen, J.R., and Prakash, C. 2012. Laboratory Optimization of an Emulsified Acid Blend for Stimulation of High-Temperature Carbonate Reservoirs. Paper SPE 150337 presented at North Africa Technical Conference and Exhibition, Cairo, Egypt, 20-22 February.

Saxon, A., Chariag, B., and Abdel Rahman, M.R. 2000. An Effective Matrix Diversion Technique for Carbonate Formations. *SPE Drilling & Completion* **15**(1): 57-62.

Schechter, R.S. and Gidley, J.L. 1969. The Change in Pore Size Distribution from Surface Reactions in Porous Media. *AIChE Jour.* **15**(3)**:** 339-350.

Sherman, P. (ed.). 1968. Emulsion Science, Academic Press, New York.

Shukla, S., Zhu, D., and Hill, A.D. 2006. The Effect of Phase Saturation Conditions on Wormhole Propagation in Carbonate Acidizing. *SPE Journal* **11**(3): 273-281.

Smith, C.F., Crowe, C.W., and Wieland, D.R. 1970. Fracture Acidizing in High Temperature Limestone. SPE Preprint 3008 presented at the SPE Deep Drilling and Production Symposium, Monahans, Texas, USA, 26-27 March**.**

Snow, S.E, and Brownlee, M.H. 1989. Practical and Theoretical Aspects of Well Testing in the Ekofisk Area chalk Fields. Paper SPE 19776 presented at the 64th Annual Technical Conference and Exhibition of the Society of Petroleum Engineers, San Antonio, Texas, USA, 8-11 October.

Solares, J.R., Al-Asiri, K., Franco, C., Vielma, J., and Izquierdo, G. 2011. Optimized HP/HT Acid Blends and Associative Polymer Diversion Proven to be Successful in Acid Fracturing a Multilayered Reservoir: A Case History from South Ghawar Gas Field in Saudi Arabia. Paper SPE 141337 presented at the SPE Production and Operations Symposium, Oklahoma City, Oklahoma, USA, 27-29 March.

Sollman, M.Y., Hunt, J.L., and Daneshi, T. 1990. Well Test Analysis Following a Closed Fracture Acidizing Treatment. *SPE Formation Evaluation* **5**(4): 369-374.

Tadros, T.F. 1994. Fundamental Principles of Emulsion Rheology and Their Applications. *Colloid Surfaces A* **91**: 39-55.

Tambini, M. 1992. An Effective Matrix Stimulation Technique for Horizontal Wells. Paper SPE 24993 presented at the European Petroleum Conference, Cannes, France, 16-18 November.

Taylor, K.C., Nasr-El-Din, H.A. and Al-Alawi, M., 1999. A Systematic Study of Iron Control Chemicals Used During Well Stimulation. *SPE Journal* **4**(1): 19-24.

Taylor, K.C., and Nasr-El-Din, H.A. 1999. A Systematic Study of Iron Control Chemicals Used During Well Stimulation - Part II. Paper SPE 50277 presented at the SPE Oilfield Chemistry, Houston, Texas, USA, 16-19 February.

Taylor, K.C., Al-Ghamdi, A.H., and Nasr-El-Din, H.A. 2003. Effect of Rock Type and Acidizing Additives on Acid Reaction Rates Using the Rotating Disk Instrument. Paper SPE 80256 presented at the International Symposium on Oilfield Chemistry, Houston, Texas, USA, 5–7 February.

Taylor, K.C., Al-Ghamdi, A.H., and Nasr-El-Din, H.A. 2004a. Effect of Additives on the Acid Dissolution Rates of Calcium and Magnesium Carbonates. *SPEPF* **19**(3): 122-127.

Taylor, K.C., Al-Ghamdi, A.H., and Nasr-El-Din, H.A. 2004b. Measurement of Acid Reaction Rates of a Deep Dolomitic Gas Reservoir. *Journal of Canadian Petroleum Technology* **43**(10): 49-56.

Taylor, K.C., and Nasr-El-Din, H.A. 2004. Anomalous Acid Reaction Rates in Carbonate Reservoir Rocks. Paper SPE 89417 presented at the SPE/DOE Fourteenth Symposium on Improved Oil Recovery, Tulsa, Oklahoma, USA, 17 – 21 April.

Taylor, K.C., Nasr-El-Din, H.A., and Mehta, S. 2006. Anomalous Acid Reaction Rates in Carbonate Reservoir Rock. *SPEJ* **11**(4): 488-496.

Terjesen, S. G., Erga, O., Thorsen, G., and Ve, A. 1961. II. Phase Boundary Processes as Rate Determining Steps in Reactions between Solids and Liquids: The Inhibitory Action of Metal Ions on the Formation of Calcium Bicarbonate by the Reaction of Calcite with Aqueous Carbon Dioxide. *Chem. Eng. Sci.* **74**: 277-288.

Tyler, T.N., Metzger, R.R., and Twyford, L.R. 1985. Analysis and Treatment of Formation Damage at Prudhoe Bay, Alaska. *Journal of Petroleum Technology* **37**(6): 1010-1018.

Van Poollen, H.K. 1967. How Acids Behave in Solution. *Oil & Gas J*, pp: 100-102.

Van Poollen, H.K. and Jargon, J. R. 1968. How Conditions Affect Reaction Rate of Well-Treating Acids. *Oil & Gas J*, pp: 84-91.

Weitz, D.A., and Pine, D.J. 1992. Diffusing-Wave Spectroscopy. In: Brown W, editor. Dynamic Light Scattering, Oxford University Press; Oxford, UK, pp: 652-720.

Weyl, P.K. 1958. The Solution Kinetics of Calcite. *J. Geol.* **66**: 163-176.

Williams, B.B., Gidley, J.L., Guin, J.A., and Schechter, R.S. 1970. Characterization of Liquid-Solid Reactions. *Industrial & Engineering Chemistry*, **9**(4): 589-596.

Williams, B.B., and Nierode, D.E. 1972. Design of Acid Fracturing Treatments. *Journal of Petroleum Technology* **24**(7): 849-859.

Wollast, R. 1990. Rate and Mechanism of Dissolution of Carbonates in the System $CaCO_3$–$MgCO_3$. In: Stuum, W. (Ed.), Aquatic Chemical Kinetics. Wiley - lnterscience, New York, USA, pp. 431–445.

Xiong, C., Zhou, F., Liu, Y., Yang, X., Liu, X., Shi, Y., Tan, Y., Zhang, F., Ji, X., Qin, S., Huang, S., and Wang, X. 2010. Application and Study of Acid Technique Using Novel Selective Emulsified Acid System. Paper SPE 131216 presented at the CPS/SPE International Oil & Gas Conference and Exhibition, Beijing, China, 8-10 June.

Yeager, V. and Shuchart, C. 1997. In-Situ Gels Improve Formation Acidizing. *OGJ* **95**(3): 70-72.